

**Rapid systems for detection of pathogen and human nucleic acids
via microfluidic amplification**

Jacquelyn Astin DuVall
Virginia Beach, Virginia

B.S. Chemistry, University of Virginia, 2010

A Dissertation presented to the Graduate Faculty of the University of Virginia in
Candidacy for the Degree of Doctor of Philosophy

Department of Chemistry

University of Virginia
April 2017

Abstract

Nucleic acid amplification serves an important role in many applications, including, but not limited to: clinical diagnostics, biomedical analyses, and forensics. Traditional amplification, either via polymerase chain reaction (PCR) or isothermal methods, is time-consuming and dependent upon expensive instrumentation and equipment. Microfluidics has emerged as a powerful tool to address these limitations, and extensive research has been focused on the application of micro total analysis systems (μ TAS) to nucleic acid amplification. This dissertation presents two specific applications of microfluidic amplification: pathogen detection and forensic human identification.

The goal of the work presented in Chapters 2 and 3 was an inexpensive and simplified method for pathogen detection. Building upon a previously described technique, chaotrope-induced aggregation (CIA), a novel magnetic bead assay was developed, and coupled to an isothermal amplification reaction, for rapid detection of multiple microorganisms, including: Rift Valley fever virus, *Escherichia coli*, *Salmonella*, Influenza H1N1, and *Clostridium difficile*. The magnetic bead assay, referred to as product-inhibited bead aggregation (PiBA), as well as the isothermal amplification, were both successfully demonstrated on a polyester microdevice. Functionality, including spinning, heating, and application of a rotating magnetic field (RMF), was achieved with a custom-built system, and image analysis allowed for detection of targeted pathogens with an inexpensive 15-megapixel cell phone camera.

Chapters 4 and 5 present work aimed at developing an inexpensive and rapid platform for human identification using short tandem repeat (STR) analysis. Multiplexed

PCR was demonstrated for the first time on a polyester microdevice, and the amplification was further integrated with upstream liquid extraction (LE) and downstream microchip electrophoresis (ME). A custom-built system was designed for rapid Peltier-mediated thermocycling, and allowed for the successful amplification of 10 genetic loci in only 15 minutes. The print, cut, laminate (PCL) method was utilized for rapid prototyping, and this approach allowed for the fabrication of a fully-integrated microdevice using inexpensive, commercially available substrates. Fluid flow control was achieved through the use of centrifugal force and laser-actuated valves, thereby eliminating the need for cumbersome external pumps and valves. Overall, a fully-integrated microdevice was demonstrated, capable of DNA extraction, multiplexed STR-based PCR amplification, and fragment separation, for rapid human identification via generation of a unique STR profile.

Acknowledgments

First and foremost, I would like to gratefully acknowledge my advisor, Dr. James Landers. Your support throughout graduate school has been invaluable, and I thank you for the opportunity to pursue my doctorate; you took a chance on me and I hope it has paid off. You have taught me many lessons, the most valuable of which is the importance of good old-fashioned hard work. To my peers in the Landers Research Group, thank you for cultivating a work environment that was enjoyable and supportive, I could not have done it without you. I would like to thank Dr. Daniel Nelson and Dr. Delphine Le Roux for their mentorship and guidance throughout this process.

To my Charlottesville family- Tristan, Courtney, Brandon, and Danielle, whom I lovingly refer to as the “nerd herd”, thank you for making these some of the best years of my life. To Brandon, my nook buddy, I cannot thank you enough for your friendship both in and out of the lab; it truly means the world to me. Thank you for keeping me sane. To my parents, Randy and Leslie, I would not be here without your unfailing support and tough love. Thank you for always believing in me, even when I forgot to believe in myself. I love you both so much. Kyle, you are the light of my life. Thank you for making me laugh through the worst of it, and for always having my back. I love you, and I cannot wait for this next great adventure with you.

Table of Contents

Abstract.....	ii
Acknowledgments.....	iv
Table of Contents.....	v
List of Figures and Tables.....	ix
Abbreviations.....	xiii

Chapter 1: Introduction 1

1.1 Overview of microfluidics.....	1
1.2 Microfluidic amplification.....	3
1.3 Pathogen detection.....	7
1.3.1 Background.....	7
1.3.2 Conventional methods for pathogen detection.....	8
1.3.3 PCR microdevices for pathogen detection.....	9
1.3.4 LAMP microdevices for pathogen detection.....	11
1.3.5 Microfluidic chip-based detection modalities.....	12
1.4 Forensic human identification.....	14
1.4.1 Background.....	14
1.4.2 STR profile generation.....	15
1.4.3 Rapid DNA.....	17
1.4.4 PCR microdevices for forensic applications.....	18
1.4.5 Integrated systems for rapid human identification.....	24
1.5 Conclusions.....	27
1.6 References.....	27

Chapter 2: Development of a novel bead aggregation assay for detection of

LAMP amplicons 43

2.1 Overview.....	43
2.2 Introduction.....	43
2.3 Materials and Methods.....	47
2.3.1 LAMP/RT-LAMP Protocol.....	47

2.3.2 DNA/RNA Extraction.....	48
2.3.2.1 Human and Animal.....	48
2.3.2.2 Bacteria.....	49
2.3.2.3 Virus.....	49
2.3.3 Quantitative real-time PCR.....	51
2.3.4 Reagent preparation.....	51
2.3.5 PiBA.....	51
2.4 Results and Discussion.....	52
2.4.1 Microbead aggregation.....	52
2.4.2 Specificity of response and concentration effect.....	54
2.4.3 Proof of concept.....	56
2.4.4 Image analysis.....	59
2.4.5 Food-borne pathogen detection.....	60
2.4.6 Detection of <i>E. coli</i> with serotype- and strain-specificity.....	63
2.4.7 Human-specific DNA detection.....	65
2.4.8 Virus detection.....	66
2.5 Conclusions.....	69
2.6 References.....	71

Chapter 3: Transitioning the PiBA assay onto a polyester microdevice

platform and integration with loop-mediated isothermal amplification.....	79
3.1 Overview.....	79
3.2 Introduction.....	80
3.3 Materials and Methods.....	85
3.3.1 On-chip LAMP.....	85
3.3.2 Chip design and fabrication.....	86
3.3.3 Spin system.....	86
3.3.4 Optimization of spin speed, direction, and duration.....	87
3.3.5 On-chip PiBA.....	87
3.3.6 <i>Clostridium difficile</i> spore isolation and culture.....	88
3.4 Results and Discussion.....	89

3.4.1 Polyester toner (PeT) microdevices and associated hardware	89
3.4.2 Optimization of PiBA on PeT microdevices	90
3.4.3 Validation of LAMP on PeT microdevices	95
3.4.4 Species-specific <i>C. difficile</i> detection and cell phone analysis	99
3.4.5 Strain-specific <i>C. difficile</i> detection.....	103
3.5 Conclusions.....	104
3.6 References.....	105

Chapter 4: Optimization of a novel Peltier clamping system and associated microdevice for multiplex PCR: applications in human identification115

4.1 Overview.....	115
4.2 Introduction.....	115
4.3 Materials and Methods.....	122
4.3.1 Chip design and instrumentation	122
4.3.2 Optimization of mixing and heating	124
4.3.3 PCR assay on-chip.....	125
4.3.4 Amplification of buccal swab samples on PeT chips	127
4.3.5 Conventional processes and data analysis	128
4.4 Results and Discussion	128
4.4.1 Dual Integrated Peltier Spin (DIPS) System.....	128
4.4.2 Sample and reagent mixing.....	131
4.4.3 Thermocycling in a PeT chip on the DIPS system	134
4.4.4 PeT chip surface effects.....	135
4.4.5 Introduction of a 6-plex custom kit and primer modifications	138
4.4.6 Introduction of a 10-plex custom kit and primer modifications	140
4.4.7 Titration of master mix components	142
4.5 Conclusions.....	147
4.6 References.....	148

Chapter 5: Integrated DNA extraction, PCR amplification, and electrophoretic separation on a rapid and portable microdevice154

5.1 Overview.....	154
5.2 Introduction.....	155
5.3 Materials and Methods.....	161
5.3.1 Chip fabrication and instrumentation.....	161
5.3.2 Spin system for integrated LE-PCR-ME	162
5.3.3 PCR primer optimization for on-chip amplification.....	163
5.3.4 PCR time reduction.....	163
5.3.5 PCR master mix optimization for on-chip amplification.....	164
5.3.6 On-chip amplification	165
5.3.7 Liquid extraction (LE)	165
5.3.8 Electrophoresis and data analysis	165
5.4 Results and Discussion	166
5.4.1 PCR time reduction with control DNA.....	166
5.4.2 ZyGEM DNA template.....	168
5.4.3 PCR time reduction with ZyGEM-extracted DNA.....	171
5.4.4 Integration of LE and PCR	173
5.4.5 Integration of PCR and ME	178
5.4.6 Integration of LE-PCR-ME.....	181
5.5 Conclusions.....	186
5.6 References.....	187
Chapter 6: Final Remarks.....	193
6.1 Conclusions.....	193
6.2 Future Directions	195
6.3 Summation	198
6.4 References.....	199

List of Figures and Tables

Chapter 1: Introduction

Figure 1-1 Example of a lab-on-a-chip device	2
Figure 1-2 Continuous-flow PCR	4
Figure 1-3 Schematic of the LAMP reaction	6
Figure 1-4 Areas of interest for pathogen detection	8
Figure 1-5 Schematics and photographs of the integrated PCR-CE microdevice	10
Figure 1-6 Schematic and image of self-heating, water-activated cartridge for LAMP....	12
Figure 1-7 Diagram of short tandem repeats (STRs)	15
Figure 1-8 Exemplary STR profile	16
Figure 1-9 Slidable SPE- μ PCR- μ CE microdevice with operation process	20
Figure 1-10 Schematics and photographs of the integrated microdevice	22
Figure 1-11 Design of the PCR-CE microchip for forensic DNA analysis	23
Figure 1-12 Microfluidic chip for “sample-in-answer-out” integrated DNA processing..	26

Chapter 2: Development of a novel bead aggregation assay for detection of LAMP amplicons

Figure 2-1 Proposed mechanism for chaotrope-induced aggregation (CIA).....	52
Figure 2-2 Magnesil beads used to detect presence of positive and negative RT-LAMP product	53
Figure 2-3 Testing specificity of inverse response for correct template.....	54
Figure 2-4 Concentration effect on aggregation inhibition.....	55
Figure 2-5 Extent of aggregation inhibition varies over the course of the RT-LAMP reaction.....	55
Figure 2-6 Schematic of proposed PiBA mechanism.....	56
Figure 2-7 PiBA proof-of-feasibility	57
Figure 2-8 Various types of trigger DNA	58
Figure 2-9 Statistical and empirical (visual) thresholds for PiBA	59
Figure 2-10 LAMP primer sequences and amplification temperature for <i>E. coli</i> O157:H7 strain EDL933, shiga toxin 2 (stx2) gene	61
Figure 2-11 PiBA for food-borne pathogen detection	62

Figure 2-12 Lower limit of <i>E. coli</i> O157:H7 detection via PiBA.....	63
Figure 2-13 Serotype-specific PiBA detection of <i>E. coli</i>	64
Figure 2-14 Strain-specific PiBA detection of <i>E. coli</i>	65
Figure 2-15 Detecting the presence of DNA specific to the human thyroid peroxidase (TPOX) gene	66
Figure 2-16 Detecting the presence of Rift Valley fever virus (RVFV) RNA	67
Figure 2-17 Results from RVFV qRT-PCR	68

Chapter 3: Transitioning the PiBA assay onto a polyester microdevice platform and integration with loop-mediated isothermal amplification

Figure 3-1 Schematic of a multilayer PeT device.....	89
Figure 3-2 Spin system built in-house for on-chip PiBA	90
Figure 3-3 Effects of distance of magnetic field to microwell	91
Figure 3-4 Effect of 1 cm RMF distance from microwell	92
Figure 3-5 Effect of increased strength of magnet.....	94
Figure 3-6 Optimization of trigger DNA concentration for on-chip PiBA	95
Figure 3-7 LAMP primer design and validation for <i>cdtA</i> primers	96
Figure 3-8 Chip design for on-chip LAMP.....	98
Figure 3-9 On-chip serpentine mixing validation.....	99
Figure 3-10 LAMP following on-chip serpentine mixing	100
Figure 3-11 Validation of cell phone for image analysis.....	101
Figure 3-12 Species-specific detection and cell phone analysis.....	102
Figure 3-13 Strain-specific <i>C. difficile</i> detection.....	103

Chapter 4: Optimization of a novel Peltier clamping system and associated microdevice for multiplex PCR: applications in human identification

Figure 4-1 Diagram of short tandem repeats (STR)	116
Figure 4-2 Dual Integrated Peltier Spinning (DIPS) System.....	129
Figure 4-3 DIPS system and PeT chips	130
Figure 4-4 Process optimization of on-chip mixing and thermocycling.....	132
Figure 4-5 Example STR profiles from tube-based amplification.....	136

Figure 4-6 PCR amplification of STR fragments on a PeT chip using the DIPS system	137
Figure 4-7 Preliminary primer modifications for 6-plex kit	139
Figure 4-8 Results from preliminary primer modifications	140
Figure 4-9 A novel 10-plex PCR amplification of STR fragments for rapid human identification	141
Figure 4-10 Optimizing primer concentration to improve on-chip peak balance and height.....	142
Figure 4-11 Polymerase titration for on-chip 15-minute PCR.....	143
Figure 4-12 Magnesium titration to determine optimal concentration in master mix	145
Figure 4-13 Exemplary results after optimization	146

Chapter 5: Integrated DNA extraction, PCR amplification, and electrophoretic separation on a rapid and portable microdevice

Figure 5-1 Time reduction study.....	167
Figure 5-2 Schematic of DNA extraction microdevice	168
Figure 5-3 Amplification of ZyGEM-extracted DNA	169
Figure 5-4 Data analysis for on-chip PCR with ZyGEM-extracted DNA	170
Figure 5-5 Rapid on-chip amplification of ZyGEM-extracted DNA	172
Figure 5-6 Early prototype for integrated device.....	173
Figure 5-7 Material inhibition study	174
Figure 5-8 Temperature control in new PCR chamber	175
Figure 5-9 Results from on-chip PCR with new design	176
Figure 5-10 Integration of LE and PCR.....	177
Figure 5-11 LE-PCR results.....	178
Figure 5-12 Integration of PCR and ME.....	179
Figure 5-13 Results from integrated PCR-ME	180
Figure 5-14 Results from integrated PCR-ME after allelic ladder was run.....	181
Figure 5-15 Fluidic flow control via laser valves	182
Figure 5-16 Final integrated device	183
Figure 5-17 Hardware for integrated functionality.....	184

Figure 5-18 Limited user interaction	184
Figure 5-19 Integrated LE-PCR-ME results	185

Abbreviations

μ TAS – micro total analysis system
LOC – lab on a chip
PDMS – polydimethylsiloxane
PMMA – poly(methyl methacrylate)
COC – cyclic olefin copolymer
PCL – print, cut, and laminate
Pe- polyethylene terephthalate
PCR- polymerase chain reaction
LAMP- loop-mediated isothermal amplification
SDA- strand displacement amplification
NASBA- nucleic acid sequence based amplification
RCA- rolling circle amplification
LIF- laser-induced fluorescence
ELISA- enzyme linked immunosorbent assay
NAAT- nucleic acid amplification test
HBV- Hepatitis B virus
MTB- *Mycobacterium tuberculosis*
HLA- human leucocyte antigen
PTFE- polytetrafluoroethylene
CCD- charged coupled device
NNV- nervous necrosis factor
VNTR- variable number tandem repeats
STR- short tandem repeat
CODIS – combined DNA index system
ESS – European standard set
SPE- solid phase extraction
CE – capillary electrophoresis
ME – microchip electrophoresis
LE- liquid extraction
IR- infrared
RMF- rotating magnetic field
POC- point of care
PiBA- product-inhibited bead aggregation
RVFV- Rift Valley fever virus
TPOX- thyroid peroxidase
HAI- hospital acquired infection
CDI- *Clostridium difficile* infection
PeT- polyethylene terephthalate toner
HSA- heat sensitive adhesive

Introduction

1.1 Overview of microfluidics

The first miniaturized (or micro) total chemical analysis system (μ TAS) was described by Manz et al. in 1990.¹ Development continued throughout the 1990s, and significant advances were made in the field, including efforts to decrease the volume of sample and reagents required for analysis, as well as efforts to decrease the overall analysis time.² As a field, μ TAS or lab-on-a-chip (LOC) systems have continued to evolve over the past twenty years, with a major focus on decreasing the overall cost, increasing the functionality, and finding utility in a wide range of applications. These applications include some of the most common centralized laboratory techniques: blood chemistries, immunoassays, nucleic acid amplification tests, and flow cytometry.³ In the beginning, the main driving force behind miniaturization was to enhance the analytical performance of the device; however, with that came an inherent reduction in size and a decrease in reagent and sample volume.^{4,5} The small size, precise microfluidic control, and automation allow for the integration of multiple processes onto a single chip, thereby reducing sample and reagent consumption, eliminating manual handling errors, and enhancing the analytical performance of the device.⁶⁻⁸ In addition to these characteristics, compact devices also allow for samples to be analyzed outside of a centralized laboratory; for this reason, LOC technologies have garnered much attention for their potential in point-of-care (POC) testing. An example of a microdevice is shown in **Figure 1-1**.

The manufacturing methods used for early microfluidic chips were those adapted from the semiconductor industry; therefore, the process was dominated by wet etching and photolithography of glass and silicon.^{9,10} In order to simplify the fabrication process, and mitigate the need for a clean room, various polymers were introduced, including: polydimethylsiloxane

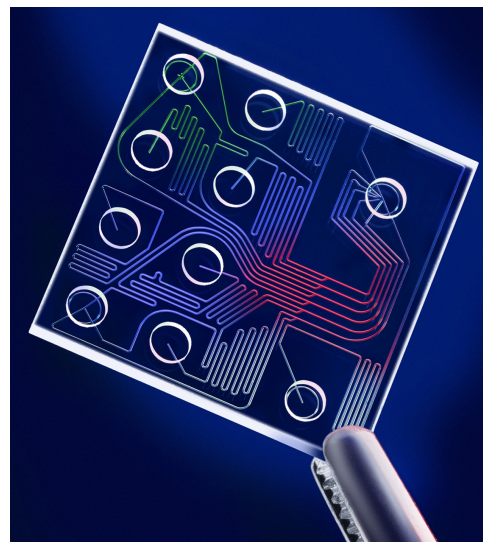


Figure 1-1. Example of a lab-on-a-chip device. Image courtesy of autogestion.ru

(PDMS), poly(methyl methacrylate) (PMMA), and cyclic olefin copolymer (COC). These polymer-based microdevices can generally be fabricated in a more rapid and inexpensive manner, using techniques such as soft lithography, injection molding, hot embossing, and laser ablation. Furthermore, these substrates are optically transparent, heat stable, and biocompatible.¹¹⁻¹³ Despite advances in new materials, however, cumbersome traditional fabrication processes remain a limiting factor in rapid and inexpensive prototyping. To address these limitations, the print, cut, laminate (PCL) method was developed in 2015, and effectively utilizes commercially available office equipment and inexpensive materials, including polyethylene terephthalate (Pe).² Briefly, a CO₂ laser is used to ablate the microfluidic architecture into Pe sheets that have been printed with ink (toner), and multilayer devices can be assembled using an office laminator. The PCL method will be described in more detail in Chapter 3.

1.2 Microfluidic amplification

Increasing the amount of target nucleic acid is often necessary and indispensable for analysis, as the amount of target present after sample preparation, or from a raw sample, can be insufficient for downstream detection.^{14, 15} Furthermore, increasing the amount of nucleic acid content through amplification allows for decreased detection sensitivity, which can simplify the associated instrumentation. The polymerase chain reaction (PCR) was developed by Kary Mullis in 1984 as a means for amplifying nucleic acid¹⁶, and it has since revolutionized many research areas, including: clinical diagnostics, biomedical analyses, and forensics.^{9, 17-19} Other amplification techniques include: loop mediated isothermal amplification (LAMP), strand-displacement amplification (SDA), nucleic acid sequence based amplification (NASBA), and rolling circle amplification (RCA); however, PCR has remained the most popular amplification method since its inception in the 1980s. Conventional PCR requires heating and cooling of the entire reaction mix, as well as the reaction chamber, which has a large thermal mass and, therefore, leads to a lengthy 1-2 hour PCR amplification.²⁰ Typically, nucleic acid amplification is faster in microdevices, owing to the enhanced kinetics; the high surface area to volume ratio allows for efficient heat transfer and rapid thermocycling.¹⁹ Many groups have devoted time to the development of microfluidic devices for PCR amplification, and these devices can be divided into three main groups: continuous-flow, droplet, and well-based.

Continuous-flow PCR involves the movement of fluid through various zones of a device which are set to specific temperatures, and these devices can be further divided

into three categories: fixed-loop, closed-loop, and oscillatory. Schematics of continuous-flow devices are shown in **Figure 1-2**. The first continuous-flow chip was developed by Kopp et al. in 1998, and the overall reaction time depends upon the flow rate of the sample through the various temperature zones.²¹ Obeid et al. developed a continuous-flow PCR chip that was combined with laser-induced fluorescence (LIF) for both DNA and RNA amplification and detection, with PCR times as low as 35 minutes.^{22, 23} In 2002, West and colleagues developed a closed-loop microdevice with a two-step PCR reaction, in which the fluid is moved via magnetohydrodynamic actuation.²⁴ Similarly, Chen et al.

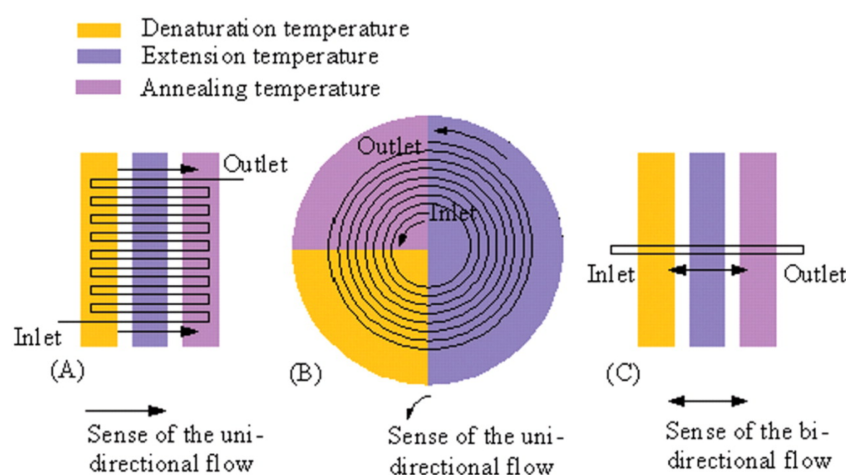


Figure 1-2. Continuous-flow PCR. A) The serpentine channel continuous-flow PCR. B) The spiral channel-based continuous-flow PCR. The sample is introduced at the inlet and pumped unidirectionally towards the outlet. C) The straight channel oscillatory-flow PCR. The sample is introduced in the inlet and pumped back and forth in a straight channel. Temperature zones are provided by three heaters. Adopted from Zhang et al. 2007.

developed a system comprised of a Teflon tube, with three distinct heating zones, which was angled such that fluid flow would be driven by convection, negating the need for an external pump.²⁵ The

successful amplification of 305 and 700 base pair fragments was shown in 73 minutes using this device. Although much progress has been made toward microdevices for continuous-flow PCR, the biggest disadvantage of this method is surface inhibition and adsorption, since the PCR reagents experience more interaction with the chamber surface while they are continuously flowing through the device.²⁰

Droplet-based PCR has garnered substantial attention in recent years. This method eliminates PCR inhibition and carryover contamination seen with continuous-flow devices. Typically, the PCR reaction is performed in a water-in-oil droplet in a microchannel, and each droplet can, therefore, be considered its own PCR reactor. Since the sample and reagents are confined to a single microdroplet, local temperature variations are small, and each microdroplet can experience a uniform temperature.²⁶ Beer et al. developed a microfluidic droplet-based PCR chip with picoliter droplets that remain stationary during thermocycling.²⁷ Owing to the small size of the droplets, a 56% cycle reduction is possible and only 18 cycles are required for single-copy amplification. In contrast to this stationary droplet-based approach, a continuous-flow droplet device was developed by Kiss et al. and can amplify a 245 base pair fragment within 35 minutes.²⁸ The drawbacks associated with this method include the challenge of reliably producing monodispersed droplets, and controlling the interaction of these droplets with the surface and each other.²⁰

Well-based PCR microdevices require the entire well, and sometimes the entire device, to be heated and cooled during thermocycling. The large thermal mass associated with this process often leads to long thermocycling times, a distinct disadvantage for well-based microfluidic PCR.²⁰ Despite this drawback, many groups have made significant progress with well-based PCR. In 2004, El-Ali et al. developed a microdevice capable of heating and cooling rates of 50°C and 30°C/second, respectively, and this device made use of integrated heaters and a total chamber volume of 20 μ L.²⁹ Another example of a well-based microfluidic PCR device is the PDMS chip developed by Liu et al. for real-time quantitative PCR. This device contains 100 wells (120 nL each) that

have pre-loaded, dried primer pairs, and heating and cooling is accomplished with a thermoelectric mechanism.³⁰ The well-based system will be the focus of the microfluidic PCR developed in Chapter 4-5 for integration with upstream DNA extraction and downstream electrophoretic separation.

Isothermal amplification techniques offer an alternative to PCR, requiring only one temperature, rather than multi-temperature thermocycling. Among the isothermal methods mentioned previously (LAMP, SDA, NASBA, and RCA), LAMP is the most widely researched and well characterized.³¹ A schematic of the LAMP reaction is shown in **Figure 1-3**. This method employs 4-6 primers and a strand displacement polymerase

(Bst); the products of the amplification are stem-loop structures with self priming capabilities.³² The reaction takes place between 60-65°C,

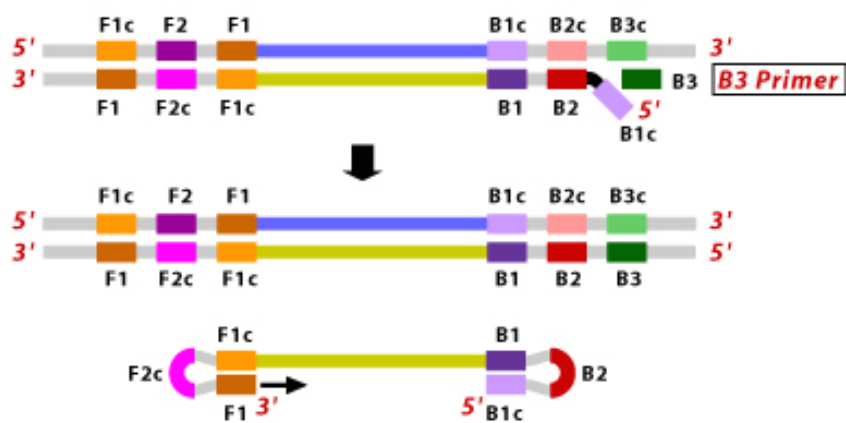


Figure 1-3. Schematic of the LAMP reaction. Image from www.premierbiosoft.com

and the combination of primers makes for a highly specific amplification, with an insoluble pyrophosphate by-product that can be visualized, via turbidity, following amplification.³³ Unlike microfluidic PCR, which has been widely applied to various fields, the bulk of research surrounding microfluidic LAMP pertains to pathogen detection, and will, therefore, be discussed in more depth in Section 1.3.3.

As mentioned previously, nucleic acid amplification techniques have revolutionized many research areas, two of which will be discussed at length: pathogen detection and forensic human identification. The focus of the work presented in this dissertation is twofold: one project is aimed at microfluidic pathogen detection utilizing a novel magnetic bead aggregation assay coupled to LAMP; and the other project is aimed at rapid human identification via a fully integrated centrifugal microdevice. Both projects use microfluidics as a tool to solve important problems, and nucleic acid amplification and detection plays a vital role.

1.3 Pathogen detection

1.3.1 Background

Infectious diseases are an ongoing threat to the populations of developing countries, despite recent advances in the availability of powerful, effective drugs.³⁴ More than half of deaths in developing countries can be attributed to infectious diseases, compared to less than 5 percent of deaths in developed nations; furthermore, infectious diseases are second only to cardiovascular disease, in terms of mortality, throughout the world.³⁵⁻³⁷ As such, timely and appropriate treatment often requires diagnostic tests that can be performed in resource-limited settings. By contrast, in developed nations, pathogen detection is important primarily for health and safety reasons, and primary concerns fall into three main categories: the food industry, water and environmental quality control, and clinical diagnostics.³⁸ **Figure 1-4** shows a diagram of the basic areas

of interest for pathogen detection. Conventional methods for pathogen detection, such as culture and colony counting methods, nucleic acid amplification testing, and immunoassays are effective, but often time-consuming and dependent on expensive laboratory equipment.

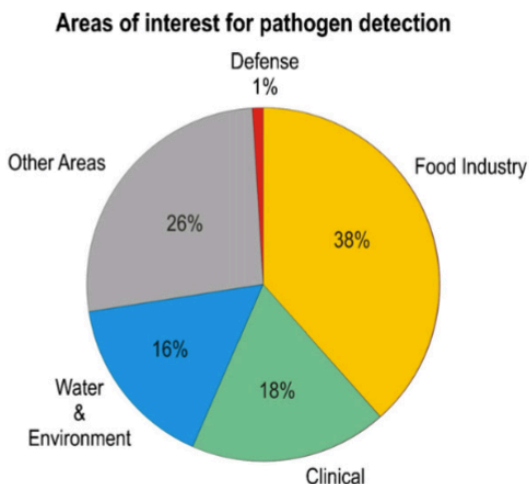


Figure 1-4. Areas of interest for pathogen detection. Adopted from Lazcka et al. 2007.

1.3.2 Conventional methods for pathogen detection

Cell culture and colony counting has long served as the gold standard for pathogen detection, despite the excessive time consumption required. Cell cultivation can require at least 3-4 days for preliminary results, and upwards of 7 days to have a final confirmatory result.⁶ Furthermore, culture runs a high risk of contamination with commensal flora, and the interpretation of results requires technical expertise.³⁹ Selective media can be used to detect specific pathogens, and detection is most often carried out using optical methods. These selective media either contain inhibitors, to stop the growth of non-targeted pathogens, or specific substrates that only the pathogen of interest is able to degrade, or that confers a distinct color to the growing colony.^{38, 40}

The most common type of immunology-based method for pathogen detection is the enzyme-linked immunosorbent assay (ELISA). This method utilizes the basic concept of an antigen binding to a specific antibody, allowing for low-level detection of multiple antigens, including: proteins, peptides, and hormones.⁴¹ The assay usually

consists of a target (antigen), an antibody to capture the antigen, and a detection antibody that will produce a signal in the presence of the target antigen.⁴² Despite the high degree of sensitivity afforded by the ELISA method, the high cost and batch-to-batch variability in the production of monoclonal antibodies are significant challenges that must be addressed.

Nucleic acid amplification tests (NAAT) are a fundamental tool of molecular biology, and involve generating many copies of short nucleic acid sequences. Over the years, there have been several PCR methods developed for pathogen detection, including: real-time PCR⁴³, multiplex PCR⁴⁴, and reverse transcriptase PCR.⁴⁵ While PCR relies on thermal cycling to produce amplicons, isothermal amplification produces nucleic acid sequences at a constant temperature, and various isothermal amplification techniques have been developed since the early 1990s to serve as alternatives to PCR.⁴⁶ Regardless of variable or constant temperature control, the largest drawback to NAAT methods is the requirement for downstream detection of the amplicons produced, as these methods often rely on fluorescence or gel electrophoresis, both of which can be cumbersome and expensive.

1.3.3 PCR microdevices for pathogen detection

Due to the inherent advantages of LOC devices for PCR mentioned previously in Section 1.2, a significant amount of work has focused on the implementation of PCR microdevices for pathogen detection. Pan et al. demonstrated an integrated device for parallel genetic analysis and detection of hepatitis B virus (HBV), *Mycobacterium tuberculosis* (MTB), and genotyping of human leucocyte antigen (HLA-B27).⁴⁷ The

device consists of three main functional units, including: temperature control, multiplex PCR, and multi-channel separation. For PCR thermocycling, a Pt/Ti microheater (covered by an aluminum block) was utilized, and a Pt-chip sensor was used for constant temperature monitoring. Four different samples were analyzed simultaneously, demonstrating the ability for multiplexed pathogen detection. A schematic of this device is shown in **Figure 1-5**. Wang et al. demonstrated a capillary-based microdevice for oscillatory-flow multiplex PCR, with a polytetrafluoroethylene (PTFE) tube serving as the reaction channel.⁴⁸ Three important food-borne pathogens, *Salmonella enterica*, *Escherichia coli* O157:H7, and *Listeria monocytogenes*, were amplified using this device. Temperature control was achieved with three copper heat blocks, each of which maintained a constant temperature during the oscillatory-flow PCR. Thaitrong and colleagues developed a two-layer integrated PCR-CE microdevice for parallel detection of respiratory viruses.⁴⁹ This device is capable of detecting pathogens, including:

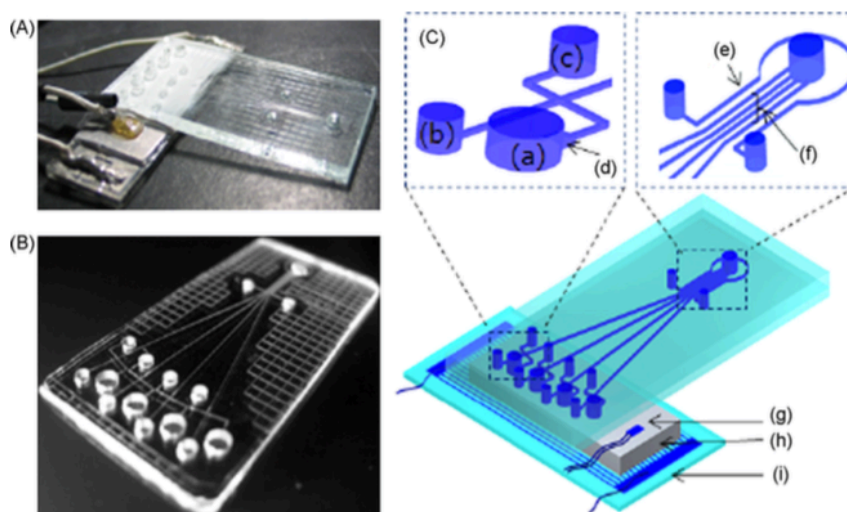


Figure 1-5. Schematics and photographs of the integrated PCR-CE microdevice. A) Pictures of the integrated microfluidic device. B) Pictures of glass chip (multiple PCR unit and multiple channel separation unit). C) Schematics of the integrated microfluidic device; (a) PCR chamber, (b) cathode reservoir, (c) sample waste reservoir, (d) expanded zone, (e) reference channel, (f) separation channels, (g) platinum-chip temperature sensor, (h) Al block, and (i) glass wafer with Pt electrodes. Adopted from Pan et al. 2010.

influenza A virus, human metapneumovirus (hMPV), human coronavirus OC43, and influenza B virus, and integrated heaters are used for thermocycling. Following PCR amplification, a streptavidin/biotin-mediated cleanup step is utilized prior to integrated separation.

1.3.4 LAMP microdevices for pathogen detection

Unlike PCR, isothermal amplification of nucleic acids does not require large thermal momentum and energy for thermocycling, thereby making this approach more energy efficient, and, subsequently, more suitable for LOC devices.³⁷ Several groups have successfully demonstrated LAMP microdevices capable of integrated pathogen detection for a wide variety of microorganisms. Fang et al. demonstrated a microdevice which utilized LAMP for the detection of pseudorabies viral DNA.⁵⁰ This device consists of 8 reaction microchannels for high-throughput analysis, and uncured PDMS is used to seal the device and prevent evaporation. Detection was achieved using a compact real-time absorbance device, but the results could also be visualized by the naked eye (via turbidity).

In another approach, Liu et al. described a LAMP reaction with the isothermal heat source provided by a water-activated, self-heating, polymeric cartridge (see **Figure 1-6**).⁵¹ This device was used for detection of *E. coli* samples in urine, and the amplified products were detected using fluorescence after 1 hour. In order to detect water-borne pathogens, Ahmad et al. developed a disposable microdevice coupled to an inexpensive charged-coupled device (CCD) camera for fluorescence imaging.⁵² Six different water-borne pathogens were detected at the single DNA copy level in less than 20 minutes,

comparable to the commercially available PCR system tested in conjunction. Using a reverse transcription step prior to LAMP (RT-LAMP) allowed Liu and colleagues to detect HIV RNA⁵³; and this device was also applied to the detection of the nervous necrosis factor (NNV) in fish larvae.⁵⁴ An array-type microheater was used to generate a uniform temperature, and the limit of detection was found to 10 fg of DNA using a compact fluorescence reader.

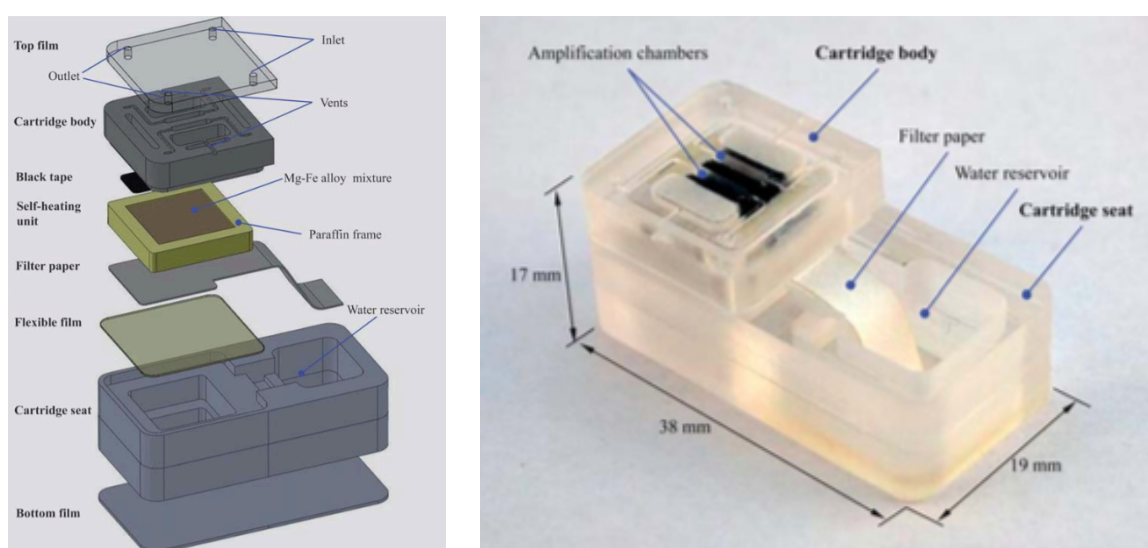


Figure 1-6. Schematic and image of self-heating, water-activated cartridge for LAMP. The cartridge consists of two main components: a cartridge body and a cartridge seat. Adopted from Liu et al. 2011.

1.3.5 Microfluidic chip-based detection modalities

Chip-based detection on microfluidic platforms has been demonstrated, both by the miniaturization of conventional techniques, as well as the incorporation of creative new approaches.¹³ The main challenge associated with microfluidic nucleic acid detection is achieving sensitivity comparable to traditional methods, without the use of the complicated and expensive instrumentation that is commonly required. This sensitivity challenge stems from the smaller detection volumes inherent to microdevices,

meaning there is a marked decrease in the number of analytes available for detection.⁵⁵ The two main factors, therefore, in choosing a detection modality for microdevices are the sensitivity and the scalability to smaller dimensions.

Three main techniques have emerged for chip-based detection, including: absorbance, chemiluminescence, and fluorescence.⁵⁵ While absorbance is the most widely used detection method for macro-scale applications, there are few examples of microdevices with absorbance-based detection; this is mainly attributed to the small channel dimensions that present problems for sensitive and reliable absorbance measurement. Chemiluminescence has several distinct advantages for chip-based detection, including: high sensitivity, low detection limits, and relatively simple instrumentation (which does not require an external light source).⁵⁶ However, there are a limited number of chemiluminescent reagents, and the reagents that do exist need to be mixed with target analytes prior to detection, therefore requiring a more complicated chip design. Lastly, fluorescence detection is the most widely used optical method for microdevices, due to the superior selectivity and sensitivity of this approach.^{4, 57} Laser-induced fluorescence (LIF) is the most common excitation source, and this technique has been successfully applied to chip-based sensors because it is easily adapted to the dimensions of a microfluidic device. A less expensive alternative, lamp-based excitation, allows for more flexibility in choosing an excitation wavelength.

Since rapid pathogen detection remains an important concern, many commercial tools have been developed to address diagnostic challenges.⁵ A variety of companies have demonstrated chip-based pathogen sensing systems. One example is the CANARY

(cellular analysis and notification of antigen risks and yield), which is a rapid biosensor for B-lymphocyte based antigen detection of multiple pathogens.⁵⁸ Another example is a SPR-based biosensor that can be implemented into a field-deployable device for detection of proteins, viruses, and whole microbes using a 24 channel SPREETA (Sensata) sensor unit.⁵⁹ Since microfluidic tools have been readily applied to the genomics research area, it is not surprising that most commercially available chip-based pathogen detection devices rely on DNA as the sole target.

1.4 Forensic human identification

1.4.1 Background

Human identification has been used for many decades, dating as far back as the 1800s when fingerprints were first used to identify criminals.⁶⁰ Since the discovery of the molecular structure of DNA in 1953⁶¹, many advances have been made toward new methods for human identification. In the early 1980s, “minisatellite” regions of the human genome were discovered and postulated to be an effective tool to identify molecular differences among individuals based on their DNA.⁶² These DNA sequences, known as variable number of tandem repeats (VNTRs), were shown to be repeated throughout the genome, and the number of repeats was found to be unique to a given individual. Shortly thereafter, in 1991, fluorescent short tandem repeat (STR) marker detection was first described.^{63,64} Whereas VNTRs are quite long, with repeats of several hundred bases, STRs are comprised of short repeats consisting of 1-6 nucleotides.⁶⁵

The same flanking regions are found across the entire human genome, regardless of the individual, making STR markers very easy to target and amplify using PCR primers (see **Figure 1-7**). At a given genetic marker, each individual has two alleles, thereby leading to polymorphism owing to these hypervariable DNA regions. When multiple markers are analyzed simultaneously, this method allows for a very high degree of discrimination among individuals. Specific STR markers have been chosen and characterized for human identification, and the Combined DNA Index System (CODIS)⁶⁶ is used in the United States, whereas a different database is used in Europe (European Standard Set (ESS)).⁶⁷ The newest STR kits combine all the markers from both databases, yielding a discriminatory power of 10^{14} times greater than the total population on Earth.

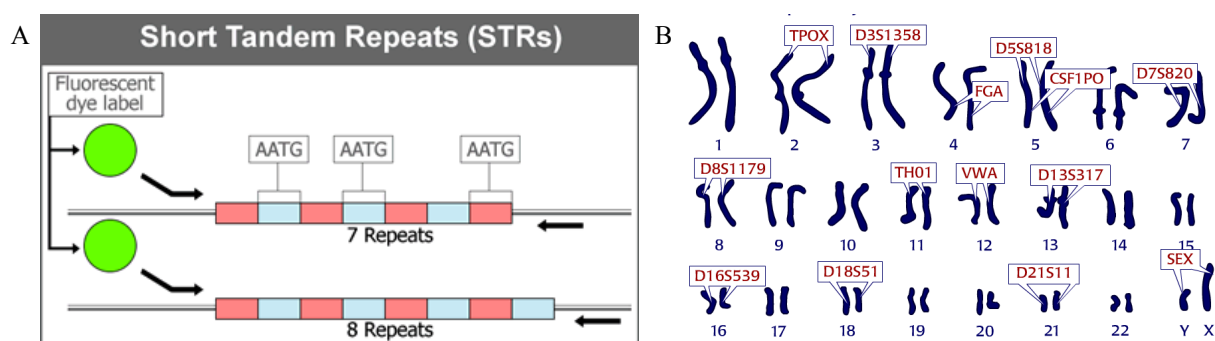


Figure 1-7. Diagram of short tandem repeats (STRs). A) The number of repeats can be the same on both alleles (homozygous) or different (heterozygous), and changes for each individual. B) Interrogating multiple STR markers within the genome allows for a high degree of discrimination among individuals. The Core 13 CODIS loci (plus Amelogenin) are shown, along with which chromosome each loci is found on.

1.4.2 STR profile generation

Amplification of STRs using PCR is only one step in the total analysis required to create a unique STR profile (exemplary STR profile shown in **Figure 1-8**). DNA has to

be extracted from biological samples prior to PCR amplification, and several extraction techniques are commonly used: phenol-chloroform, solid-phase, and ZyGEM.⁶⁸⁻⁷¹ The phenol-chloroform method works by partitioning proteins into an organic layer and nucleic acids into an aqueous layer.⁷² Solid phase extraction (SPE) uses a silica-based solid phase to reversibly bind DNA under high salt conditions. Lastly, ZyGEM liquid extraction utilizes a thermostable enzyme that is able to liberate DNA from the cell.^{73, 74}

Following DNA extraction and PCR amplification of STRs, the fragments must be separated and detected. Capillary electrophoresis (CE) has been, and continues to be, the preferred method for separation of STR fragments.^{75, 76} The underlying principle of this method lies in the negative charge associated with DNA, which, when an electric field is applied, causes the DNA to migrate through a capillary toward a positive

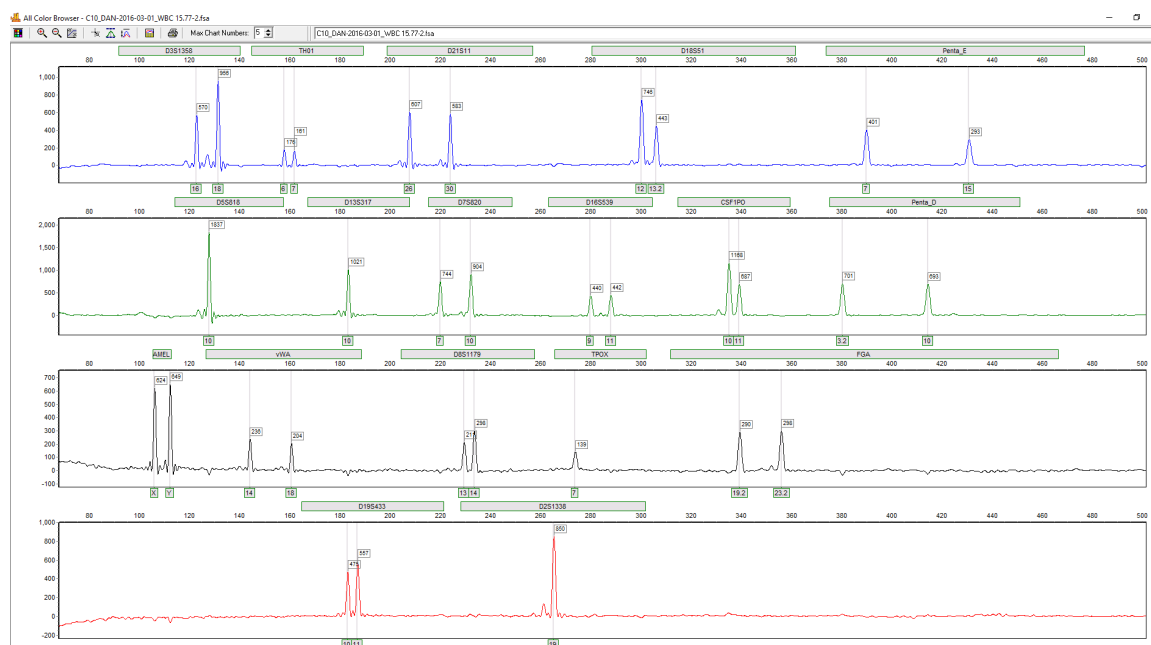


Figure 1-8. Exemplary STR profile. 18 genetic markers were amplified and separated on an ABI 3130 instrument. Each marker (labeled with grey boxes above electropherogram) has either one or two peaks, based on whether the individual is homozygous or heterozygous, respectively. The peak heights (RFU) are labeled in boxes above each peak. Allele numbers are labeled below each peak and represent the number of repeats for a given marker.

electrode (anode). Larger DNA fragments take longer to migrate through a sieving matrix (polymer) than short fragments; therefore, size-based separation is achieved using CE. Compared to slab gels, this method affords higher voltages, and thus a faster DNA migration rate.⁷² Furthermore, CE systems contain a detection system and a laser excitation source for detection of fluorescently labeled PCR amplicons.

1.4.3 Rapid DNA

Although the field of human identification has progressed significantly since its inception, the entire analytical process required for generating a STR profile requires multiple instruments (centrifuge, thermocycler, CE, etc.) and individual steps are often performed in different rooms to mitigate the effects of DNA contamination. The time associated with the STR analysis, from raw sample to result, is often between 7-10 hours if the sample is analyzed singularly. However, this time frame is often much longer when samples must be batched, and a significant backlog of samples exists in many laboratories. Rapid DNA has emerged as a primary interest in the forensics community to address these concerns. The aim of this field is threefold: (i) reduce sample backlog, (ii) provide rapid sample-to-answer STR analysis, and (iii) simplify the analytical processes so they can be performed by untrained users. Specifically, Rapid DNA is defined by the FBI as the fully automated process of generating a STR profile from a reference buccal swab, known as “swab in-profile out”.⁷⁷ Furthermore, the process must consist of automated extraction, amplification, separation, detection, and allele calling. In essence, the entire laboratory is reduced to a single instrument capable of performing each step required for generation of a STR profile.

To meet the demands of Rapid DNA, the microfluidic regime has been investigated, owing to the distinct advantages of this platform, including: time reduction, faster analysis times, lower reagent/sample consumption, and portability. Microfluidic systems for STR analysis enable the fluidic integration of each step in the process, resulting in faster analysis times (with the goal of less than 90 minutes) and a significantly decreased risk of sample loss or contamination. Although the ultimate goal of Rapid DNA is to create a fully-integrated microdevice with “swab in-profile out” capabilities, stand-alone microfluidic systems for each of the individual processes are not without merit. These stand-alone systems can be integrated into the conventional workflow in an effort to drastically reduce the processing time.

1.4.4 PCR microdevices for forensic applications

PCR microdevices have been extensively investigated for their utility in forensic and Rapid DNA applications. Devices have been developed for each of the individual genetic analysis assays, including: DNA extraction and preparation from biological samples, multiplex PCR for full STR typing, as well as Y chromosomal-STR typing, and fragment separation via capillary electrophoresis (CE). Devices have also been demonstrated that are either partially or completely integrated for genetic analysis. In forensic applications, it is often important to have a method for rapidly screening suspects, specifically when time is limited, or when a large number of samples need to be processed quickly. In these settings, the ability to rapidly perform Y-chromosomal STR typing would greatly enhance the speed with which the forensic analysis could be completed.⁷⁸

Lagally et al. demonstrated an integrated PCR-CE silicon microdevice for multiplex sex determination from human genomic DNA.⁷⁹ The device includes microfabricated heaters and resistance temperature detectors (RTDs) within the PCR chambers to create uniform heating and fast thermal response times, while minimizing the power required to operate the device. The RTDs are specifically designed to enable rapid thermal response and an accurate measurement of the temperature within the PCR chamber during thermocycling. With this approach, the authors were able to achieve heating and cooling rates of 20°C/second, and 20 cycles of PCR were completed in 10 minutes. In 2016, Kim et al. developed an integrated, slidable glass microchip for mini Y-chromosome STR typing.⁸⁰ This device effectively eliminates the requirement for micropumps or microvalves, allowing for a portable system that is capable of on-site Y-STR typing. SPE is used upstream of PCR, and a portable fluorescence detector is used following microchip electrophoresis (ME). The entire process, from extraction to detection, is completed in 60 minutes, and PCR requires 35 cycles, both for single-plex and multiplex amplification of mini Y-STR markers. The authors further demonstrated the device for use in mixed samples, whereby both male and female DNA is present, which is most often the case in sexual assault samples. A schematic of this device is shown in **Figure 1-9**.

In addition to Y-STR typing for rapid screening applications, full STR typing for human identification has also been demonstrated on various microfluidic platforms. Much effort has been aimed at improving microfluidic PCR amplification of STR fragments. Schmidt et al. successfully demonstrated a 16-plex PCR reaction on glass microscope slides with 60 reaction compartments (1 μ L reaction volume), and these open

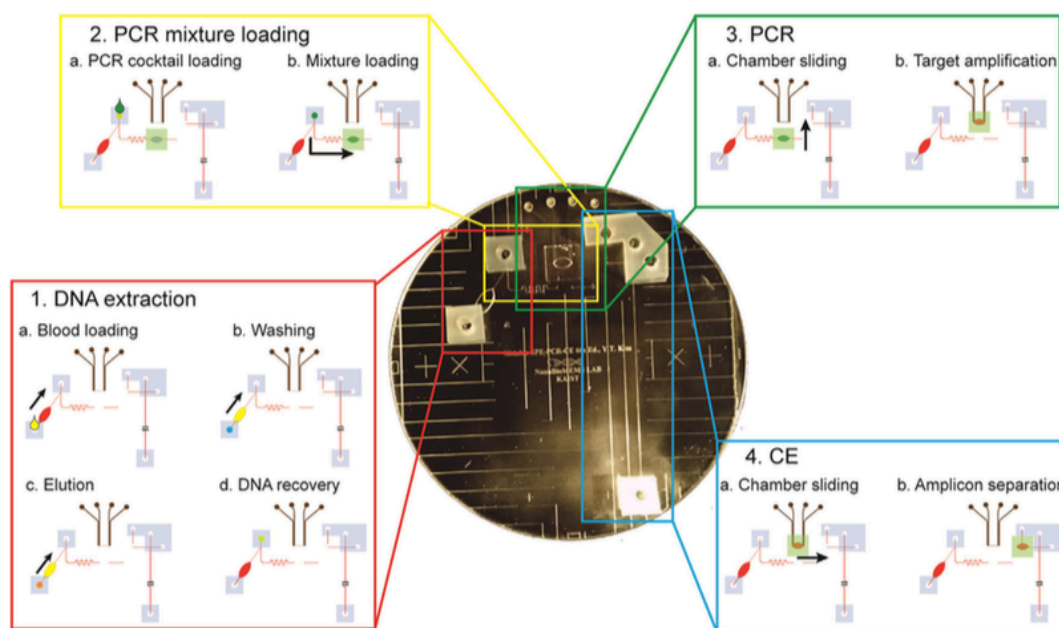


Figure 1-9. An image of the slidable SPE- μ PCR- μ CE microdevice with operation process. 1) Solid phase DNA extraction step. Human whole blood sample loading, washing buffer injection, and DNA elution were serially performed. 2) PCR mixture loading step. Purified DNA and PCR cocktail mixture were introduced to the slidable chip. 3) PCR step. The slidable chip was moved to the PCR region and PCR thermal cycling was performed. 4) CE step. Following target amplification, the slidable chamber slid to the CE region for amplicon separation and detection. Adopted from Kim et al. 2016.

wells were covered with oil during PCR to prevent evaporation and contamination.⁸¹ Sun and colleagues developed a closed-loop PMMA device for rapid 16-plex STR amplification.⁸² This microdevice is unique in that it comprises an external magnet, which drives a small ferrofluidic plug, which moves the PCR reaction mixture through the various temperature zones for thermocycling. The number of cycles can, therefore, be controlled by the number of rotation cycles of the magnet. In 2013, Lounsbury et al. demonstrated a disposable PMMA microdevice capable of 16-plex STR amplification in 30 minutes.⁸³ This device utilizes IR-mediated thermocycling, with heating and cooling rates of 7-9°C/second. Furthermore, the device can be used in a multi-chamber format, whereby a positive and negative control, as well as the samples of interest, can be amplified simultaneously. Geng et al. proposed a novel approach to STR typing of

individual cells, with amplification taking place in 1.5 nL agarose-in-oil droplets.⁸⁴ These monodisperse droplets were generated with a high frequency using a PDMS-glass microdevice; single cells and primer-functionalized microbeads are compartmentalized in the droplets for PCR amplification of 9 STR markers.

Toward the end goal of full integration, several groups have demonstrated the integration of the first two steps: DNA extraction and STR-based PCR amplification. Bienvenue et al. published the first example of an integrated DNA extraction and amplification system for human identification in 2010.⁸⁵ The microdevice consists of a micro-sample processing device (μ SPD) that utilizes a silica solid phase with syringe pump-driven flow for DNA extraction, followed by integrated, on-chip PCR amplification of STR fragments. Standard, commercially available STR kits (COfiler™ 7-plex and Profiler Plus™ 10-plex) were used, and the microdevice was placed in a laboratory thermal cycler for PCR amplification. In 2013, Lounsbury et al. demonstrated a disposable PMMA microdevice capable of liquid extraction (LE) via ZyGEM reagents, and multiplex PCR amplification of 16 genetic markers.⁸⁶ This device has an on-chip swab receptacle that accepts a portion of a dried buccal swab, effectively bridging the gap between the macro- and micro-scale processes (**Figure 1-10**). Adhesive valves are used for fluid flow control, without any surface activation or modification, and non-contact infrared (IR)-mediated PCR thermocycling is used to generate partial STR profiles (12 out of 16 loci present) in <45 minutes. Gan et al. developed an integrated PMMA-PDMS extraction-PCR device with filter paper serving as the DNA extraction component.⁸⁷ A Fusion 5 membrane disc was used to capture DNA in a low-cost and automated manner, and the feasibility of this method was demonstrated with a variety of raw samples,

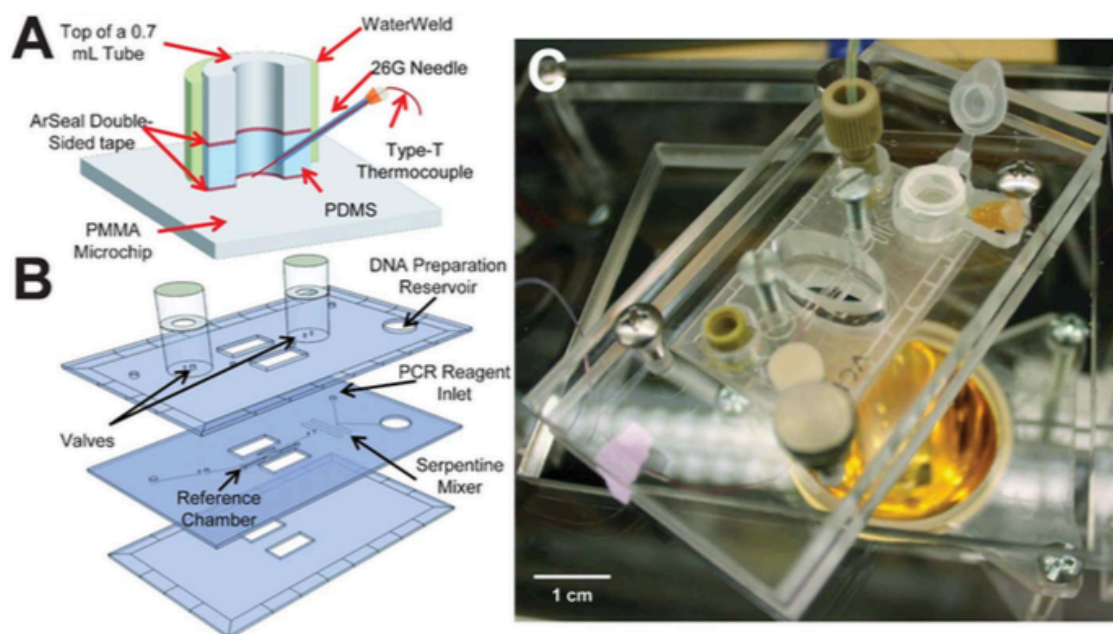


Figure 1-10. Schematics and photograph of the integrated microdevice. A) Rendering of the barrel for enzyme-based DNA preparation. A portion of a foam swab is loaded into the barrel and heated in the enzyme-based reagents using the IR-PCR system. B) Expanded 3-D view of the layers for an integrated microchip, showing the microarchitecture, including a serpentine mixer and two manually actuated adhesive valves. Overall dimensions: 3 x 5 cm; Channel dimensions: 146.9 +/- 7.2 μm wide x 315.4 +/- 15.7 μm deep; PCR chamber: a = 1.5 mm, b = 0.375 mm, depth = 0.5 mm, volume = 884 nL. C) Photograph of the assembled microdevice prior to an integrated analysis run. Adopted from Lounsbury et al. 2013.

including: human whole blood, dried blood stains, FTA™ cards, buccal swabs, saliva, and cigarette butts. A novel, “in-situ” PCR amplification was performed in the same chamber as the DNA extraction, thereby eliminating the possibility of sample dilution, while simplifying the overall microdevice design. 15 genetic loci were amplified, and the device was sealed and placed on top of a conventional, bench-top thermal cycler, resulting in a lengthy PCR.

Several groups have taken the microfluidic approach one step further, successfully demonstrating integration of all three assays: DNA extraction, PCR amplification of STR fragments, and separation. In 2008, Liu et al. demonstrated an integrated device for PCR-CE; however, DNA extraction and purification was performed

off-chip.⁸⁸ This glass-PDMS device is comprised of a 160 nL PCR chamber, as well as an on-chip heater and temperature sensor for amplification of a 9-plex STR-based PCR. The total process, from sample introduction to STR profile can be performed in 2 hours and 30 minutes (**Figure 1-11**). Hopwood and colleagues developed a completely closed device; a pre-filled polycarbonate cartridge is used for DNA extraction, PCR, and post-PCR manipulation, and separation is performed in a glass chip.⁸⁹ This device utilizes electrochemical pumps for fluid flow control, and PCR thermocycling is Peltier-driven. A mini high voltage power supply is integrated into the device hardware, allowing for STR fragment separation of 16 genetic markers for human identification. The integrated device is capable

of generating a STR profile in under 4 hours from buccal swabs. Taking a slightly different approach,

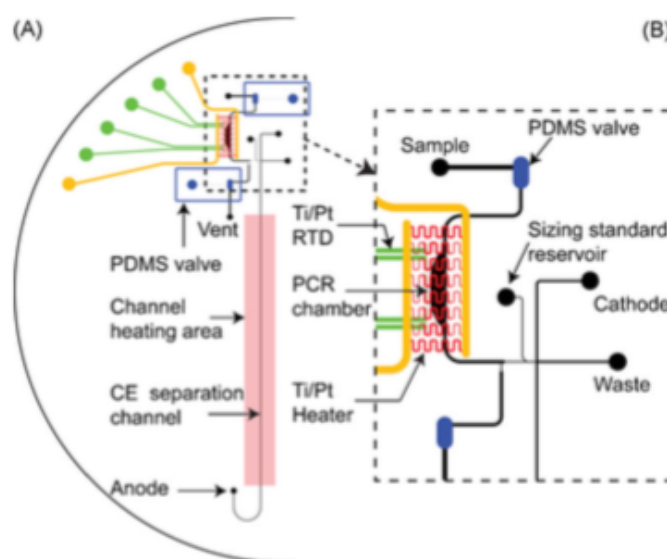


Figure 1-11. Design of the PCR-CE microchip for forensic DNA analysis. A) The integrated device consists of 7-cm-long electrophoretic separation channels (black), 160-nL PCR chambers (black), RTDs (green), PCR heaters (red), and PDMS microvalves (blue). A co-injector, including a co-injection channel and a sizing standard reservoir is incorporated into the microdevice. B) Expanded view of the heater, RTD, PCR chamber and CE co-injector. Adopted from Liu et al. 2008.

Reedy et al. demonstrated a modular microfluidic system for STR analysis.⁹⁰ Solid phase extraction of buccal swab lysate is performed, followed by IR-mediated PCR thermocycling of a 9-plex STR amplification, and laser-induced fluorescence detection of separated fragments. The entire process is complete in less than 3 hours, and the modular

approach provides flexibility in terms of how to proceed with sample processing, based upon information gained or already known about the sample.

1.4.5 Integrated systems for rapid human identification

As a natural extension of the research surrounding microfluidic extraction, PCR, and separation, several companies have focused on the development of an integrated forensic DNA analysis system to fulfill the requirements set forth by the Rapid DNA community. Here, four different systems aimed at meeting the goals of Rapid DNA will be briefly discussed: IntegenX RapidHIT™, Netbio/GE DNAscan™, NEC Portable DNA Analyzer, and the MicroLab IntrepID.

The IntegenX RapidHIT™ system has proven to be the most successful for STR profiling and rapid human identification, with CODIS profiles generated in <90 minutes.⁹¹⁻⁹³ The system, however, is not portable, and requires 4 microfluidic cartridges; 2 cartridges for DNA extraction and PCR amplification, and 2 cartridges for electrophoretic separation. Furthermore, separation takes place on a conventional CE instrument (not on the microdevice itself) that is incorporated into the system. Fluidic movement is achieved through the use of valves and pumps, notably the patented Microscale On-chip Valves (MOVE™) technology, which allows for metering and mixing of volumes as small as 10 nL. Extraction is performed via SPE, and thermocycling for PCR amplification is Peltier-driven. Despite its many advantages in terms of assay quality, the RapidHIT™ system is expensive (\$250,000 USD for the instrument and \$250-300 USD for consumables) and lacks portability.

Netbio/GE has developed the DNAscan™ system, and it is the first truly integrated device for rapid human identification.⁹⁴ A STR profile is generated in approximately 84 minutes, with lyophilized reagents allowing for room temperature storage of the injection molded BioChipSet cassette. Rapid multiplex PCR (probing 16 genetic markers) is achieved in 20 minutes. After insertion of the buccal swab into the cartridge, it is placed into the instrument, and the entire process is automated. Unlike the RapidHIT™ system, the DNAscan™ system has on-chip separation, and an allelic ladder can be generated with each sample that is run on the instrument. However, this instrument suffers from the same disadvantages, namely cost of the instrument and consumables, as well as a lack of portability.

The NEC Portable DNA Analyzer adopts a new approach to microfluidic PCR for STR profiling.⁹⁵ This instrument features multiple chambers for simultaneous single-plex and 2-plex PCR, rather than a large multiplex, and the overall PCR amplification time is 30 minutes with Peltier-driven thermocycling. Following PCR, the product is separated on-chip with multiple ME channels; short channel lengths are sufficient since there are only one or two PCR amplicons per line, and ME can, therefore, be achieved in as little as 5 minutes. Overall analysis time is 50 minutes, representing a distinct advantage of this system over the two previously described; however, since a commercial STR kit is not used, external validation in the forensic community will be required, and the cost of the device is still high.

Lastly, the MicroLab Intrepid system (**Figure 1-12**) was developed by Le Roux et al. to interface DNA extraction via ZyGEM reagents with non-contact PCR

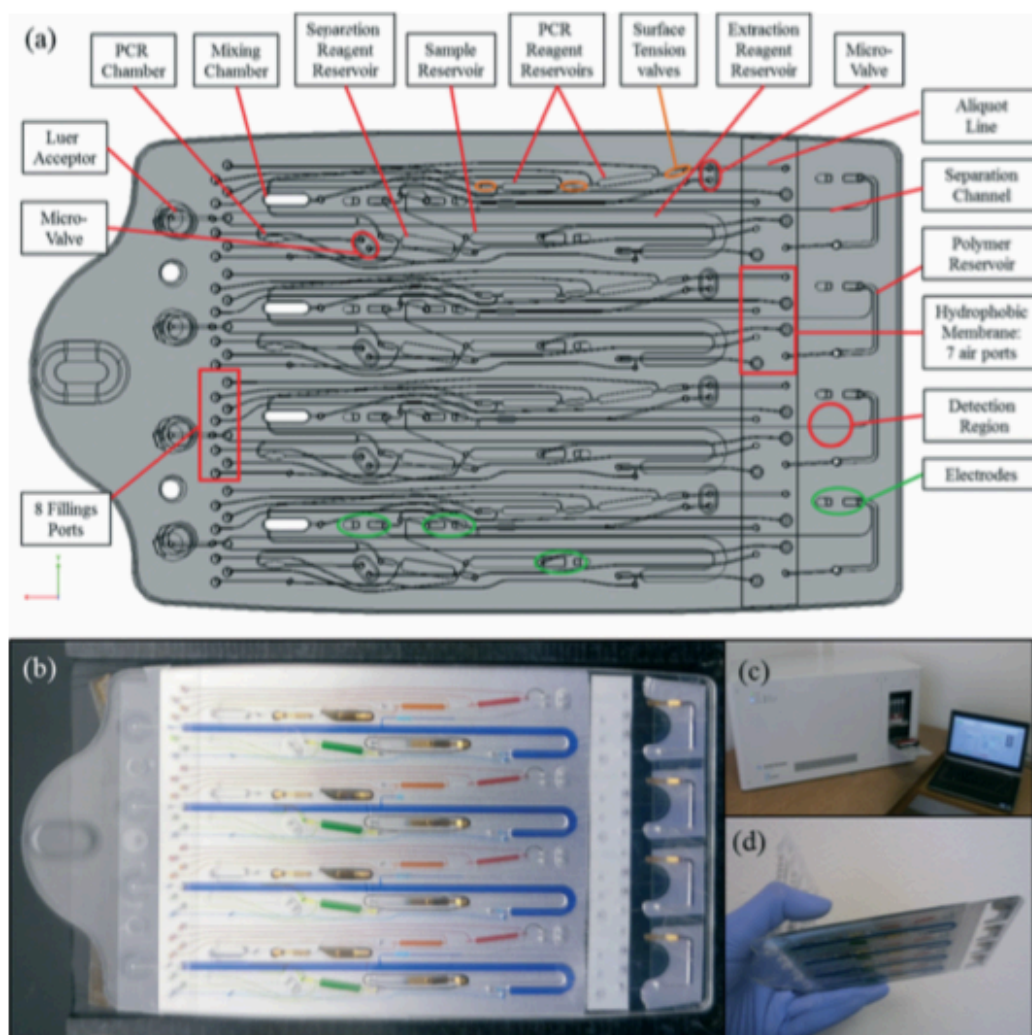


Figure 1-12. Microfluidic chip for “sample-in-answer-out” integrated DNA processing. A) Schematic representation of the microchip with major microfluidic features. B) Bottom view of the cartridge containing the fluidic layout with blue reagents in the extraction reagent reservoir, red and orange reagents in the PCR reagent reservoirs, green reagents in the separation reagent reservoir and polymer in the polymer reservoir. C) Microchip inside the instrument enabling its functionality with swabs attached and computer for software control. D) View of the microchip with swabs attached to it with a hand scale. Adopted from Le Roux et al. 2014

amplification of 18 genetic markers (18-plex).^{96,97} ZyGEM reagents were used for liquid enzymatic DNA liberation prior to PCR, and the non-contact amplification was driven by an IR lamp that provided rapid heating and cooling for thermocycling with simplified instrumentation. ME was performed in a 7 cm microchannel with a unique, self-coating polymer. Although the footprint of the microdevice itself was reduced, the inclusion of

pneumatic pumps and valves for fluid flow control required undesirable bulk to be added to the system, thereby decreasing portability and increasing cost.

1.5 Conclusions

This Chapter has introduced the concept of microfluidics as a tool with which to solve a wide range of scientific problems. Microfluidic amplification has been described in detail, specifically as it pertains to two distinct areas: pathogen detection and forensic human identification. In the pathogen detection realm, substantial progress has been made in developing rapid point-of-care microdevices that can be utilized in resource-limited settings, and microfluidics lends itself well to the specific requirements of such devices. For forensic human identification, many groups have dedicated themselves to fulfilling the requirements set forth by the Rapid DNA community, and microdevices have been developed with varying degrees of assay integration and automation.

1.6 References

1. Manz, A.; Graber, N.; Widmer, H. M., MINIATURIZED TOTAL CHEMICAL-ANALYSIS SYSTEMS - A NOVEL CONCEPT FOR CHEMICAL SENSING. *Sensors and Actuators B-Chemical* **1990**, *1* (1-6), 244-248.
2. Thompson, B. L.; Ouyang, Y. W.; Duarte, G. R. M.; Carrilho, E.; Krauss, S. T.; Landers, J. P., Inexpensive, rapid prototyping of microfluidic devices using overhead

transparencies and a laser print, cut and laminate fabrication method. *Nature Protocols* **2015**, *10* (6), 875-886.

3. Yager, P.; Edwards, T.; Fu, E.; Helton, K.; Nelson, K.; Tam, M. R.; Weigl, B. H., Microfluidic diagnostic technologies for global public health. *Nature* **2006**, *442* (7101), 412-418.

4. Reyes, D. R.; Iossifidis, D.; Auroux, P. A.; Manz, A., Micro total analysis systems. 1. Introduction, theory, and technology. *Analytical Chemistry* **2002**, *74* (12), 2623-2636.

5. Mairhofer, J.; Roppert, K.; Ertl, P., Microfluidic Systems for Pathogen Sensing: A Review. *Sensors* **2009**, *9* (6), 4804-4823.

6. Kim, T. H.; Park, J.; Kim, C. J.; Cho, Y. K., Fully Integrated Lab-on-a-Disc for Nucleic Acid Analysis of Food-Borne Pathogens. *Analytical Chemistry* **2014**, *86* (8), 3841-3848.

7. Haeberle, S.; Zengerle, R., Microfluidic platforms for lab-on-a-chip applications. *Lab on a Chip* **2007**, *7* (9), 1094-1110.

8. Daw, R.; Finkelstein, J., Lab on a chip. *Nature* **2006**, *442* (7101), 367-367.

9. Vilchner, T.; Janasek, D.; Manz, A., Micro total analysis systems. Recent developments. *Analytical Chemistry* **2004**, *76* (12), 3373-3385.

10. Fiorini, G. S.; Chiu, D. T., Disposable microfluidic devices: fabrication, function, and application. *Biotechniques* **2005**, *38* (3), 429-446.
11. Gubala, V.; Harris, L. F.; Ricco, A. J.; Tan, M. X.; Williams, D. E., Point of Care Diagnostics: Status and Future. *Analytical Chemistry* **2012**, *84* (2), 487-515.
12. Kumar, S.; Ali, M. A.; Anand, P.; Agrawal, V. V.; John, R.; Maji, S.; Malhotra, B. D., Microfluidic-integrated biosensors: Prospects for point-of-care diagnostics. *Biotechnology Journal* **2013**, *8* (11), 1267-1279.
13. Sloane, H. Nucleic Acid Analysis via Hybridization-Induced Microbead Aggregation:

Opportunities for Genetic Testing. University of Virginia, Charlottesville, VA USA, 2016.
14. Lee, T. M. H.; Hsing, I. M., DNA-based bioanalytical microsystems for handheld device applications. *Analytica Chimica Acta* **2006**, *556* (1), 26-37.
15. Zhang, C. S.; Xing, D., Miniaturized PCR chips for nucleic acid amplification and analysis: latest advances and future trends. *Nucleic Acids Research* **2007**, *35* (13), 4223-4237.
16. Bartlett, J.; Stirling, D., *A short history of the polymerase chain reaction*. PCR Protocols: 2003; p 3-6.

17. Auroux, P. A.; Iossifidis, D.; Reyes, D. R.; Manz, A., Micro total analysis systems. 2. Analytical standard operations and applications. *Analytical Chemistry* **2002**, *74* (12), 2637-2652.
18. Auroux, P. A.; Koc, Y.; deMello, A.; Manz, A.; Day, P. J. R., Miniaturised nucleic acid analysis. *Lab on a Chip* **2004**, *4* (6), 534-546.
19. Chen, L.; Manz, A.; Day, P. J. R., Total nucleic acid analysis integrated on microfluidic devices. *Lab on a Chip* **2007**, *7* (11), 1413-1423.
20. Zhang, Y. H.; Ozdemir, P., Microfluidic DNA amplification-A review. *Analytica Chimica Acta* **2009**, *638* (2), 115-125.
21. Kopp, M. U.; de Mello, A. J.; Manz, A., Chemical amplification: Continuous-flow PCR on a chip. *Science* **1998**, *280* (5366), 1046-1048.
22. Obeid, P. J.; Christopoulos, T. K., Continuous-flow DNA and RNA amplification chip combined with laser-induced fluorescence detection. *Analytica Chimica Acta* **2003**, *494* (1-2), 1-9.
23. Obeid, P. J.; Christopoulos, T. K.; Crabtree, H. J.; Backhouse, C. J., Microfabricated device for DNA and RNA amplification by continuous-flow polymerase chain reaction and reverse transcription-polymerase chain reaction with cycle number selection. *Analytical Chemistry* **2003**, *75* (2), 288-295.

24. West, J.; Karamata, B.; Lillis, B.; Gleeson, J. P.; Alderman, J.; Collins, J. K.; Lane, W.; Mathewson, A.; Berney, H., Application of magnetohydrodynamic actuation to continuous flow chemistry. *Lab on a Chip* **2002**, *2* (4), 224-230.
25. Chen, Z. Y.; Qian, S. Z.; Abrams, W. R.; Malamud, D.; Bau, H. H., Thermosiphon-based PCR reactor: Experiment and modeling. *Analytical Chemistry* **2004**, *76* (13), 3707-3715.
26. Zhang, C. S.; Xu, J. L.; Ma, W. L.; Zheng, W. L., PCR microfluidic devices for DNA amplification. *Biotechnology Advances* **2006**, *24* (3), 243-284.
27. Beer, N. R.; Hindson, B. J.; Wheeler, E. K.; Hall, S. B.; Rose, K. A.; Kennedy, I. M.; Colston, B. W., On-chip, real-time, single-copy polymerase chain reaction in picoliter droplets. *Analytical Chemistry* **2007**, *79* (22), 8471-8475.
28. Kiss, M. M.; Ortoleva-Donnelly, L.; Beer, N. R.; Warner, J.; Bailey, C. G.; Colston, B. W.; Rothberg, J. M.; Link, D. R.; Leamon, J. H., High-Throughput Quantitative Polymerase Chain Reaction in Picoliter Droplets. *Analytical Chemistry* **2008**, *80* (23), 8975-8981.
29. El-Ali, J.; Perch-Nielsen, I. R.; Poulsen, C. R.; Bang, D. D.; Telleman, P.; Wolff, A., Simulation and experimental validation of a SU-8 based PCR thermocycler chip with integrated heaters and temperature sensor. *Sensors and Actuators a-Physical* **2004**, *110* (1-3), 3-10.

30. Liu, H. B.; Ramalingam, N.; Jiang, Y.; Dai, C. C.; Hui, K. M.; Gong, H. Q., Rapid distribution of a liquid column into a matrix of nanoliter wells for parallel real-time quantitative PCR. *Sensors and Actuators B-Chemical* **2009**, *135* (2), 671-677.
31. Craw, P.; Balachandran, W., Isothermal nucleic acid amplification technologies for point-of-care diagnostics: a critical review. *Lab on a Chip* **2012**, *12* (14), 2469-2486.
32. Notomi, T.; Okayama, H.; Masubuchi, H.; Yonekawa, T.; Watanabe, K.; Amino, N.; Hase, T., Loop-mediated isothermal amplification of DNA. *Nucleic Acids Research* **2000**, *28* (12), 7.
33. Mori, Y.; Nagamine, K.; Tomita, N.; Notomi, T., Detection of loop-mediated isothermal amplification reaction by turbidity derived from magnesium pyrophosphate formation. *Biochemical and Biophysical Research Communications* **2001**, *289* (1), 150-154.
34. Urdea, M., Penny, L.A., Olmsted, S.S., Giovanni, M.Y., Kaspar, P., Shepherd, A., Wilson, P., Dahl, C.A., Buchsbaum, S., Moeller, G., Burgess, D.C.H., Requirements for high impact diagnostics in the developing world. *Nature*: 2006; Vol. 444, pp 73-79.
35. Morens, D. M.; Folkers, G. K.; Fauci, A. S., The challenge of emerging and re-emerging infectious diseases. *Nature* **2004**, *430* (6996), 242-249.
36. Fauci, A. S., Infectious diseases: Considerations for the 21st century. *Clinical Infectious Diseases* **2001**, *32* (5), 675-685.

37. Foudeh, A. M.; Didar, T. F.; Veres, T.; Tabrizian, M., Microfluidic designs and techniques using lab-on-a-chip devices for pathogen detection for point-of-care diagnostics. *Lab on a Chip* **2012**, *12* (18), 3249-3266.
38. Lazcka, O.; Del Campo, F. J.; Munoz, F. X., Pathogen detection: A perspective of traditional methods and biosensors. *Biosensors & Bioelectronics* **2007**, *22* (7), 1205-1217.
39. Singh, R.; Das Mukherjee, M.; Sumana, G.; Gupta, R. K.; Sood, S.; Malhotra, B. D., Biosensors for pathogen detection: A smart approach towards clinical diagnosis. *Sensors and Actuators B-Chemical* **2014**, *197*, 385-404.
40. Fratamico, P. M., Comparison of culture, polymerase chain reaction (PCR), TaqMan Salmonella, and Transia Card Salmonella assays for detection of Salmonella spp. in naturally-contaminated ground chicken, ground turkey, and ground beef. *Molecular and Cellular Probes* **2003**, *17* (5), 215-221.
41. Gan, S. D.; Patel, K. R., Enzyme Immunoassay and Enzyme-Linked Immunosorbent Assay. *Journal of Investigative Dermatology* **2013**, *133* (9), E10-E12.
42. Toh, S. Y.; Citartan, M.; Gopinath, S. C. B.; Tang, T. H., Aptamers as a replacement for antibodies in enzyme-linked immunosorbent assay. *Biosensors & Bioelectronics* **2015**, *64*, 392-403.
43. Rodriguez-Lazaro, D.; D'Agostino, M.; Herrewegh, A.; Pla, M.; Cook, N.; Ikonomopoulos, J., Real-time PCR-based methods for detection of Mycobacterium avium

- Subsp paratuberculosis in water and milk. *International Journal of Food Microbiology* **2005**, *101* (1), 93-104.
44. Jofre, A.; Martin, B.; Garriga, M.; Hugas, M.; Pla, M.; Rodriguez-Lazaro, D.; Aymerich, T., Simultaneous detection of *Listeria monocytogenes* and *Salmonella* by multiplex PCR in cooked ham. *Food Microbiology* **2005**, *22* (1), 109-115.
45. Deisingh, A. K.; Thompson, M., Strategies for the detection of *Escherichia coli* O157 : H7 in foods. *Journal of Applied Microbiology* **2004**, *96* (3), 419-429.
46. Zhao, Y. X.; Chen, F.; Li, Q.; Wang, L. H.; Fan, C. H., Isothermal Amplification of Nucleic Acids. *Chemical Reviews* **2015**, *115* (22), 12491-12545.
47. Pan, X. Y.; Jiang, L.; Liu, K. Y.; Lin, B. C.; Qin, J. H., A microfluidic device integrated with multichamber polymerase chain reaction and multichannel separation for genetic analysis. *Analytica Chimica Acta* **2010**, *674* (1), 110-115.
48. Wang, H. Y.; Zhang, C. S.; Xing, D., Simultaneous detection of *Salmonella enterica*, *Escherichia coli* O157:H7, and *Listeria monocytogenes* using oscillatory-flow multiplex PCR. *Microchimica Acta* **2011**, *173* (3-4), 503-512.
49. Thaitrong, N.; Liu, P.; Briese, T.; Lipkin, W. I.; Chiesl, T. N.; Higa, Y.; Mathies, R. A., Integrated Capillary Electrophoresis Microsystem for Multiplex Analysis of Human Respiratory Viruses. *Analytical Chemistry* **2010**, *82* (24), 10102-10109.

50. Fang, X. E.; Liu, Y. Y.; Kong, J. L.; Jiang, X. Y., Loop-Mediated Isothermal Amplification Integrated on Microfluidic Chips for Point-of-Care Quantitative Detection of Pathogens. *Analytical Chemistry* **2010**, *82* (7), 3002-3006.
51. Liu, C. C.; Mauk, M. G.; Hart, R.; Qiu, X. B.; Bau, H. H., A self-heating cartridge for molecular diagnostics. *Lab on a Chip* **2011**, *11* (16), 2686-2692.
52. Ahmad, F.; Seyrig, G.; Turlousse, D. M.; Stedtfeld, R. D.; Tiedje, J. M.; Hashsham, S. A., A CCD-based fluorescence imaging system for real-time loop-mediated isothermal amplification-based rapid and sensitive detection of waterborne pathogens on microchips. *Biomedical Microdevices* **2011**, *13* (5), 929-937.
53. Liu, C. C.; Geva, E.; Mauk, M.; Qiu, X. B.; Abrams, W. R.; Malamud, D.; Curtis, K.; Owen, S. M.; Bau, H. H., An isothermal amplification reactor with an integrated isolation membrane for point-of-care detection of infectious diseases. *Analyst* **2011**, *136* (10), 2069-2076.
54. Wang, C. H.; Lien, K. Y.; Wang, T. Y.; Chen, T. Y.; Lee, G. B., An integrated microfluidic loop-mediated-isothermal-amplification system for rapid sample pre-treatment and detection of viruses. *Biosensors & Bioelectronics* **2011**, *26* (5), 2045-2052.
55. Kuswandi, B.; Nuriman; Huskens, J.; Verboom, W., Optical sensing systems for microfluidic devices: A review. *Analytica Chimica Acta* **2007**, *601* (2), 141-155.

56. Lee, S. H.; Cho, S. I.; Lee, C. S.; Kim, B. G.; Kim, Y. K., Microfluidic chip for biochemical reaction and electrophoretic separation by quantitative volume control. *Sensors and Actuators B-Chemical* **2005**, *110* (1), 164-173.
57. Hata, K.; Kichise, Y.; Kaneta, T.; Imasaka, T., Hadamard transform microchip electrophoresis combined with diode laser fluorometry. *Analytical Chemistry* **2003**, *75* (7), 1765-1768.
58. Rider, T. H.; Petrovick, M. S.; Nargi, F. E.; Harper, J. D.; Schwoebel, E. D.; Mathews, R. H.; Blanchard, D. J.; Bortolin, L. T.; Young, A. M.; Chen, J. Z.; Hollis, M. A., A B cell-based sensor for rapid identification of pathogens. *Science* **2003**, *301* (5630), 213-215.
59. Chinowsky, T. M.; Quinn, J. G.; Bartholomew, D. U.; Kaiser, R.; Elkind, J. L., Performance of the Spreeta 2000 integrated surface plasmon resonance affinity sensor. *Sensors and Actuators B-Chemical* **2003**, *91* (1-3), 266-274.
60. Yeatts, T., Forensics: Solving the Crime. The Oliver Press, Inc.: 2001; Vol. No. 9.
61. Watson, J. D.; Crick, F. H., Letters to Nature: molecular structure of nucleic acid. *Nature*: 1953; Vol. 171, p 738.
62. Jeffreys, A. J.; Wilson, V.; Thein, S. L., HYPERVARIABLE MINISATELLITE REGIONS IN HUMAN DNA. *Nature* **1985**, *314* (6006), 67-73.

63. Edwards, A.; Civitello, A.; Hammond, H. A.; Caskey, C. T., DNA TYPING AND GENETIC-MAPPING WITH TRIMERIC AND TETRAMERIC TANDEM REPEATS. *American Journal of Human Genetics* **1991**, 49 (4), 746-756.
64. Edwards, A.; Hammond, H.; Jin, L.; Caskey, C.; Chakraborty, R., Genetic variation at five trimeric and tetrameric tandem repeat loci in four human population groups. *Genomics*: 1992; Vol. 12, pp 241-253.
65. Pena, S. D. J.; Chakraborty, R.; Epplen, J. T.; Jeffreys, A. J., *DNA Fingerprinting: State of the Science ; Progress in Systems and Control Theory*. Birkhäuser Basel: 1993.
66. Butler, J. M., Genetics and genomics of core short tandem repeat loci used in human identity testing. *Journal of Forensic Sciences* **2006**, 51 (2), 253-265.
67. Gill, P.; Fereday, L.; Morling, N.; Schneider, P. M., The evolution of DNA databases - Recommendations for new European STR loci. *Forensic Science International* **2006**, 156 (2-3), 242-244.
68. Tan, S. C.; Yiap, B. C., DNA, RNA, and Protein Extraction: The Past and The Present. *Journal of Biomedicine and Biotechnology* **2009**, 10.
69. Stray JE, L. J., Brevnov MG, Shewale JG, Extraction of DNA from Forensic Biological Samples for Genotyping. *Forensic Science Review*: 2010; Vol. 22, pp 159-175.

70. Miller, S. A.; Dykes, D. D.; Polesky, H. F., A SIMPLE SALTING OUT PROCEDURE FOR EXTRACTING DNA FROM HUMAN NUCLEATED CELLS. *Nucleic Acids Research* **1988**, *16* (3), 1215-1215.
71. Valgren C, W. S., Hansson O, A comparison of three automated DNA purification methods in Forensic casework. *Forensic Science International: Genetics Supplement Series*: 2008; Vol. 1, pp 76-77.
72. Butler, J. M., *Fundamentals of forensic DNA typing*. Academic Press: 2009.
73. Lounsbury, J. A.; Coult, N.; Miranian, D. C.; Cronk, S. M.; Haverstick, D. M.; Kinnon, P.; Saul, D. J.; Landers, J. P., An enzyme-based DNA preparation method for application to forensic biological samples and degraded stains. *Forensic Science International-Genetics* **2012**, *6* (5), 607-615.
74. Moss, D.; Harbison, S. A.; Saul, D. J., An easily automated, closed-tube forensic DNA extraction procedure using a thermostable proteinase. *International Journal of Legal Medicine* **2003**, *117* (6), 340-349.
75. McCord, B. R.; McClure, D. L.; Jung, J. M., CAPILLARY ELECTROPHORESIS OF POLYMERASE CHAIN REACTION-AMPLIFIED DNA USING FLUORESCENCE DETECTION WITH AN INTERCALATING DYE. *Journal of Chromatography A* **1993**, *652* (1), 75-82.

76. McCord, B. R.; Jung, J. M.; Holleran, E. A., HIGH-RESOLUTION CAPILLARY ELECTROPHORESIS OF FORENSIC DNA USING A NON-GEL SIEVING BUFFER. *Journal of Liquid Chromatography* **1993**, *16* (9-10), 1963-1981.
77. <https://www.fbi.gov/about-us/lab/biometric-analysis/codis/rapid-dna-analysis>.
78. Gibson-Daw, G.; Albani, P.; Gassmann, M.; McCord, B., Rapid microfluidic analysis of a Y-STR multiplex for screening of forensic samples. *Analytical and Bioanalytical Chemistry* **2017**, *409* (4), 939-947.
79. Lagally, E. T.; Emrich, C. A.; Mathies, R. A., Fully integrated PCR-capillary electrophoresis microsystem for DNA analysis. *Lab on a Chip* **2001**, *1* (2), 102-107.
80. Kim, Y. T.; Lee, D.; Heo, H. Y.; Sim, J. E.; Woo, K. M.; Kim, D. H.; Im, S. G.; Seo, T. S., Total integrated slidable and valveless solid phase extraction-polymerase chain reaction-capillary electrophoresis microdevice for mini Y chromosome short tandem repeat genotyping. *Biosensors & Bioelectronics* **2016**, *78*, 489-496.
81. Schmidt, U.; Lutz-Bonengel, S.; Weisser, H. J.; Sanger, T.; Pollak, S.; Schon, U.; Zacher, T.; Mann, W., Low-volume amplification on chemically structured chips using the PowerPlex16 DNA amplification kit. *International Journal of Legal Medicine* **2006**, *120* (1), 42-48.
82. Sun, Y.; Kwok, Y. C.; Nguyen, N. T., A circular ferrofluid driven microchip for rapid polymerase chain reaction. *Lab on a Chip* **2007**, *7* (8), 1012-1017.

83. Lounsbury, J. A.; Landers, J. P., Ultrafast Amplification of DNA on Plastic Microdevices for Forensic Short Tandem Repeat Analysis. *Journal of Forensic Sciences* **2013**, *58* (4), 866-874.
84. Geng, T.; Novak, R.; Mathies, R. A., Single-Cell Forensic Short Tandem Repeat Typing within Microfluidic Droplets. *Analytical Chemistry* **2014**, *86* (1), 703-712.
85. Bienvenue, J. M.; Legendre, L. A.; Ferrance, J. P.; Landers, J. P., An integrated microfluidic device for DNA purification and PCR amplification of STR fragments. *Forensic Science International-Genetics* **2010**, *4* (3), 178-186.
86. Lounsbury, J. A.; Karlsson, A.; Miranian, D. C.; Cronk, S. M.; Nelson, D. A.; Li, J. Y.; Haverstick, D. M.; Kinnon, P.; Saul, D. J.; Landers, J. P., From sample to PCR product in under 45 minutes: a polymeric integrated microdevice for clinical and forensic DNA analysis. *Lab on a Chip* **2013**, *13* (7), 1384-1393.
87. Gan, W. P.; Zhuang, B.; Zhang, P. F.; Han, J. P.; Li, C. X.; Liu, P., A filter paper-based microdevice for low-cost, rapid, and automated DNA extraction and amplification from diverse sample types. *Lab on a Chip* **2014**, *14* (19), 3719-3728.
88. Liu, P.; Yeung, S. H. I.; Crenshaw, K. A.; Crouse, C. A.; Scherer, J. R.; Mathies, R. A., Real-time forensic DNA analysis at a crime scene using a portable microchip analyzer. *Forensic Science International-Genetics* **2008**, *2* (4), 301-309.
89. Hopwood, A. J.; Hurth, C.; Yang, J. N.; Cai, Z.; Moran, N.; Lee-Edghill, J. G.; Nordquist, A.; Lenigk, R.; Estes, M. D.; Haley, J. P.; McAlister, C. R.; Chen, X.; Brooks,

C.; Smith, S.; Elliott, K.; Koumi, P.; Zenhausern, F.; Tully, G., Integrated Microfluidic System for Rapid Forensic DNA Analysis: Sample Collection to DNA Profile. *Analytical Chemistry* **2010**, *82* (16), 6991-6999.

90. Reedy, C. R.; Price, C. W.; Sniegowski, J.; Ferrance, J. P.; Begley, M.; Landers, J. P., Solid phase extraction of DNA from biological samples in a post-based, high surface area poly(methyl methacrylate) (PMMA) microdevice. *Lab on a Chip* **2011**, *11* (9), 1603-1611.

91. LaRue, B. L.; Moore, A.; King, J. L.; Marshall, P. L.; Budowle, B., An evaluation of the RapidHIT (R) system for reliably genotyping reference samples. *Forensic Science International-Genetics* **2014**, *13*, 104-111.

92. L. K. Hennessy, H. F., Y. Li, J. Buscaino, K. Chear, J. Gass, N. Mehendale, S. Williams, S. Jovanovich, D.; 2 3 Harris, K. E., W. Nielsen, Developmental validation studies on the RapidHIT^M Human DNA identification system. *Forensic Science International: Genetics Supplement Series* **2013**, *4* (1), e7-e8.

93. Verheij, S.; Harteveld, J.; Sijen, T., A protocol for direct and rapid multiplex PCR amplification on forensically relevant samples. *Forensic Science International-Genetics* **2012**, *6* (2), 167-175.

94. Vallone, P.,

http://www.cstl.nist.gov/strbase/pub_pres/Vallone_BCC_Talk_Sept2013.pdf.

95. Asogawa, M., Sugisawa, M., Aoki, K., Hagiwara, H., Mishina, Y., Yamashita, S., Yamada, Y., Development of portable and rapid human DNA analysis system aiming on-site screening. *Twelfth International Conference on Miniaturized Systems for Chemistry and Life Sciences (MicroTAS)*: 2008.
96. Le Roux, D.; Root, B. E.; Hickey, J. A.; Scott, O. N.; Tsuei, A.; Li, J. Y.; Saul, D. J.; Chassagne, L.; Landers, J. P.; de Mazancourt, P., An integrated sample-in-answer-out microfluidic chip for rapid human identification by STR analysis. *Lab on a Chip* **2014**, *14* (22), 4415-4425.
97. Le Roux, D.; Root, B. E.; Reedy, C. R.; Hickey, J. A.; Scott, O. N.; Bienvenue, J. M.; Landers, J. P.; Chassagne, L.; de Mazancourt, P., DNA Analysis Using an Integrated Microchip for Multiplex PCR Amplification and Electrophoresis for Reference Samples. *Analytical Chemistry* **2014**, *86* (16), 8192-8199.

Development of a novel bead aggregation assay for detection of LAMP amplicons

2.1 Overview

DNA-paramagnetic silica bead aggregation in a rotating magnetic field (RMF) facilitates the quantification of DNA with femtogram sensitivity, but yields no sequence-specific information.¹ Described herein is the use of bead aggregation inhibition for the detection of DNA and RNA in a sequence-specific manner following loop-mediated isothermal amplification (LAMP). The fragments generated via LAMP fail to induce chaotrope-mediated bead aggregation; however, due to their ability to passivate the bead surface, they effectively inhibit bead aggregation by longer trigger DNA. We demonstrate the utility of aggregation inhibition as a method for the detection of bacterial and viral pathogens with sensitivity that approaches single copies of the target. We successfully apply this methodology to the detection of notable food-borne pathogens *Escherichia coli* O157:H7 and *Salmonella enterica*, as well as Rift Valley fever virus, a weaponizable virus of national security concern. We also show the concentration dependence of aggregation inhibition, suggesting the potential for quantification of target nucleic acid in clinical and environmental samples.

2.2 Introduction

Pathogenic microorganisms represent a substantive threat to human and animal health and safety, making the detection of such organisms of paramount importance. Conventional methods for pathogen detection, such as culture and colony counting

methods, nucleic acid amplification testing, and immunoassays are effective, but often time-consuming and dependent on expensive laboratory equipment. Cell culture and colony counting has long served as the gold standard for pathogen detection, despite the excessive time consumption required. Cell cultivation can require at least 3-4 days for preliminary results, and upwards of 7 days to have a final confirmatory result.² Selective media can be used to detect specific pathogens and detection is most often carried out using optical methods.³

Nucleic acid amplification tests (NAAT) are a fundamental tool of molecular biology, and involve generating many copies of short nucleic acid sequences. Polymerase chain reaction (PCR) is a technique for nucleic acid amplification developed by Mullis in the mid 1980s⁴; it was the first NAAT, and remains the most popular to this day.⁵ Over the years, there have been several PCR methods developed for pathogen detection, including: real-time PCR⁶, multiplex PCR⁷, and reverse transcriptase PCR.⁸ While PCR relies on thermal cycling to produce amplicons, isothermal amplification produces nucleic acid sequences at a constant temperature, and various isothermal amplification techniques have been developed since the early 1990s to serve as alternatives to PCR.⁵ Regardless of variable or constant temperature control, the largest drawback to NAAT methods is the requirement for downstream detection of the amplicons produced, as these methods often rely on fluorescence or gel electrophoresis, which can be cumbersome and expensive.

The most common type of immunology-based method for pathogen detection is the enzyme-linked immunosorbent assay (ELISA). This method utilizes the basic

concept of an antigen binding to a specific antibody, allowing for low-level detection of multiple antigens, including: proteins, peptides, and hormones.⁹ The assay usually consists of a target (antigen), an antibody to capture the antigen, and a detection antibody that will produce a signal in the presence of the target antigen.¹⁰ Despite the high degree of sensitivity afforded by the ELISA method, the high cost and batch-to-batch variability in the production of monoclonal antibodies are significant challenges that must be addressed.

As stated, current methods for the detection of pathogenic microorganisms are effective, but often time-consuming and dependent upon expensive laboratory equipment and highly trained personnel. Most commonly, the expense of the instrumentation is due to the requirement for fluorescence detection (which is often laser-induced) or for rapid thermal cycling.^{11,12} To facilitate using NAATs that preclude detection of fluorescence, there is a need for new analytical platforms for amplicon detection. Standard methods for NAAT, including PCR, nucleic acid sequence-based amplification (NASBA), and loop-mediated isothermal amplification (LAMP), have proven incredibly sensitive and specific for detection of microbial pathogens. However, in order to be portable and cost-effective in a point-of-care (POC) setting, an alternative to these methods is needed for detection of amplicons generated using NAATs.

Molecular diagnostic-based detection and characterization of microbial pathogens is of immense utility for emerging diseases, which include multi-drug resistant bacteria and rapidly mutating viruses capable of evading the immune response.¹³⁻¹⁶ Although NAAT methods share similar processes for generation of nucleic acid sequence-specific

amplicons, the technique of efficient amplicon detection is fundamental to whether this can be done in a portable and cost-effective manner. Several groups have successfully demonstrated NAAT microdevices for pathogen detection. For example, Pan et al. demonstrated an integrated device for parallel genetic analysis and detection of hepatitis B virus (HBV), *Mycobacterium tuberculosis* (MTB), and genotyping of human leucocyte antigen (HLA-B27).¹⁷ The device consists of three main functional units, including: temperature control, multiplex PCR, and multi-channel separation. A unique isothermal microdevice for the detection of *E. coli* in urine was developed by Liu et al., and the heat source was provided by a water-activated, self-heating, polymeric cartridge.¹⁸ Although both devices are capable of pathogen detection, the cost associated with fluorescence detection remains a distinct disadvantage.

Here, the focus is on the utilization of paramagnetic silica beads, developed for nucleic acid isolation and image analysis, as a replacement for fluorophores or fluorophore-quenching probes. By eliminating complicated wavelength specific optical detection and thermal cycling equipment we abrogate the necessity for expensive and cumbersome instrumentation. We propose that Product-inhibited Bead Aggregation (PiBA) represents the potential for rapid and robust detection of pathogen-specific amplicons at a fraction of the cost of conventional methods. We apply this technology to the detection of food-borne pathogens, including *E. coli* and *Salmonella*, Rift Valley fever virus (RVFV), a weaponizable RNA virus of national security concern, and human-specific DNA via the thyroid peroxidase (TPOX) gene.

Demonstrated here is the sequence-specific detection of both DNA and RNA from human, bacterial, and viral sources with a detection platform that requires only a rudimentary heat source, an inexpensive camera, and a simple computer algorithm. The description of PiBA as the inhibition of chaotropic nucleic acid-induced bead aggregation is the core concept behind this novel detection modality. This method exploits the original use of an existing reagent (paramagnetic beads) to effectively circumvent the need for expensive fluorophores or dual-labeled probes. The detection of bead aggregation inhibition involves analysis of an image captured by a camera; inexpensive and portable when compared to the hardware required for laser-induced fluorescence detection and thermal cycling. DNA and RNA target amplification is driven by LAMP. This multi-primer amplification system provides exquisite target specificity and low copy number target sensitivity without the complexities of thermal cycling and fluorophore detection.

By coupling the PiBA assay to LAMP, we demonstrate that the requirement for thermal cycling is eliminated, and the assay can effectively be performed on a simple heat block or water bath. The simplicity of both heat control and optical detection makes this technology suitable for resource-limited and rural settings that lack access to important clinical diagnostic facilities.

2.3 Materials and Methods

2.3.1 LAMP/RT-LAMP protocol

All LAMP primer sequences and amplification temperatures can be found in Table S4. Primers were purchased from Eurofins MWG Operon. Reactions were carried out using a LoopAmp DNA Amplification Kit and a LoopAmp RNA Amplification Kit (Eiken Chemical Co., Ltd. Tokyo, Japan). For all reactions the following amounts of primers were used: 5 pmol each of F3 and B3, 20 pmol each LF and LB, and 40 pmol each of FIP and BIP. Positive and negative controls were included in each run. For primers designed in-house, LAMP PrimerExplorer V4 software was used (<http://primerexplorer.jp/elamp4.0.0/index.html>; Eiken Chemical Co., Ltd. Tokyo, Japan).

2.3.2 DNA/RNA extraction

2.5.2.1 Human and animal

DNA was extracted from human and animal blood for TPOX amplification using a QIAamp DNA mini kit (Qiagen, Netherlands) according to manufacturer protocol. Animal samples were provided by the University of Virginia Center for Comparative Medicine in accordance with the University of Virginia Institutional Animal Care and Use Committee (ACUC). Blood collection was specifically approved by the UVA ACUC for diagnostic and research purposes under the animal protocol used in this study. Blood was collected from the following animals: pig, ferret, rabbit, rat, and mouse. Human samples were de-identified, prior to the authors receiving them, and scheduled for discard by the University of Virginia Medical Laboratories. All samples were stored at -20°C until use.

2.3.2.2 *Bacteria*

E. coli cultures were grown overnight in LB media (Fisher Scientific) with antibiotics to an O.D.600 of approximately 1.5. Strains EDL933, 86-24, TW14359, and O42 were grown with streptomycin (Sigma-Aldrich), final concentration 100 µg/mL. Strain O127 (E2348/69) was grown in nalidixic acid (Sigma-Aldrich), final concentration 100µg/mL. Strain 86-24 was isolated from a patient in 1986¹⁹, strain O42 was isolated from an infected patient in 1983²⁰, strain O127 was isolated from a case of infantile diarrhea in 1969²¹, strain TW14359 was isolated from a spinach outbreak in 2006²², and strain EDL933 was isolated from raw hamburger (ground beef) implicated with outbreaks in 1982.²³ These samples were generously provided by Dr. Kendall at the University of Virginia. DNA was extracted using 1mL of culture and a GenElute Bacterial Genomic DNA Kit (Sigma Aldrich, St. Louis, MO). Genomic DNA was eluted with water and allowed to sit for five minutes prior to centrifugation. All samples were stored at -20°C until use.

2.3.2.3 *Virus*

Rift Valley fever virus (RVFV) strain MP12, a recombinant vaccine strain (arMP12), was generated using an RVFV reverse-genetics system and then passaged in Vero cells. The vaccine strain was originally derived from the RVFV ZH548 strain that had been isolated in 1977 from a patient with uncomplicated RVFV.²⁴ These samples were generously provided by the University of Texas Medical Branch, Galveston, TX. The Venezuelan Equine Encephalitis Virus (VEEV) strain TC83 was obtained from BEI Resources (NR63). VEEV TC83 was propagated by infecting Vero cells at 80-90%

confluence at an MOI of 0.1 in supplemented media. Influenza A/California/04/09 and Influenza B/Taiwan/2/62 strains of Influenza viruses were obtained from BEI Resources. Influenza viruses were propagated by infecting MDCK cells at 80-90% confluence at an MOI of 0.1 in Influenza Growth Media (DMEM supplemented with 1% bovine serum albumin, 1% non-essential amino acids, 1% L-glutamine, and 1% penicillin/streptomycin). TPCK-treated trypsin from bovine pancreas (Sigma-Aldrich) was added to the Influenza Growth Media at a final concentration of 200 ng/mL. Viral titers were determined by plaque assays as previously described.²⁵⁻²⁷

Viral RNA was isolated from cell-free viral supernatants using Trizol LS according to manufacturer's recommendations (Life Technologies, Inc.) and DNase treated. RNA quantification was performed using the Quant-iT™ RiboGreen® RNA assay (Invitrogen) using the DTX 880 Multimode Detector plate reader (Beckman Coulter). The concentration of the sample was determined using the Multimode Analysis software (Version 3.3.09). All samples (RVFV and the four blinded RNA samples) were then diluted to 5E+07 genomic copies/5 µL. The final concentration (in g/µL) for 5E+07 genomic copies per 5µL was determined by multiplying the mass of the genome (1.6E-17 for RVFV; L, M, and S segment genome sizes are added together) by the genomic copies wanted (5E+07), then dividing the number by 5µL. The final volume for 5E+07 per 5µL was determined by multiplying the stock sample concentration by the stock sample volume, then dividing the number by the concentration wanted (for RVFV, 0.16 ng/µL for 5E+07 genomic copies per 5µL). Total RNA was extracted from mock-infected (media containing no virus) and MP12 infected Vero cells using RNeasy Mini Kit

(Qiagen). RNA quantification was performed using the NanoDrop™ 2000 Spectrophotometer (Thermo Scientific).

2.3.3 Quantitative real-time PCR

For RVFV and VEEV samples, qRT-PCR with viral specific primers and TaqMan fluorogenic probes was performed using RNA UltraSense One-Step Quantitative RT-PCR System (Life Technologies) as previously described. For Influenza A and Influenza B samples, qRT-PCR with viral specific primers (Figure S12) was performed using the SYBR® green real-time PCR System (Life Technologies).

2.3.4 Reagent preparation

30 μ L of stock Magnesil beads (purchased from Promega, Madison, WI) were washed three times with guanidine hydrochloride (GdnHCl) solution (8M, 1X TE, adjusted to pH 6.1 with 100 mM MES) and resuspended in a total volume of 1000 μ L GdnHCl solution.

2.3.5 PiBA

The following was added to each 20 μ L well: 13 μ L of GdnHCl solution, 4 μ L stock Magnesil beads, 2 μ L LAMP sample, 0.5 μ L pre-purified human genomic DNA ('trigger' DNA, 1.0 ng/ μ L, purchased from Promega). Mixture was exposed to a RMF at 2200 rpm for 5 min and vortexer was used at ~500 rpm to agitate the samples during assay. Images of microwells were captured using a Canon Rebel EOS Rebel T1i, 15.1-megapixel camera. Image files were processed using an isodata algorithm written in Mathematica software.

2.4 Results and Discussion

2.4.1 Microbead aggregation

It has long been established that DNA released from lysed cells binds to silica beads in the presence of a chaotropic salt (e.g., guanidine). The interaction between DNA and the silica surface is thought to be entropically driven, and this phenomenon is the basis for most commercial DNA

purification kits used today.²⁸⁻³¹

However, under the same chaotropic conditions in a RMF, paramagnetic silica beads are aggregated by DNA, with the extent of aggregation quantitatively linked to the mass of DNA present, a phenomenon referred

to as the ‘pinwheel effect’ (**Figure 2-1**).¹ The entanglement that leads to DNA-bead aggregation requires a

threshold DNA length >10 Kb, and since most DNA released from cells under denaturing conditions is close to full length, direct quantification is possible using this method. This technique can be used directly on crude samples (e.g., whole blood) whereby DNA mass can be quantified and used as a new method for cell counting.³²

Shorter fragments (<3 Kb), however, fail to induce aggregation, being physically too short to entangle the micron-scale beads. While smaller beads (400 nm) have an

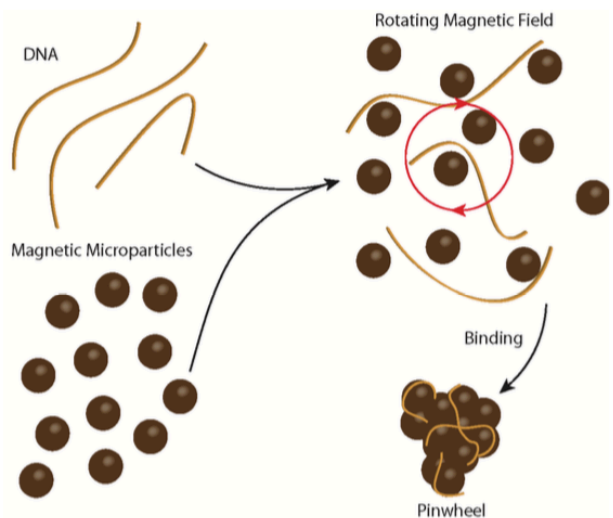


Figure 2-1. Proposed mechanism for chaotrope-induced aggregation (CIA). Long strands of DNA bind to silica-coated magnetic beads in a chaotropic environment. Aggregation is induced using a rotating magnetic field, and visible aggregates are formed. Figure taken from Leslie et al.

increased tolerance for shorter DNA, fragments <5 Kb are still problematic. NAAT assays generate DNA amplicons <1 Kb in order to facilitate assay speed with specificity, therefore, it is not possible to use bead aggregation as a detection mode for these short sequences.¹

The inability of short double-stranded nucleic acid fragments to induce entanglement and, subsequently, aggregation, does not mean that these shorter DNA fragments will not bind to the silica bead surface. In fact, there is significant literature that supports this ionic interaction phenomenon.^{33, 34} In order to test this theory, RT-LAMP product (positive and negative, target: RVFV) was spiked into microwells containing silica-coated beads and trigger DNA. Trigger DNA refers to long strands of

human genomic DNA that would induce aggregation of the beads under normal, chaotropic conditions in the presence of a RMF.

Figure 2-2 shows the results from this experiment, with a visual

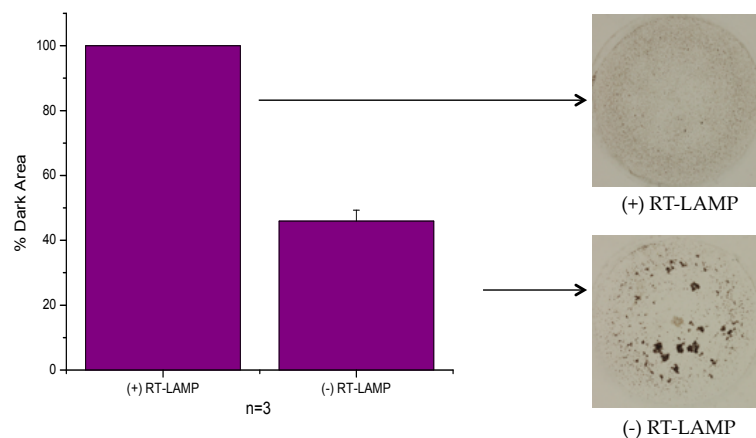


Figure 2-2. Magnesil beads used to detect presence of positive and negative RT-LAMP product. Inverse effect of CIA is seen with RT-LAMP product where the negative causes aggregation and the positive remains dispersed in the presence of a RMF and trigger DNA.

aggregate forming in the microwell containing the (-) RT-LAMP product, and complete dispersion of the beads in the microwell containing the (+) RT-LAMP product. % Dark area (% DA) refers to the percentage of pixels that are dark in the cropped image of the microwell (high % DA corresponds to dispersed beads and low % DA corresponds to

aggregated beads). This phenomenon is the inverse of what is seen with chaotrope-induced aggregation as described previously.

2.4.2 Specificity of response and concentration effect

In order to test the specificity of this inverse response, RT-LAMP was performed using correct template (RNA control provided in LoopAmp RT-LAMP kit), incorrect (in this case, viral) template, and no template (negative). These samples were then probed for the extent of aggregation inhibition (AI) in the presence of trigger DNA. As shown in **Figure 2-3**, the response remains specific for the correct template nucleic acid. When incorrect template is introduced into the RT-LAMP amplification, no product is generated, therefore failing to inhibit aggregation, whereas the correct template amplifies and produces short amplicons that inhibit aggregation.

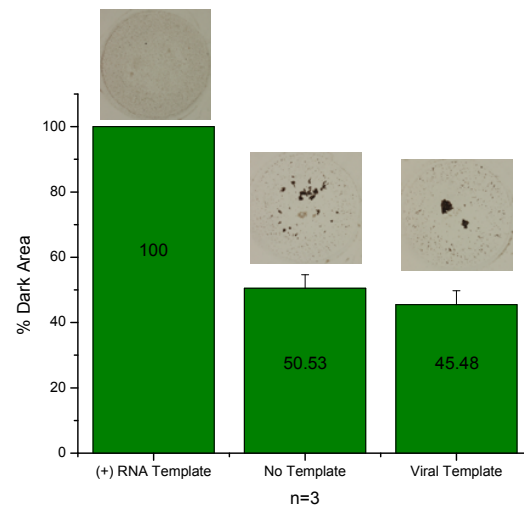


Figure 2-3. Testing specificity of inverse response for correct template. Positive RNA template is the correct template for the given primer set. Viral template is incorrect template for primers and therefore should not amplify. Results show that inverse response is specific for the correct template for a given set of primers.

The effect of RT-LAMP product concentration was also tested in order to determine if there was a quantitative aspect to the assay. **Figure 2-4** shows the dilution of a sample of RT-LAMP product compared to a control sample (human genomic DNA, set to 100% aggregation). The % Aggregation for a sample containing only (+) RT-

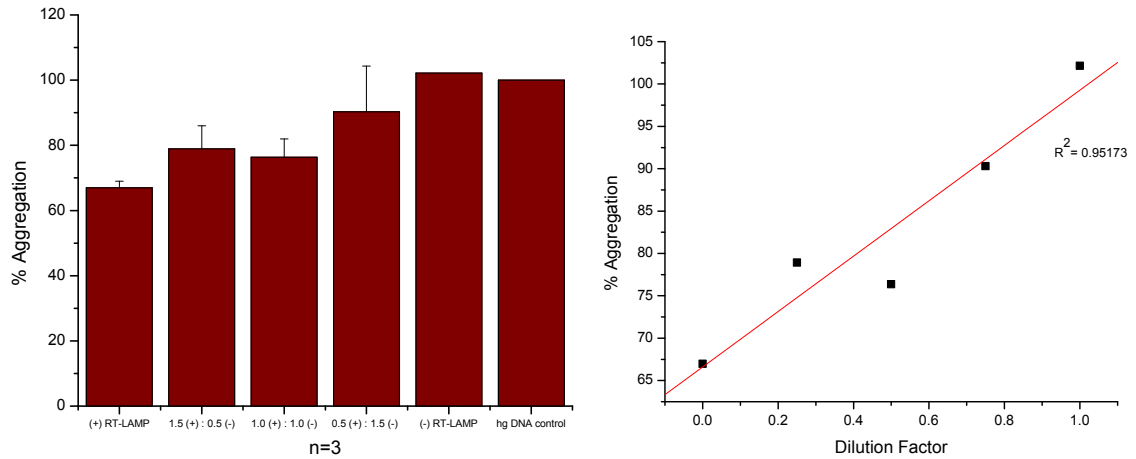


Figure 2-4. Concentration effect on aggregation inhibition. Concentration of LAMP product was varied to determine if the extent of aggregation inhibition changes accordingly. Human genomic DNA used as 100% aggregation control.

LAMP product is around 65%, and this number increases as the sample is further diluted with (-) RT-LAMP product. Accordingly, the sample containing only (-) RT-LAMP product is almost fully aggregated. To further prove out this effect, the extent of aggregation inhibition was demonstrated over the course of the RT-LAMP amplification reaction. As with PCR, the LAMP amplification proceeds exponentially.³⁵ To test

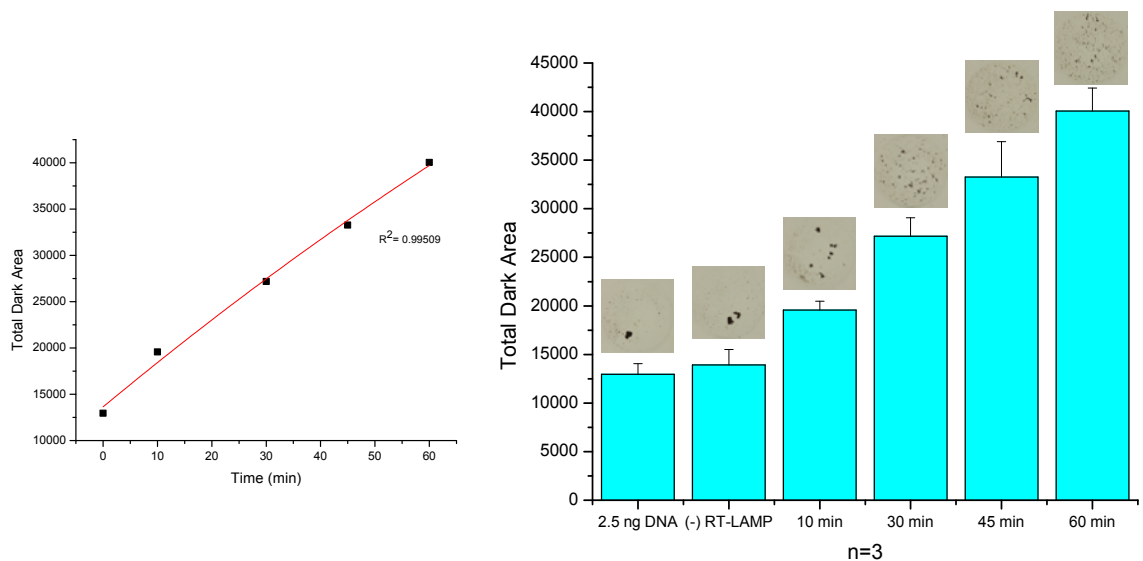


Figure 2-5. Extent of aggregation inhibition varies over the course of the RT-LAMP reaction. Tubes were pulled from various time points during the reaction and probed for AI. Total dark area increases as AI increases.

whether PiBA could be used to monitor the production of RT-LAMP product in a temporal manner, tubes were removed from the heat source at various time points during the amplification. **Figure 2-5** shows the results from this experiment, with the total dark area increases as the reaction proceeds (i.e., the more product present, the more inhibited the aggregation becomes and therefore the higher the dark area).

2.4.3 Proof of concept

The proposed mechanism of action for PiBA is shown in **Figure 2-6**, whereby the short fragments generated by RT-LAMP or LAMP (depending on RNA or DNA template, respectively) bind to and coat the surface of the magnetic beads in a chaotropic environment. When trigger DNA is introduced, it can no longer access the surface of the magnetic beads, and therefore in the presence of a RMF, the trigger DNA no longer induces aggregation (i.e., aggregation is inhibited). In this way, the presence of aggregation signals a failed LAMP amplification (i.e., the target was not present) and the

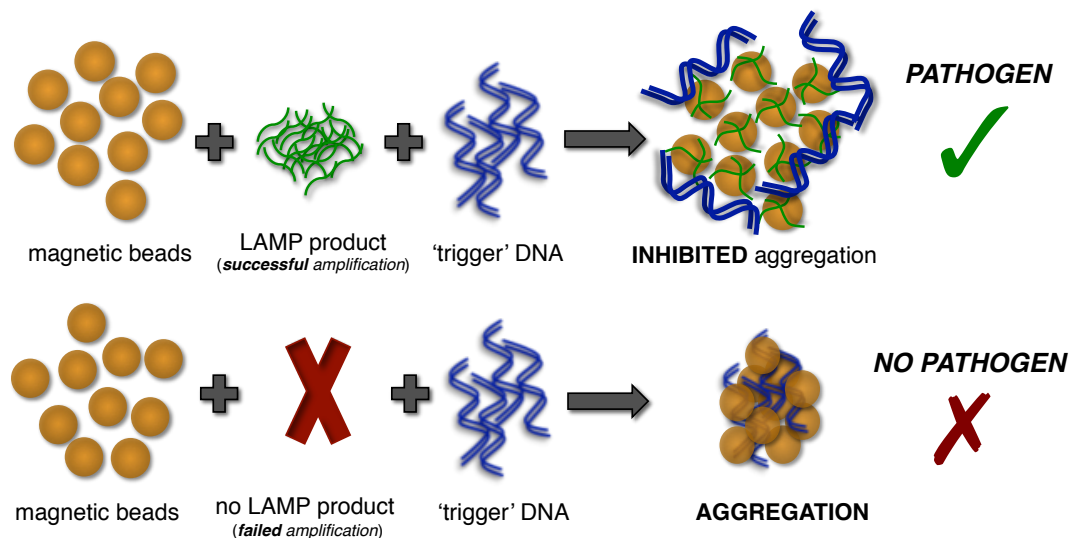


Figure 2-6. Schematic of proposed PiBA mechanism. LAMP product is added to a sample of magnetic beads. If the amplification was successful, the presence of short fragments of the target sequence inhibits aggregation by trigger DNA.

absence of aggregation (the dispersion of the beads) signals a successful LAMP amplification.

Figure 2-7 shows the result of measuring the impact that an abundance of shorter DNA fragments has on the ability of full length DNA to induce microbead aggregation. As expected, the LAMP product alone failed to induce bead aggregation as a result of

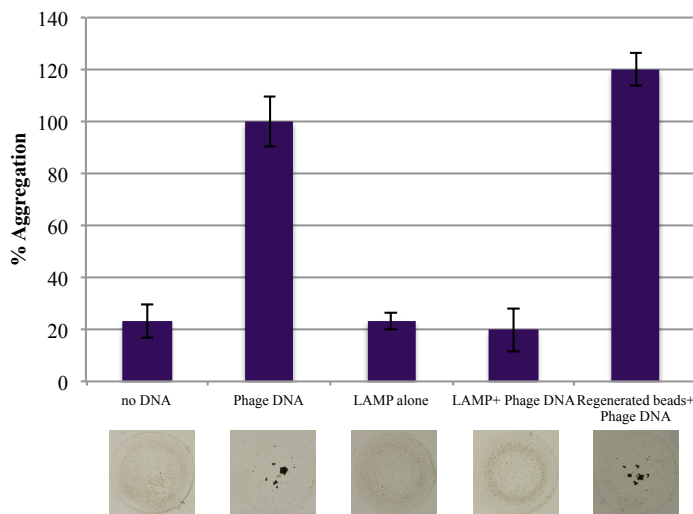


Figure 2-7. PiBA proof-of-feasibility. Results suggesting LAMP product is too short to induce bead aggregation, but still capable of binding to silica surface of beads and inhibiting aggregation by 'trigger' DNA.

inadequate length. More importantly, in the presence of the LAMP products, λ -phage trigger DNA (~48 Kb) fails to induce bead aggregation. This supports our theory that small DNA fragments bind avidly to the silica surface and prevent the binding of very long double-stranded DNA

fragments that would normally aggregate the beads. When these same beads are "cleansed" of the small double-stranded fragments by elution of bound DNA with TE buffer, exposure anew to λ -phage DNA results in bead aggregation, indicating the integrity of the beads for DNA binding. It is worth noting that λ -phage DNA was set as '100% Aggregation' for these experiments and that the regenerated beads+ phage DNA, as well as the human DNA, both aggregated more than the sample of λ -phage DNA. For this reason, human genomic DNA was used to normalize the data (i.e., set to 100% Aggregation) presented in the remainder of the experiments described herein.

The data shown in Figure 2-7 supports the theory that the inhibition of bead aggregation by full length DNA could be an indicator of the presence of an inhibiting concentration of smaller DNA fragments. These fragments effectively compete for a limited number of ionic binding sites on the beads in a non-specific manner with regard to DNA sequence. However, the specificity of LAMP in generating double-stranded DNA fragments is known to be high, owing to multiple primers (no fewer than 6) required for successful product amplification,³⁵ thus it is the inhibition of bead aggregation by trigger DNA that we propose as a new detection modality based on the non-specific binding competition mechanism. Here, if the smaller fragments of DNA have occupied the binding sites on the beads, full length DNA cannot lash together

adjacent beads to induce aggregation. In other words, a standard trigger DNA is used to probe the susceptibility of the silica beads to DNA-induced aggregation. This non-specific stoichiometric competitive binding is further demonstrated in **Figure 2-8** where DNA from a variety of different sources

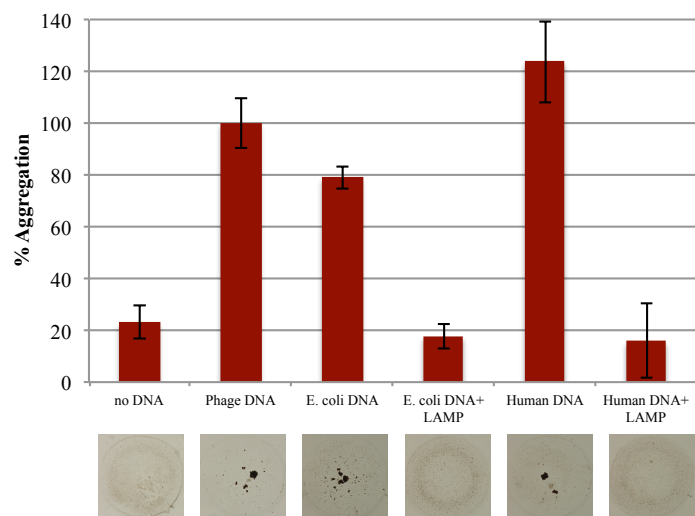


Figure 2-8. Various types of trigger DNA. *PiBA* was tested using different trigger DNA to determine if aggregation inhibition is seen. LAMP product induced AI in presence of three types of trigger DNA.

readily aggregates the beads, but aggregation is consistently inhibited by the presence of LAMP product, supporting the proposed binding competition mechanism. This indicates

that (LAMP) fragments, amplified as a result of the presence of a specific nucleic acid target, can be readily detected by inhibition of trigger DNA-induced bead aggregation.

2.4.4 Image analysis

We sought to evaluate the utility of PiBA for the detection of DNA and RNA targets specific to a select group of infectious pathogens. In order to accomplish this, aggregation controls had to be established for each target: negative, with no template nucleic acid, and positive, with template for a known target. **Figure 2-9A-B** shows how the optical images are first analyzed, using a Mathematica algorithm, in terms of “%

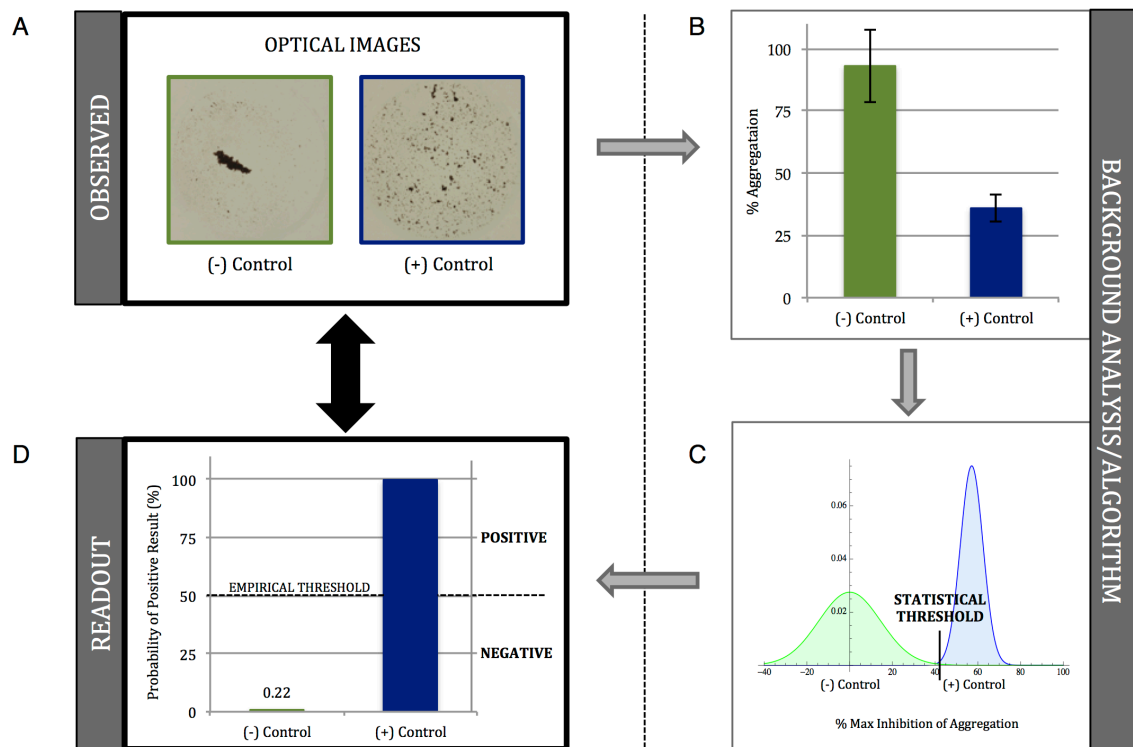


Figure 2-9. Statistical and empirical (visual) thresholds for PiBA. A) Optical images of (+/-) Controls. B) Graph of “% Aggregation”, error bars represent standard deviation, $n=3$. C) Probability distribution functions (PDF) calculated for (+/-) Controls. Threshold set as $[\mu-3\sigma]$ for (+) Control. X axis shows “% Maximum Inhibition of Aggregation”, (-) Control set as “0%”. D) Graphical representation of PDF. “Probability of Positive Result” represents likelihood of value to cross the calculated statistical threshold. Empirical threshold serves as visual representation of (+/-) results. For all data represented, the empirical threshold is set at 50%. Values above this threshold are considered positive and values below are considered negative.

Aggregation” based on the total number of dark pixels present. In this algorithm, dispersed beads, as well as bead aggregates, are counted as “dark”, and areas devoid of beads are counted as “bright”. In this manner, the number of pixels in an image can be used as a measure of aggregation.¹ The negative control is then used to normalize the data to “% Inhibition of Aggregation” by setting it to 0%. The probability distribution function (PDF) of the positive control is plotted and the statistical threshold is set as 3 times the standard deviation of the mean value (**Figure 2-9C**). A second Mathematica algorithm then analyzes the PDF of each piece of data and calculates the probability of any given curve crossing over the statistical threshold. Results are presented as “% Probability of Positive Result” simply for ease of interpretation so that a Yes/No, qualitative answer is immediately evident when looking at the data (**Figure 2-9D**). Since this analysis uses both the sample mean and standard deviation in the probability distribution function, error bars are absent in these plots. A visual threshold is determined empirically for ease of result interpretation, and this is shown as 50% for all data presented. Any sample above this threshold is considered positive, while any sample below is considered negative for the target of interest.

2.4.5 Food-borne pathogen detection

Pathogen detection in the food industry is important due to the potentially disastrous consequences of failing to detect certain bacteria, and the ensuing public health crisis.^{16, 36} The Centers for Disease Control (CDC) estimates that food-borne pathogens account for roughly 128,000 hospitalizations and 3,000 deaths each year in America. *Escherichia coli* alone causes approximately 73,000 cases of diarrheal illness in the U.S.

each year and further life-threatening complications, including hemolytic uremic syndrome (HUS), occur in about 4% of these cases.³⁷ Additionally, studies have shown that as few as 10-100 *E. coli* cells are enough to cause infection in humans.^{37, 38}

To address this, we wanted to explore the potential utility of this approach for detecting food-borne infectious agents, specifically, *E. coli*, *Salmonella*, and *Listeria*. A set of eight unique LAMP primers (**Figure 2-10**) was used to target sequences in the shiga toxin 2 (*stx2*) gene of *E.*

coli O157:H7, strain EDL933 isolated from ground beef associated with the 1982 *E. coli* outbreak in Michigan.³⁹

Using these to evaluate specificity, **Figure 2-11A**

shows the clear-cut detection of *E. coli* O157:H7; no aggregation inhibition was seen

Primer	Length	Sequence (5' - 3')
stx2 F3	20	CGCTTCAGGCAGATACAGAG
stx2 B3	19	CCCCCTGATGATGGCAATT
stx2 F2	20	GTCAGGCACTGTCTGAAACT
stx2 F1c	21	TTCGCCCCAGTTCAGAGTGA
stx2 B2	19	CAGTCCCAGTATCGCTGA
stx2 B1c	21	TGCTCCGGAGTATCGGGGAG
stx2 LF	22	GCGTCATCGTATACACAGGAGC
stx2 LB	22	GATGGTGTCTCAGAGTGGGGAGAA

Figure 2-10. LAMP primer sequences and amplification temperature for *E. coli* O157:H7 strain EDL933, shiga toxin 2 (*stx2*) gene. Primers were designed using Primer Explorer software and optimized for temperatures between 61-65°C.

with *Salmonella* or *Listeria* template. The specificity of PiBA was further evaluated by testing the same samples with a primer set specific for target sequences in the Invasion A (*invA*) gene of *Salmonella* (**Figure 2-11B**). Again, only the target organism of interest (in this case, *Salmonella*) showed dramatic aggregation inhibition, indicating that PiBA is specific for the bacterial pathogens of interest. In both cases, with both *E. coli* and

Salmonella primers, there is no non-specific amplification of off-target bacterial species, and 200 genomic copies of each target were used for amplification.

Having shown (at least with the targets tested) that PiBA had the desired specificity for infectious pathogen detection, the sensitivity of the assay was evaluated

using the primer set specific for *E.*

coli O157:H7 stx2 gene sequence.

Solutions prepared through serial

dilution provided starting template

concentrations that varied from 2 to

a high of 2000 genomic copies (per

amplification reaction). **Figure 2-**

12 shows that the aggregation

inhibition with template

concentrations from 2000 copies

down to 20 copies was unequivocal.

At a template concentration of 2

copies, significant aggregation

inhibition was observed in 2 of 3

analyses. As expected, further dilution to less than 1 copy per reaction (0.2 copies)

produced no observable aggregation inhibition. Thus, we conclude that the limit of

detection lies around 20 starting copies of genomic DNA. Research has shown that *E.*

coli contains approximately 4 genomic copies/cell⁴⁰; therefore, the findings are

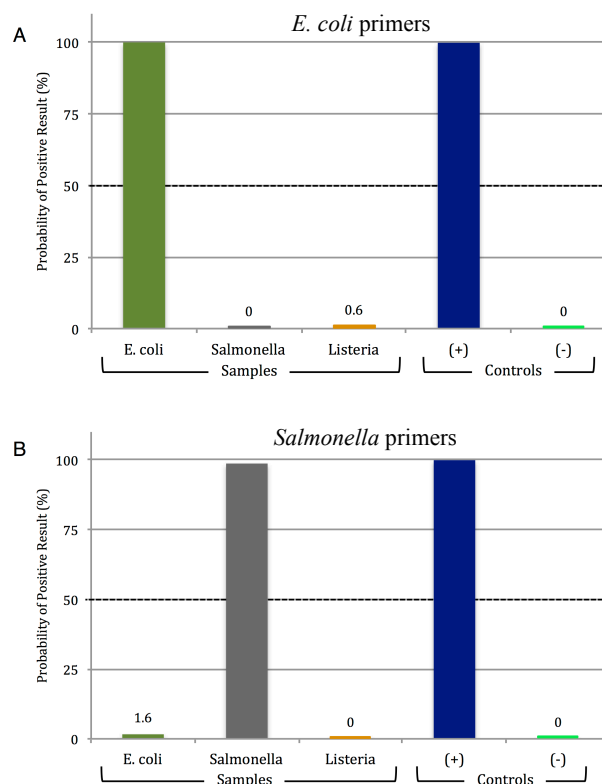


Figure 2-11. PiBA for food-borne pathogen detection. A) PiBA using primers specific to *Escherichia coli*. B) PiBA using primers specific to *Salmonella enterica*. *Listeria monocytogenes* was used as an off-target control.

significant for food-borne pathogen detection, as we have demonstrated the ability to detect <10 cells in a sample.

2.4.6 Detection of *E. coli* with serotype- and strain-specificity

Differentiation of various serotypes/strains of the same bacteria has important implications for food-safety and clinical pathology.⁴¹ To address this, *E. coli* was used

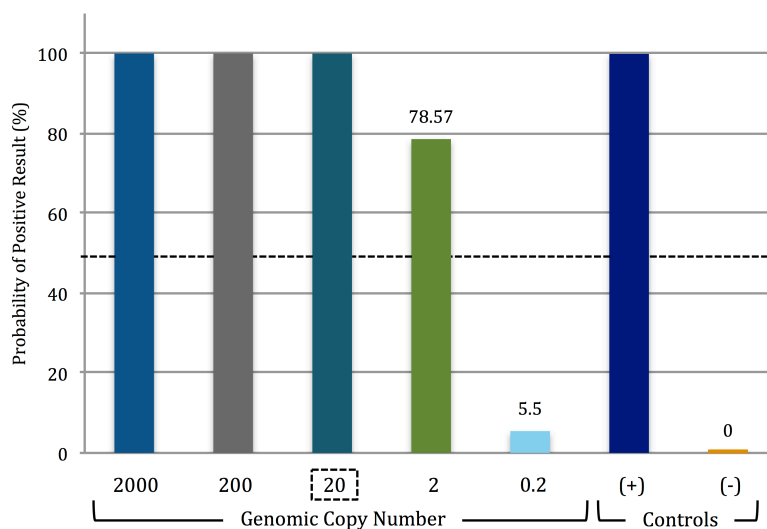


Figure 2-12. Lower limit of *Escherichia coli* O157:H7 detection via PiBA. Limit of detection was determined to be conservatively 20 copies (2 out of 3 analyses were positive using 2 genomic copies of template DNA). Each starting template amount was tested three times, $n=3$. The LOD was determined using *Escherichia coli* O157:H7 strain EDL933 isolated from ground beef.

as the model organism.

E. coli O157 affects the food supply and, therefore, has potential impact on patient health. As such, it is critical to have technology capable of detecting bacterial DNA isolated from various types of

samples. Enterohemorrhagic (EHEC), Enteroaggregative (EAEC), and Enteropathogenic (EPEC) are three serotypes of *E. coli*, and the corresponding strains involved here are O157, O42, and O127, respectively. For the EHEC serotype O157 there are multiple sub-strains, including EDL933, 86-24, and TW14359. The primer set used here is specific to *E. coli* O157 and targets the *rfbE* gene (O-antigen transporter), which is common to all sub-strains (EDL933, 86-24, and TW14359) but absent in O42 and O127.

The primer set specific for EAEC O42 targets sequences in the *aggR* gene (a transcriptional activator of aggregative adherence fimbria)⁴², which is absent in the EDL933, 86-24, and TW14359 sub-strains.

Figure 2-13 shows the results of PiBA detection following amplification of O157, O42, and O127 DNA using the *rfbE* (O157) and *aggR* (O42) gene primer sets (200 genomic copies used as starting template for each). Significant aggregation inhibition was only observed with amplified products specific to the target, i.e., O157 primers were largely ineffective with

O42 and O127 template DNA. Similar results were obtained with the O42 primers, which were ineffective with the O157 and O127 *E. coli* strains. EPEC O127 template

DNA was used as an off-target control and, as seen in the figure, there was

minimal aggregation inhibition observed with either primer set. Again, there is no evidence to suggest non-specific amplification with the O157 primers. However, in experiments with O42 primers there was a slightly higher probability of positive result, though still sufficiently below the empirical threshold. This is attributed to primer

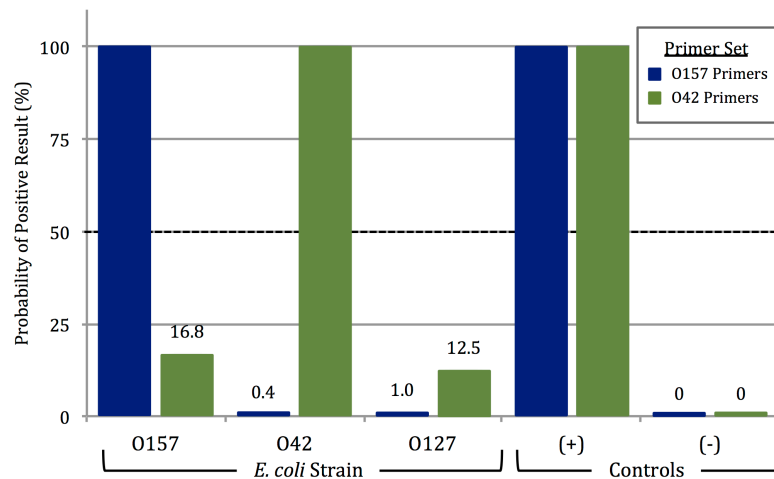


Figure 2-13. Serotype-specific PiBA detection of *E. coli*. PiBA detection of Enterohemorrhagic *E. coli* O157:H7 (EHEC) using primers specific to *rfbE* gene, shown in blue. Enteroaggregative *E. coli* O42 (EAEC) detection using primers specific to *aggR* gene, shown in green.

design, and continued optimization of both primer sequence and amplification temperature in future studies will likely decrease this.

Having successfully demonstrated the detection of *E. coli* O157 isolated from ground beef, we sought to further validate the LAMP-PiBA assay using the same starting

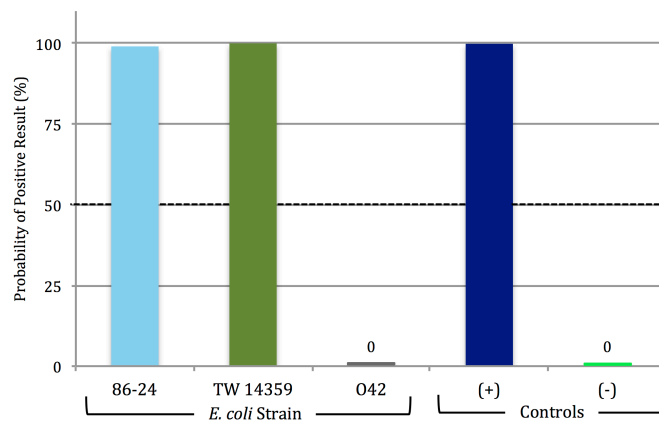


Figure 2-14. Strain-specific PiBA detection of *E. coli*. Detection of *E. coli* O157 DNA extracted from human stool. 86-24 and TW14359 are O157 strains isolated from outbreaks in 1985 and 2006, respectively. EAEC O42 was

contaminated beef.³⁷ Results in **Figure 2-14** show that both TW14359 and 86-24 exhibit aggregation inhibition, correlating with a high probability of a positive result. A complete lack of aggregation inhibition with *E. coli* O42 indicates minimal (or no) non-specific amplification. These results support the potential for future use of PiBA with various starting sample types (food, human stool, etc.).

2.4.7 Human-specific DNA detection

To demonstrate the full bandwidth of the LAMP-PiBA assay, we focused on human genomic DNA pertinent to a forensic application. For forensic DNA analysis, where a number of genetic loci are probed for tetra- and penta-nucleotide repeats, it is

template amount (200 copies) with human stool samples associated with other outbreaks. O157 strain TW14359 was responsible for the spinach-associated outbreak in 2006, while strain 86-24 was associated with an outbreak in 1985 traced back to

critical to define that casework samples have DNA of human origin.⁴³ The thyroid peroxidase (TPOX) gene is a commonly probed locus that is human-specific. To test PiBA in this capacity,

LAMP primers were specifically designed to target the TPOX gene, and used for amplification of DNA from multiple species with a starting template concentration of 1 ng/ μ L.

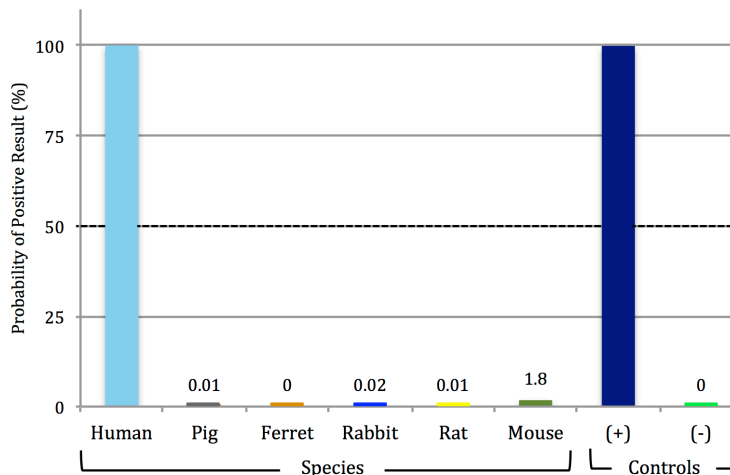


Figure 2-15. Detecting the presence of DNA specific to the human thyroid peroxidase (TPOX) gene. PiBA for detection of human-specific DNA from whole blood. Primers were designed to target the TPOX gene and DNA from multiple species was used as template for the LAMP reaction.

Figure 2-15 shows that the only template to elicit a

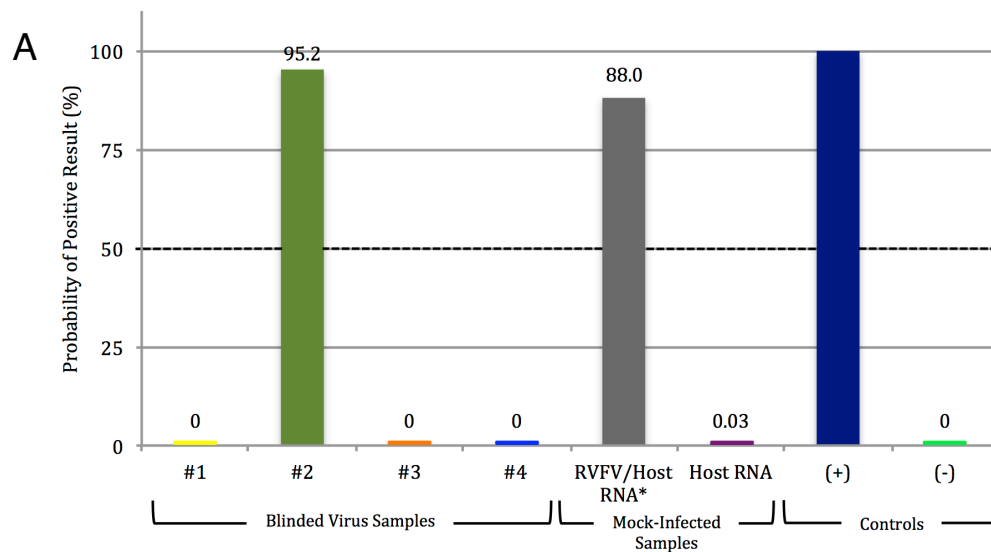
positive response (again, inhibited aggregation) was the sample of human origin, which is consistent with the presence of the TPOX gene.

2.4.8 Virus detection

Having shown success of the LAMP-PiBA assay for detection of bacterial and human DNA, we were curious as to the effectiveness of aggregation inhibition as a means to detect viral RNA targets. The capability of PiBA for detection of an RNA virus is demonstrated here for RVFV-MP12, a mosquito-borne pathogen, which along with other viruses such as Ebola, is known to cause viral hemorrhagic fever (VHF). In 1999, the CDC classified all viruses capable of producing VHF as Category A Bioweapon Agents, due in part to the lack of vaccines available to the general public.⁴⁴ RVFV

outbreaks occur routinely in rural parts of Africa and the ability to have a PiBA-based POC platform would be extremely beneficial for field diagnostics.

In order to detect RVFV-MP12, LAMP primers specific for the L Polymerase gene (L pol) were utilized. Four blinded viral samples (purified RNA), potentially containing RVFV-MP12, were obtained and tested using L pol primers. **Figure 2-16A** shows that, of the four samples, only sample #2 was positive for RVFV-MP12. The scoring of the trials with blinded samples is given in **Figure 2-16B**. With samples #1, 3,



B

SAMPLE	Unknown				RVFV	Host RNA
	1	2	3	4		
Blind Call	RVFV negative	RVFV positive	RVFV negative	RVFV negative	RVFV positive	RVFV negative
Post-Analysis	Influenza A	RVFV	VEEV	Influenza B		
Score	✓	✓	✓	✓		

Figure 2-16. Detecting the presence of Rift Valley fever virus (RVFV) RNA. A) RVFV detection from infected (viral RNA in a background of host RNA) samples. #1-4 represent blinded viral samples. B) Results of blinded analysis of samples.

and 4 containing RNA template from Influenza A, Influenza B, and Venezuelan Equine Encephalitis Virus (VEEV TC83), respectively. The RT-LAMP-PiBA assay proved effective in defining the only sample with RVFV-MP12 (#2). This was confirmed by conventional qRT-PCR (**Figure 2-17**).

Also positive was the RVFV-MP12 infected sample which consisted of RVFV RNA in a background of host RNA at a ratio of ~1: 10,000. This is significant as it suggests that RT-LAMP-PiBA may have potential for use with samples that have undergone minimal upstream enrichment procedures. Additionally, it proves the feasibility to perform the PiBA assay following RT-LAMP, as well as LAMP. Furthermore, we have developed a rapid technique for nucleic acid amplicon detection without the requirement for fluorescence, which can be expensive and necessitate complex instrumentation, simply by using image analysis of magnetic bead aggregation and inhibition. By demonstrating proof of feasibility with various bacterial and viral

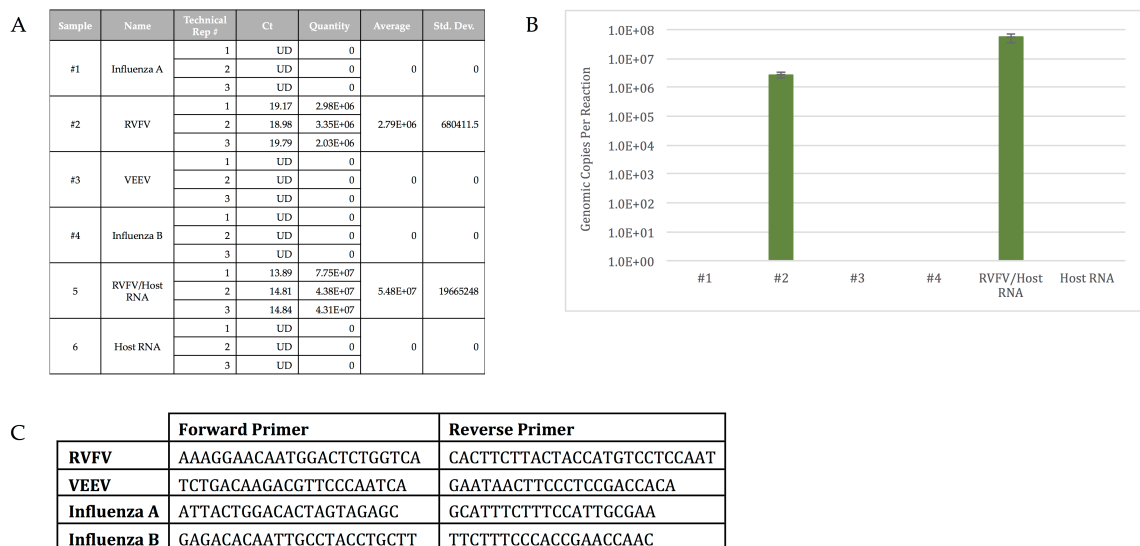


Figure 2-17. Results from RVFV qRT-PCR. A) Table of results from RVFV qRT-PCR. B) Graph of genomic copies per reaction, confirming blinded viral sample results. C) Primer sequences used.

pathogens in the present study, we believe our technique could reasonably be extended to apply to any target pathogen for which specific primers can be designed.

2.5 Conclusions

Fluorescence dominated as a sensitive detection modality for nucleic acid testing, and obviously played a key role in the sequencing of the human genome.^{45, 46} While powerful, it is tethered to the use of specialized reagents that must be purchased commercially, and are often expensive. In addition, hardware demands are high when lasers are used for excitation and sophisticated optical systems are required for detection. Traditional LAMP can be interpreted by comparing the turbidity, however, this can lead to subjectivity and misinterpretation on the part of the reader if they are untrained. For point-of-care devices, it is advantageous to have test results that are presented in a simple, Yes/No manner to avoid misinterpretation. It is for these reasons that there is intense interest in label-free detection technologies. If inexpensive reagents and simplified optical components are involved, a more portable and cost-effective instrument becomes possible. With LAMP-PiBA, reagent requirements include only fluor-free primers for amplification, unlabeled commercially-available magnetic beads, and guanidine. Likewise, detection with PiBA consists of simple image capture and analysis with an inexpensive cell phone-like camera.

The case can be made for the broad range utility of LAMP-PiBA, showing its effectiveness for sequence-specific DNA and RNA detection, as well as applicability to

bacteria, virus, and human sequences. On the amplification front, specificity is driven by the 6-8 primers needed for LAMP, where incomplete hybridization of any one primer results in failed amplification.⁴⁷ Comparing the per run reagent costs for LAMP with PCR, the primer cost differential is negligible at $\sim 7\phi$ and 1ϕ , respectively, while the fluorescence reagents for qPCR (SYBR green or Taqman probes) total $\sim \$1$; cost of beads for PiBA is a fraction of a cent. Consequently, the overall cost differential is ~ 10 -fold.

While cost reduction is not without value, the true paradigm shift with PiBA is in the hardware. The ‘pinwheel effect’ was discovered using the RMF generated by a laboratory stir plate. This is currently being miniaturized as an electromagnetic array that interrogates 5 mm microwells in a small (2 cm^2) microchip. The excitation source (lamp or laser) and photo-detection system (optics, photodiode, CCD) required for fluorescence detection are circumvented in PiBA by a camera (minimum 3 MP) for image capture with no need for elaborate back-lighting. Together, these represent a significant simplification in the hardware for detection. The image analysis (an algorithm in Mathematica) is simple and could potentially be converted into a cell phone application (app) in the future. These characteristics make PiBA a potentially powerful tool in resource-limited settings where infectious disease diagnostics are of critical importance. Cited as an invaluable criteria for point-of-care testing, simple ‘Yes/No detection’ is required in order to avoid misinterpretation of results by untrained users.⁴⁸

Based on these preliminary results, we believe this technology represents the potential for a fully-automated, inexpensive, and portable device suitable for resource-

limited settings. Integration onto a rotationally-driven microdevice (RDM), costing <\$1 to fabricate, would allow for multiplexed results in tens of minutes. Such a device could be driven by the equivalent of a Sony Discman, relying solely on battery power, which is significant because of the departure from conventional electricity-dependent devices. The potential of PiBA to be integrated into such a device stems from the limited equipment requirements: basic heat source, cell phone camera, and custom app.

2.6 References

1. D. C. Leslie, J. Y. Li, B. C. Strachan, M. R. Begley, D. Finkler, L. A. L. Bazydlo, N. S. Barker, D. M. Haverstick, M. Utz and J. P. Landers, *Journal of the American Chemical Society*, 2012, **134**, 5689-5696.
2. T. H. Kim, J. Park, C. J. Kim and Y. K. Cho, *Analytical Chemistry*, 2014, **86**, 3841-3848.
3. P. M. Fratamico, *Molecular and Cellular Probes*, 2003, **17**, 215-221.
4. K. Mullis, F. Faloona, S. Scharf, R. Saiki, G. Horn and H. Erlich, *Cold Spring Harbor Symposia on Quantitative Biology*, 1986, **51**, 263-273.
5. Y. X. Zhao, F. Chen, Q. Li, L. H. Wang and C. H. Fan, *Chemical Reviews*, 2015, **115**, 12491-12545.

6. D. Rodriguez-Lazaro, M. D'Agostino, A. Herrewegh, M. Pla, N. Cook and J. Ikonomopoulos, *International Journal of Food Microbiology*, 2005, **101**, 93-104.
7. A. Jofre, B. Martin, M. Garriga, M. Hugas, M. Pla, D. Rodriguez-Lazaro and T. Aymerich, *Food Microbiology*, 2005, **22**, 109-115.
8. A. K. Deisingh and M. Thompson, *Journal of Applied Microbiology*, 2004, **96**, 419-429.
9. S. D. Gan and K. R. Patel, *Journal of Investigative Dermatology*, 2013, **133**, E10-E12.
10. S. Y. Toh, M. Citartan, S. C. B. Gopinath and T. H. Tang, *Biosensors & Bioelectronics*, 2015, **64**, 392-403.
11. D. S. Leland and C. C. Ginocchio, *Clinical Microbiology Reviews*, 2007, **20**, 49-78.
12. K. Küllerich-Pedersen, J. Dapra, S. Cherre and N. Rozlosnik, *Biosensors & Bioelectronics*, 2013, **49**, 374-379.
13. D. M. Morens, G. K. Folkers and A. S. Fauci, *Nature*, 2004, **430**, 242-249.
14. A. S. Fauci, *Clinical Infectious Diseases*, 2001, **32**, 675-685.
15. A. M. Foudeh, T. F. Didar, T. Veres and M. Tabrizian, *Lab on a Chip*, 2012, **12**, 3249-3266.

16. O. Lazcka, F. J. Del Campo and F. X. Munoz, *Biosensors & Bioelectronics*, 2007, **22**, 1205-1217.
17. X. Y. Pan, L. Jiang, K. Y. Liu, B. C. Lin and J. H. Qin, *Analytica Chimica Acta*, 2010, **674**, 110-115.
18. C. C. Liu, M. G. Mauk, R. Hart, X. B. Qiu and H. H. Bau, *Lab on a Chip*, 2011, **11**, 2686-2692.
19. P. M. Griffin, S. M. Ostroff, R. V. Tauxe, K. D. Greene, J. G. Wells, J. H. Lewis and P. A. Blake, *Annals of Internal Medicine*, 1988, **109**, 705-712.
20. R. R. Chaudhuri, M. Sebahia, J. L. Hobman, M. A. Webber, D. L. Leyton, M. D. Goldberg, A. F. Cunningham, A. Scott-Tucker, P. R. Ferguson, C. M. Thomas, G. Frankel, C. M. Tang, E. G. Dudley, I. S. Roberts, D. A. Rasko, M. J. Pallen, J. Parkhill, J. P. Nataro, N. R. Thomson and I. R. Henderson, *Plos One*, 2010, **5**, 19.
21. S. X. Wu and R. Q. Peng, *Acta Paediatrica Scandinavica*, 1991, **80**, 1019-1024.
22. C. F. E. R. Team, *Journal*, 2007.
23. J. G. Wells, B. R. Davis, I. K. Wachsmuth, L. W. Riley, R. S. Remis, R. Sokolow and G. K. Morris, *Journal of Clinical Microbiology*, 1983, **18**, 512-520.
24. T. Ikegami and S. Makino, *Vaccine*, 2009, **27**, D69-D72.
25. B. A. Szretter K, Katz J, *Curr Protoc Microbiol*, 2005.

26. N. Shafagati, A. Narayanan, A. Baer, K. Fite, C. Pinkham, C. Bailey, F. Kashanchi, B. Lepene and K. Kehn-Hall, *Plos Neglected Tropical Diseases*, 2013, **7**, 12.
27. L. Lundberg, C. Pinkham, A. Baer, M. Amaya, A. Narayanan, K. M. Wagstaff, D. A. Jans and K. Kehn-Hall, *Antiviral Research*, 2013, **100**, 662-672.
28. J. M. Bienvenue, N. Duncalf, D. Marchiarullo, J. P. Ferrance and J. P. Landers, *Journal of Forensic Sciences*, 2006, **51**, 266-273.
29. M. C. Breadmore, K. A. Wolfe, I. G. Arcibal, W. K. Leung, D. Dickson, B. C. Giordano, M. E. Power, J. P. Ferrance, S. H. Feldman, P. M. Norris and J. P. Landers, *Analytical Chemistry*, 2003, **75**, 1880-1886.
30. K. A. Hagan, J. M. Bienvenue, C. A. Moskaluk and J. P. Landers, *Analytical Chemistry*, 2008, **80**, 8453-8460.
31. H. J. Tian, A. F. R. Huhmer and J. P. Landers, *Analytical Biochemistry*, 2000, **283**, 175-191.
32. J. Y. Li, Q. Liu, L. Xiao, D. M. Haverstick, A. Dewald, L. Columbus, K. Kelly and J. P. Landers, *Analytical Chemistry*, 2013, **85**, 11233-11239.
33. R. Boom, C. J. A. Sol, M. M. M. Salimans, C. L. Jansen, P. M. E. Wertheimvandillen and J. Vandernoordaa, *Journal of Clinical Microbiology*, 1990, **28**, 495-503.

34. B. Vogelstein and D. Gillespie, *Proceedings of the National Academy of Sciences of the United States of America*, 1979, **76**, 615-619.
35. T. Notomi, H. Okayama, H. Masubuchi, T. Yonekawa, K. Watanabe, N. Amino and T. Hase, *Nucleic Acids Research*, 2000, **28**, 7.
36. V. Velusamy, K. Arshak, O. Korostynska, K. Oliwa and C. Adley, *Biotechnology Advances*, 2010, **28**, 232-254.
37. K. L. Mohawk, A. R. Melton-Celsa, T. Zangari, E. E. Carroll and A. D. O'Brien, *Microbial Pathogenesis*, 2010, **48**, 131-142.
38. Z. Y. Yao, G. Wei, H. Z. Wang, L. S. Wu, J. J. Wu and J. M. Xu, *Applied and Environmental Microbiology*, 2013, **79**, 1755-1756.
39. L. W. Riley, R. S. Remis, S. D. Helgerson, H. B. McGee, J. G. Wells, B. R. Davis, R. J. Hebert, E. S. Olcott, L. M. Johnson, N. T. Hargrett, P. A. Blake and M. L. Cohen, *New England Journal of Medicine*, 1983, **308**, 681-685.
40. S. P. Luisi PL, *The minimal cell: the biophysics of cell compartment and the origin of cell functionality. A biophysical chemists thoughts about the lower limit of cell sizes*, Springer, 2010.
41. J. C. Paton and A. W. Paton, *Clinical Microbiology Reviews*, 1998, **11**, 450-+.
42. J. P. Nataro, Y. K. Deng and K. Walker, *Journal of Bacteriology*, 1994, **176**, 4691-4699.

43. W. G. Dirks, and Hans G. Drexler, *Journal*, **13**, 27-38.
44. A. Narayanan, C. Bailey, F. Kashanchi and K. Kehn-Hall, *Expert Opinion on Investigational Drugs*, 2011, **20**, 239-254.
45. M. Schena, D. Shalon, R. Heller, A. Chai, P. O. Brown and R. W. Davis, *Proceedings of the National Academy of Sciences of the United States of America*, 1996, **93**, 10614-10619.
46. E. S. Lander, C. Int Human Genome Sequencing, L. M. Linton, B. Birren, C. Nusbaum, M. C. Zody, J. Baldwin, K. Devon, K. Dewar, M. Doyle, W. FitzHugh, R. Funke, D. Gage, K. Harris, A. Heaford, J. Howland, L. Kann, J. Lehoczyk, R. LeVine, P. McEwan, K. McKernan, J. Meldrim, J. P. Mesirov, C. Miranda, W. Morris, J. Naylor, C. Raymond, M. Rosetti, R. Santos, A. Sheridan, C. Sougnez, N. Stange-Thomann, N. Stojanovic, A. Subramanian, D. Wyman, J. Rogers, J. Sulston, R. Ainscough, S. Beck, D. Bentley, J. Burton, C. Clee, N. Carter, A. Coulson, R. Deadman, P. Deloukas, A. Dunham, I. Dunham, R. Durbin, L. French, D. Grafham, S. Gregory, T. Hubbard, S. Humphray, A. Hunt, M. Jones, C. Lloyd, A. McMurray, L. Matthews, S. Mercer, S. Milne, J. C. Mullikin, A. Mungall, R. Plumb, M. Ross, R. Shownkeen, S. Sims, R. H. Waterston, R. K. Wilson, L. W. Hillier, J. D. McPherson, M. A. Marra, E. R. Mardis, L. A. Fulton, A. T. Chinwalla, K. H. Pepin, W. R. Gish, S. L. Chissoe, M. C. Wendl, K. D. Delehaunty, T. L. Miner, A. Delehaunty, J. B. Kramer, L. L. Cook, R. S. Fulton, D. L. Johnson, P. J. Minx, S. W. Clifton, T. Hawkins, E. Branscomb, P. Predki, P. Richardson, S. Wenning, T. Slezak, N. Doggett, J. F. Cheng, A. Olsen, S. Lucas,

C. Elkin, E. Uberbacher, M. Frazier, R. A. Gibbs, D. M. Muzny, S. E. Scherer, J. B. Bouck, E. J. Sodergren, K. C. Worley, C. M. Rives, J. H. Gorrell, M. L. Metzker, S. L. Naylor, R. S. Kucherlapati, D. L. Nelson, G. M. Weinstock, Y. Sakaki, A. Fujiyama, M. Hattori, T. Yada, A. Toyoda, T. Itoh, C. Kawagoe, H. Watanabe, Y. Totoki, T. Taylor, J. Weissenbach, R. Heilig, W. Saurin, F. Artiguenave, P. Brottier, T. Bruls, E. Pelletier, C. Robert, P. Wincker, A. Rosenthal, M. Platzer, G. Nyakatura, S. Taudien, A. Rump, H. M. Yang, J. Yu, J. Wang, G. Y. Huang, J. Gu, L. Hood, L. Rowen, A. Madan, S. Z. Qin, R. W. Davis, N. A. Federspiel, A. P. Abola, M. J. Proctor, R. M. Myers, J. Schmutz, M. Dickson, J. Grimwood, D. R. Cox, M. V. Olson, R. Kaul, N. Shimizu, K. Kawasaki, S. Minoshima, G. A. Evans, M. Athanasiou, R. Schultz, B. A. Roe, F. Chen, H. Q. Pan, J. Ramser, H. Lehrach, R. Reinhardt, W. R. McCombie, M. de la Bastide, N. Dedhia, H. Blocker, K. Hornischer, G. Nordsiek, R. Agarwala, L. Aravind, J. A. Bailey, A. Bateman, S. Batzoglou, E. Birney, P. Bork, D. G. Brown, C. B. Burge, L. Cerutti, H. C. Chen, D. Church, M. Clamp, R. R. Copley, T. Doerks, S. R. Eddy, E. E. Eichler, T. S. Furey, J. Galagan, J. G. R. Gilbert, C. Harmon, Y. Hayashizaki, D. Haussler, H. Hermjakob, K. Hokamp, W. H. Jang, L. S. Johnson, T. A. Jones, S. Kasif, A. Kasprzyk, S. Kennedy, W. J. Kent, P. Kitts, E. V. Koonin, I. Korf, D. Kulp, D. Lancet, T. M. Lowe, A. McLysaght, T. Mikkelsen, J. V. Moran, N. Mulder, V. J. Pollara, C. P. Ponting, G. Schuler, J. R. Schultz, G. Slater, A. F. A. Smit, E. Stupka, J. Szustakowki, D. Thierry-Mieg, J. Thierry-Mieg, L. Wagner, J. Wallis, R. Wheeler, A. Williams, Y. I. Wolf, K. H. Wolfe, S. P. Yang, R. F. Yeh, F. Collins, M. S. Guyer, J. Peterson, A. Felsenfeld,

- K. A. Wetterstrand, A. Patrinos, M. J. Morgan and C. Int Human Genome Sequencing, *Nature*, 2001, **409**, 860-921.
47. X. H. Zhao, Y. M. Li, L. Wang, L. J. You, Z. B. Xu, L. Li, X. W. He, Y. Liu, J. H. Wang and L. S. Yang, *Molecular Biology Reports*, 2010, **37**, 2183-2188.
48. P. Yager, T. Edwards, E. Fu, K. Helton, K. Nelson, M. R. Tam and B. H. Weigl, *Nature*, 2006, **442**, 412-418.

Transitioning the PiBA assay onto a polyester microdevice platform and integration with loop-mediated isothermal amplification

3.1 Overview

Pathogen detection has traditionally been accomplished by utilizing methods such as cell culture, immunoassays, and nucleic acid amplification tests; however, these methods are not easily implemented in resource-limited settings because special equipment for detection and thermal cycling is often required. Presented herein is a magnetic bead aggregation assay coupled to an inexpensive microfluidic fabrication technique that allows for cell phone detection and analysis of a notable pathogen in less than one hour. Detection is achieved through the use of a custom-built system that allows for fluid flow control via centrifugal force, as well as manipulation of magnetic beads with an adjustable rotating magnetic field (RMF). Cell phone image capture and analysis is housed in a 3D-printed case with LED backlighting and a lid-mounted Android phone. A custom-written application (app) is employed to interrogate images for the extent of aggregation present following loop-mediated isothermal amplification (LAMP) coupled to product-inhibited bead aggregation (PiBA) for detection of target sequences. *Clostridium difficile* is a pathogen of increasing interest due to its causative role in intestinal infections following antibiotic treatment, and was therefore chosen as the pathogen of interest in the present study to demonstrate the rapid, cost-effective, and sequence-specific detection capabilities of the microfluidic platform described herein.

3.2 Introduction

Detection of pathogenic microorganisms has long been considered important; however, in recent years the rise of antibiotic resistant bacterial pathogens has caused what experts in the field consider to be an antibiotic resistant ‘crisis’.¹ In fact, antimicrobial resistance is poised to threaten effective prevention and treatment of a wide range of infections caused by various types of pathogens (i.e., bacteria, parasites, viruses, and fungi), according to the World Health Organization (WHO).² This risk is especially prevalent in resource-limited settings where sanitation is poor, as antibiotics are the main weapon used to decrease morbidity and mortality associated with infectious diseases.¹ Even in the developed world, antibiotic resistant strains of pathogenic bacteria have become more common in places such as hospitals over the last several decades.³

Current techniques utilized for the detection of pathogens include cell culture, immunoassays, and nucleic acid amplification tests (NAAT) such as the polymerase chain reaction (PCR).⁴ While these tests have proven effective in the past, they are often time-consuming and expensive, owing to the requirement for specialized equipment and instrumentation. Specifically, NAATs usually require the capacity for fluorescence detection (often laser-induced) as well as thermal cycling, making it challenging to implement these techniques in resource-limited or point-of-care (POC) settings.^{5,6}

To address the limitations associated with traditional NAATs, a novel magnetic bead-based aggregation assay (product-inhibited bead aggregation, PiBA) has been described that requires minimal hardware and a simple camera for image capture and analysis.⁷ The basis for this detection platform relies on the *inhibition* of silica bead

aggregation by long DNA strands that would normally induce aggregation of the beads under chaotropic conditions in a rotating magnetic field. Additionally, this technology is coupled to an isothermal amplification method (loop-mediated isothermal amplification, LAMP)⁸ that effectively eliminates the requirement for thermal cycling, and thereby drastically simplifies the associated heating elements. Furthermore, polyethylene terephthalate (Pe) is used for fabrication of simple and inexpensive microfluidic devices capable of carrying out LAMP-PiBA.

The first miniaturized (or micro) total chemical analysis system (μ TAS) was described by Manz et al. in 1990.⁹ Throughout the 1990s, development continued and significant advances were made in the field, including efforts to decrease the volume of sample and reagents, as well as speeding up the analysis time required for μ TAS platforms.¹⁰ As a field, μ TAS or lab-on-a-chip (LOC) systems have continued to evolve over the past twenty years with a major focus on decreasing the cost, increasing the functionality, and finding value in a wide swath of applications. These applications include the most common centralized laboratory techniques: blood chemistries, immunoassays, nucleic-acid amplification tests, and flow cytometry.¹¹ In the beginning, the main driving force behind miniaturization was to enhance the analytical performance of the device¹²; however, with that came an inherent reduction in size and a decrease in reagent and sample volume.¹³ Owing to the small size and volume requirements, LOC technologies have garnered much attention for their potential in point-of-care (POC) testing. Cited as the most desirable qualities of such systems are the ability to quickly analyze small volumes of samples, and to do so without the requirement for trained personnel.¹¹

Specifically, in the realm of pathogen detection, extensive research has been done and microfluidic devices have been successfully employed by a number of groups.¹³⁻¹⁹ Microfluidic nucleic acid, protein/enzyme, and cell counting-based methods represent the most common LOC platforms for pathogen detection.¹³ Nucleic acid-based pathogen detection has been achieved either by directly probing the target, or probing the target following amplification (leading to increased sensitivity). Both reverse-transcriptase PCR and real-time PCR have been successfully applied to microfluidic platforms for pathogen sensing.^{20, 21} As far as protein/enzyme-based methods, a highly integrated and portable device based on antibody interactions was recently described for the detection of *Escherichia coli* O157:H7.²² However, one major drawback to antibody-based detection modalities is the requirement for surface modifications to introduce functional groups for protein coupling, often using poly(dimethylsiloxane) (PDMS), which can be expensive and time-consuming.²³ Lastly, cell counting-based assays have been incorporated into LOC devices and allow for direct identification, differentiation, and quantification of cellular systems for pathogen detection. Several applications of these devices include microchips capable of CD4⁺ cell counting for monitoring the progress of HIV in AIDS patients^{24, 25} and miniaturized culture assays for identifying drug-resistant strains of pathogenic bacteria.^{26, 27}

While much progress has been made in LOC systems for integrated pathogen detection, the necessity for microfluidic devices that can be fabricated inexpensively, rapidly, and in a disposable manner persists. The manufacturing methods used for early microfluidic chips were those utilized by the semiconductor industry, therefore, the process was dominated by wet etching and photolithography of glass and silicon (often

requiring a clean room environment for fabrication).^{28,29} Eventually, a shift was made to various polymers, including PDMS, poly(methyl methacrylate) (PMMA), and cyclic olefin copolymer (COC), which simplified the bonding process through the use of surface oxidation (plasma).^{30, 31} Despite advances in new materials, cumbersome traditional fabrication processes remain a limiting factor in rapid and inexpensive prototyping. For example, photolithography requires a custom mask, whereas the channel architecture in PMMA and COC chips must be embossed or injection molded, making these methods perilously slow when an efficient prototyping platform is desired.^{32,33} In answer to this, the print, cut, laminate (PCL) method was developed by Thompson et al. and makes use of commercial office equipment and inexpensive materials. A CO₂ laser is used to ablate the microfluidic architecture into polyester sheets that have been printed with ink-toner (PeT), and multilayer devices can then be assembled using a simple office laminator.¹⁰ This technique allows for rapid prototyping of microfluidic devices in a cost-effective manner, utilizing inexpensive overhead transparencies as the substrate. Due to the inexpensive nature of these PeT devices they are readily disposable, decreasing the risk of contamination to both the user and the sample, which is a distinct advantage for pathogen-related applications.

The centrifugal microfluidic platform has become the focus of intense research in recent years as a natural extension of current LOC systems.³⁴ Utilizing this approach, fluidic steps (such as metering and mixing) can be automated through the implementation of spin profiles, and PeT devices lend themselves well to this method.³⁵⁻³⁷ A small motor can be used for fluid flow, thereby eliminating the need for external pumps and valves. The major advantage of this platform lies in the potential for an entirely hands-off

system, which would reduce time, cost, and error due to human handling, while increasing portability.³⁴

We describe the novel coupling of PiBA to a simple and inexpensive fabrication technique for polyester toner microdevices. A custom-built system allows for fluid flow control via centrifugal force, and an adjustable rotating magnetic field is used for manipulation of commercially available magnetic beads. Imaging is carried out using a cell phone camera, and results are compared to those obtained using a standard 15 Megapixel camera. Furthermore, imaging and analysis takes place in a 3D-printed case, representing the potential for a fully portable device in the future.

To demonstrate the functionality of this system, *Clostridium difficile* (*C. difficile*) was chosen as the target organism. *C. difficile* is a hypervirulent, spore-forming bacterium responsible for infectious diarrhea and pseudomembranous colitis.³⁸⁻⁴² It is the leading cause of hospital-associated gastrointestinal illness and can lead to death.⁴ *C. difficile* infection (CDI) spreads via a fecal-oral route, and individuals receiving antibiotic treatment are most at risk for infection because antibiotics suppress the normal bacteria of the gut, allowing *C. difficile* to flourish.^{43, 44} Whereas the rates of most other hospital-acquired infections (HAI) have been declining for the past two decades, CDI-related hospital stays in the U.S. have increased from 85,700 in 1993 to 336,600 in 2009. Furthermore, in 2011 nearly a half million *C. difficile* infections were reported in the United States alone.

This work describes the rapid, cost-effective, and strain-specific detection of *C. difficile* using a previously described magnetic bead-based assay coupled to a centrifugal

microfluidic platform. Several groups have successfully detected *C. difficile* and other bacterial species on microfluidic platforms; however these methods largely rely on either fluorescent or luminescent probes and/or detection modalities.⁴⁵⁻⁴⁹ In contrast, the microdevice described herein uses inexpensive magnetic beads and a completely fluor-free detection method. Furthermore, this device is fabricated using a simplistic technique and an inexpensive polyester substrate. Total analysis time is less than one hour, and image analysis can be simplified by the utilization of a cell phone camera for microchamber image capture following PiBA. The findings described herein are specific to *C. difficile*; however, the target can easily be interchanged by simply re-designing the LAMP primers, and, therefore, the desired pathogenic microorganism.

3.3 Materials and Methods

3.3.1 On-chip LAMP

For 3 μ L on-chip amplification the following reagent volumes were used: 1.5 μ L reaction mix, 0.204 μ L primers, 0.12 μ L enzyme, 0.876 μ L diH₂O, and 0.3 μ L template DNA. For 5 μ L on-chip amplification the following reagent volumes were used: 2.5 μ L reaction mix, 0.34 μ L primers, 0.2 μ L enzyme, 0.96 μ L diH₂O, and 1.0 μ L template DNA. All reactions were carried out using a LoopAmp DNA Amplification Kit (Eiken Chemical Co., Ltd., Tokyo, Japan). In each reaction, the concentration of primers were as follows: 5 pM for each outer primer (F3 and B3), 40 pM for each inner primer (FIP and BIP), and 20 pM for each loop primer (LF and LB). Following amplification, fluid was

extracted from the chip using filtered 1.0 μL pipette tips and samples were analyzed on the Agilent 2100 Bioanalyzer.

3.3.2 Chip design and fabrication

All microfluidic chips described in this study were designed and fabricated as described in previous work from our group.¹⁰ Briefly, polyester toner (PeT) chips were designed using CorelDraw Software and printed using an HP LaserJet printer. The microfluidic architecture was laser cut using a VersaLaser [model VLS 3.50] and the five layers of the chip were laminated together using an Akiles UltraLam 250B.

3.3.3 Spin system

The spin device featured a Sanyo Denki Sanmotion series stepper motor controlled by a Pololu DRV8825 stepper motor driver in full step mode. The motor was mounted on a custom made 3-arm support structure cut from PMMA, which functioned to immobilize the motor during sample rotation. Motion control profiles were generated using a Parallax Propeller microcontroller, programmed in its native programming language, called Spin. A printed circuit board was designed using EAGLE CAD software, and contained the microcontroller, motor drivers, and the associated components for power regulation, heat sinking, and serial communication with an external computer terminal.

The magnet-containing disc was rotated in a similar fashion as described for the sample disc above, and also mounted to a 3-arm PMMA support structure. This support structure was fastened to a set of carriage nuts, which could move freely on a set of 3 lead

screws. Each lead screw was attached to a Sanyo Denki stepper motor so that rotation of the motors would allow for vertical height adjustment of the magnets with respect to the sample platform.

3.3.4 Optimization of spin speed, direction, and duration

For all on-chip PiBA assays the following spin protocol was used: 2000 RPM (spin platform) for 20 seconds to spin all reagents and LAMP sample into the PiBA chamber, 200 RPM (rotating magnet) for 60 seconds to bring all beads to one side of the chamber, and 10 cycles of 200 RPM (rotating magnet) for 30 seconds in opposite directions to ensure maximum contact between magnetic beads, trigger DNA, and LAMP sample. Following the last step, the rotating magnet was turned off and images were captured using either a 15 Mp Canon Rebel EOS Rebel T1i camera or an Android cell phone camera.

3.3.5 On-chip PiBA

All on-chip PiBA was carried out with the following reagent volumes and concentrations: 3.0 μL magnetic beads (Magesil, purchased from Promega, Madison, WI.), 2.5 μL guanidine hydrochloride (GdnHCl, 6M), 1.0 μL λ -phage trigger DNA (Life Technologies, Inc.), and 0.5 μL LAMP product. Results are presented as ‘% Difference in Aggregation’ with all data normalized to a sample containing only magnetic beads, trigger DNA, and GdnHCl (no LAMP product), and set to ‘100% Aggregation’. Following optimization of discrimination between positive and negative samples, results were normalized to a ‘negative’ sample (i.e., LAMP reagents without template DNA)

which was set to 100% Aggregation. Equation 1 describes ‘% Difference in Aggregation’ (%DA), and Equation 2 describes ‘% Aggregation’. Results are presented in both %DA and %Aggregation. %Aggregation reflects the raw values such that the negative control is taken into account, whereas %DA is used for ease of interpretation of the normalized values.

$$\% DA = \left(\frac{\text{dark area neg.} - \text{dark area pos.}}{\text{average dark area}} \right) * 100 \quad (1)$$

$$\% Aggregation = \left(\frac{\text{dark area blank}}{\text{dark area sample}} \right) * 100 \quad (2)$$

3.3.6 Clostridium difficile spore isolation and culture

Clostridium difficile strains were grown in BHI broth for one week anaerobically. The cultures were spun at 12000 RPM for 5 min followed by 5 washes with distilled water. The pellet was then resuspended in PBS with 0.1% Tween-80 (ST-80 solution) and vortexed for 10 minutes. Spores were pelleted and suspended in fresh ST-80 solution and heated at 65°C for 15 minutes with shaking. Spores were washed 3 times with distilled water, resuspended in PBS and stored at 4°C. *C. diff* strains were as follows: R20191 (A+B+C+), R20291 cdtB- (A+B+), 630 delta-ermB- (A+ B+), VPI10463 (A+B+).

3.4 Results and Discussion

3.4.1 Polyester toner (PeT) microdevices and associated hardware

Polyester toner (PeT) was chosen as the microdevice substrate due to the many advantages afforded, including: rapid prototyping, inexpensive materials, and a facile fabrication methodology. The PCL method was employed to fabricate the devices used for pathogen detection via LAMP-PiBA, and consisted of 5 layers of transparency that had laser-ablated microfluidic architecture and were bonded using an office laminator. The purpose of the ink-toner used in this methods is three-fold: (i) substrate bonding, (ii) passive hydrophobic valving, and (iii) defining the microfluidic architecture.¹⁰ **Figure 3-1** shows a schematic for how the PeT devices are assembled from multiple transparency layers.

Fluid flow control is achieved using a custom-built system with a compact motor

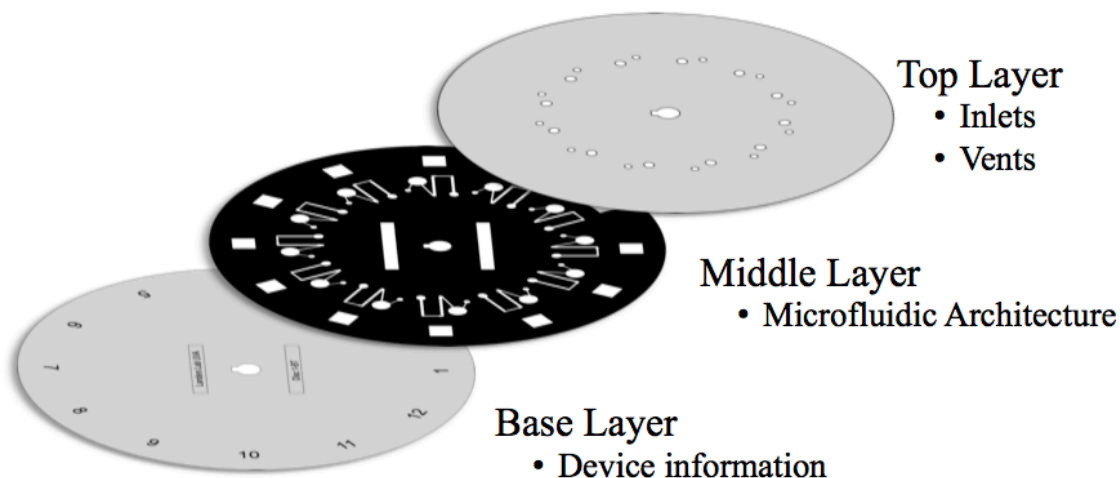


Figure 3-1. Schematic of a multilayer PeT device. Top and base layers consist of non toner-printed polyethylene terephthalate (Pe). Middle layers have toner printed for microfluidic architecture and bonding via an office laminator. Schematic from Thompson et al. 2016³⁷.

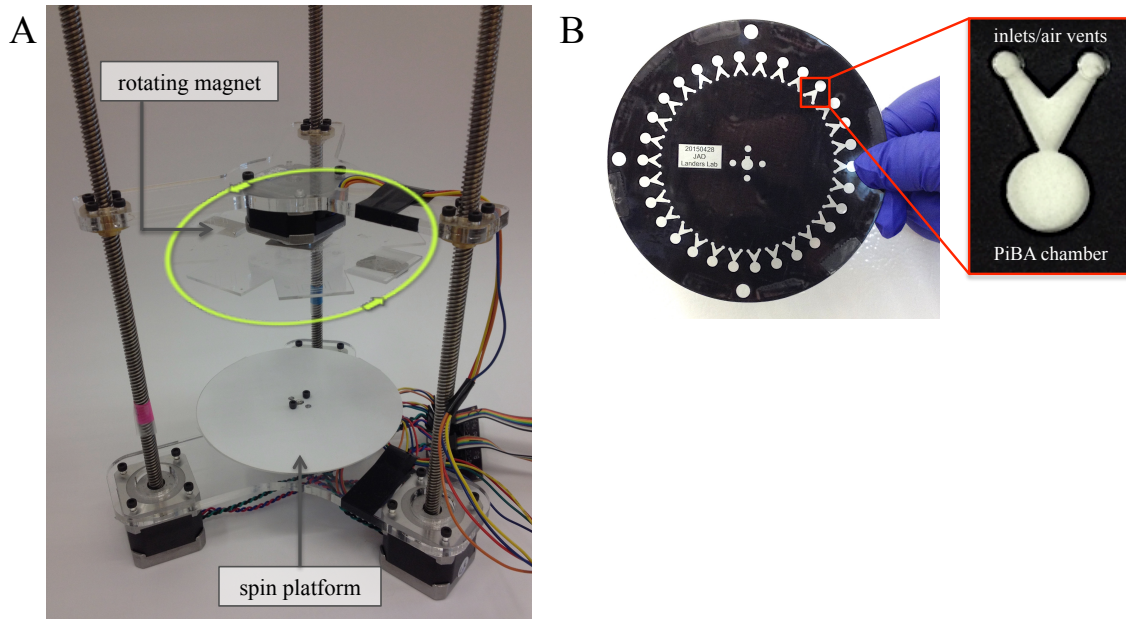


Figure 3-2. Spin system built in-house for on-chip PiBA. A) Spin system with spin platform for fluid flow control and rotating magnet for on-chip PiBA detection. B) Design of 5 layer PeT chip for optimization of PiBA assay. Microwells are designed to contain 6 μ L.

for disc spinning via centrifugal force. For the PiBA assay, a rotating magnetic field (RMF) is necessary for magnetic bead manipulation⁷, and this functionality was therefore built into the system shown in **Figure 3-2A**. The spin platform provides fluidic movement following the on-chip LAMP assay, but remains stationary during PiBA. In contrast, the magnets for bead manipulation are fixed to a PMMA disc that is attached to a top motor, which, when engaged, provides an adjustable RMF that can be deployed at a variable distance from the spin platform. **Figure 3-2B** shows the PeT chip designed for on-chip PiBA, with 6 μ L wells (30 wells on each disc) in a five-layer device.

3.4.2 Optimization of PiBA on PeT microdevice

Preliminary proof of concept studies for PiBA on PeT microdevices and the custom-built spin system described above were conducted using Influenza H1N1 as the target pathogen. In our initial description of PiBA, the RMF provided magnetic bead

manipulation in an open microwell (20 μ L) and agitation (in this case, with a re-purposed lab vortexer) was required for complete dispersion of the beads in the absence of trigger DNA, a phenomenon referred to as dual force aggregation (DFA).⁵⁰ Naturally, moving the assay to closed microwells on the PeT microdevice necessitated some additional optimization of three important parameters: distance of RMF from the PiBA microwell, strength of RMF used for bead manipulation, and trigger DNA concentration.

Initial studies were carried out at a distance of 2 cm (from microwell to magnet).

Figure 3-3 shows the results from initial experiments using positive and negative LAMP product. The control consisted of trigger DNA and beads, and this microwell was set to 100% Aggregation. Visible aggregation inhibition (AI) is seen in the microwell containing (+) LAMP product, as expected; however, the beads in the (-) LAMP sample

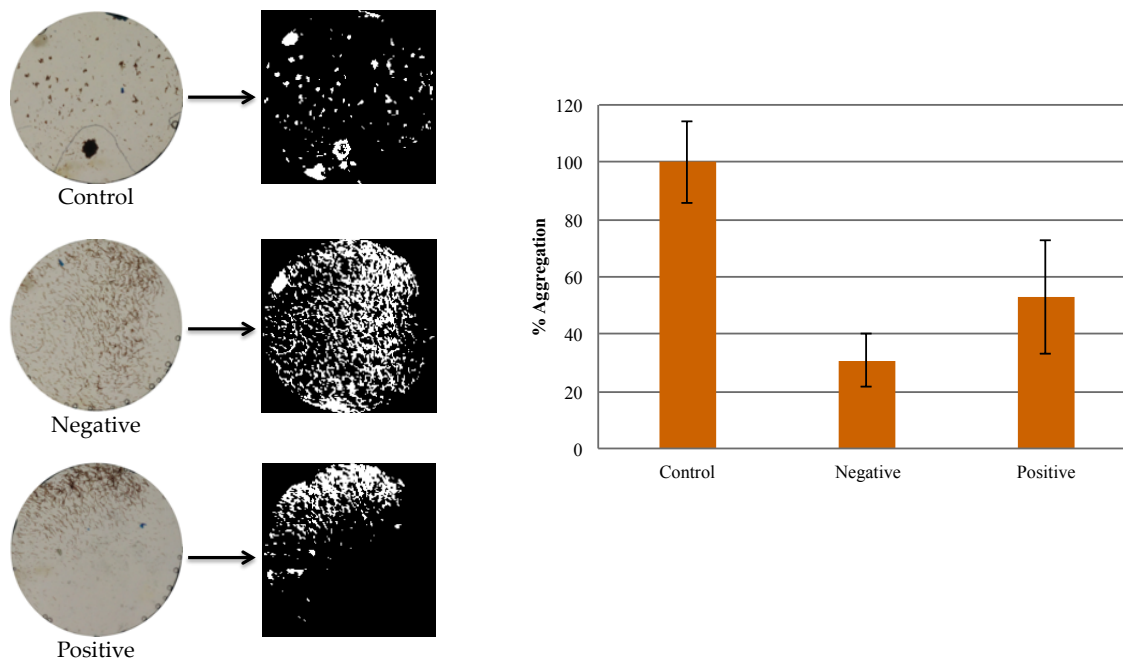


Figure 3-3. Effect of distance of magnetic field to microwell. Custom-built system with RMF was used for on-chip PiBA and the distance from microwell to magnet was 2 cm in preliminary studies. Good discrimination between control and positive LAMP product (here shown with H1N1 for proof of principle); however, poor discrimination between positive and negative LAMP product.

are also dispersed following PiBA interrogation. Therefore, no discrimination is present between the (+) and (-) LAMP samples. Based on these results, it was hypothesized that the primers in the (-) LAMP sample were inducing AI due to their short length, in a manner similar to what is seen when the amplicons produced in the LAMP reaction coat the surface of the magnetic beads and prevent the adherence and subsequent aggregation of the beads by long strands of trigger DNA (in the (+) sample).

The RMF was then moved to a distance of 1 cm (microwell to magnet) for further optimization studies, and **Figure 3-4** shows the results of PiBA run at this RMF distance.

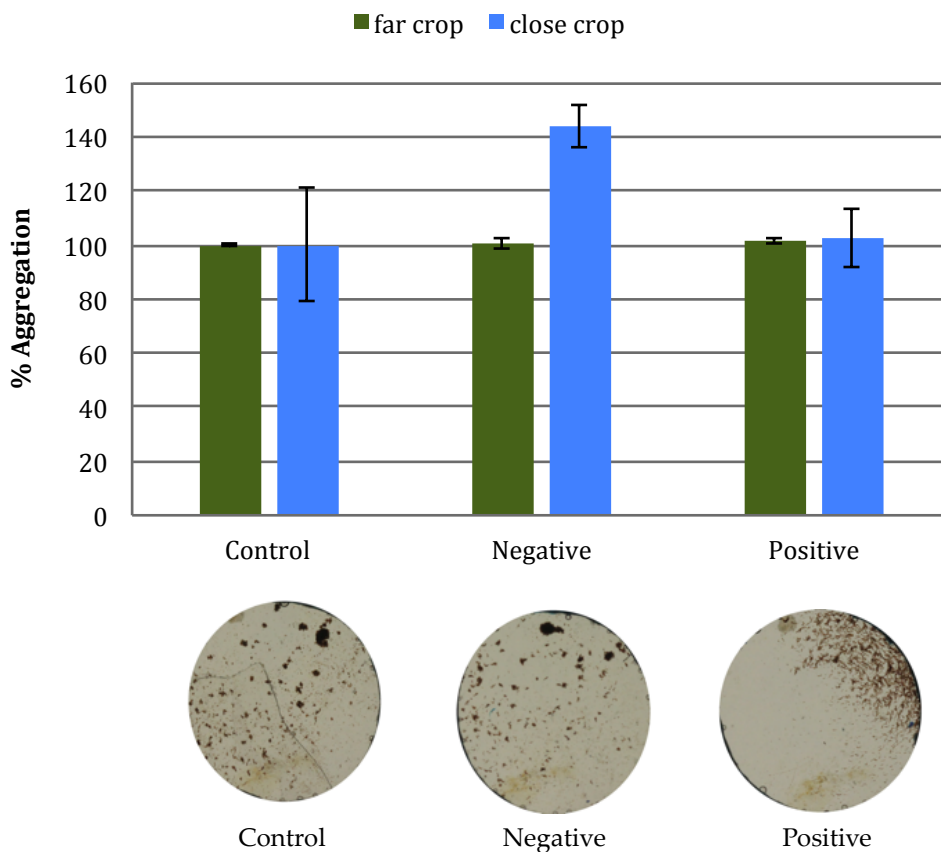


Figure 3-4. Effect of 1 cm RMF distance from microwell. Visual discrimination is present between positive and negative; however the algorithm is not picking up the difference in dark area. Two different cropping methods were utilized. Results suggest beads need to be in center of the well.

As seen in the images of the microwells, the control and the (-) LAMP product are both aggregated, while the (+) LAMP product demonstrates AI, as expected. However, the graph shows the results of two different cropping methods (using Image J) for image analysis, and no discrimination is present among any of the three microwells. The most likely cause of this is the bead position in the (+) sample, wherein all magnetic beads are swept against the side of the microwell. Despite the lack of aggregation, the image analysis algorithm looks only at dark area and the overall dark area is visually similar in all three samples.

To address this, the magnetic field strength was increased to 2777 Gauss (by doubling the number of magnets fixed to the PMMA disc). For initial optimization, the spin parameter consisted of 10 cycles of 200 RPM for 30 seconds in opposite directions. In addition to increasing the strength of the RMF, the final spin step was decreased to 5 seconds so that the beads were oriented in the center of the microwell at the conclusion of the PiBA assay. **Figure 3-5** shows the results from these experiments, and visual discrimination is again seen between the (+) and (-) LAMP samples. The stronger RMF yielded a tighter aggregate in both the control and (-) LAMP sample. Furthermore, with the magnetic beads positioned in the center of the microwell, the image analysis algorithm is able to better discriminate between the samples.

The concentration of trigger DNA in the PiBA assay is another important parameter that was optimized after transitioning the assay onto the PeT microdevice platform. **Figure 3-6** shows the results of varying the concentration of trigger DNA during on-chip PiBA using (+/-) LAMP product. Images of the microwells are shown in

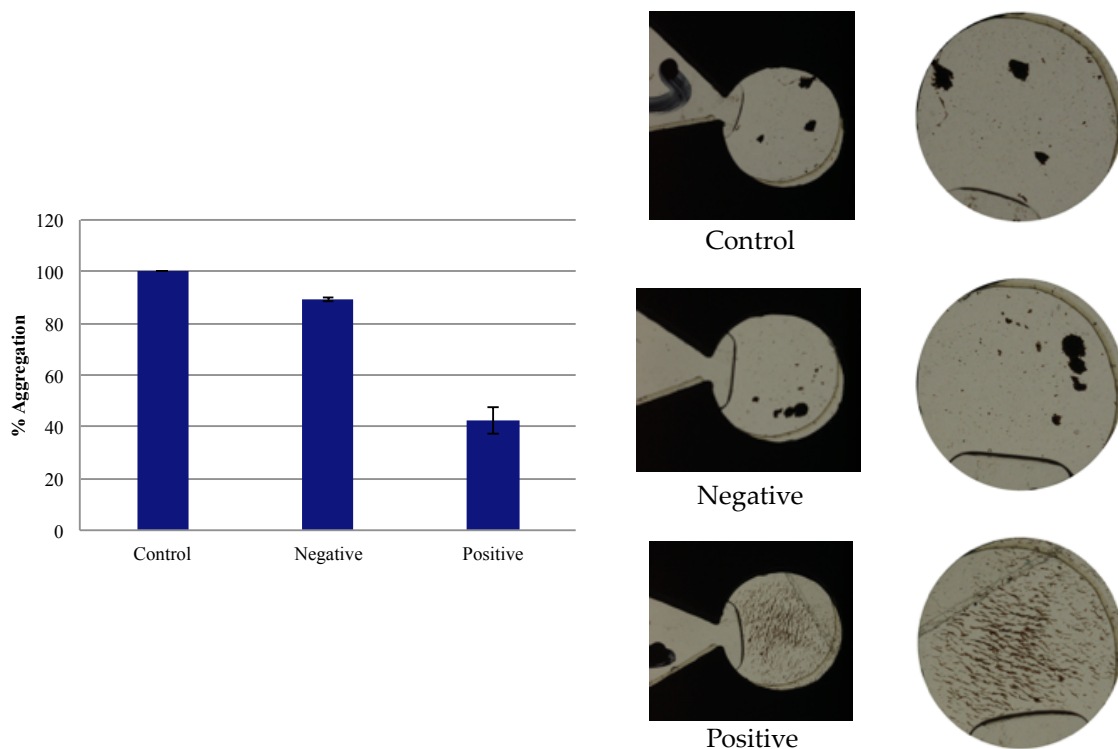


Figure 3-5. Effect of increased strength of magnet. RMF strength was increased, and spin intervals were shortened such that RMF is removed when beads are swept into the center of the well for better imaging. Algorithm is now able to properly differentiate between +/- LAMP samples.

Figure 3-6A, and the varying extent of aggregation allows for visual discrimination between (+/-) LAMP samples. In the 0.5 ng/ μ L images, the magnetic beads in both samples appear dispersed, likely due to the low concentration of trigger DNA that is unable to induce aggregation in the (-) LAMP sample. On the other hand, in the 10 ng/ μ L images, both samples show aggregated beads, which is indicative that the trigger DNA concentration is too high and is able to overcome the (+) LAMP product and induce aggregation regardless of the coating of the short amplicons on the surface of the beads. **Figure 3-6B** shows the results for the % Difference in Aggregation between (+/-) LAMP samples, and 2.5 ng/ μ L yielded the greatest discrimination between samples, therefore, this concentration was determined to be optimal for PiBA on PeT microdevices.

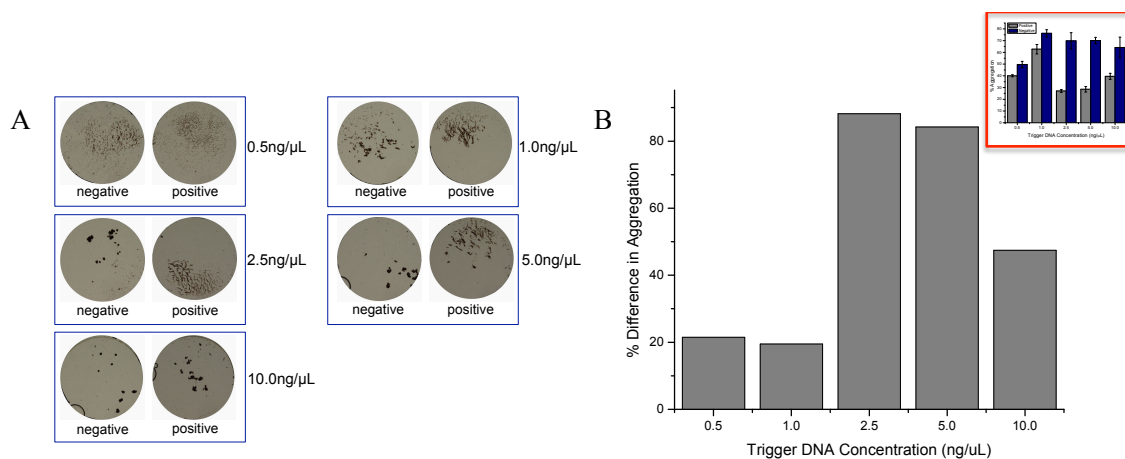


Figure 3-6. Optimization of trigger DNA concentration for on-chip PiBA. A) Images of microwells following on-chip PiBA. B) Results from on-chip PiBA with varying concentrations of trigger DNA. 2.5 ng/μL yields greatest % Difference in Aggregation between positive and negative. Inset shows results in terms of % Aggregation.

Results are presented in terms of ‘Percent Difference in Aggregation’ (**Equation 1**) and images are analyzed for the dark area present (high dark area corresponds to positive samples and inhibition of aggregation, while low dark area corresponds to negative samples and a high degree of aggregation). To arrive at this value, a ‘blank’ (i.e., a microchamber with magnetic beads, GdnHCl, and trigger DNA only) is used to normalize the data. Using this metric, a high % Difference in Aggregation signifies a positive sample, and a low % Difference in Aggregation signifies a negative sample. The inset of Figure 3-6B shows the results in terms of ‘Percent Aggregation’, which is calculated using **Equation 2**. Error bars show the standard deviation for each sample.

3.4.3 Validation of LAMP on PeT microdevices

For LAMP validation, the target organism was chosen to be *Clostridium difficile* (*C. difficile*). This pathogen is known to produce two primary toxins: toxin A and toxin B, representing the main virulence factors. These toxins belong to a group of large clostridial cytotoxins (LCT), a group that includes single-stranded protein toxins with

molecular weights ranging from 250-308 kDa.⁵¹ A third toxin was discovered in 1988, binary toxin CDT, and is associated with hypervirulent strains of *C. difficile*.⁵² CDT toxin is comprised of a catalytic component (CDTa) as well as a binding component (CDTb).⁵³ In order to target the gene encoding toxin B (tcdB gene) primers were found in the literature⁵⁴; however, primers were designed in-house to target the gene encoding the catalytic component of toxin CDT (cdtA gene).

Figure 3-7A shows the primer sequences used to target the *C. difficile* cdtA gene, present in strains R20291 and R20291 B-. Primers were designed using Primer Explorer Software. Loop forward (LF) and loop backward (LB) primers were added for increased speed and sensitivity of the LAMP reaction. Primers were first validated in-tube to optimize the amplification temperature, and 62°C for 40 minutes proved to be ideal for the cdtA primer set.

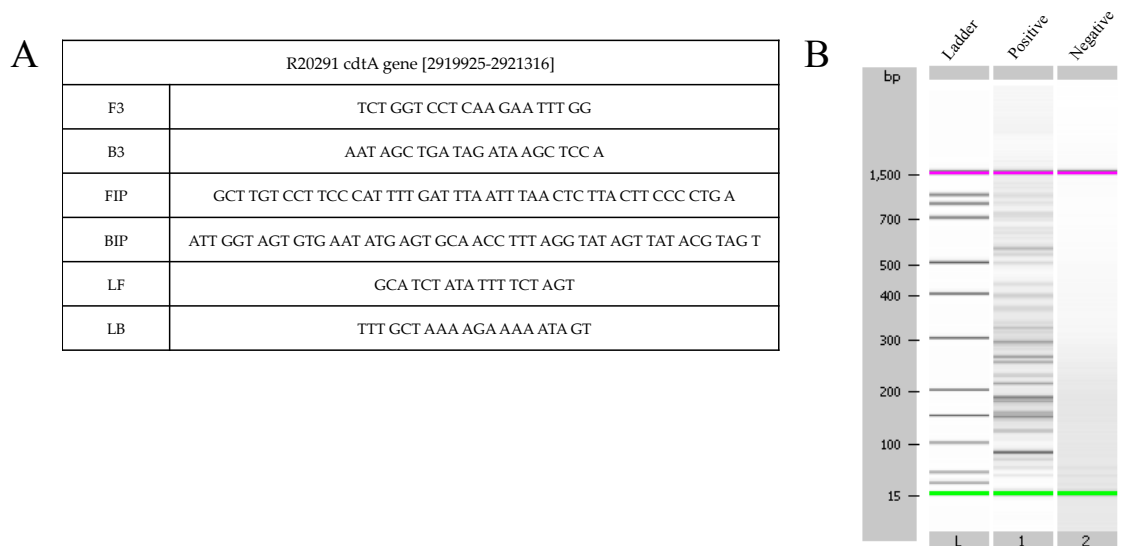


Figure 3-7. LAMP primer design and validation for cdtA primers. A) Primer sequences for cdtA gene LAMP primers. B) Results from 3 μ L on-chip amplification of cdtA primers with *C. difficile* strain R20291. Lane 1 is positive (containing template DNA), and lane 2 is negative (cdtA primers with no template DNA).

Figure 3-7B shows the microchip electrophoretic results (using Agilent Bioanalyzer) following a 3 μL on-chip amplification of strain R20291 using *cdtA* primers. LAMP product is generated in a range of sizes and therefore appears as a smear of bands (varying in size and, as a consequence, mobility).⁸ The sample was added to the PeT chip and amplified for 40 minutes using a heat block with a constant temperature of 62°C. The results indicate that the LAMP reaction is not inhibited by the PeT and, therefore, potentially amenable to point-of-care use in this manner due to the desirable properties of these PeT microfluidic devices.

Portability is one of the main advantages afforded by microfluidics; however, thorough reagent mixing is an important component that is required prior to amplification. Specifically, microfluidic mixing can be challenging due to the low Reynolds numbers and decreased turbulent mixing associated with fluid flow through microchannels. In these devices, diffusive mixing must be enhanced to achieve adequate mixing in shorter mixing channels.⁵⁵ Lee et al. has reviewed different types of microfluidic mixing; however, due to the small size of the device presented here, we sought to use a serpentine^{55,56} chip design that would allow for adequate on-chip reagent mixing upstream of isothermal amplification. Chips were designed and fabricated with three chambers: one for *C. difficile* template, one for the LAMP reagents (reaction mix and primers), and one in which the LAMP reaction takes place. **Figure 3-8** shows the chip design.

Initial studies were conducted using dye to analyze the on-chip mixing efficiency. **Figure 3-9A** shows results from these experiments (n=3). Chips were designed with

either a straight channel or a serpentine channel and filled with red (1 μL) and yellow (4 μL) dye, then spun at 2000 RPM for 10 seconds. The chips were then scanned and the standard deviation of the hue value was analyzed via histograms generated using Image J (**Figure 3-9B**). A sharp peak (bottom left, Fig. 3-9A) indicates the presence of a single color, and therefore thorough mixing, while a broad peak (bottom right, Fig. 3-9A) indicates the presence of more than one color, and therefore less efficient mixing. Histograms for red, yellow, and pre-mixed orange dye can be found in **Figure 3-9C**. These results indicate that the serpentine channel design yields more efficient mixing than the straight channel design.

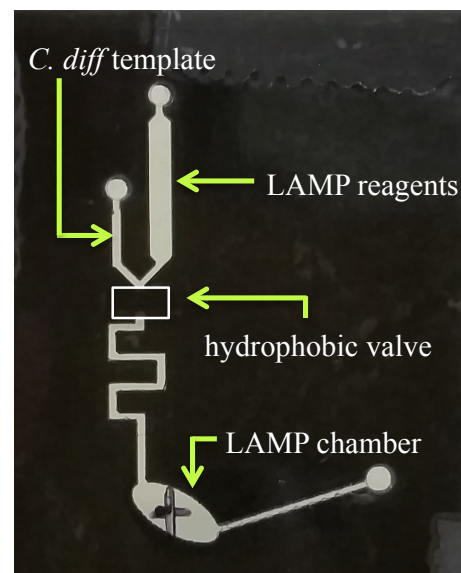


Figure 3-8. Chip design for on-chip LAMP. Design of PeT microdevice used for on-chip mixing and amplification. Three chambers were designed for: (i) *C. difficile* template, (ii) LAMP reagents (reaction mix and primers), and (iii) amplification.

Valving was achieved through the use of a hydrophobic toner patch⁵⁷ that kept the template and LAMP reagents in their respective chambers prior to mixing. The microdevice was spun at 2000 RPM for 10 seconds prior to amplification on a heat block. **Figure 3-10A** shows the results from 5 μL on-chip amplification of *C. difficile* strain 10463 with tcdB primers (40 minutes, 62°C) downstream of serpentine mixing, suggesting that this microfluidic architecture allows for adequate reagent mixing prior to LAMP. Furthermore, **Figure 3-10B** shows results from amplification downstream of either a serpentine channel or a straight channel. The amplification with serpentine

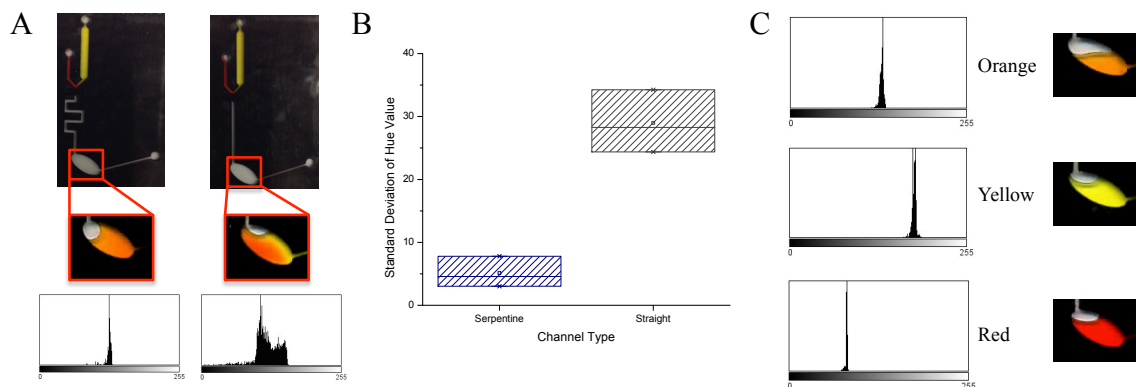


Figure 3-9. On-chip serpentine mixing validation. A) Results from dye studies indicating more efficient mixing with the serpentine channel design. Bottom left shows histogram of well-mixed serpentine channel design, and bottom right shows histogram of poorly-mixed straight channel design. B) Standard deviation of hue value was analyzed ($n=3$) to confirm more efficient mixing utilizing serpentine design. C) Histograms for each of the colored dyes used in the mixing study.

mixing was successful, while amplification with a straight channel was not, suggesting that this design is not only sufficient, but essential for adequate on-chip mixing.

3.4.4 Species-specific *C. difficile* detection and cell phone analysis

Up to this point, all PiBA results have been analyzed using a standard 15Mp camera and a *Mathematica* algorithm for image analysis (as described in Materials and Methods); however, a cell phone camera and custom-written app were investigated for primary image capture and analysis, which has the potential for true portability when integrated with PiBA. The app and the standard algorithm both interrogate images in the same manner, i.e., looking at the number of dark pixels in a given cropped area. Cropping is done manually, and involves dragging a box of adjustable size over the desired area. **Figure 3-11** shows the preliminary results for image analysis using the cell phone method. All (-) LAMP samples were below 5% dark area, whereas all (+) LAMP samples were above 30% dark area, providing good discrimination. Furthermore, each

sample (n=3) was interrogated with PiBA in triplicate, and each microwell was imaged and analyzed via cell phone in triplicate.

Prior to testing various strains of *C. difficile*, experiments were first performed to ensure that the *cdtA* primers were species-specific. **Figure 3-12A** shows the results of PiBA analysis of

three different bacterial species, *C. difficile*, *Salmonella*, and *Listeria* utilizing the *cdtA* primers and 200 genomic copies of starting template DNA (n=3). It has previously been established that the limit of detection for the PiBA assay falls between 2-20 genomic copies of starting template DNA.⁷ The *C. difficile* sample was the only sample found to be positive in these analyses, suggesting that the *cdtA* primers are indeed species-specific.

The *C. difficile* *tcdB* gene is relatively well conserved among strains, making it a common and viable target for detection of the bacterial pathogen.⁵⁸ Of the four strains tested here, all contain the *tcdB* gene and are therefore expected to amplify using the *tcdB* primer set.⁵⁴ **Figure 3-12B-C** shows the results of PiBA detection of toxin B in four

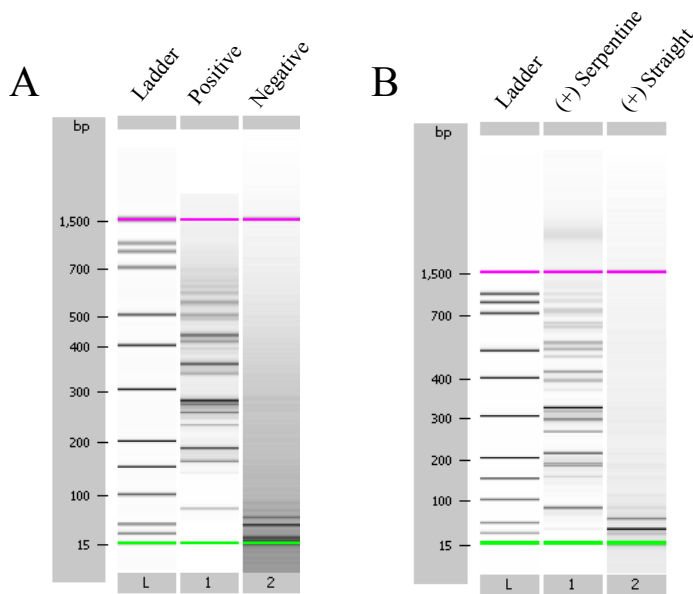


Figure 3-10. LAMP following on-chip serpentine mixing. A) Results from 5 μ L on-chip amplification downstream of serpentine mixing using *tcdB* primers and *C. difficile* strain 10463. Lane 1 is positive, Lane 2 is negative. B) Results from 5 μ L on-chip amplification with serpentine channel (lane 1) and with straight channel (lane 2), suggesting serpentine channel is essential for adequate mixing on-chip.

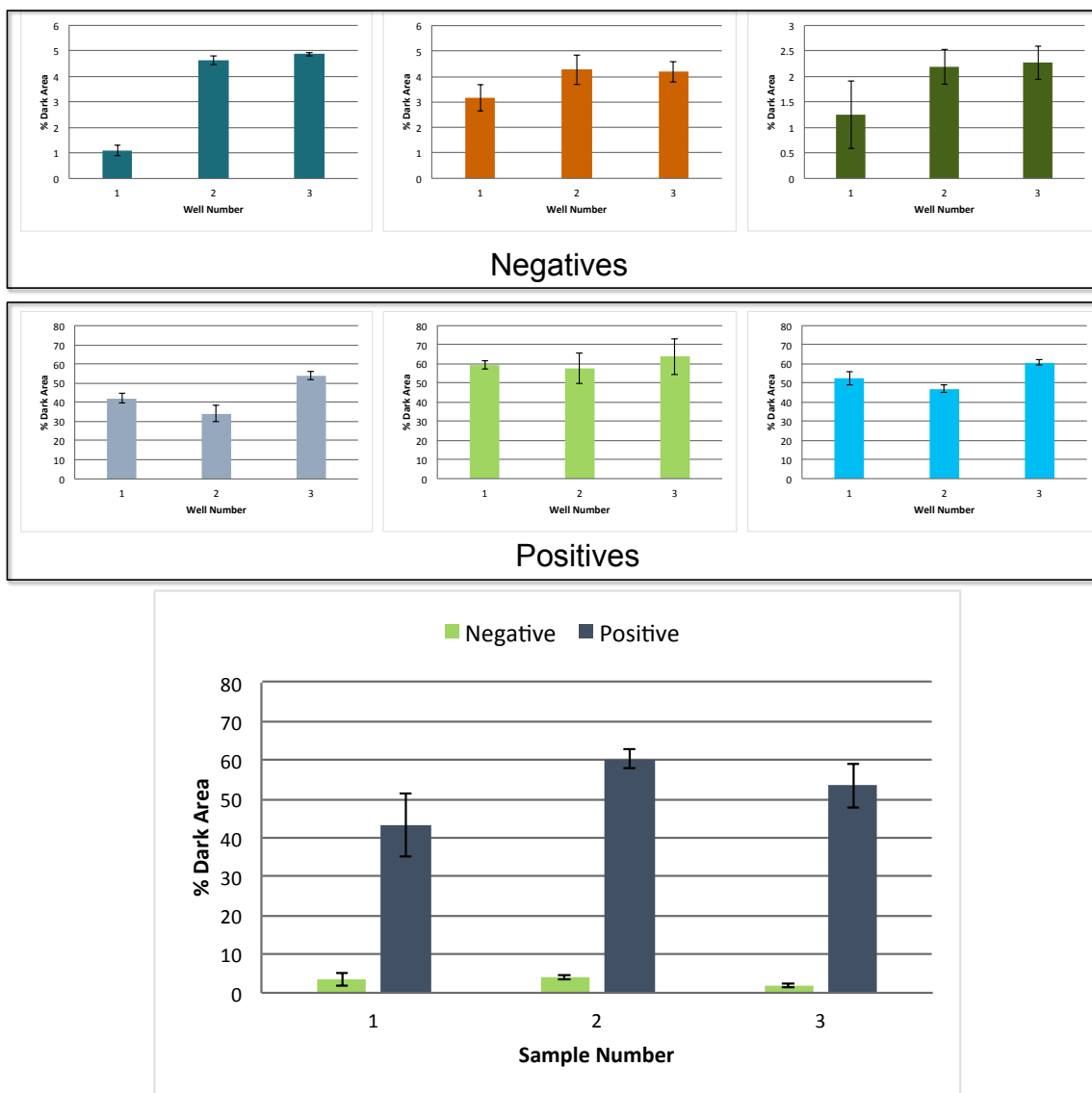


Figure 3-11. Validation of cell phone for image analysis. Results show good agreement among all negative and all positive samples ($n=3$). Data is presented as % Dark Area which is the raw data output of the app.

different *C. difficile* strains. These experiments were carried out with a starting template amount of 200 genomic copies per LAMP reaction ($n=3$). Following amplification, the LAMP products were run with PiBA to determine the presence or absence of the *C. difficile* target (*tcdB* gene). Here, the negative refers to a LAMP reaction containing no template DNA. Based on the PiBA results, all four strains are determined positive for the *tcdB* gene.

The microchambers were first analyzed using a 15 Mp camera and the images are shown in **Figure 3-12D**, demonstrating the naked eye differentiation between positive (non-aggregated) and negative (aggregated) samples when probed with the PiBA assay. Next, the images were analyzed using an Android cell phone mounted in a 3D-printed casing shown in **Figure 3-12E**. The case contains a small LED light and microchambers are manually aligned with the camera. Figure 3-12C shows the results of cell phone image analysis, and results agree well with those shown in Figure 3-12B. It is interesting to note that the discrimination between positive and negative samples is actually greater using the cell phone method, and this is likely due to the decreased resolution of the

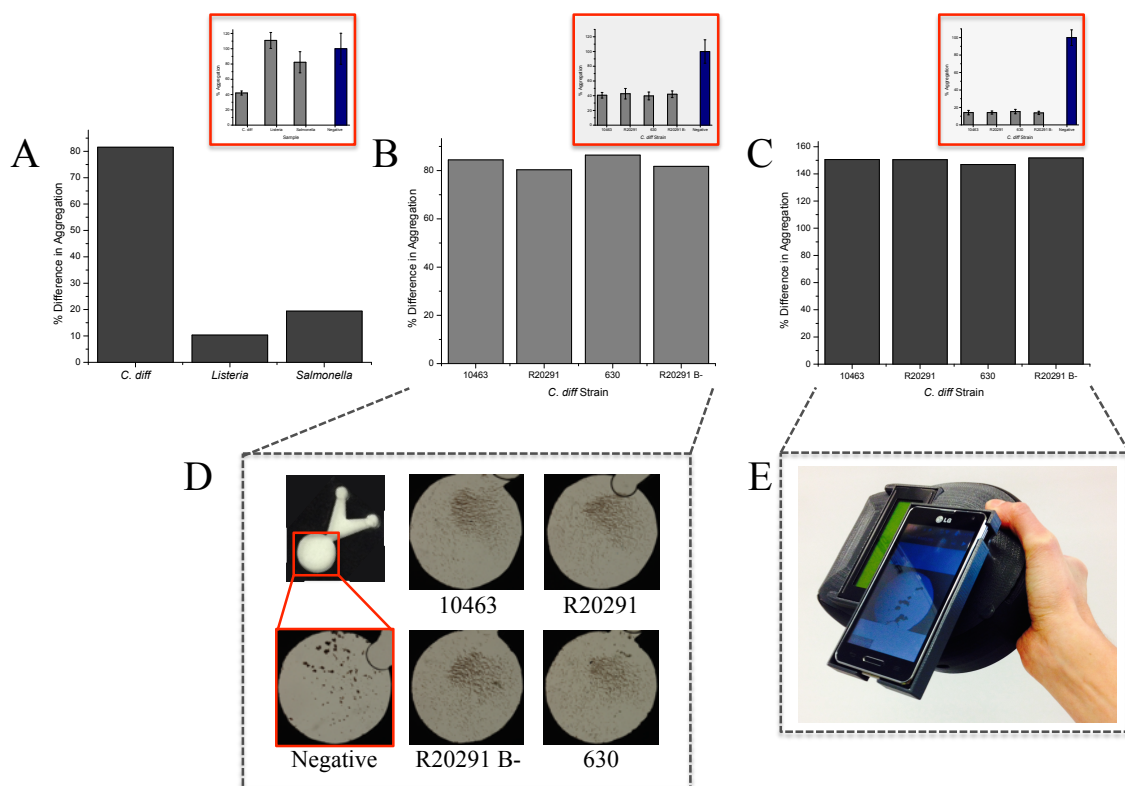


Figure 3-12. Species-specific detection and cell phone analysis. A) Results showing species specificity of *cdtA* LAMP primers. B) Results from on-chip PiBA using 15 Mp camera and Mathematica algorithm for image analysis. C) Results from on-chip PiBA using Android cell phone and custom-written application (app) for image analysis. For B and C, $n=3$ (each of 3 samples analyzed 3 times with PiBA assay). D) Images of microwells following on-chip PiBA using 15 Mp camera. E) 3D printed casing with lid-mounted cell phone for image analysis. Insets show results in % Aggregation.

images captured. Decreased resolution allows for a more pronounced difference between aggregation and inhibited aggregation in terms of dark area present, as the resolution of the aggregates is not as important as simply the number of dark pixels that are comprised within the aggregate. This phenomenon will be explored further in future studies.

3.4.5 Strain-specific *C. difficile* detection

The CDT binary toxin is associated with hypervirulent strains of *C. difficile*, making it an important clinical target.⁵¹ In many cases, it is critical to be able to

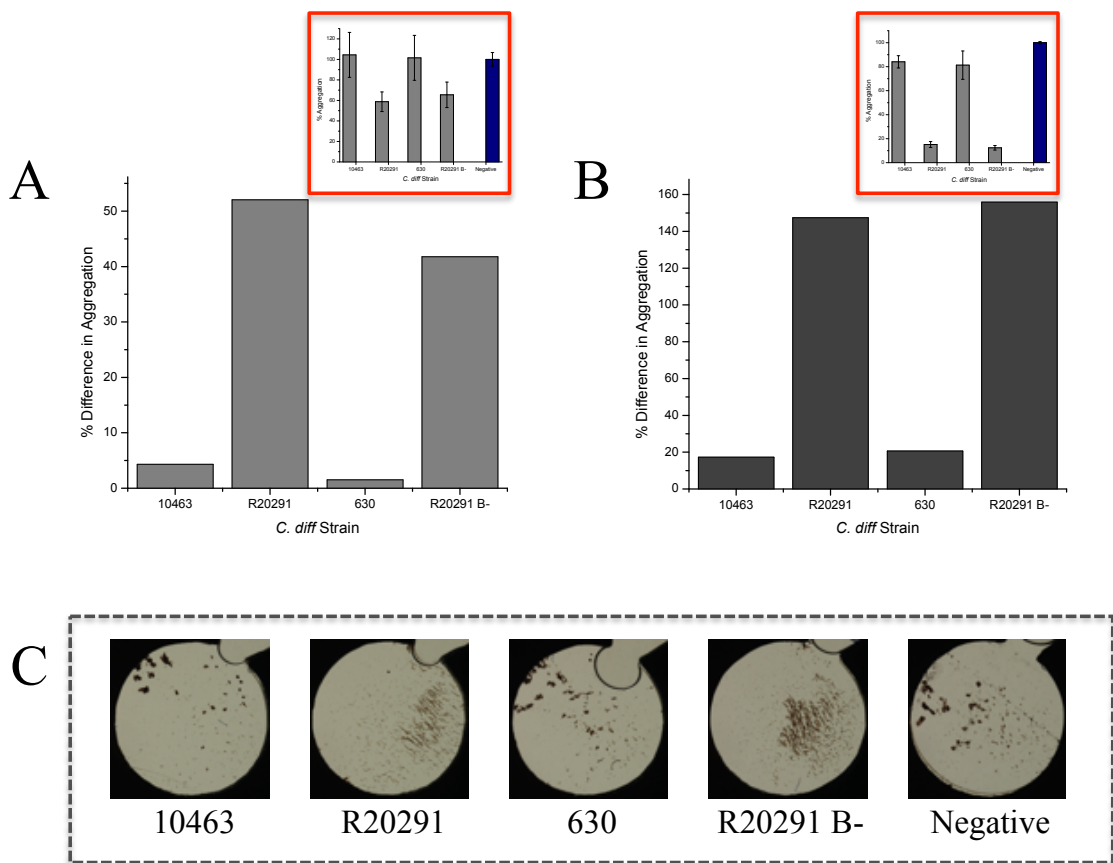


Figure 3-13. Strain-specific *C. difficile* detection. A) Results from on-chip PiBA using 15 Mp camera and Mathematica algorithm for image analysis. B) Results from on-chip PiBA using Android cell phone and custom-written application (app) for image analysis. For A and B, $n=3$ (each of 3 samples analyzed 3 times with PiBA assay) C) Images of microwells following on-chip PiBA using 15 Mp camera. Insets show results in % Aggregation.

differentiate between non-hypervirulent and hypervirulent strains of the bacteria, and for this reason we chose to target the *cdtA* gene using PiBA. Of the four *C. difficile* strains tested, strains 10463 and 630 contain a 2kB deletion in the *cdtA* gene, whereas strains R20291 and R20291 B- do not. **Figure 3-13A-B** show the results of amplification of all four strains using the *cdtA* primer set shown in Figure 1A, again with 200 genomic copies of starting template DNA (n=3).

Figure 3-13A shows the results of image analysis using the 15 Mp camera, while Figure 3-13B shows the results from the cell phone method. Following PiBA analysis, only strains R20291 and R20291 B- are found to be positive for the *cdtA* gene. These results are significant because they suggest that we are not only able to detect the presence of *C. difficile*, but also able to distinguish between non-hypervirulent (10463 and 630) and hypervirulent (R20291 and R20291 B-) strains of the bacteria.

3.5 Conclusions

Clostridium difficile is an important pathogen because of the predominant role it plays in hospital-acquired infections, and the emergence of hypervirulent strains of the bacteria. An opportunistic pathogen, *C. difficile* is capable of taking over the healthy gastrointestinal flora of an individual, often leading to antibiotic resistance and further complications. Point-of-care detection of the bacteria is important because of the nature of the infection, often occurring in hospitals and requiring immediate treatment at the patient's bedside. Additionally, the ability to monitor a *C. difficile* infection from home

would allow for patients to test themselves and transmit their results to a physician for interpretation and rapid decision-making in terms of diagnosis and treatment.

Here, we have demonstrated the viability of our previously described magnetic bead aggregation assay for use with an inexpensive and commercially available substrate, polyester. Utilizing the print, cut, and laminate method for microdevice fabrication, the cost to manufacture a disposable chip is less than \$1.^{59, 60} Furthermore, by utilizing centrifugal force and hydrophobic toner patches the device requires no external pumps or valves for fluid flow control. Detection is achieved through the use of a simple camera and image analysis program, circumventing the need for expensive fluors and labels commonly associated with other NAAT detection modalities. All of these characteristics lend themselves toward complete integration of a system that is rapid, sensitive, and portable for use in point-of-care settings.

While both amplification and detection have proven successful when carried out on a PeT microdevice, future work will be done toward the full integration of both processes onto a single microdevice housed completely in the 3D-printed casing shown in this work.

3.6 References

1. Rossolini, G. M.; Arena, F.; Pecile, P.; Pollini, S., Update on the antibiotic resistance crisis. *Current Opinion in Pharmacology* **2014**, *18*, 56-60.

2. Beatson, S. A.; Walker, M. J., Tracking antibiotic resistance. *Science* **2014**, *345* (6203), 1454-1455.
3. Fischbach, M. A.; Walsh, C. T., Antibiotics for Emerging Pathogens. *Science* **2009**, *325* (5944), 1089-1093.
4. Surawicz, C. M.; Brandt, L. J.; Binion, D. G.; Ananthkrishnan, A. N.; Curry, S. R.; Gilligan, P. H.; McFarland, L. V.; Mellow, M.; Zuckerbraun, B. S., Guidelines for Diagnosis, Treatment, and Prevention of Clostridium difficile Infections. *American Journal of Gastroenterology* **2013**, *108* (4), 478-498.
5. Leland, D. S.; Ginocchio, C. C., Role of cell culture for virus detection in the age of technology. *Clinical Microbiology Reviews* **2007**, *20* (1), 49-78.
6. Kiilerich-Pedersen, K.; Dapra, J.; Cherre, S.; Rozlosnik, N., High sensitivity point-of-care device for direct virus diagnostics. *Biosensors & Bioelectronics* **2013**, *49*, 374-379.
7. DuVall, J. A.; Borba, J. C.; Shafagati, N.; Luzader, D.; Shukla, N.; Li, J. Y.; Kehn-Hall, K.; Kendall, M. M.; Feldman, S. H.; Landers, J. P., Optical Imaging of Paramagnetic Bead-DNA Aggregation Inhibition Allows for Low Copy Number Detection of Infectious Pathogens. *Plos One* **2015**, *10* (6), 16.
8. Notomi, T.; Okayama, H.; Masubuchi, H.; Yonekawa, T.; Watanabe, K.; Amino, N.; Hase, T., Loop-mediated isothermal amplification of DNA. *Nucleic Acids Research* **2000**, *28* (12), 7.

9. Manz, A.; Graber, N.; Widmer, H. M., MINIATURIZED TOTAL CHEMICAL-ANALYSIS SYSTEMS - A NOVEL CONCEPT FOR CHEMICAL SENSING. *Sensors and Actuators B-Chemical* **1990**, *1* (1-6), 244-248.
10. Thompson, B. L.; Ouyang, Y. W.; Duarte, G. R. M.; Carrilho, E.; Krauss, S. T.; Landers, J. P., Inexpensive, rapid prototyping of microfluidic devices using overhead transparencies and a laser print, cut and laminate fabrication method. *Nature Protocols* **2015**, *10* (6), 875-886.
11. Yager, P.; Edwards, T.; Fu, E.; Helton, K.; Nelson, K.; Tam, M. R.; Weigl, B. H., Microfluidic diagnostic technologies for global public health. *Nature* **2006**, *442* (7101), 412-418.
12. Reyes, D. R.; Iossifidis, D.; Auroux, P. A.; Manz, A., Micro total analysis systems. 1. Introduction, theory, and technology. *Analytical Chemistry* **2002**, *74* (12), 2623-2636.
13. Mairhofer, J.; Roppert, K.; Ertl, P., Microfluidic Systems for Pathogen Sensing: A Review. *Sensors* **2009**, *9* (6), 4804-4823.
14. Lagally, E. T.; Scherer, J. R.; Blazej, R. G.; Toriello, N. M.; Diep, B. A.; Ramchandani, M.; Sensabaugh, G. F.; Riley, L. W.; Mathies, R. A., Integrated portable genetic analysis microsystem for pathogen/infectious disease detection. *Analytical Chemistry* **2004**, *76* (11), 3162-3170.

15. Easley, C. J.; Karlinsey, J. M.; Bienvenue, J. M.; Legendre, L. A.; Roper, M. G.; Feldman, S. H.; Hughes, M. A.; Hewlett, E. L.; Merkel, T. J.; Ferrance, J. P.; Landers, J. P., A fully integrated microfluidic genetic analysis system with sample-in-answer-out capability. *Proceedings of the National Academy of Sciences of the United States of America* **2006**, *103* (51), 19272-19277.
16. Beyor, N.; Yi, L. N.; Seo, T. S.; Mathies, R. A., Integrated Capture, Concentration, Polymerase Chain Reaction, and Capillary Electrophoretic Analysis of Pathogens on a Chip. *Analytical Chemistry* **2009**, *81* (9), 3523-3528.
17. Dharmasiri, U.; Witek, M. A.; Adams, A. A.; Osiri, J. K.; Hupert, M. L.; Bianchi, T. S.; Roelke, D. L.; Soper, S. A., Enrichment and Detection of Escherichia coli O157:H7 from Water Samples Using an Antibody Modified Microfluidic Chip. *Analytical Chemistry* **2010**, *82* (7), 2844-2849.
18. Chen, Y. W.; Wang, H.; Hupert, M.; Witek, M.; Dharmasiri, U.; Pingle, M. R.; Barany, F.; Soper, S. A., Modular microfluidic system fabricated in thermoplastics for the strain-specific detection of bacterial pathogens. *Lab on a Chip* **2012**, *12* (18), 3348-3355.
19. Kim, T. H.; Park, J.; Kim, C. J.; Cho, Y. K., Fully Integrated Lab-on-a-Disc for Nucleic Acid Analysis of Food-Borne Pathogens. *Analytical Chemistry* **2014**, *86* (8), 3841-3848.
20. Felbel, J.; Reichert, A.; Kielpinski, A.; Urban, M.; Henkel, T.; Hafner, N.; Durst, M.; Weber, J., Reverse transcription-polymerase chain reaction (RT-PCR) in flow-

through micro-reactors: Thermal and fluidic concepts. *Chemical Engineering Journal* **2008**, *135*, S298-S302.

21. Csordas, A. I.; Delwiche, M. J.; Barak, J. D., Nucleic acid sensor and fluid handling for detection of bacterial pathogens. *Sensors and Actuators B-Chemical* **2008**, *134* (1), 1-8.

22. Mujika, M.; Arana, S.; Castano, E.; Tijero, M.; Vilares, R.; Ruano-Lopez, J. M.; Cruz, A.; Sainz, L.; Berganza, J., Magnetoresistive immunosensor for the detection of *Escherichia coli* O157:H7 including a microfluidic network. *Biosensors & Bioelectronics* **2009**, *24* (5), 1253-1258.

23. Makamba, H.; Kim, J. H.; Lim, K.; Park, N.; Hahn, J. H., Surface modification of poly(dimethylsiloxane) microchannels. *Electrophoresis* **2003**, *24* (21), 3607-3619.

24. Chin, C. D.; Linder, V.; Sia, S. K., Lab-on-a-chip devices for global health: Past studies and future opportunities. *Lab on a Chip* **2007**, *7* (1), 41-57.

25. Liu, Q.; Chernish, A.; DuVall, J. A.; Ouyang, Y. W.; Li, J. Y.; Qian, Q.; Bazydlo, L. A. L.; Haverstick, D. M.; Landers, J. P., The ART mu S: a novel microfluidic CD4+T-cell enumeration system for monitoring antiretroviral therapy in HIV patients. *Lab on a Chip* **2016**, *16* (3), 506-514.

26. Balagadde, F. K.; You, L. C.; Hansen, C. L.; Arnold, F. H.; Quake, S. R., Long-term monitoring of bacteria undergoing programmed population control in a microchemostat. *Science* **2005**, *309* (5731), 137-140.

27. Futai, N.; Gu, W.; Song, J. W.; Takayama, S., Handheld recirculation system and customized media for microfluidic cell culture. *Lab on a Chip* **2006**, *6* (1), 149-154.
28. Vilkner, T.; Janasek, D.; Manz, A., Micro total analysis systems. Recent developments. *Analytical Chemistry* **2004**, *76* (12), 3373-3385.
29. Fiorini, G. S.; Chiu, D. T., Disposable microfluidic devices: fabrication, function, and application. *Biotechniques* **2005**, *38* (3), 429-446.
30. Unger, M. A.; Chou, H. P.; Thorsen, T.; Scherer, A.; Quake, S. R., Monolithic microfabricated valves and pumps by multilayer soft lithography. *Science* **2000**, *288* (5463), 113-116.
31. Becker, H.; Gartner, C., Polymer microfabrication technologies for microfluidic systems. *Analytical and Bioanalytical Chemistry* **2008**, *390* (1), 89-111.
32. Ren, K. N.; Zhou, J. H.; Wu, H. K., Materials for Microfluidic Chip Fabrication. *Accounts of Chemical Research* **2013**, *46* (11), 2396-2406.
33. McDonald, J. C.; Whitesides, G. M., Poly(dimethylsiloxane) as a material for fabricating microfluidic devices. *Accounts of Chemical Research* **2002**, *35* (7), 491-499.
34. Gorkin, R.; Park, J.; Siegrist, J.; Amasia, M.; Lee, B. S.; Park, J. M.; Kim, J.; Kim, H.; Madou, M.; Cho, Y. K., Centrifugal microfluidics for biomedical applications. *Lab on a Chip* **2010**, *10* (14), 1758-1773.

35. Krauss, S. T.; Remcho, T. P.; Monazami, E.; Thompson, B. L.; Reinke, P.; Begley, M. R.; Landers, J. P., Inkjet printing on transparency films for reagent storage with polyester-toner microdevices. *Analytical Methods* **2016**, *8* (39), 7061-7068.
36. Krauss, S. T.; Remcho, T. P.; Lipes, S. M.; Aranda, R.; Maynard, H. P.; Shukla, N.; Li, J.; Tontarski, R. E.; Landers, J. P., Objective Method for Presumptive Field-Testing of Illicit Drug Possession Using Centrifugal Microdevices and Smartphone Analysis. *Analytical Chemistry* **2016**, *88* (17), 8689-8697.
37. Thompson, B. L.; Gilbert, R. J.; Mejia, M.; Shukla, N.; Haverstick, D. M.; Garner, G. T.; Landers, J. P., Hematocrit analysis through the use of an inexpensive centrifugal polyester-toner device with finger-to-chip blood loading capability. *Analytica Chimica Acta* **2016**, *924*, 1-8.
38. Bartlett, J. G.; Taylor, N. S.; Chang, T. W.; Dzink, J. A., CLINICAL AND LABORATORY OBSERVATIONS IN CLOSTRIDIUM DIFFICILE COLITIS. *American Journal of Clinical Nutrition* **1980**, *33* (11), 2521-2526.
39. Bartlett, J. G., CLOSTRIDIUM-DIFFICILE - CLINICAL CONSIDERATIONS. *Reviews of Infectious Diseases* **1990**, *12*, S243-S251.
40. Gilligan, P. H.; McCarthy, L. R.; Genta, V. M., RELATIVE FREQUENCY OF CLOSTRIDIUM DIFFICILE IN PATIENTS WITH DIARRHEAL DISEASE. *Journal of Clinical Microbiology* **1981**, *14* (1), 26-31.

41. Lyerly DM, K. H., Wilkins TD, Clostridium difficile: its disease and toxins. *Clinical Microbiology Reviews* **1988**, *1* (1), 1-18.
42. Staneck, J. L.; Weckbach, L. S.; Allen, S. D.; Siders, J. A.; Gilligan, P. H.; Coppitt, G.; Kraft, J. A.; Willis, D. H., Multicenter evaluation of four methods for Clostridium difficile detection: ImmunoCard C-difficile, cytotoxin assay, culture, and latex agglutination. *Journal of Clinical Microbiology* **1996**, *34* (11), 2718-2721.
43. DM, L., Clostridium difficile testing. *Clinical Microbiology Newsletter* **1995**, *17* (3), 17-22.
44. McDonald, L. C.; Owings, M.; Jernigan, D. B., Clostridium difficile infection in patients discharged from US short-stay hospitals, 1996-2003. *Emerging Infectious Diseases* **2006**, *12* (3), 409-415.
45. Tsaloglou, M. N.; Watson, R. J.; Rushworth, C. M.; Zhao, Y.; Niu, X.; Sutton, J. M.; Morgan, H., Real-time microfluidic recombinase polymerase amplification for the toxin B gene of Clostridium difficile on a SlipChip platform. *Analyst* **2015**, *140* (1), 258-264.
46. Seise, B.; Pahlow, S.; Klapper, M.; Pollok, S.; Seyboldt, C.; Neubauer, H.; Weber, K.; Popp, J., Clostridium spp. discrimination with a simple bead-based fluorescence assay. *Analytical Methods* **2014**, *6* (9), 2943-2949.
47. Ju, Q.; Noor, M. O.; Krull, U. J., Paper-based biodetection using luminescent nanoparticles. *Analyst* **2016**, *141* (10), 2838-2860.

48. Foudeh, A. M.; Didar, T. F.; Veres, T.; Tabrizian, M., Microfluidic designs and techniques using lab-on-a-chip devices for pathogen detection for point-of-care diagnostics. *Lab on a Chip* **2012**, *12* (18), 3249-3266.
49. Cho, Y. K.; Lee, J. G.; Park, J. M.; Lee, B. S.; Lee, Y.; Ko, C., One-step pathogen specific DNA extraction from whole blood on a centrifugal microfluidic device. *Lab on a Chip* **2007**, *7* (5), 565-573.
50. Nelson, D. A.; Strachan, B. C.; Sloane, H. S.; Li, J. Y.; Landers, J. P., Dual-force aggregation of magnetic particles enhances label-free quantification of DNA at the sub-single cell level. *Analytica Chimica Acta* **2014**, *819*, 34-41.
51. Rupnik, M.; Grabnar, M.; Geric, B., Binary toxin producing *Clostridium difficile* strains. *Anaerobe* **2003**, *9* (6), 289-294.
52. Popoff, M. R.; Rubin, E. J.; Gill, D. M.; Boquet, P., ACTIN-SPECIFIC ADP-RIBOSYLTRANSFERASE PRODUCED BY A CLOSTRIDIUM-DIFFICILE STRAIN. *Infection and Immunity* **1988**, *56* (9), 2299-2306.
53. Perelle, S.; Gibert, M.; Bourlioux, P.; Corthier, G.; Popoff, M. R., Production of a complete binary toxin (actin-specific ADP-ribosyltransferase) by *Clostridium difficile* CD196. *Infection and Immunity* **1997**, *65* (4), 1402-1407.
54. Kato H, Y. T., Kato H, Arakawa Y, Rapid and Simple Method for Detecting the Toxin B Gene of *Clostridium difficile* in Stool Specimens by Loop-Mediated Isothermal Amplification. *Journal of Clinical Microbiology* **2005**, *43* (12), 6108-6112.

55. Lee, C. Y.; Chang, C. L.; Wang, Y. N.; Fu, L. M., Microfluidic Mixing: A Review. *International Journal of Molecular Sciences* **2011**, *12* (5), 3263-3287.
56. La, M.; Park, S. J.; Kim, H. W.; Park, J. J.; Ahn, K. T.; Ryew, S. M.; Kim, D. S., A centrifugal force-based serpentine micromixer (CSM) on a plastic lab-on-a-disk for biochemical assays. *Microfluidics and Nanofluidics* **2013**, *15* (1), 87-98.
57. Ouyang, Y. W.; Wang, S. B.; Li, J. Y.; Riehl, P. S.; Begley, M.; Landers, J. P., Rapid patterning of 'tunable' hydrophobic valves on disposable microchips by laser printer lithography. *Lab on a Chip* **2013**, *13* (9), 1762-1771.
58. Voth, D. E.; Ballard, J. D., Clostridium difficile toxins: Mechanism of action and role in disease. *Clinical Microbiology Reviews* **2005**, *18* (2), 247-+.
59. Ouyang, Y.; Duarte, G. R. M.; Poe, B. L.; Riehl, P. S.; dos Santos, F. M.; Martin-Didonet, C. C. G.; Carrilho, E.; Landers, J. P., A disposable laser print-cut-laminate polyester microchip for multiplexed PCR via infra-red-mediated thermal control. *Analytica Chimica Acta* **2015**, *901*, 59-67.
60. do Lago, C. L.; da Silva, H. D. T.; Neves, C. A.; Brito-Neto, J. G. A.; da Silva, J. A. F., A dry process for production of microfluidic devices based on the lamination of laser-printed polyester films. *Analytical Chemistry* **2003**, *75* (15), 3853-3858.

Optimization of a novel Peltier clamping system and associated microdevice for multiplex PCR: applications in human identification

4.1 Overview

We demonstrate the capabilities of a centrifugal polyethylene terephthalate toner (PeT) microdevice for integrated on-chip reagent mobilization, mixing, and PCR amplification for genetic analysis of short tandem repeats (STR). Fluid flow, including reagent mobilization and mixing, is achieved by centrifugal force, eliminating the need for bulky instrumentation. The use of a passive valve also eradicates the need for extra hardware and simplifies the chip and the device design. A custom-built system is capable of thermocycling through a dual Peltier clamping system, as well as variable rate spinning with a DC motor. A multiplex PCR amplification of alleles associated with 18 genomic loci was successfully performed on-chip, followed by capillary electrophoretic separation, which showed efficient amplification of DNA from multiple sources. The genetic profiles generated were 100% concordant with those obtained using conventional PCR methods. The resultant system represents a novel microfluidic PCR amplification platform that uses inexpensive PCR microdevices that are simple to fabricate, yet effective for complex, multiplexed PCR.

4.2 Introduction

Human identification has been used for many decades, dating as far back as the 1800s when fingerprints were first used to identify criminals.¹ Since the discovery of the

molecular structure of DNA in 1953², many advances have been made toward new methods for human identification. In the early 1980s, “minisatellite” regions of the human genome were discovered and postulated to be an effective tool to identify molecular differences among individuals based on their DNA.³ These DNA sequences, known as variable number of tandem repeats (VNTRs), were shown to be repeated throughout the genome and the number of repeats was found to be unique to a given individual. Shortly thereafter, in 1991, fluorescent short tandem repeat (STR) marker detection was first described.^{4,5} Whereas VNTRs were quite long, with repeats of several hundred bases, STRs are comprised of short repeats consisting of 1-6 nucleotides.⁶

The same flanking regions are found across the entire human genome, regardless of the individual, making STR markers very easy to target and amplify using PCR primers (see **Figure 4-1**). At a given genetic marker each individual has two alleles, thereby leading to polymorphism owing to these hypervariable DNA regions. When multiple markers are analyzed simultaneously, this method allows for a very high degree of discrimination among individuals. Specific STR markers have been chosen and

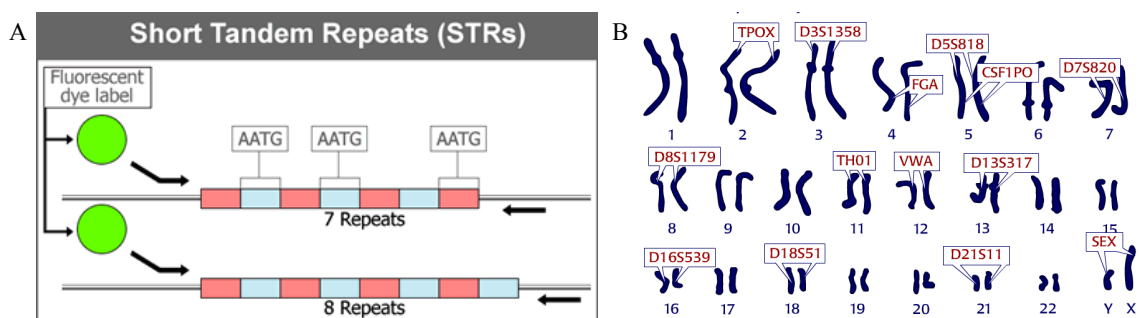


Figure 4-1. Diagram of short tandem repeats (STRs). A) The number of repeats can be the same on both alleles (homozygous) or different (heterozygous), and changes for each individual. B) Interrogating multiple STR markers within the genome allows for a high degree of discrimination among individuals. The Core 13 CODIS loci (plus Amelogenin) are shown, along with which chromosome each loci is found on.

characterized to be used for human identification, and the Combined DNA Index System (CODIS)⁷ is used in the United States, whereas a different database is used in Europe (European Standard Set (ESS)).⁸ The newest STR kits combine all the markers from both databases, yielding a discriminatory power of 10^{14} times greater than the total population on Earth.

Amplification of STRs using PCR is only one step in the total analysis required to create a unique STR profile. DNA has to be extracted from biological samples prior to PCR amplification, and several extraction techniques are commonly used: phenol-chloroform, solid-phase, and ZyGEM.⁹⁻¹² The phenol-chloroform method works by partitioning proteins into an organic layer and nucleic acids into an aqueous layer.¹³ Solid phase extraction (SPE) uses a silica-based solid phase to reversibly bind DNA under high salt conditions. Lastly, ZyGEM extraction utilizes a thermostable enzyme that is able to liberate DNA from the cell.^{14, 15}

Following DNA extraction and PCR amplification of STRs, the fragments must be separated and detected. Capillary electrophoresis (CE) has been, and continues to be, the preferred method for separation of STR fragments.^{16, 17} The underlying principle of this method lies in the negative charge associated with DNA, which, when an electric field is applied, causes the DNA to migrate through a capillary toward a positive electrode (anode). Larger DNA fragments take longer to migrate through a sieving matrix (polymer) than short fragments; therefore, size-based separation is achieved using CE. Compared to slab gels, this method affords higher voltages, and thus a faster DNA

migration rate.¹³ Furthermore, CE systems contain a detection system and a laser excitation source for detection of fluorescently labeled PCR amplicons.

Although the field of human identification has progressed significantly since its inception, the entire analytical process required for generating a STR profile requires multiple instruments (centrifuge, thermocycler, CE, etc.) and individual steps are often performed in different rooms to mitigate the effects of DNA contamination. The time associated with the STR analysis, from raw sample to result, is often between 7-10 hours if the sample is analyzed singularly. However, this time frame is often much longer when samples must be batched, and a significant backlog of samples exists in many laboratories.

Rapid DNA has emerged as a primary interest in the forensics community to address these concerns. The aim of this field is threefold: (i) reduce sample backlog, (ii) provide rapid sample-to-answer STR analysis, and (iii) simplify the analytical processes so they can be performed by untrained users. Specifically, Rapid DNA is defined by the FBI as the fully automated process of generating a STR profile from a reference buccal swab, known as “swab in-profile out”.¹⁸ Furthermore, the process must consist of automated extraction, amplification, separation, detection, and allele calling. In essence, the entire laboratory is reduced to a single instrument capable of performing each step required for generation of a STR profile. Several attempts at a Rapid DNA system have been made, and these will be discussed further in Chapter 5.

To meet the demands of Rapid DNA, the microfluidic regime has been investigated, owing to the distinct advantages of this platform that have been described in

previous Chapters (cost reduction, faster analysis times, lower reagent/sample consumption, portability, etc.). Microfluidic systems for STR analysis enable the fluidic integration of each step in the process, resulting in faster analysis times (with the goal of less than 90 minutes) and a significantly decreased risk of sample loss or contamination. Although the ultimate goal of this work is to create a fully-integrated microdevice with “swab in-profile out” capabilities, stand-alone microfluidic systems for each of the individual processes is not without merit. These stand-alone systems can be integrated into the conventional workflow in an effort to drastically reduce the processing time.

The focus of the work presented in this Chapter is on microfluidic PCR, and integration with DNA extraction and separation will be discussed in Chapter 5. Since DNA amplification is a key step in STR profile generation, extensive work has been done toward adapting PCR to the microscale. From this work, three major classes of microfluidic PCR have emerged: stationary, continuous-flow, and droplet. Briefly, stationary PCR just refers to conventional PCR that has been miniaturized to the microfluidic platform, and the reagents are kept stationary in a PCR chamber during thermocycling. The first example of this was in 1993 when Northrup et al.¹⁹ demonstrated a silicon-based PCR chip with a chamber volume of 25-50 μL , effectively increasing the speed of the reaction, while decreasing the power consumption. The review by Zhang et al.²⁰ thoroughly discusses the research that has been devoted to stationary microfluidic PCR in the ensuing years. Continuous flow PCR is capable of moving the PCR liquid through various zones on a microfluidic device that are set to specific temperatures, thereby achieving rapid thermocycling. Nakano et al.²¹ was the first group to demonstrate continuous flow PCR, and this was accomplished in 10% of

the time required for conventional PCR, while Kopp et al.²² demonstrated this phenomenon on a glass microchip. Lastly, droplet-based PCR is generally suited toward single molecule and low copy number DNA amplification. Recently, Geng et al.²³ has demonstrated microfluidic droplet PCR for forensic single cell analysis, with the main advantage of this system relying on the rapid thermocycling possible for such small volumes of PCR reagents (picoliter to nanoliter range).

While there are obvious advantages to the incorporation of LOC devices for PCR, the main disadvantage is the large surface area to volume ratio, which increases surface area effects. Namely, this increases the likelihood for various components of the PCR reaction mixture, such as polymerase, dNTPs, primers, and MgCl₂, to adsorb to the surface of the microdevice and adversely affect the efficiency of the reaction.²⁴ This phenomenon will be explored further in the Results and Discussion section.

The review by Zhang, et al.²⁰ presented microfluidic PCR devices that had been shown to be functional and it was clear that the substrates and associated instrumentation were not readily translatable to a form for rapid, cost-effective, and automated analysis, especially if integrated with upstream and downstream analytical processes. The goal with most microfluidic platforms is to reduce their footprint to that approaching the size of the microchip. However, this is difficult when bulky external hardware is required for functionality²⁵, e.g., on-chip mobilization of fluids driven by air/vacuum pumps and active valves that require mechanical actuation.²⁶ Utilizing this approach, the systems can quickly become complex and, as a result, expensive.

The focus of this work is a simple, spin-based PCR system utilizing inexpensive polyester microdevices that, when encased by minimal external hardware, is capable of exquisite fluid flow control for reagent mobilization and mixing, driven solely by centrifugal force. Centrifugal microfluidics or “lab-on-a-CD” devices have been described previously, and have emerged for various biological analyses and applications, including PCR.²⁷⁻²⁹ Passive flow control is accomplished with printed toner valves³⁰ that provide a hydrophobic barrier. The polyester toner (PeT) microdevices are thin (~300 μm), providing a small thermal mass for heat transfer and rapid temperature cycling. These devices are also inexpensive (materials <50¢ USD per chip), disposable, and easy to fabricate using a simplified laser print, cut, and laminate technique previously described by our lab.³¹ Collectively, the simplicity and cost of device fabrication, the simple hardware components required to assist in assay function, and the increased temperature transitioning speed facilitated by a small dual Peltier heating system, lead to a powerful PCR microfluidic platform. Exploiting several unique aspects of microfluidics on a single device (hydrophobic valves, centrifugal fluidic movement, and mixing) allows for the design of a small, simple PCR platform that circumvents the need for bulky, expensive hardware.

In this study, we demonstrate the functionality of the PCR platform for multiplex amplification of short tandem repeat sequences for use in forensic human identification. Complimenting the use of PeT microchips, centrifugal force and toner valves, is a novel dual Peltier system for rapid thermocycling. PCR reagents can be loaded independently and then mixed prior to temperature cycling. The functionality of the system is evaluated with the amplification of DNA samples from multiple different donors, with the

electrophoretic analysis of the PCR products of multiplexes consisting of 18, 10, or 6 genetic markers showing that the process is 100% concordant with conventional PCR methods.

4.3 Materials and Methods

4.3.1 Chip design and instrumentation

A simple microfluidic chip was designed for preliminary PCR and Peltier heating system validation. This chip was made of commercially available overhead transparencies (TransNS, Film Source, Maryland Heights, MD, USA) following the laser print, cut, and laminate fabrication method developed in our lab and described by Thompson, et al.³¹ The chip consisted of five layers of polyester transparencies, and contained one PCR chamber of approximately 10 μ L and two PCR loading arms connected to the inlet and outlet, which are necessary to vent the chamber. The arms were designed such that the inlet and outlet ports remain outside of the heating zone, thereby limiting evaporation issues. A second iteration of the PeT chip was designed for on-chip mixing and amplification. This chip was designed with three different loading chambers (one for the PCR master mix, one for DNA and water, and one for the PCR primers) that join into a single chamber after passing through a toner valve into the final PCR chamber with the same dimensions as the preliminary chip. The toner valve, as described by Ouyang et al³⁰, prevents the liquid from mixing prior to centrifugation and mobilization of the reagents into the PCR chamber.

The instrument used for this assay was designed to achieve two main functions: centrifugal mixing of the reagents, and PCR amplification. Therefore, a spinning device was integrated with a heating system capable of clamping the chip and heating it from both sides. The heating component is moveable so that it does not obstruct the movement of the chip when the chip is spinning. This Peltier stack was opened and closed around the sample using a HiTec HS-645MG servomotor and clamp mechanism controlled by Propeller software. The two Peltier heating/cooling modules are controlled by a Laird PR-59 Thermoelectric Controller (TEC) running a PID algorithm. The Peltier plates were attached to a heat sink and fan to aid with the cooling steps of the cycle, as well as an embedded thermistor to provide feedback to the TEC. The heating element is controlled by an in-house Labview interface designed to allow entry of PCR parameters (i.e., set point temperatures, cycle duration, and cycle number) while the spinning/clamping functions are controlled by Parallax software (parameters of centrifugal mixing were sent to a Parallax Propeller microcontroller using a serial terminal interface with a custom command menu). The spinning of the device was achieved through the use of a Pololu 37 mm diameter DC brushed motor receiving a Pulse Width Modulated (PWM) signal from the microcontroller. Spin speeds were monitored and kept constant by the microcontroller in a closed-loop fashion using readouts from a Hall Effect quadrature encoder and a PID controller. Additionally, the encoder readout was used to aid in the alignment of the sample disc between the Peltier heaters.

4.3.2 Optimization of mixing and heating

The different functionalities of the system were optimized individually prior to the integration of these components for mixing and PCR amplification. A preliminary mixing study was performed with colored dye in water. Different parameters were tested to improve the mixing using the in-house system including: stop flow mixing, bead mixing, varying the distance of the final chamber from the center, channel width, spinning times, spinning acceleration rates, and spinning sequence. The mixing efficiency was assessed by calculating the standard deviation of the hue value (from the dye studies) inside the PCR chamber using the open source software ImageJ at the end of the mixing steps. A total of eight chips per spinning test were analyzed to characterize the reproducibility of the mixing protocol. The mixing standard deviation of the hue value was compared against the same value calculated for premixed reagents and introduced into the PCR chamber.

The heating protocol was optimized to ensure that the temperature inside the chip matched the temperature recommended for the chemistry used. Also, PID adjustments were made to minimize overshooting at the different set temperatures. The temperature optimization was performed with a thermocouple housed inside the simple PCR chip filled with liquid. An in-house Labview software program allowed for the temperature to be recorded from the thermocouple while running the PCR with the dual Peltier clamping apparatus. A direct comparison was then made between the set temperatures for the dual Peltier and the actual temperatures inside the PCR chamber. The dual Peltier

temperatures were then adjusted so the temperatures inside the chamber matched the temperatures required for the PCR assay.

4.3.3 PCR assay on-chip

First, premixed PCR reagents were pipetted into the outlet port to fill the PCR chamber. The 18-plex PowerPlex® 18 Fast System (Promega Corp., Madison, WI, USA) previously demonstrated for PCR on plastic chips was used.²⁶ 10 μ L of primers were mixed with 5 μ L of master mix and 10 μ L of DNA plus water. The chip was then spun for 20 sec at 1200 rpm and heated at 96°C for 60 seconds. The Dual Integrated Peltier Spin (DIPS) System was then clamped to allow thermocycling inside the chip. This first heating/spinning step allowed for bubble degassing and limited future evaporation or bubble formation. After the degassing step, the clamp was opened and the chip was again spun down for 10 seconds at 1200 rpm. Finally, the chip was clamped and the PCR cycling profile was applied allowing for a 45 min PCR with the following protocol: 96°C for 60 seconds, 30 cycles of 94°C for 10 seconds and 60°C for 60 seconds, and finally 60°C for 120 seconds. The PCR times were not further optimized for this assay.

Prior to integration with on-chip mixing, studies were first conducted to validate successful mobilization of premixed PCR reagents from the loading ports, through the toner valve, and into the PCR chamber. These studies were performed to test for a potential drop in PCR efficiency due to surface effects/adsorption and inhibition by the toner comprising the hydrophobic valve prior to on-chip mixing. To test this, 10 μ L of premixed reagents were introduced into both of the larger loading chambers and 5 μ L of the same mix was introduced into the smaller loading chamber. The mixing protocol

previously optimized was applied to the reagents prior to the degassing and PCR steps. It consisted of 5 seconds at 1200 rpm followed by 3 steps at 800 rpm for 20 sec (each), and finally 10 seconds at 1200 rpm.

Following these studies, full integration of mixing on-chip and STR-based PCR amplification using the DIPS system was performed. All previously described steps (mobilization, mixing, degassing) were performed here in the same manner. Briefly, 10 μ L of primers were added into the left loading chamber, 5 μ L of master mix was loaded into the center chamber, and 10 μ L of DNA and water was added into the right loading chamber.

A custom 6-plex and a custom 10-plex kit were developed in this work. The main goal was to be able to amplify either 5 or 9 core CODIS loci plus Amelogenin (for 6-plex and 10-plex, respectively) with amplicons no larger than 300 base pairs to be suitable for downstream fast microfluidic separation. Different arrangements of markers were designed and tested in preliminary studies and a unique combination was chosen and used for this study, composed of three different dye colors (FAM, JOE and ET-CRX). The custom kits were first amplified conventionally using the PowerPlex[®] Fusion System amplification master mix following the manufacturer's recommendations for thermocycling. The primers were used at the same proprietary concentration in the original 6-plex and 10-plex primer pair mixes. The amplification was performed in 35 and 27 minutes using the DIPS system for 6-plex and 10-plex, respectively. The thermocycling parameters were: 96°C for 1 minute, followed by 30 cycles of 94°C for 10 seconds, 59°C for 20 seconds, and 72°C for 15 seconds, with a final extension at 60°C

for 60 seconds. The individual primer pair concentrations were adjusted based on the on-chip amplification results to optimize the inter-locus balance within the kits for on-chip amplification.

After on-chip amplification, the PCR product was recovered by inverting the chip and pipetting the liquid off the chip via the outlet port. The PCR products were then gently vortexed and 1 μL was added into a ILS 500: Hi Di Formamide mix (1 μL : 14 μL), heat snap cooled, and separated on an ABI 310 instrument.

4.3.4 Amplification of buccal swab samples on PeT chips

The preliminary PCR tests to develop the PCR on PeT chips were performed using 10 μL of DNA plus water (0.5 μL of enzymatically-extracted DNA plus 9.5 μL of water). All experiments completed complied with IRB #12548, and approved by the University of Virginia Health System; all participants gave informed consent. The enzymatic extraction was performed as follows: a cheek swab was placed into 100 μL of ZyGEM reaction mix (98 μL of prepGEM™ Saliva buffer and 2 μL prepGEM™ Saliva EA1 enzyme, (ZyGEM Corp., Hamilton, New Zealand)), vortexed, and placed in a conventional thermocycler (Eppendorf Mastercycler epgradient S) at 75°C for two minutes followed by 95°C for two minutes.

Ten different DNA samples enzymatically-extracted on-chip were then used to demonstrate the potential integration of both extraction and amplification on a PeT-based centrifugal microfluidic device. 1 μL of on-chip enzymatically-extracted DNA was loaded with 9 μL of water for the ten repeats. For PCR using on-chip extracted DNA, the

DNA input was doubled (from 0.5 μ L to 1 μ L) as the DNA yield from on-chip enzymatic extraction was found to be slightly lower than the conventional extraction method.

4.3.5 Conventional processes and data analysis

Conventional processes were also used to obtain genetic profiles from the different donors in order to ensure concordance with on-chip results. PCR in-tube was performed following the manufacturer's instructions and amplified in an Eppendorf Mastercycler ep Gradient S thermocycler (Eppendorf, Hamburg, Germany). The capillary electrophoresis of the samples was performed on an ABI Genetic Analyzer 310 (Life Technologies, Carlsbad, CA, USA), injecting at 15 kV for 5 seconds and with separation conditions of 15 kV for 1680 seconds. Data analysis was conducted using GeneMarker human identification software (SoftGenetics LLC, State College, PA, USA). Genetic profiles were generated, automatically analyzed through the run wizard, and validated manually.

4.4 Results and Discussion

4.4.1 Dual Integrated Peltier Spin (DIPS) System

The DIPS system (**Figure 4-2**) was constructed in-house as part of a novel platform that brings together passive valving and centrifugally-driven fluid flow for PCR in an inexpensive and easy-to-fabricate microdevice. Specifically, it was designed to facilitate Peltier-driven heating/cooling of a PeT PCR chip from both sides. The bi-directional heating is not a new approach, as Kim et al.³² showed that it improved the thermal response of the PCR system. Not surprisingly, the heating and cooling ability of

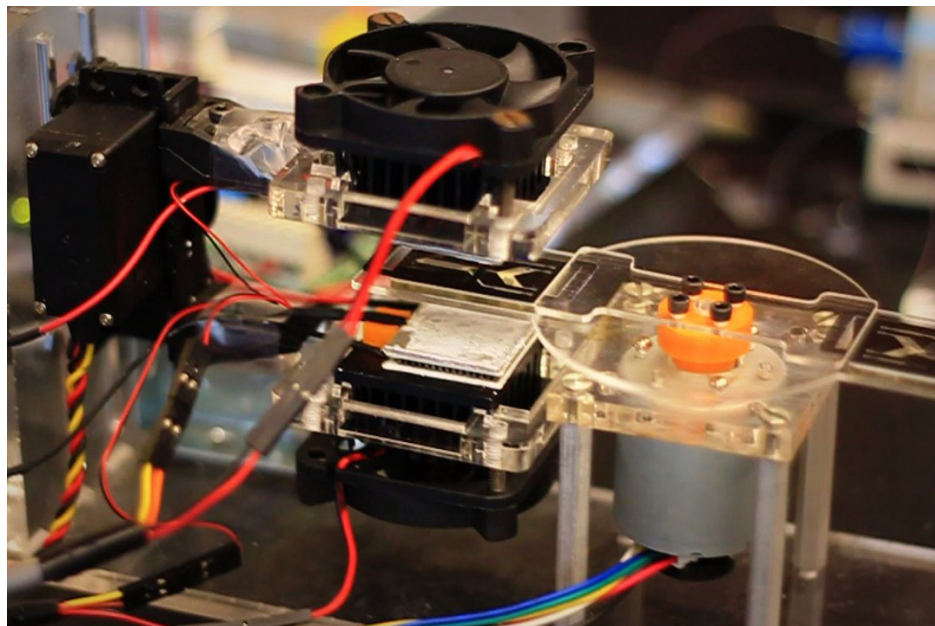


Figure 4-2. Dual Integrated Peltier Spinning (DIPS) System. The custom-built system includes a top and bottom Peltier for rapid thermal cycling, as well as a spin motor for fluidic flow control via centrifugal force. The DIPS system is capable of clamping at various heights, allowing for liquid extraction (LE) and PCR to take place using the same heating elements.

the DIPS system was found to be superior to the single Peltier system used initially (2°C/sec for heating with a simple Peltier versus 5°C/sec on a dual Peltier system). The clamping ‘closed’ position was optimized in preliminary studies (data not shown) based on the temperature effects seen inside the PCR chamber.

The Peltiers were mounted on a motorized clamping system that facilitated engagement/disengagement of the Peltier units with the chip (**Figure 4-3**). The motorized clamping functionality was essential to disengaging the Peltiers from the chip to accommodate rotation of the chip so that centrifugal force could be exploited for mobilization and mixing of pre-loaded reagents. As described previously³¹, the chip was fabricated from polyethylene terephthalate, which served as a perfect substrate for printing toner as an adhesive, as well as printing valves that provide a hydrophobic barrier to fluidic movement (passive valving). In addition, with the capping and base

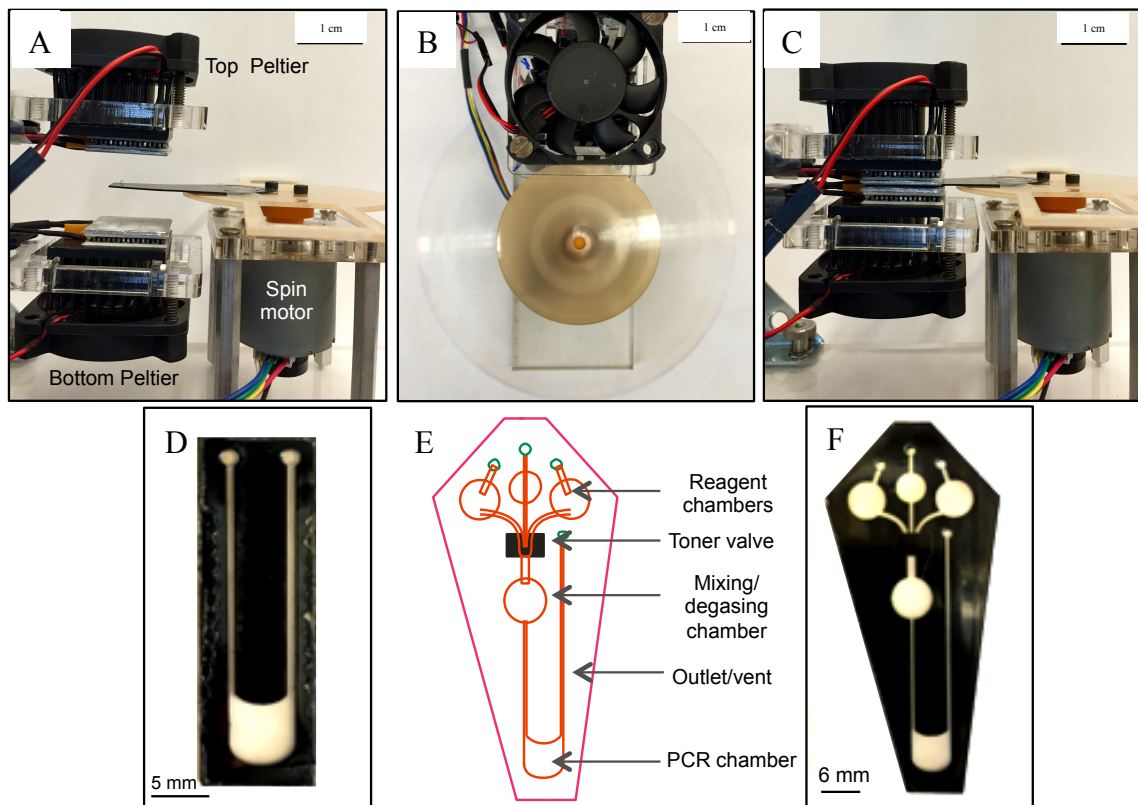


Figure 4-3. DIPS system and PeT chips. A) DIPS in open position allowing the motor and the chip acceptor to rotate in between the dual heating system. B) DIPS spinning to allow for different fluidic movements. C) DIPS in closed position allowing thermocycling inside the PCR chip. D) Simple PCR PeT chip used for preliminary tests and development. E) Schematic of the mixing/PCR chip showing the different features. F) Image of the final mixing/PCR PeT chip used for the integrated assay.

layers $\sim 100\ \mu\text{m}$ thick, the thermal responsiveness needed for rapid heat transfer could be achieved.

Figure 4-3A shows the system with two Peltier heaters that clamp onto the PeT PCR chip in the ‘open’ position prior to engagement for simultaneous heating/cooling from the top and bottom when the system is in the ‘closed’ position (**Figure 4-3C**). **Figure 4-3B** is a still image of the DIPS system captured in spin mode, with fluidic movement providing mobilization and mixing of the PCR-ready DNA with the PCR reagents (as described in the *Materials and Methods* section). **Figure 4-3D** shows the design of the preliminary PeT chip used for optimization of the on-chip thermocycling

and the system heating parameters. Finally, **Figure 4-3E-F** shows the finalized PCR chip design where the PCR chamber in Figure 4-3D is integrated with chambers for sample and reagents; this was used for testing on-chip reagent loading, mixing, and STR-based PCR amplification. The two larger chambers contain the primers and the DNA (in water), and the smaller loading chamber contains the master mix. The design of this chip can easily be altered to accommodate different volumes used for other amplification chemistries (for initial proof of principle studies, the PowerPlex® 18 Fast System was used, consisting of 17 genetic loci plus Amelogenin). The fabrication of this 5-layer microchip is rapid (<10 minutes), costs <50¢ USD in materials, and requires only a laser cutter, printer, and office laminator.³¹ While a non-disc PCR chip has been previously demonstrated by our group for chip-based infrared (IR) PCR³³, that chip was simpler in design, utilizing a single-plex system, and didn't have architectural features amenable to reagent pre-loading and mixing.

4.4.2 Sample and reagent mixing

The mixing capabilities of the spin device were optimized for efficient PCR reagent mixing by evaluating the acceleration rate. This is consistent with the parameters deemed important by Ren et al.³⁴ **Figure 4-4A** provides the pictorial results of spin-induced on-chip mixing where the efficiency of mixing was defined by the reduction of the standard deviation in the hue value of the solution in the PCR chamber after all three solutions have been mobilized. For use as a reference to evaluate the efficiency of on-chip mixing, a thoroughly premixed green solution was added to the chip and a hue value calculated; a standard deviation in the hue was ~4. A low standard deviation (<5)

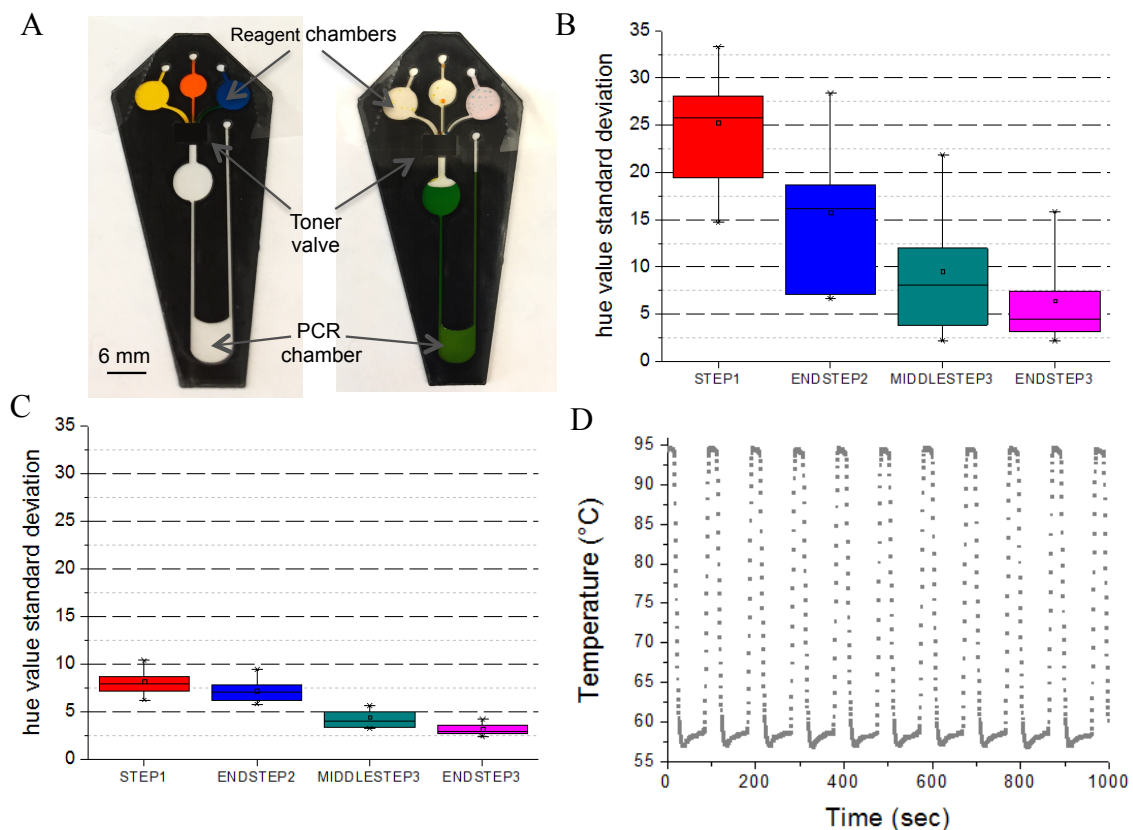


Figure 4-4. Process optimization of on-chip mixing and thermocycling. A) Colorimetric results prior to mixing (left) and pre-mixed reagents mobilized through the toner valve as a mixing reference (right). B) Standard deviation of hue values at four different steps of the mixing protocol with the original rotating system. C) Standard deviation of hue values after optimization of the acceleration rate. D) Temperatures recorded inside the PCR chamber for 10 cycles after temperature optimization of the dual peltier heating system.

represents homogenous mixing, and demonstrates a thoroughly well mixed solution. A uniform color (meaning a well-mixed solution) yields a low standard deviation, while a poorly mixed solution has different shades of color within the sample chamber, thus a higher standard deviation.

To determine the best spin protocol for effective mixing of the sample and reagents, the original mixing protocol was performed with a stepper motor capable of a maximum acceleration of 40 rpm/sec. Three spin steps were applied to the chip, based on preliminary results that showed a high spin rate was needed to burst the hydrophobic valve, followed by a quick, low spin rate to create stopped flow mixing. Following this,

several steps at higher speeds were used to increase the vortical flow mixing: a first step for 5 sec at 1200 rpm, a second step at 500 rpm for 1 sec in both directions, and a third step of 20 sec at 1000 rpm. These steps were applied alternating between clockwise and counterclockwise rotation, four times. This was used to improve the vortical flow mixing, which is rapid relative to passive molecular diffusion. In addition, Grumann, et al.³⁵ showed that changing the spin direction also enhanced the mixing of reagents. As a result, the spin device was brought to a complete stop between each sequence of spin steps. Eight repeats were carried out on 8 different chips in a single day, and the hue and associated standard deviation of the mixed solution were calculated. The box plots in **Figure 4-4B** indicate poor reproducibility and inefficient mixing, as evidenced by a large standard deviation of hue value. Moreover, when flow was monitored using a stroboscopic set-up, the solutions in the three loading chambers did not break through the toner valve at the same time, and this was deemed to be the result of a slow acceleration in rotation speed.

In order to obtain better acceleration, the stepper motor was replaced with a more powerful DC brushed motor with an acceleration rate specification rating for >10,000 rpm/sec. The mixing experiments described earlier were repeated and the results, shown in **Figure 4-4C**, indicate a marked improvement in mixing efficiency. The boxplots were narrowed significantly in comparison with Figure 4-4B, indicating that the mixing method was not only efficient, but also very reproducible. Considering this improvement, these mixing parameters were used, and the total mixing process time was reduced to <90 sec by increasing the acceleration rate. The optimized spin protocol was deemed to be: 1200 rpm for 10 sec, followed by 3 spin steps at 800 rpm for 20 sec, with the last step at

1200 rpm for 10 sec. All tests performed with this mixing protocol yielded hue values that had standard deviations <5 and, thus, were determined to be sufficient for the PCR assay. These results were confirmed after successful amplification of solutions mixed with this protocol, and amplified on a conventional thermocycler within the PCR microchip. The results (data not shown) showed good correlation between the PCR efficiency of reagents that were premixed and those mixed on-chip using the optimized mixing protocol.

4.4.3 Thermocycling in a PeT chip on the DIPS System

In order to carry out on-chip PCR using the custom-built system, the dual Peltier heating system needed to be optimized for thermocycling. The PID control system was first tuned using the Ziegler-Nichols method to improve heating efficiency and speed, that is, by reducing temperature overshoot while increasing the heating and cooling rates. The P value was increased until the system started to oscillate with I and D values set to zero. This allowed for calculating the PID gains, and was performed independently for each of the Peltier systems. A thermocouple was introduced into the simple PeT chip shown in Figure 4-3D, to serve as a reference chamber for temperature optimization. It was then possible to record the solution temperature while simultaneously recording the temperature between the Peltier heaters using an external thermistor; the read from the thermistor provided the feedback for closed-loop control of the system temperature. This was necessary to calibrate the set temperature of the system, taking into account the temperature lag and difference between the Peltier surface and the fluid in the PCR chamber. The actual set temperatures were modified based on the results of the

temperature inside the chamber. For example, if the chamber solution temperature was 97°C for the initial denaturation step instead of the desired set temperature of 96°C, the set temperature was decreased by 1°C. This was performed for each of the cycling temperatures. At the end of this optimization, the temperatures recorded inside the chip matched the temperatures recommended for the STR chemistry amplification as shown by the overlapping temperature profiles for 60°C and 94°C shown in **Figure 4-4D**.

4.4.4 PeT chip surface effects

The PCR chamber is comprised of Pe and toner (used as adhesive) with the former being the dominating surface. In addition, mobilization of the individual reagents to the PCR chamber involves brief exposure to a surface that is largely toner (hydrophobic valve). Hydrophobic toner valves developed in our lab have previously been described and characterized.³⁰ As a result of their hydrophobicity (contact angle of 111°), they function well as a hydrophobic barrier to impede aqueous fluid flow. The end-goal is to incorporate these valves into the final PCR chip design as part of a mechanism that ensures reagents (master mix and primer pairs) and sample remain isolated (separate chambers for all three) prior to amplification. As a result, it was essential to determine that neither the Pe surface nor the hydrophobic toner valve had inhibitory effects on chip-based PCR. In order to evaluate this, the efficiency of the STR fragment amplification (i.e., resulting peak height in RFU) was used as the metric. The PowerPlex® 18 Fast System was used in this work and is a multiplexed PCR system that has been optimized by the manufacturer for amplification of tetra- and penta-nucleotide repeats (short tandem repeats, STR) at 17 locations in the genome (non-coding DNA; no

known function; presumably no clinical relevance). It allows for the probing of the number of repeats at each location, which is specific to an individual and revealed by capillary electrophoresis (CE). An exemplary STR profile (full profile, obtained in conventional tube-based amplification) is shown in **Figure 4-5A** when DNA is extracted from the buccal swab using conventional liquid extraction, amplified on a conventional thermocycler, and the products separated on a CE instrument. While this commercial STR chemistry is very robust, it is also very sensitive to specific inhibitors (**Figure 4-5B**, showing a failed amplification.)

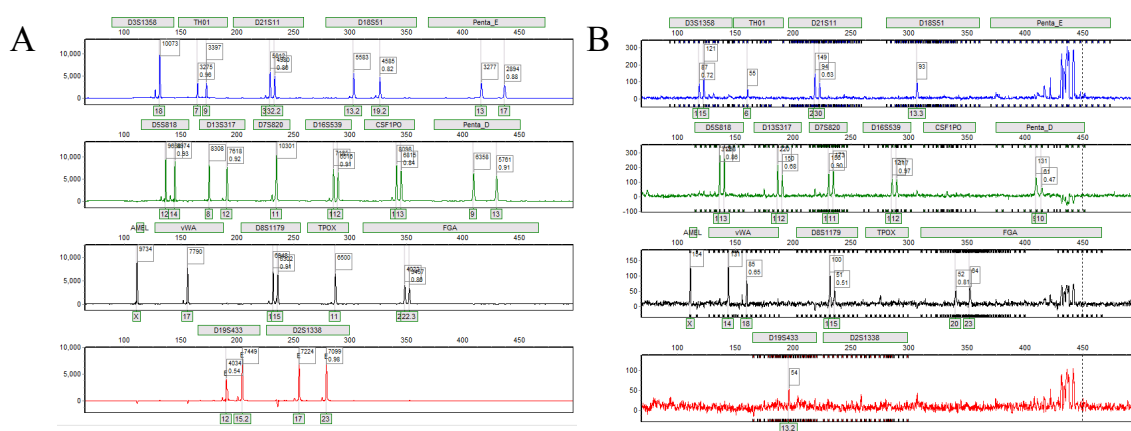


Figure 4-5. Example STR profiles from tube-based amplification. A) Exemplary profile for PowerPlex® 18 Fast System amplified conventionally in-tube. B) Profile demonstrating a poor amplification. Y-axis scale for profile on the left is 10,000 RFU vs. 300 RFU on the right.

The first step evaluated the effect of the PCR chamber surface alone (primarily Pe) on PCR amplification. This involved pipetting premixed sample/reagents directly into the PCR chamber through the vent (see Figure 4-3E), thus, bypassing the toner valve. This was then thermocycled utilizing the DIPS system, and PCR efficiency was determined by how complete the STR profile was (i.e., all alleles present) and how strong the fluorescence signal was on the CE (desired peak height is > 500 RFU) when compared to the profile obtained from conventional tube-based amplification. **Figure 4-**

6A shows a profile containing all of the expected alleles at each of the 18 markers represented by the gray boxes shown above each dye color (full profile), following reagent exposure to the chamber only, signifying a lack of inhibition caused by the Pe surface of the PCR chamber. The X-axis shows the DNA fragment size (base pairs) and the Y-axis is the peak height of each allele in relative fluorescent units (RFU); each peak has a label showing the associated specific peak height. The next step involved premixing the reagents (sample, master mix, and buffer); this mixture was then added to the three loading chambers, and spun into the PCR chamber where it was exposed to the toner valve, albeit intermittently, prior to the thermocycling step. **Figure 4-6B** shows that a full profile resulted, indicating that amplification was successful following the exposure of all PCR reagents to the hydrophobic barrier. The profiles in **Figures 4-6** show both strong peak height and good intralocus balance (the ratio of peak heights for heterozygous alleles) greater than 60%. This is important because heterozygous alleles with low intralocus balance are not considered valid by the forensic community. All peaks were greater than 1000 RFU, except one Penta E peak in both profiles,

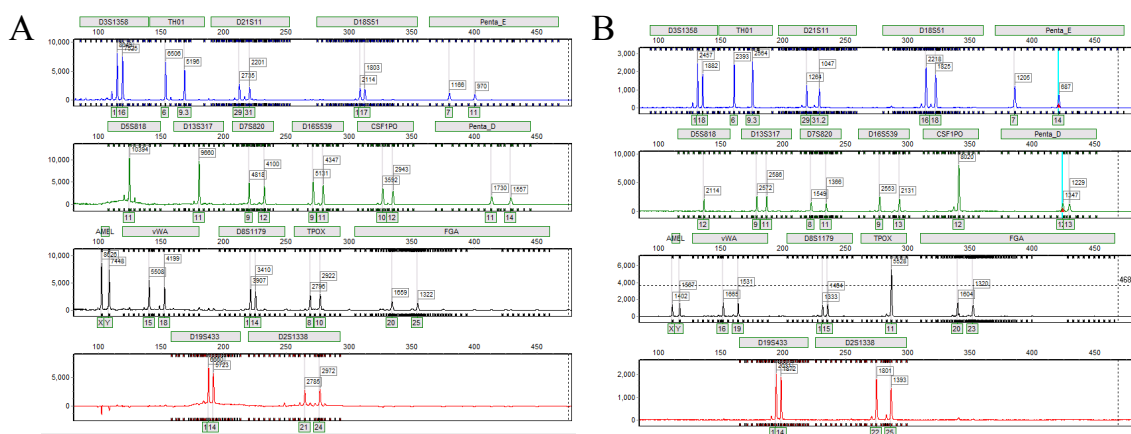


Figure 4-6. PCR amplification of STR fragments on a PeT chip using the DIPS system. A) Amplification of PowerPlex® 18 Fast System with premixed reagents introduced into the PCR chamber without passing through the toner valve. B) Amplification of PowerPlex® 18 Fast System with premixed reagents mobilized through the toner valve from the loading ports.

demonstrating strong signals, and therefore, good PCR efficiency. This data suggests that the toner valve does not have obvious inhibitory effects on PCR of the STR fragments. Collectively, these studies confirm that multiplex STR amplification is possible on PeT microdevices using the custom-built DIPS system.

4.4.5. Introduction of a 6-plex custom kit and primer modifications

Following initial proof of principle studies using the commercially available 18-plex kit described above, a novel 6-plex kit was designed in collaboration with Promega for human identification. The loci in this kit (5 genetic markers plus Amelogenin) were chosen for ease of integration with ultimate downstream microchip electrophoresis (ME), and therefore, certain characteristics were desired; namely, the kit has markers in only two colors (i.e., PCR primers labeled with either Fluorescein or JOE dye) and all amplicons generated via PCR are smaller than 300 base pairs. These criteria will be discussed further in Chapter 5.

Interlocus balance is an important parameter to consider when optimizing STR-based PCR amplifications. Preferential amplification can occur, whereby certain loci amplify very well while other loci do not, often leading to an imbalanced profile and even dropout of certain alleles (i.e., alleles completely absent in resulting STR profile), which can negatively impact the overall amplification efficiency. Interlocus balance is commonly measured by the contribution of each locus to the overall peak height; in a well-balanced amplification, each locus should contribute roughly equally to the overall peak height (combined RFU for each allele). For the 6-plex kit, if each locus were contributing equally, a contribution of 0.16 (16%) is expected. Accordingly, **Figure 4-**

7A shows the results of a conventional tube-based amplification of the 6-plex kit and the resulting contribution of each locus. The amplification is well balanced, and each locus contributes approximately the expected 0.16. Likewise, the results in **Figure 4-7B** show the same study performed on-chip using a PeT microdevice, with a much larger spread in terms of the contribution of each locus. Some markers perform quite well (Amelogenin), while others perform very poorly, or dropout completely (D8S1179).

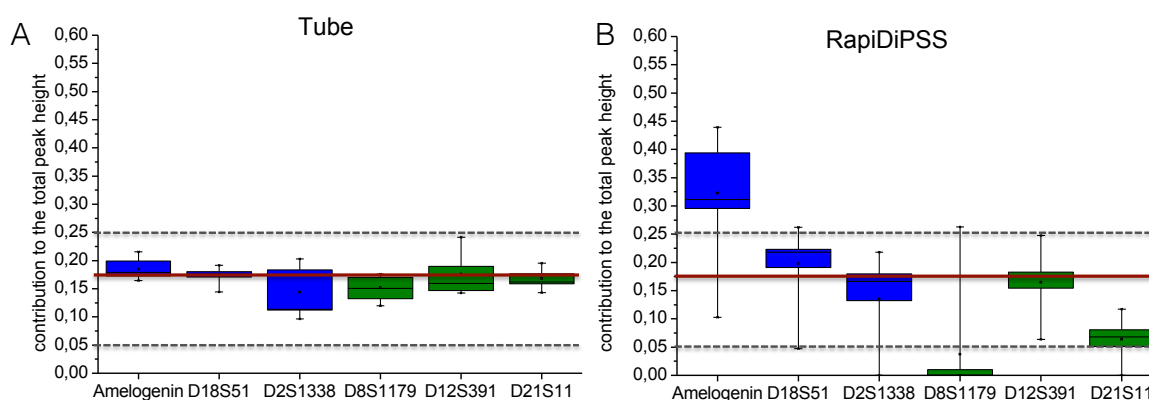


Figure 4-7. Preliminary primer modifications for 6-plex kit. A) Contribution of each marker to the total peak height. Since there are 6 markers, if each marker were contributing equally, the contribution of each would be 0.16 (on Y-axis). Amplification in tube yields results that are very well balanced and each marker is contributing roughly 16%. B) Amplification on-chip yields results that are not as well balanced, indicating preferential amplification of some markers over others. Dotted lines show acceptable range for contribution of each marker.

To address this problem, primer modifications were deemed necessary to improve the interlocus balance and overall amplification efficiency. Each primer is added into the primer mix individually, allowing for modifications of primer concentration in the final mix. The concentrations for loci that performed well on-chip were decreased, while the concentrations for loci that performed poorly were increased; the results for the conventional tube-based amplification are shown in **Figure 4-8A**. The results for this primer modification are the inverse of what is seen in the amplification on-chip (using

non-modified primer concentrations) shown in Figure 4-7B, which should ideally lead to a well balanced profile when amplified on-chip. The loci that were previously low are now exaggerated to be much higher, and the loci that were previously high are now much lower. The STR profile from on-chip amplification for these optimized primer modifications is shown in **Figure 4-8B**, with each marker demonstrating comparable peak heights. Importantly, D8S1179 is now present on-chip, where it was often completely absent prior to primer modifications.

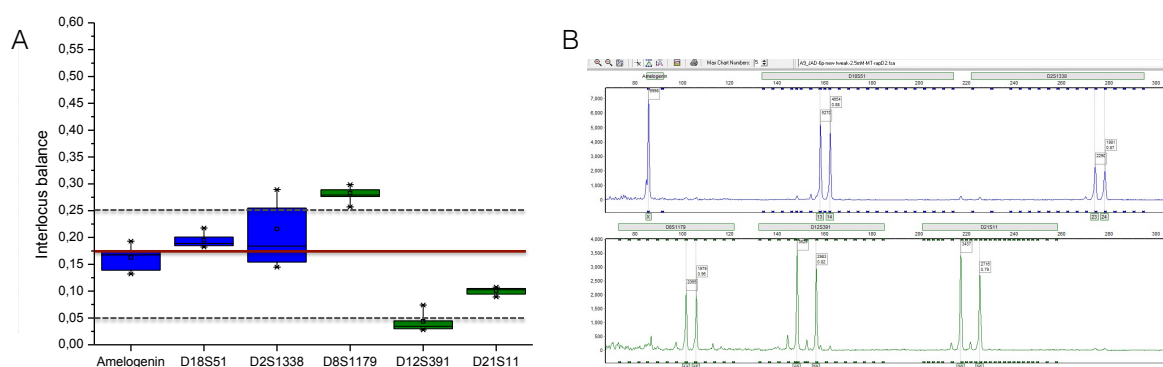


Figure 4-8. Results from preliminary primer modifications. A) Tube amplification shows the inverse of the results seen in Fig 4-7B (i.e., markers that are strong on-chip were lowered and markers that were weak on-chip were increased in concentration). D8 is consistently absent for on-chip amplifications, so the concentration of this marker was increased significantly. B) STR profile using modified primers showing good interlocus balance (all peaks contributing roughly equally to overall peak height). The concentration of the D8 primers has been increased significantly, and the marker is now visible for on-chip amplifications.

4.4.6. Introduction of a 10-plex custom kit and primer modifications

Similar to the 6-plex kit described above, further work was done to design and optimize a 10-plex kit for the same ultimate goal of rapid human identification. This kit introduced markers labeled with a new dye (ET-CRX), but all amplicons generated are

still smaller than 300 base pairs. This 10-plex was designed to increase the power of discrimination compared to the 6-plex, and will be discussed further in Chapter 5 as it pertains to the integration of DNA extraction, PCR amplification, and separation via ME. As with the 6-plex, this novel 10-plex was first optimized in terms of primer modifications to achieve well balanced on-chip profiles and PCR efficiency leading to STR profiles with peaks >500 RFU (determined to be necessary for downstream ME using a custom-built system; discussed further in Chapter 5). **Figure 4-9A** shows the preliminary results for conventional tube-based amplification of the 10-plex kit, and a strong, well balanced STR profile is observed. The PeT microdevice used for on-chip amplification is shown in **Figure 4-9B**, and the results for the first on-chip amplification of the 10-plex kit are shown in **Figure 4-9C**. Similar to the 6-plex kit, marker D8S1179 is completely absent in the resultant STR profile (green circle). All other loci have peak heights >800 RFU, which was very encouraging for preliminary on-chip amplification.

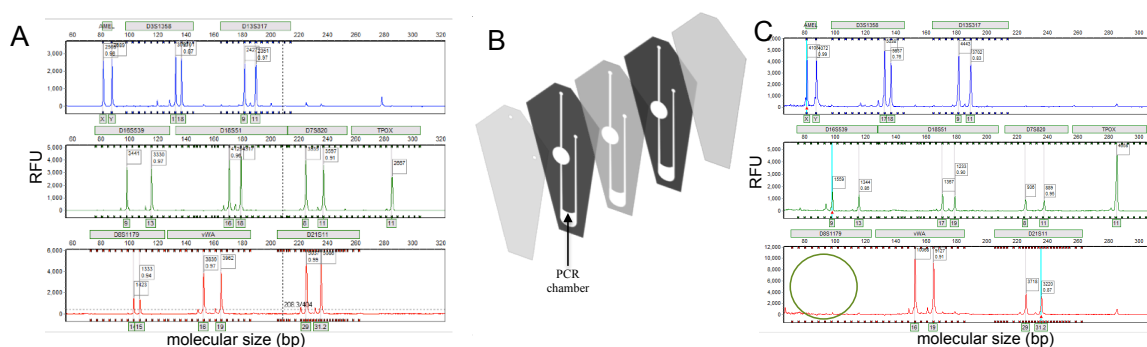


Figure 4-9. A novel 10-plex PCR amplification of STR fragments for rapid human identification. A) Conventional tube-based PCR amplification of Control DNA (2800M) using the 10-plex with primers at equal concentrations with the PowerPlex[®] Fusion Master Mix following the manufacturer's recommendations. B) Picture of the chip used for this study. C) On-chip amplification of Control DNA using the 10-plex with primers at equal concentrations with a custom master mix based on the PowerPlex[®] Fusion Master Mix (27 minute PCR using polyester-toner [PeT] microdevice and DIPS system). The on-chip amplification reaction shows drop off of D8S1179 and strong inter-locus imbalance.

Unlike the 6-plex kit, the 10-plex kit required multiple rounds of iterative primer modifications. **Figure 4-10A** shows the results of on-chip amplification following multiple rounds of primer modifications, where each locus should contribute 0.1 (10%) to the overall peak height. The blue line delineates the contribution of each marker prior to primer modifications, with the D8S1179 marker hovering around 0, and the vWA marker up around 0.2. The green line represents the final round of primer modifications, and D8S1179 is now around 0.08 and vWA is around 0.12; both of these values are much closer to the desired value of 0.1. Not only do these primer modifications yield better interlocus balance, they also result in more efficient PCR as demonstrated by the increased peak heights (all peaks >2000 RFU) shown in **Figure 4-10B**.

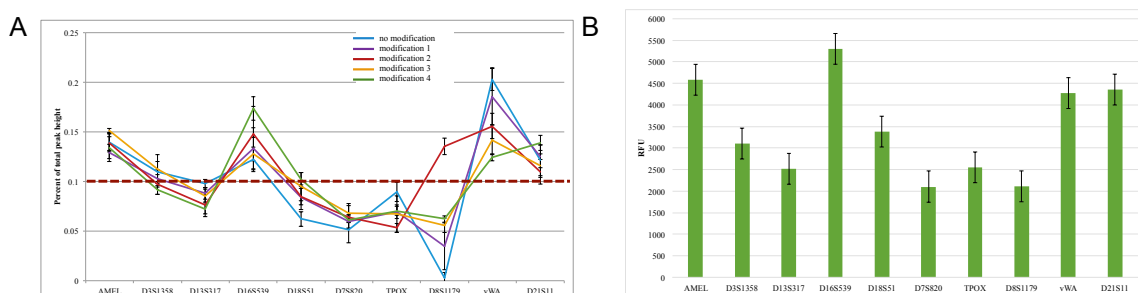


Figure 4-10. Optimizing primer concentration to improve on-chip peak balance and height. A) Mean value of each peak compared to the overall peak height over various rounds of primer modifications, showing good balance (each peak close to 10% contribution). Final modification shown in green. B) Total peak height for each locus, with all peaks >2000 RFU. Y-axis shows peak height in RFU.

4.4.7. Titration of master mix components

The results shown up to this point for 6-plex and 10-plex amplifications were generated using a master mix with proprietary concentrations and intended for use with the PowerPlex® Fusion 6c multiplex kit. As discussed in the Introduction to this Chapter, one of the main disadvantages to using the microfluidic platform for PCR amplification is the large surface area to volume ratio, often leading to detrimental

adsorption of reaction components to the chip surface. To combat this effect, a polymerase titration was utilized to explore the possibility for increased PCR efficiency by increasing the amount of polymerase in the overall on-chip amplification. This would, in theory, compensate for some polymerase adsorbing to the Pe chip surface without negatively impacting the efficiency and peak heights in the STR profile. Surface passivation is also a viable option; however, we opted against this technique, as it would add substantial time and effort to the streamlined microdevice fabrication process.

The polymerase titration was performed with concentrations ranging from 200-1000 units/ μL , and the results are shown in **Figure 4-11A**. In addition to improving the peak heights, the polymerase titration was performed in an attempt to decrease the overall reaction time from 27 minutes to 15 minutes. This parameter is important for integration, and will be discussed more extensively in Chapter 5. Each condition was tested in

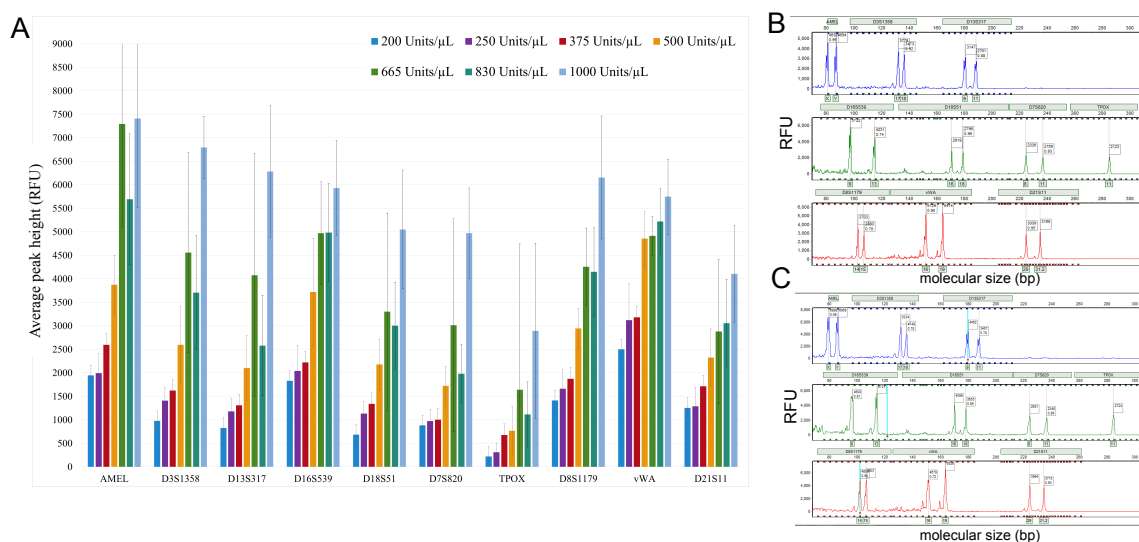


Figure 4-11. Polymerase titration for on-chip 15 min PCR. A) Three on-chip amplification reactions were tested for each of the polymerase concentrations, the average signal per marker across three repeat experiments is represented in the bar graph, showing a consistent increase in peak height as the polymerase concentration is increased. (B) and (C) are two representative profiles of the polymerase titration for on-chip 15 min amplification with 10X (500 units/ μL) polymerase (B) and 16.6X (830 units/ μL) polymerase (C).

triplicate and the mean peak height values were calculated for each polymerase concentration. The peak heights clearly increase as the polymerase concentration increases using 15-minute thermocycling parameters. Although the result for 1000 units/ μL polymerase yielded strong peak heights, the profiles generated had unwanted artifact peaks present in the baseline, making it difficult to correctly identify the appropriate alleles. Representative profiles for amplification with 500 units/ μL and 830 units/ μL polymerase are shown in **Figure 4-11B-C**, and all peak heights exceed 2000 RFU. In addition to peak height, other parameters must be considered when choosing the optimized conditions moving forward. 500 units/ μL was chosen as the optimal polymerase concentration because it yielded peak heights >1500 RFU when the overall amplification reaction time was 15 minutes, but also because it is more cost-effective than 1000 units/ μL . Although the polymerase titration was performed with a reaction time of 15 minutes, this was increased slightly to 19 minutes because of heating and cooling limitations inherent to the DIPS system. Therefore, 19-minute PCR with 500 units/ μL of polymerase was chosen as the optimized condition for further testing.

In addition to polymerase, another component to consider when optimizing on-chip amplification is MgCl_2 as it is also at risk for adsorbing to the large chip surface area. **Figure 4-12** shows the results for the MgCl_2 titration performed with optimized conditions from the polymerase titration. As the MgCl_2 concentration is increased from 2.5-3.5 mM, the peak heights of the resulting STR profiles also increase. These results indicate that increasing the MgCl_2 concentration beyond 3.5 mM might further improve the peak heights; however, increasing the MgCl_2 concentration also decreases the specificity of the reaction because it stabilizes incorrect primer annealing to the target

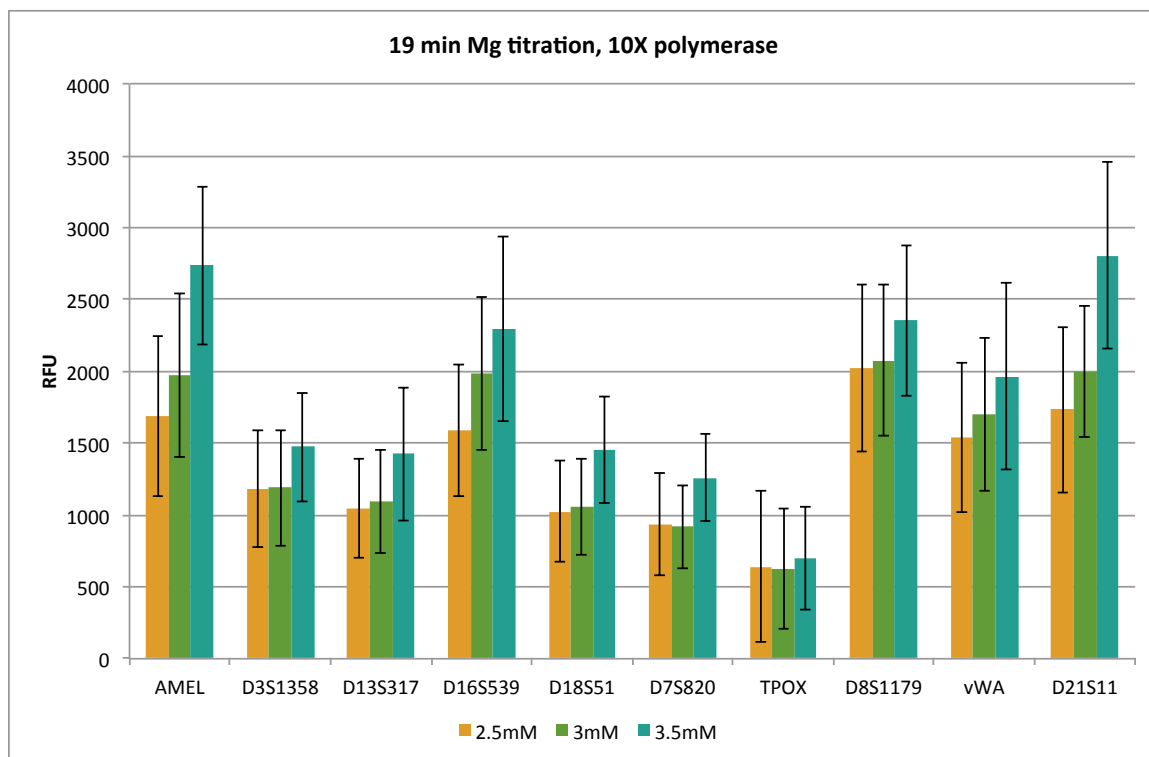


Figure 4-12. Magnesium titration to determine optimal concentration in master mix. Titration was carried out using 500 units/ μ L polymerase and 19 min total on-chip amplification time.

sequence. Therefore, 500 units/ μ L and 3.5 mM MgCl_2 were chosen as the optimized conditions for 19-minute on-chip amplification of the 10-plex kit. Similar titrations were performed previously for the 6-plex kit (data not shown) and the optimized conditions were 200 units/ μ L and 2.5 mM MgCl_2 .

Figure 4-13 shows the exemplary STR profiles for the optimized 6-plex and 10-plex kits. The 6-plex kit was optimized at 35 minutes for on-chip amplification and was successfully demonstrated with downstream ME using a custom-built system. 15 PCR reactions were run using these conditions (5 repeats for each of 3 donors) and the 5 overlaid STR profiles for one donor are shown in **Figure 4-13A**, with peak heights >7000 RFU for all loci. Similarly, the results shown in **Figure 4-13B** demonstrate the success of the 10-plex kit for on-chip amplification with all peak heights >3500 RFU. These kits

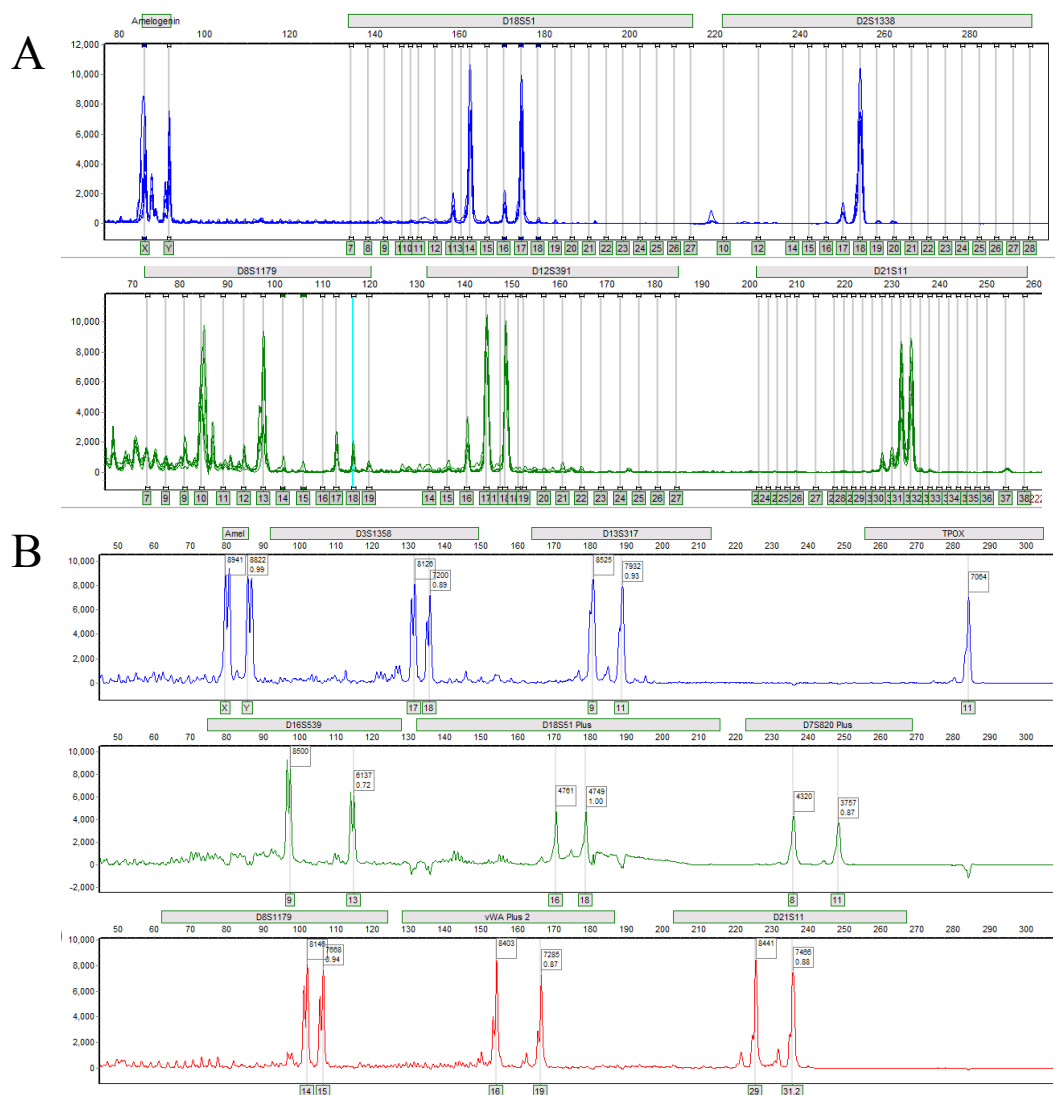


Figure 4-13. Exemplary results after optimization. A) Overlaid profiles for 5 PCR runs from the same donor for 6-plex kit. All peaks >6000 RFU. B) Profile from one donor after optimization of 10-plex kit. Peaks are oversaturated, leading to abnormal peak shape. All peaks >3500 RFU.

were optimized in terms of individual primer concentrations, polymerase, and $MgCl_2$. Further work toward integration, including material inhibition, ZyGEM template DNA, time reduction, and integration with upstream DNA extraction and downstream ME will be discussed at length in Chapter 5.

4.5 Conclusions

An inexpensive and easy to fabricate microdevice made from commercially available overhead transparencies has been demonstrated for successful STR-based PCR amplification in less than 1 hour. Fluid flow is governed by centrifugal force, and a custom-built system capable of variable rate spinning is utilized in place of bulky external pumps or valves. Thermocycling is achieved with the same system, making use of a dual Peltier clamping mechanism for accurate temperature control. Integrated on-chip reagent mobilization, mixing, and amplification is demonstrated, suggesting the potential for full integration of DNA extraction, PCR amplification, and electrophoretic separation in the future. Furthermore, 100% of the profiles generated using the chip-based STR amplification method are concordant with profiles generated using the conventional method. The signals obtained for the amplifications on this microdevice are strong enough to be suitable for microchip electrophoresis, indicating the possibility for a fully integrated device capable of a complete forensic analysis workflow, from sample preparation to genetic profile. Thus, the demonstration of this PeT chip-DIPS system is a critical step toward the integration of a genetic analysis device with “sample in-answer out” capabilities. The hardware used and the simple, inexpensive nature of the chip fabrication method have unprecedented advantages. While this system is demonstrated here for human identification applications, it can be easily adaptable to other applications and analytical assays as the amplification component is easily modifiable and the microchip can be designed and fabricated in less than one hour.

Overall, a device has been demonstrated that meets many of the fundamental criteria for lab-on-a-chip platforms: low cost, ease of fabrication, lack of external pumps and valves, simple hardware requirements, and rapid speed. This device has yielded strong, full profiles for multiple STR kits, both commercially available (PowerPlex® 18 Fast System) and custom-designed (novel 6-plex and 10-plex), reproducibly validating successful on-chip reagent mixing and STR-based PCR amplification. Chemistry optimization was performed with titrations for important components of the PCR reaction, including: primer concentration, polymerase, and MgCl₂. Future integration will allow for a microdevice capable of the full spectrum of genetic analysis, from DNA extraction, to PCR amplification, to separation via microchip electrophoresis. Additionally, there is the potential for this system to be used as a standalone PCR system for rapid thermocycling. This system, although not yet fully integrated with up and downstream analysis steps for a total integrated human identification system, represents a critical step toward a small, automated, portable, integrated human identification device.

4.6 References

1. Yeatts, T., *Forensics: Solving the Crime*. The Oliver Press, Inc.: 2001; Vol. No. 9.
2. Watson, J. D.; Crick, F. H., Letters to Nature: molecular structure of nucleic acid. *Nature*: 1953; Vol. 171, p 738.
3. Jeffreys, A. J.; Wilson, V.; Thein, S. L., HYPERVARIABLE MINISATELLITE REGIONS IN HUMAN DNA. *Nature* **1985**, 314 (6006), 67-73.

4. Edwards, A.; Civitello, A.; Hammond, H. A.; Caskey, C. T., DNA TYPING AND GENETIC-MAPPING WITH TRIMERIC AND TETRAMERIC TANDEM REPEATS. *American Journal of Human Genetics* **1991**, 49 (4), 746-756.
5. Edwards, A.; Hammond, H.; Jin, L.; Caskey, C.; Chakraborty, R., Genetic variation at five trimeric and tetrameric tandem repeat loci in four human population groups. *Genomics*: 1992; Vol. 12, pp 241-253.
6. Pena, S. D. J.; Chakraborty, R.; Epplen, J. T.; Jeffreys, A. J., *DNA Fingerprinting: State of the Science ; Progress in Systems and Control Theory*. Birkhäuser Basel: 1993.
7. Butler, J. M., Genetics and genomics of core short tandem repeat loci used in human identity testing. *Journal of Forensic Sciences* **2006**, 51 (2), 253-265.
8. Gill, P.; Fereday, L.; Morling, N.; Schneider, P. M., The evolution of DNA databases - Recommendations for new European STR loci. *Forensic Science International* **2006**, 156 (2-3), 242-244.
9. Tan, S. C.; Yiap, B. C., DNA, RNA, and Protein Extraction: The Past and The Present. *Journal of Biomedicine and Biotechnology* **2009**, 10.
10. Stray JE, L. J., Brevnov MG, Shewale JG, Extraction of DNA from Forensic Biological Samples for Genotyping. *Forensic Science Review*: 2010; Vol. 22, pp 159-175.

11. Miller, S. A.; Dykes, D. D.; Polesky, H. F., A SIMPLE SALTING OUT PROCEDURE FOR EXTRACTING DNA FROM HUMAN NUCLEATED CELLS. *Nucleic Acids Research* **1988**, *16* (3), 1215-1215.
12. Valgren C, W. S., Hansson O, A comparison of three automated DNA purification methods in Forensic casework. *Forensic Science International: Genetics Supplement Series*: 2008; Vol. 1, pp 76-77.
13. Butler, J. M., *Fundamentals of forensic DNA typing*. Academic Press: 2009.
14. Lounsbury, J. A.; Coult, N.; Miranian, D. C.; Cronk, S. M.; Haverstick, D. M.; Kinnon, P.; Saul, D. J.; Landers, J. P., An enzyme-based DNA preparation method for application to forensic biological samples and degraded stains. *Forensic Science International-Genetics* **2012**, *6* (5), 607-615.
15. Moss, D.; Harbison, S. A.; Saul, D. J., An easily automated, closed-tube forensic DNA extraction procedure using a thermostable proteinase. *International Journal of Legal Medicine* **2003**, *117* (6), 340-349.
16. McCord, B. R.; McClure, D. L.; Jung, J. M., CAPILLARY ELECTROPHORESIS OF POLYMERASE CHAIN REACTION-AMPLIFIED DNA USING FLUORESCENCE DETECTION WITH AN INTERCALATING DYE. *Journal of Chromatography A* **1993**, *652* (1), 75-82.

17. McCord, B. R.; Jung, J. M.; Holleran, E. A., HIGH-RESOLUTION CAPILLARY ELECTROPHORESIS OF FORENSIC DNA USING A NON-GEL SIEVING BUFFER. *Journal of Liquid Chromatography* **1993**, *16* (9-10), 1963-1981.
18. <https://www.fbi.gov/about-us/lab/biometric-analysis/codis/rapid-dna-analysis>.
19. Northrup MA, C. M., White RM, Watson RT In *DNA amplification in a microfabricated reaction chamber* 7th International Conference on Solid-State Sensors and Actuators, Yokohama, Japan, Yokohama, Japan, 1993; pp 924-926.
20. Zhang, C. S.; Xu, J. L.; Ma, W. L.; Zheng, W. L., PCR microfluidic devices for DNA amplification. *Biotechnology Advances* **2006**, *24* (3), 243-284.
21. Nakano, H.; Matsuda, K.; Yohda, M.; Nagamune, T.; Endo, I.; Yamane, T., HIGH-SPEED POLYMERASE CHAIN-REACTION IN CONSTANT FLOW. *Bioscience Biotechnology and Biochemistry* **1994**, *58* (2), 349-352.
22. Kopp, M. U.; de Mello, A. J.; Manz, A., Chemical amplification: Continuous-flow PCR on a chip. *Science* **1998**, *280* (5366), 1046-1048.
23. Geng, T.; Novak, R.; Mathies, R. A., Single-Cell Forensic Short Tandem Repeat Typing within Microfluidic Droplets. *Analytical Chemistry* **2014**, *86* (1), 703-712.

24. Shewale, J. G.; Liu, R. H., *Forensic DNA Analysis: Current Practices and Emerging Technologies*. CRC Press: 2013.
25. Zhang, C. S.; Xing, D.; Li, Y. Y., Micropumps, microvalves, and micromixers within PCR microfluidic chips: Advances and trends. *Biotechnology Advances* **2007**, *25* (5), 483-514.
26. Le Roux, D.; Root, B. E.; Reedy, C. R.; Hickey, J. A.; Scott, O. N.; Bienvenue, J. M.; Landers, J. P.; Chassagne, L.; de Mazancourt, P., DNA Analysis Using an Integrated Microchip for Multiplex PCR Amplification and Electrophoresis for Reference Samples. *Analytical Chemistry* **2014**, *86* (16), 8192-8199.
27. Gorkin, R.; Park, J.; Siegrist, J.; Amasia, M.; Lee, B. S.; Park, J. M.; Kim, J.; Kim, H.; Madou, M.; Cho, Y. K., Centrifugal microfluidics for biomedical applications. *Lab on a Chip* **2010**, *10* (14), 1758-1773.
28. GJ, M. M. a. K. In *Systems and Technologies for Clinical Diagnostics and Drug Discovery*, SPIE 3259, San Jose, CA, Cohn GE and Katzir A: San Jose, CA, 1998.
29. Kellogg GJ, A. T., Carvalho BL, Duff DC, Sheppard NF MicroTAS, A. van den Berg, W. O., P. Bergveld, Ed. 2000; pp 239-242.
30. Ouyang, Y. W.; Wang, S. B.; Li, J. Y.; Riehl, P. S.; Begley, M.; Landers, J. P., Rapid patterning of 'tunable' hydrophobic valves on disposable microchips by laser printer lithography. *Lab on a Chip* **2013**, *13* (9), 1762-1771.

31. Thompson, B. L.; Ouyang, Y. W.; Duarte, G. R. M.; Carrilho, E.; Krauss, S. T.; Landers, J. P., Inexpensive, rapid prototyping of microfluidic devices using overhead transparencies and a laser print, cut and laminate fabrication method. *Nature Protocols* **2015**, *10* (6), 875-886.
32. Kim, J.; Byun, D.; Mauk, M. G.; Bau, H. H., A disposable, self-contained PCR chip. *Lab on a Chip* **2009**, *9* (4), 606-612.
33. Ouyang, Y.; Duarte, G. R. M.; Poe, B. L.; Riehl, P. S.; dos Santos, F. M.; Martin-Didonet, C. C. G.; Carrilho, E.; Landers, J. P., A disposable laser print-cut-laminate polyester microchip for multiplexed PCR via infra-red-mediated thermal control. *Analytica Chimica Acta* **2015**, *901*, 59-67.
34. Ren, Y.; Leung, W. W. F., Numerical and experimental investigation on flow and mixing in batch-mode centrifugal microfluidics. *International Journal of Heat and Mass Transfer* **2013**, *60*, 95-104.
35. Grumann, M.; Geipel, A.; Riegger, L.; Zengerle, R.; Ducree, J., Batch-mode mixing on centrifugal microfluidic platforms. *Lab on a Chip* **2005**, *5* (5), 560-565.

Integrated DNA extraction, PCR amplification, and electrophoretic separation on a rapid and portable microdevice

5.1 Overview

Forensic DNA analysis requires several steps, including DNA extraction, PCR amplification, and electrophoretic separation of PCR fragments. The goal of Rapid DNA platforms is to develop an instrument that is capable of rapid “sample-to-answer” short tandem repeat (STR) analysis in a simplified manner. In order for this goal to be achieved, all of the analytical processes required for STR analysis must be integrated into a single device. Here, the focus is first on the optimization of a novel multiplex PCR chemistry that is capable of integration with upstream DNA extraction and downstream separation. In order to reach the end goal of complete STR analysis in <90 minutes, the PCR amplification time was reduced. As the design of the integrated microdevice is more complex than the simple, PCR only device shown previously, additional materials were necessary for complete fluidic control and assay functionality. To meet this need, PCR was optimized for multiple different microdevice substrates, including black polyethylene terephthalate (black Pe) and heat sensitive adhesive (HSA). Utilizing a centrifugal microfluidic platform, custom-built system, and simplified microdevice fabrication procedure, the integration of extraction, PCR, and separation was achieved in less than 90 minutes. STR profiles generated from these integrated analyses are 100% concordant with results obtained using conventional methods.

5.2 Introduction

Microfluidic or lab-on-a-chip (LOC) devices offer many distinct advantages for forensic genotyping and DNA analysis via short tandem repeat (STR) profiling. These include: reduced risk of contamination, rapid analysis times, reduced reagent and sample consumption, and the ability for on-site analysis at a crime scene or point of interdiction.¹ In a typical forensic laboratory, the entire DNA analysis process, including DNA extraction, PCR amplification, and electrophoretic separation, can take up to 7-10 hours for a single sample, or a few days when samples are batched.² This prolonged analysis timeframe can render the results from genetic profiling less relevant to the initial phases of criminal investigations. Furthermore, the long analysis times contribute significantly to the drastic sample backlog currently experienced by forensic laboratories.³⁻⁵ Owing to the unique advantages attributed to the LOC platform, these devices are poised to address the limitations inherent to conventional genetic analysis techniques for human identification.

PCR amplification is a critical component in the complete sample in-answer out analytical process involving STR profiling for DNA forensic applications. Generally accepted as a time-consuming and labor-intensive process, PCR has long been the focus of efforts to increase speed and automation to reduce overall analysis time and, therefore, aid in minimizing continued growth of casework backlogs in criminal laboratories.⁶ Significant work has been done toward the development of an analysis platform that is both rapid and inexpensive in order to improve DNA analysis in the forensic community, referred to as Rapid DNA.⁷⁻¹² Specifically with PCR, the earlier commercially-available

STR kits could require up to 3.5 hours; however, that time has been decreased dramatically with newer kits that are faster (as low as 45 min) and substantially more robust to PCR inhibitors. Efforts over the last decade have been focused on rapid PCR methods to decrease the time needed for fully-automated human genotyping.¹³⁻¹⁵ STR amplification in a conventional manner has been successfully reported in as little as 14 minutes for a 16-plex by improving the chemistry.¹⁶ Unfortunately, the capability for integration of this rapid PCR with upstream and downstream analysis is not straightforward and manual steps are still required. The past decade has seen the development of a wide variety of microfluidic devices for DNA amplification via PCR. These devices have a low thermal mass compared to conventional thermocyclers, allowing for heating and cooling rates upwards of 10-50°C/second.^{17, 18} Microdevices for PCR amplification can be divided into three main categories: continuous-flow, droplet, and well-based.

Continuous-flow PCR involves the movement of fluid through various zones of a device which are set to specific temperatures, and these devices can be further divided into three categories: fixed-loop, closed-loop, and oscillatory. The first continuous-flow chip was developed by Kopp et al. in 1998, and the overall reaction time depends upon the flow rate of the sample through the various temperature zones.¹⁹ Obeid et al. developed a continuous-flow PCR chip that was combined with laser-induced fluorescence (LIF) for both DNA and RNA amplification and detection, with PCR times as low as 35 minutes.^{20, 21} In 2002, West and colleagues developed a closed-loop microdevice with a two-step PCR reaction, in which the fluid is moved via magnetohydrodynamic actuation.²² Similarly, Chen et al. developed a system comprised

of a Teflon tube, with three distinct heating zones, that was angled such that fluid flow would be driven by convection, negating the need for an external pump.²³ The successful amplification of 305 and 700 base pair fragments was shown in 73 minutes using this device. Although much progress has been made toward microdevices for continuous-flow PCR, the biggest disadvantage of this method is surface inhibition and adsorption, since the PCR reagents experience more interaction with the chamber surface while they are continuously flowing through the device.²⁴

Droplet-based PCR has garnered substantial attention in recent years. This method eliminates PCR inhibition and carryover contamination seen with continuous-flow devices. Typically, the PCR reaction is performed in a water-in-oil droplet in a microchannel, and each droplet can, therefore, be considered its own PCR reactor. Since the sample and reagents are confined to a single microdroplet, local temperature variations are small, and each microdroplet can experience a uniform temperature.²⁵ Beer et al. developed a microfluidic droplet-based PCR chip with picoliter droplets that remain stationary during thermocycling.²⁶ Owing to the small size of the droplets, a 56% cycle reduction is possible and only 18 cycles are required for single-copy amplification. In contrast to this stationary droplet-based approach, a continuous-flow droplet device was developed by Kiss et al. and can amplify a 245 base pair fragment within 35 minutes.²⁷ The drawbacks associated with this method include the challenge of reliably producing monodispersed droplets, and how to control the interaction of these droplets with the surface and each other.²⁴

Well-based PCR microdevices require the entire well, and sometimes the entire device, to be heated and cooled during thermocycling. The large thermal mass associated with this process often leads to long thermocycling times, a distinct disadvantage for well-based microfluidic PCR.²⁴ Despite this drawback, many groups have made significant progress with well-based PCR. In 2004, El-Ali et al. developed a microdevice capable of heating and cooling rates of 50°C and 30°C/second, respectively, and this device made use of integrated heaters and a total chamber volume of 20 μL .¹⁸ Another example of a well-based microfluidic PCR device is the polydimethylsiloxane (PDMS) chip developed by Liu et al. for real-time quantitative PCR. This device contains 100 wells (120 nL each) that have pre-loaded, dried primer pairs, and heating and cooling is accomplished with a thermoelectric mechanism.²⁸ The well-based system will be the focus of the microfluidic PCR developed in this Chapter for integration with upstream DNA extraction and downstream electrophoretic separation. This approach was chosen because of the relatively simple mechanism for temperature control (dual-Peltier), which allows for PCR thermocycling, constant temperature application for DNA extraction (75°C), and rapid heat-snap cool prior to separation.

As a natural extension of the research surrounding microfluidic PCR, several groups have focused on the development of an integrated forensic DNA analysis system to fulfill the requirements set forth by the Rapid DNA community. Here, four different systems aimed at meeting the goals of Rapid DNA will be briefly discussed: IntegenX RapidHIT™, Netbio/GE DNAscan™, NEC Portable DNA Analyzer, and the MicroLab Intrepid.

The IntegenX RapidHIT™ system has proven the most successful for STR profiling and rapid human identification, with CODIS profiles generated in <90 minutes.^{8, 29, 30} The system, however, is not portable, and requires 4 microfluidic cartridges; 2 cartridges for DNA extraction and PCR amplification, and 2 cartridges for electrophoretic separation. Furthermore, separation takes place on a conventional capillary electrophoresis (CE) instrument (not on the microdevice itself) that is incorporated into the system. Fluidic movement is achieved through the use of valves and pumps, notably the patented Microscale On-chip Valves (MOVE™) technology, which allows for metering and mixing of volumes as small as 10 nL. Extraction is performed via solid-phase extraction (SPE), and thermocycling for PCR amplification is Peltier-driven. Despite its many advantages in terms of assay quality, the RapidHIT™ system is expensive (\$250,000 USD for the instrument and \$250-300 USD for consumables) and lacks portability.

Netbio/GE has developed the DNAscan™ system, and it is the first truly integrated device for rapid human identification.³¹ A STR profile is generated in approximately 84 minutes, with lyophilized reagents allowing for room temperature storage of the injection molded BioChipSet cassette. Rapid multiplex PCR (probing 16 genetic markers) is achieved in 20 minutes. After insertion of the buccal swab into the cartridge, it is placed into the instrument, and the entire process is automated. Unlike the RapidHIT™ system, the DNAscan™ system has on-chip microchip electrophoresis (ME), and an allelic ladder can be generated with each sample that is run on the instrument. However, this instrument suffers from the same disadvantages, namely cost of instrument and consumables, as well as a lack of portability.

The NEC Portable DNA Analyzer adopts a new approach to microfluidic PCR for STR profiling.³² This instrument features multiple chambers for simultaneous single-plex and 2-plex PCR, rather than a large multiplex, and the overall PCR amplification time is 30 minutes with Peltier-driven thermocycling. Following PCR, the product is separated on-chip with multiple ME channels; short channel lengths are sufficient since there are only one or two PCR amplicons per line, and ME can, therefore, be achieved in as little as 5 minutes. Overall analysis time is 50 minutes, representing a distinct advantage of this system over the two previously described; however, since a commercial STR kit is not used, external validation in the forensic community will be required, and the cost of the device is still high.

Lastly, the MicroLab IntrepID system was developed to interface DNA extraction via ZyGEM reagents with non-contact PCR amplification of 18 genetic markers (18-plex).^{1,33} ZyGEM reagents were used for liquid enzymatic DNA liberation prior to PCR, and the non-contact amplification was driven by an infrared (IR) lamp that provided rapid heating and cooling for thermocycling with simplified instrumentation. ME was performed in a 7 cm microchannel with a unique, self-coating polymer. Although the footprint of the microdevice itself was reduced, the inclusion of pneumatic pumps and valves for fluid flow control required undesirable bulk to be added to the system, thereby decreasing portability and increasing cost.

As described, all of the systems developed for rapid human identification via STR profiling fall short of the goal of an inexpensive, portable instrument for genetic analysis. This work focuses on the development of a centrifugally-driven microdevice that is

fabricated from inexpensive substrates and requires no external pumps or valves for fluid flow control, although the bulk of research was aimed at the optimization of PCR for integration. The amplification of 10 genetic markers (10-plex) is demonstrated in 15 minutes via Peltier-driven temperature control and thermocycling, and the same dual-Peltier is also used for enzymatic DNA extraction prior to PCR. Substantial effort was devoted to the reduction of overall PCR amplification time, the demonstration of PCR compatibility with both ZyGEM-extracted DNA and various new materials required for integrated microdevice fabrication. All three assays, DNA extraction, PCR amplification, and ME, are integrated onto a single device capable of generating a STR profile in an automated manner in just 74 minutes. To further demonstrate the utility of this centrifugal microfluidic platform, referred to as the FaSTR system, 40 individual runs were performed in conjunction with an outside investigator. Buccal swabs were collected from 18 individuals, and the entire process, including DNA extraction, PCR amplification, and electrophoretic separation, was run in an automated manner. STR profiles generated from these runs, where the user simply inserted the swab into the chamber, loaded the disc on the instrument, and pressed “start”, were 100% concordant with the truth data collected from conventional assay processing.

5.3 Materials and Methods

5.3.1 Chip fabrication and instrumentation

Microfluidic chips were made out of commercially available overhead transparencies (TransNS, Film Source, Maryland Heights, MD, USA) using the print, cut, laminate method previously described by Thompson, et al.³⁴ The design of the

microchips was the same as previously described by our lab.³⁵ HSA (EL-7970-39, Adhesives Research, Glen Rock, PA, USA) was used in place of toner to adhere the layers of the device together in some experiments. Black Pe (Lumirror X30-75, Tokyo Film Service Co. Ltd., Tokyo, Japan) was also used to test the compatibility of PCR with this material prior to integration with upstream and downstream analysis requiring laser valves to fluidically isolate the different assays.

5.3.2 Spin system for integrated LE-PCR-ME

The spin device for integrated LE-PCR-ME consisted of a custom-built speed controlled motor apparatus which contained a DC brushed motor (Pololu #2821) driven by a pulse width modulated signal from a Parallax Propeller microcontroller (Parallax #32150). A DRV8801 based breakout board (Pololu #2136) was used to amplify the logic level signal, in order to bring the command signal to the appropriate voltage for the motor. In order to calculate the disc RPM, a Hall effect encoder built into the motor was used, and the speed was kept constant through the use of a Proportional-Integral controller. Commands were sent to the microcontroller over USB, including the desired RPM and spin direction (both entered into the graphical user interface (GUI)). A 700 mW, 638 nm laser diode (Thorlabs, Inc., Newton, NJ, USA) was used to actuate the laser valves, and this was placed 2 cm below the disc on the integrated system. The dual-Peltier clamping apparatus was as described previously (Chapter 4).

5.3.3 PCR primer optimization for on-chip amplification

A custom 10-plex kit was developed in this work. The main goal was to be able to amplify 9 core CODIS loci and Amelogenin with amplicons no larger than 350 bp to be suitable for downstream fast microfluidic separation. Different arrangements of markers were designed and tested in preliminary studies and a unique combination was chosen and used for this study, composed of three different dye colors (FAM, JOE and ET-CRX). The custom 10-plex was first amplified conventionally using the PowerPlex[®] Fusion System amplification master mix following the manufacturer's recommendations for thermocycling. The 10 primers were used at the same proprietary concentration in the original 10-plex primer pair mix.

The 10-plex primer pair mix was then used for on-chip amplification with a proprietary master mix based on the PowerPlex[®] Fusion System, but enhanced for rapid on-chip PCR. The amplification was performed in 27 minutes using the DIPS system. The thermocycling parameters were: 96°C for 1 minute, followed by 30 cycles of 94°C for 10 seconds, 59°C for 20 seconds, and 72°C for 15 seconds, with a final extension at 60°C for 60 seconds. The individual primer pair concentrations were adjusted based on the on-chip amplification results to optimize the inter-locus balance within the 10-plex for on-chip amplification.

5.3.4 PCR time reduction

The on-chip PCR time was reduced to meet fast PCR time expectations. The first step in the time reduction was to simplify the PCR thermocycling by using an anneal-

extension temperature (60°C) instead of using two separate temperatures. This allowed for faster ramping and cooling rates with the PID controlled DIPS system. Each of the hold times were also reduced so that the total 30 cycle PCR times reached 19 min (94°C for 5 sec and 60°C for 25 sec for each cycle) and 15 min (94°C for 3 sec followed by 60°C for 20 sec for each cycle). The final extension was 60 sec for all PCR times. The total PCR time was reduced as low as 10 min total (94°C for 3 sec followed by 60°C for 10 sec for each cycle) in this study according to the hardware limitations of the DIPS system, which allowed for rapid thermocycling.

5.3.5 PCR master mix optimization for on-chip amplification

A master mix was optimized with a lyo-compatible buffer, making it suitable for future lyophilization. A magnesium and polymerase titration was performed to determine the optimal conditions for on-chip applications with the addition of MgCl₂ and DNA polymerase (Promega Corporation, Madison, WI, USA). The optimized master mix was formulated to be 2.5X in a total volume of 25 µL, where 1X polymerase was equal to 50 units/µL. The polymerase titration was performed by adding in DNA polymerase to the lyo-compatible buffer with a MgCl₂ concentration of 3.5 mM (determined to be optimal in a preliminary study). In this study, up to 20X (1000 units/µL) polymerase was added to the final PCR reaction. The lyo-compatible buffer volume remains the same for the experiments where the high polymerase concentration is increased gradually. Amplification on-chip at different times was tested for different polymerase concentration to determine the limits of the system.

5.3.6 On-chip amplification

The DNA and PCR reagents were mixed off-chip and introduced into the chip prior to amplification. Depending on the study, either 5 ng of 2800M control DNA or 2 μ L of ZyGEM extracted DNA were used as the source of template DNA. Each study included at least three replicates. The PCR reagents were degassed as follows: clamp Peltier onto PCR chamber and heat to 96°C for 1 minute, release clamped Peltier, and spin chip for 10 seconds at 1200 RPM prior to the thermocycling protocol.

5.3.7 Liquid extraction (LE)

Zygem EA1 enzyme (ZyGEM Corp., Hamilton, New Zealand) was used to perform on-chip liquid extraction prior to on-chip PCR amplification. 10 μ L of 10X prepGEM™ Saliva buffer and 2 μ L of prepGEM™ Saliva EA1 enzyme were added to 88 μ L of water. Buccal cells from nine different donors were collected for 30 seconds using bristle swabs. A buccal swab was placed into the on-chip extraction chamber and the reagent mixture was added and heated at 75°C for two minutes followed by 95°C for two minutes. The same liquid mix was used for tube extractions; 100 μ L of extraction liquid was placed into a PCR tube along with a buccal swab. After vortexing thoroughly, the same heating protocol was performed in a conventional thermocycler. Following LE, 2 μ L of ZyGEM extracted DNA was mixed into the final 25 μ L PCR reaction.

5.3.8 Electrophoresis and data analysis

All PCR results were analyzed using an ABI 310 Genetic analyzer (Life Technologies, Carlsbad, CA, USA). The injection and separation conditions were: 15

kV for 5 seconds and 15 kV for 1680 seconds, respectively. GeneMarker[®] HID software (Softgenetics LLC, State College, PA, USA) was used to analyze the profiles using panels created for the 10-plex. A 10-plex specific allelic ladder was provided by Promega.

5.4 Results and Discussion

5.4.1 PCR time reduction with control DNA

As described in Chapter 4, a novel 10-plex PCR chemistry was developed for STR-based forensic analysis of human DNA. The primers were designed with certain specifications for ease of integration with eventual downstream microchip electrophoresis (ME). These specifications included: use of amplicons < 300 base pairs (owing to the short length of the separation channel dictated by overall microdevice size constraints), and primers labeled with a maximum of three distinct fluorescent dyes. The optimization of this kit was described in Chapter 4, in regards to master mix components; however, in order to reach the goal of complete STR analysis in <90 minutes, the PCR amplification time had to be reduced.

The 10-plex amplification was originally performed using 3 temperature cycling steps: denaturation (94°C), annealing (59°C), and extension (72°C). The hold times (i.e., the time the reaction mixture is held at a given temperature during thermocycling) for 27-minute PCR (30 cycles) were 10, 20, and 15 seconds for denaturation, annealing, and extension, respectively. In order to decrease the overall amplification time, a joint

anneal/extend step (at 60°C) was used to replace the two separate steps, thereby reducing the time required for ramping the Peltiers to heat and cool. **Figure 5-1A** shows the temperature profiles for 3-step versus 2-step thermocycling. The results indicate that the 2-step cycling is not only faster overall, but the Peltier heating and cooling ramp rates are faster as well (shown at bottom of Figure 5-1A). The ramp rate for 2-step cycling is approximately 13°C/second, whereas the ramp rate for 3-step cycling is approximately 10°C/second.

In addition to reducing the number of set temperatures required for thermocycling, the hold times at each set temperature were also reduced. For 19-minute PCR, the hold times were 5 seconds at 94°C and 25 seconds at 60°C. For 15-minute PCR, the hold times were further reduced to 3 and 20 seconds, respectively. **Figure 5-1B** shows the results from five on-chip PCR reactions, using 5 ng of 2800M control DNA, with decreased overall amplification times. The Y-axis is shown as the total peak height, meaning the peak heights for all 10 markers were added together. With a threshold set at

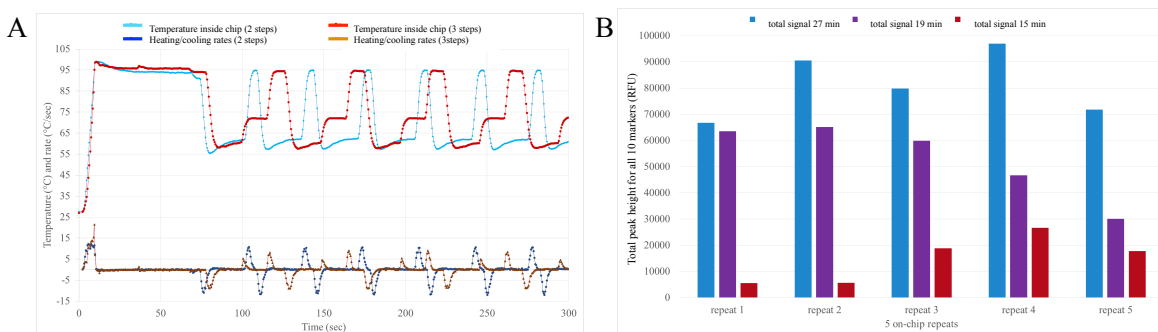


Figure 5-1. Time reduction study. A) Temperature optimization for time reduction, from the 3-step PCR cycling profile to the 2-step PCR cycling profile. The Y axis is in degrees Celsius for the temperature profile and in degrees per second for the heating and cooling rates, the X axis is in seconds. B) Data from five repeat experiments of on-chip PCR with different PCR times using the same reagents (200 units/ μ L polymerase) showing that 19 min total time has the capability to yield profiles as strong as 27 min PCR (repeat 1). A large drop in efficiency is seen between 27 min and 15 min; however 19 min shows strong profiles.

1000 RFU for each peak, and 19 peaks present in 2800M DNA (9 loci are heterozygous (18 peaks) and 1 locus is homozygous (1 peak)), the expected total peak height is 19,000 RFU. These results suggest that 19-minute PCR can yield peak heights comparable to those seen with 27-minute PCR.

5.4.2 ZyGEM DNA template

ZyGEM EA1 is a thermostable enzyme that is capable of liberating DNA from the cell. Previous work has demonstrated the success of on-chip ZyGEM extraction using a simple PeT microdevice,³⁶ and Figure 5-2 provides a schematic of this device. The device is fabricated primarily from PeT; however, poly(methyl methacrylate) (PMMA) was incorporated to allow for the introduction of the large volume required for

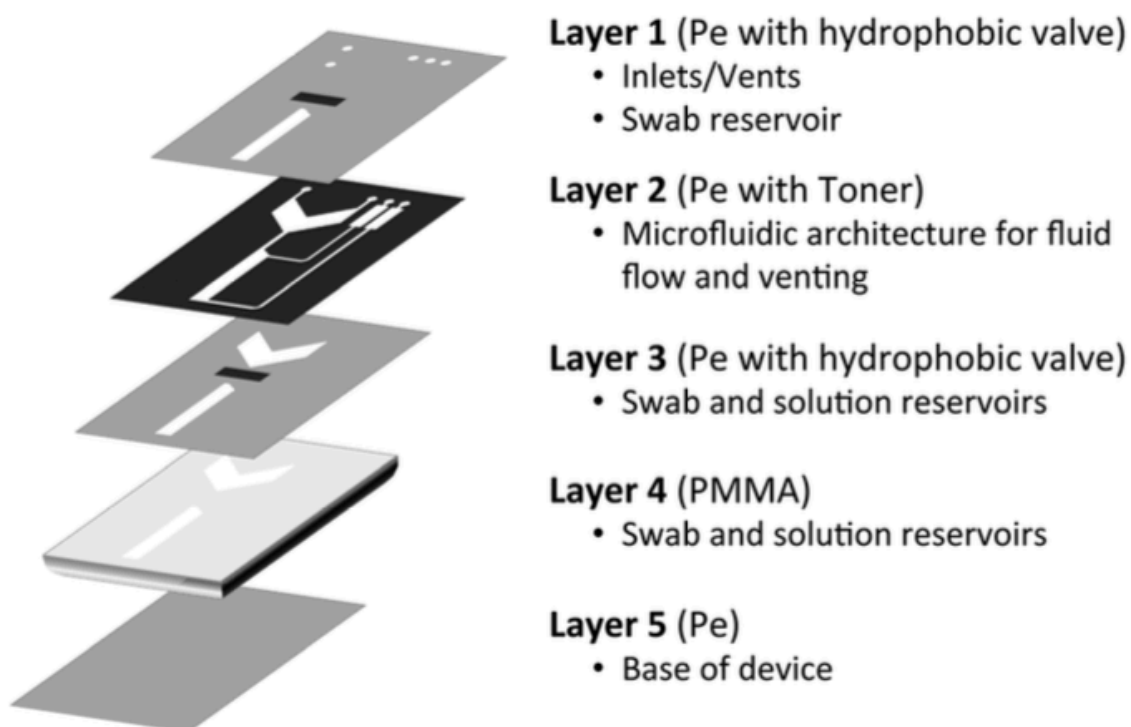


Figure 5-2. Schematic of DNA extraction microdevice. ZyGEM EA1 thermostable enzyme is used to liberate DNA from cells prior to on-chip PCR amplification. This device is fabricated from PeT, PMMA, and pressure sensitive adhesive (PSA). Taken from Thompson et al. 2016.

ZyGEM extraction (100 μ L). The PMMA layer accommodates the larger volume, while also serving as the chamber into which the buccal swab can be directly inserted. As integration of on-chip liquid extraction (LE) and PCR requires the use of ZyGEM-extracted DNA, it was important to prove the compatibility of such DNA with the 10-plex PCR chemistry.

Figure 5-3A shows the result of on-chip 10-plex amplification using conventional ZyGEM-extracted DNA (DNA extracted in tube using ZyGEM EA1 enzyme) and the DIPS system described in Chapter 4 (27 minute overall amplification time for initial studies). The average peak height per marker, for all 10 markers, is >500 RFU. The experiment was performed without prior quantification of the ZyGEM-extracted DNA. This is important because a conventional STR analysis requires quantification of the

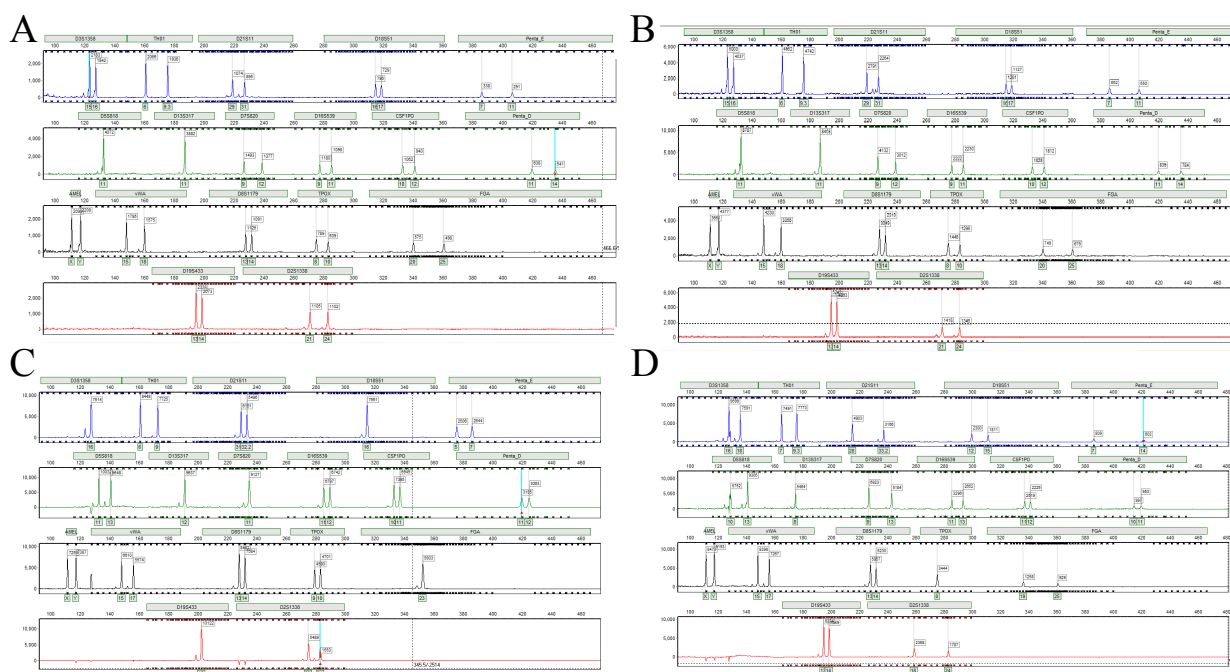


Figure 5-3. Amplification of ZyGEM-extracted DNA. A) Enzymatically-derived (extracted in tube) DNA from donor 1. B-D) Enzymatically-derived (extracted on-chip) DNA from donor 1, 2, and 3. Note: DNA input for A is 0.5 μ L compared to 1 μ L for B, C, and D explaining the difference in RFU

extracted DNA before PCR amplification; however, full on-chip integration of extraction, PCR, and separation requires the PCR to proceed without quantification of the amount of DNA present in the sample, in order to simplify the instrumentation. Each assay is optimized individually prior to integration, and the quality and/or efficiency of each assay suffers when the process is fully integrated. This is most often due to fluidic issues, such as valving, metering, and mixing; all of which are difficult to incorporate on a microfluidic device. For this reason, the peak heights in Figure 5-3A, generated using 0.5 μL template DNA, are lower than desired for a PCR-only result. To demonstrate on-chip PCR with template DNA that

was extracted on-chip (using the device shown in Figure 5-2 and ZyGEM reagents), 1.0 μL of DNA was used as template in an effort to increase the peak heights. An 18-plex amplification was used for these experiments, and the results were translated to the 10-plex amplification. **Figure 5-3B-D** shows the results from these experiments, with 3 different donors. For each

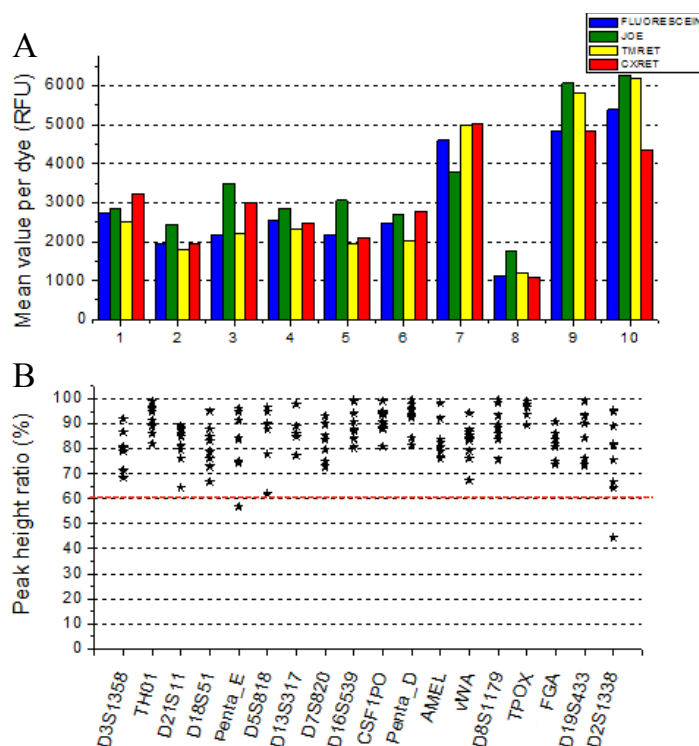


Figure 5-4. Data analysis for on-chip PCR with ZyGEM extracted DNA. A) Peak height mean value per dye color for each of the 10 samples. These profiles are considered full profiles with a threshold fixed at 500 RFU. B) Peak height ratio for the 10 samples, 98.5% of the ratios are greater than 60%.

STR profile generated, the average peak height per marker is >600 RFU, with the majority of peaks >1000 RFU. A more thorough analysis of the 10 samples amplified from on-chip ZyGEM-extracted DNA template is shown in **Figure 5-4**. The mean peak height across each of the 4 dye colors is shown in **Figure 5-4A**, with all peak heights >500 RFU. **Figure 5-4B** shows the peak height ratio (intralocus balance) across the same set of data. The peak height ratio threshold is set to 60%, meaning that for heterozygous alleles, the ratio of the two peaks should be at least 60%. By this metric, 98.5% of the STR profiles generated had peak height ratios that were >60%.

5.4.3 PCR time reduction with ZyGEM-extracted DNA

After on-chip ZyGEM-extracted DNA template was demonstrated to be suitable for on-chip PCR amplification, the next step was to reduce the overall PCR reaction time, mimicking the thermocycling parameters described previously. Furthermore, the same polymerase concentrations were used for each individual amplification time, as described in Chapter 4. **Figure 5-5A** shows the average peak height per marker across 9 different DNA donors, where DNA was extracted on-chip using ZyGEM reagents. The peak heights for 15-minute PCR are higher than the other on-chip conditions (27-min and 19-min PCR), likely due to the increased concentration of polymerase (1000 units/ μ L versus 200 units/ μ L and 500 units/ μ L, respectively). **Figure 5-5B** shows the profile for each color dye overlaid, and all peaks are >1000 RFU. Collectively, these results indicate that either 15-minute or 19-minute PCR is suitable for integration and rapid STR analysis; however, despite the increase in peak height seen with 15-minute PCR, it was determined that the cost of using this amount of polymerase would be prohibitive moving forward

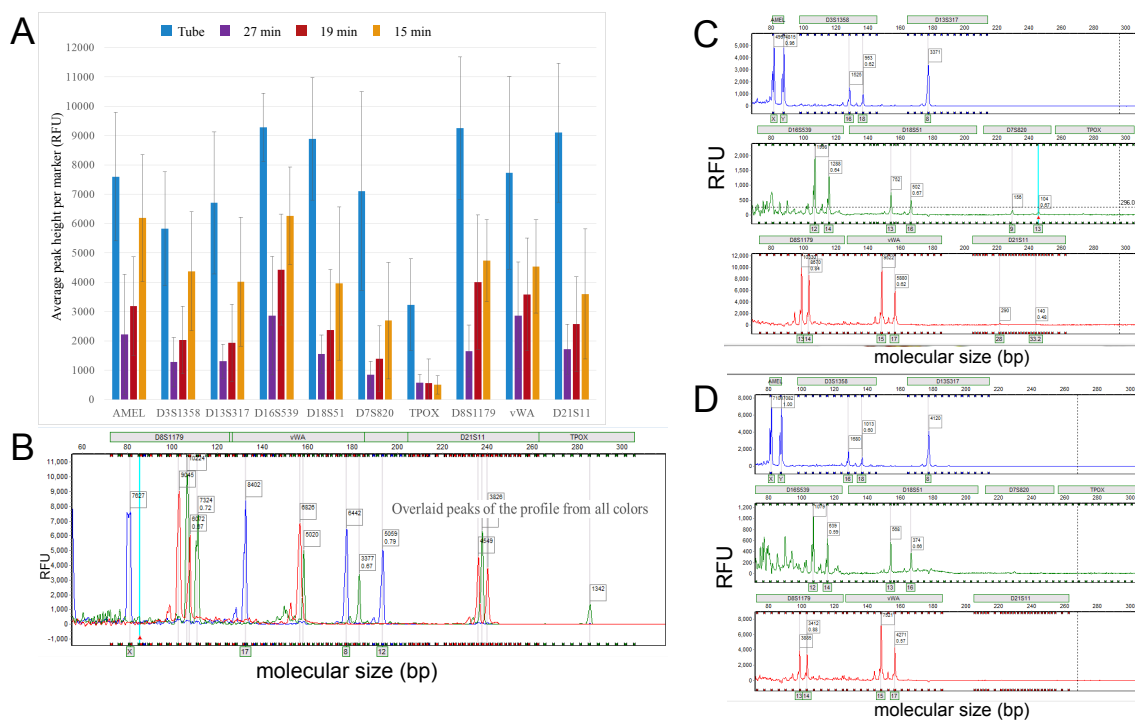


Figure 5-5. Rapid on-chip amplification of ZyGEM extracted DNA. A) Average peak height for all 10 markers for each of the 9 DNA donors. Tube amplification is shown compared to 27, 19, and 15-minute PCR. B) STR profile with ZyGEM-extracted DNA resulting from 15-min on-chip amplification. All peaks are overlaid in this representation. C) A 13-min on-chip PCR using ZyGEM extracted DNA. D) A 10-min on-chip PCR using DNA from the same donor.

with future tests. Moreover, across nine different donors (ZyGEM-extracted DNA) the peak heights for 90% of the amplified loci were >1000 RFU with 19-minute PCR, which was satisfactory to move forward with integration. While the optimal conditions were established, further time reduction was tested to try to reach the limitation of the chemistry. **Figure 5-5C-D** are two profiles obtained using DNA extracted on-chip with ZyGEM reagents from a male donor and amplified on-chip, with master mix containing 1000 units/ μ L polymerase, in 13 and 10 minutes, respectively. While all the peaks larger than 300 bp begin to drop out for a PCR time of 13 minutes (D7S820 and D21S11 show very low peaks), they are completely absent at 10 minutes, which indicates the limit of polymerase incorporation of dNTPs. This is due to the shortened anneal/extension time, which does not allow the full extension of fragments >200 bases, as the polymerase

extension rate is approximately 35-100 dNTPs/second. Despite the fact that these profiles are partial, they indicate the potential for very fast miniSTR amplification on-chip. This, when coupled to upstream and downstream analysis, could be used as a rapid screening tool for loci shorter than 200 bp.

5.4.4 Integration of LE and PCR

Since PCR is positioned between LE and ME in the integrated STR analysis workflow, work had to be done to integrate PCR with upstream and downstream assays separately, before full integration.

Figure 5-6 shows a schematic of an early design for the fully integrated human identification device, with separate regions of the microdevice devoted to extraction, PCR, and separation. In order to move forward with integration of on-chip PCR with LE and ME, a material was needed that would be compatible with all of these assays. Previously in our

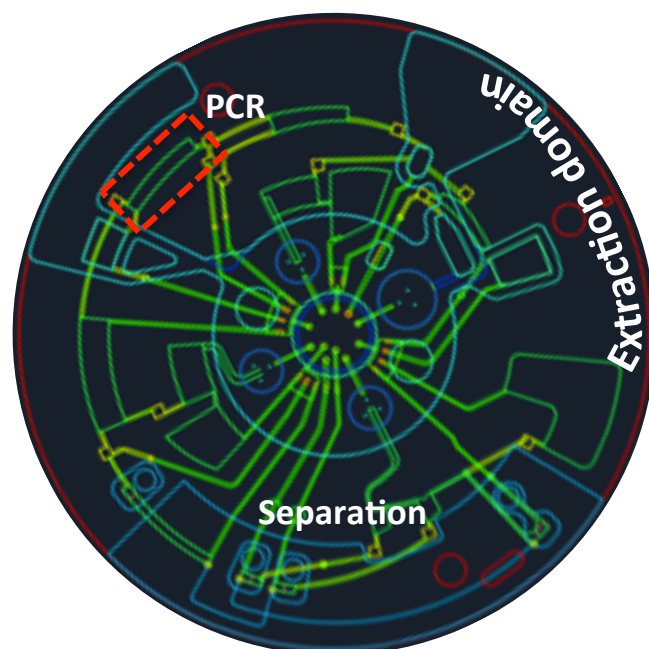


Figure 5-6. Early prototype for integrated device. Extraction, PCR, and separation domains are shown in schematic. Courtesy of Dr. Jingyi Li.

group, all work has been done using chips fabricated out of polyethylene terephthalate (Pe) printed with toner (known as a PeT device), with the toner functioning as the adhesive. However, for the separation component of the device, a COC chip must be adhered to the PeT using pressure sensitive adhesive (PSA), and the PeT devices were

found to frequently de-laminate under the pressure required for PSA adhesion. A switch was, therefore, made to heat sensitive adhesive (HSA) in lieu of toner, resulting in microdevices that were much more flexible and robust. HSA also simplifies the fabrication process, because various layers can be easily aligned prior to bonding. Additionally, the final device makes use of laser valves, which are actuated when a dark material (in this case, black Pe) absorbs the energy from an infrared laser and a hole is burned, through which the liquid can flow.

Accordingly, it was necessary to test these two new materials, HSA and black Pe, for inhibition of the 10-plex PCR demonstrated previously. **Figure 5-7** shows the results of the PCR performed on chips fabricated from Pe + HSA, and black Pe + HSA. The

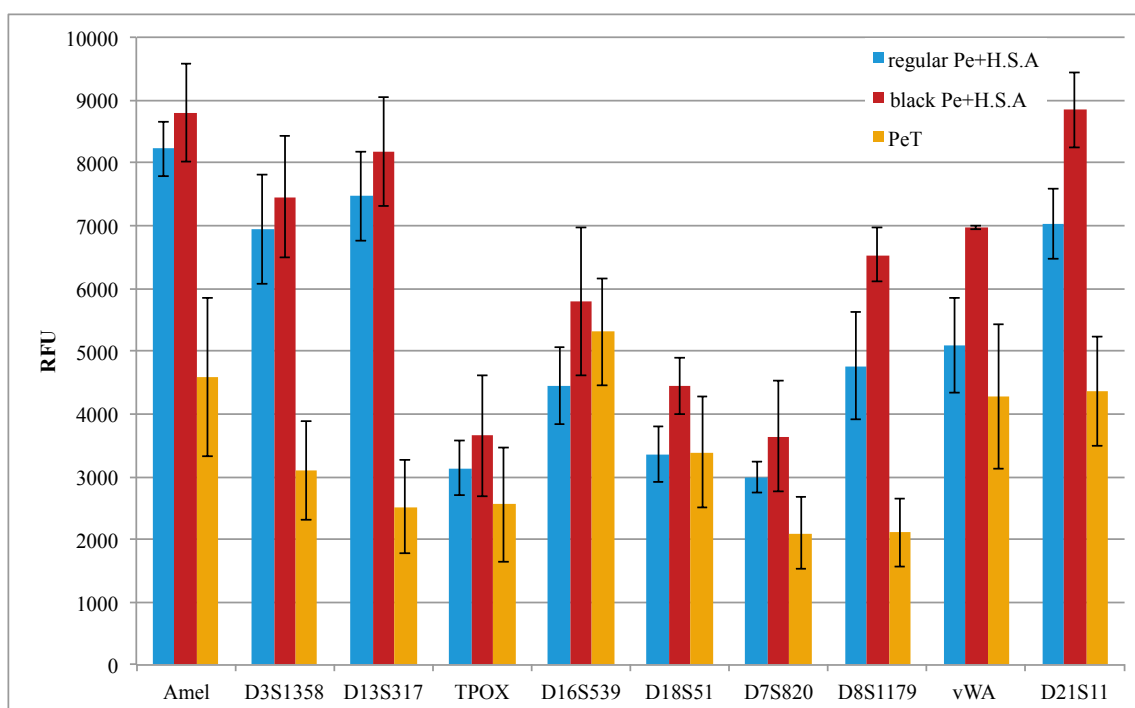


Figure 5-7. Material inhibition study. A) Optimized conditions (10X (500 units/ μ L) polymerase, 3.5mM $MgCl_2$, and 19 min amplification) were tested using various different materials. Heat sensitive adhesive (HSA) was tested as an alternative to toner in adhering the layers of Pe together in the microdevice. Black Pe was also tested as a future alternative for incorporating laser valves for integrated device linking the liquid extraction and on-chip PCR domains together.

profiles generated were very strong, with peak heights for all loci >2000 RFU. These results suggest that the incorporation of the new materials into a final integrated microdevice design will not be detrimental to the 10-plex PCR and will still allow for rapid PCR in 19 minutes.

In addition to new materials, the integrated microdevice also incorporates a new PCR chamber design, shown in **Figure 5-8A**. The PCR chamber was designed with certain constraints, including device “real estate”. The main challenges for integrated microdevice design include limited space (120 mm diameter), and maintaining components that require heating (via dual-Peltier stack) to be in the same radial plane (i.e., approximately the same radius from the center), since the Peltiers are stationary. The new design was tested for temperature gradients by inserting a thermocouple into various regions of the PCR chamber and recording the temperature. **Figure 5-8B** shows the results of these experiments, with temperatures ranging from 92.5-95°C, depending on which region of the PCR chamber the thermocouple was measuring. Despite the slight temperature gradient seen here, PCR was performed in PeT chips with the standard design (referred to as “coffin shape”) and with the new design (“integrated”), and the results are shown in **Figure 5-9**. The drop in peak height seen between the coffin shape

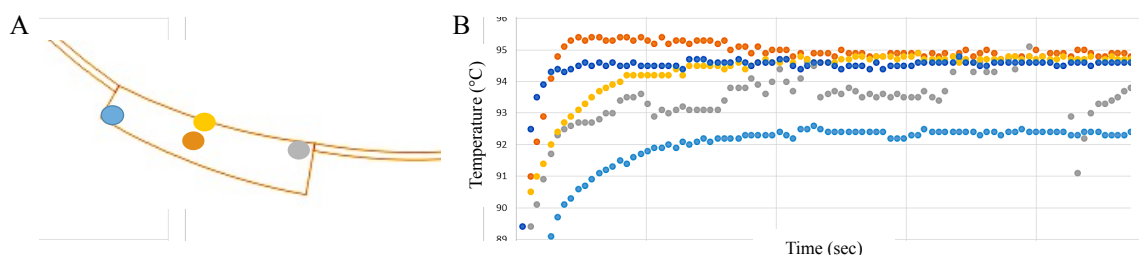


Figure 5-8. Temperature control in new PCR chamber. A) PCR chamber with designated thermocouple locations. B) Resultant temperature profiles for initial denaturation step during on-chip thermocycling of new PCR chamber design.

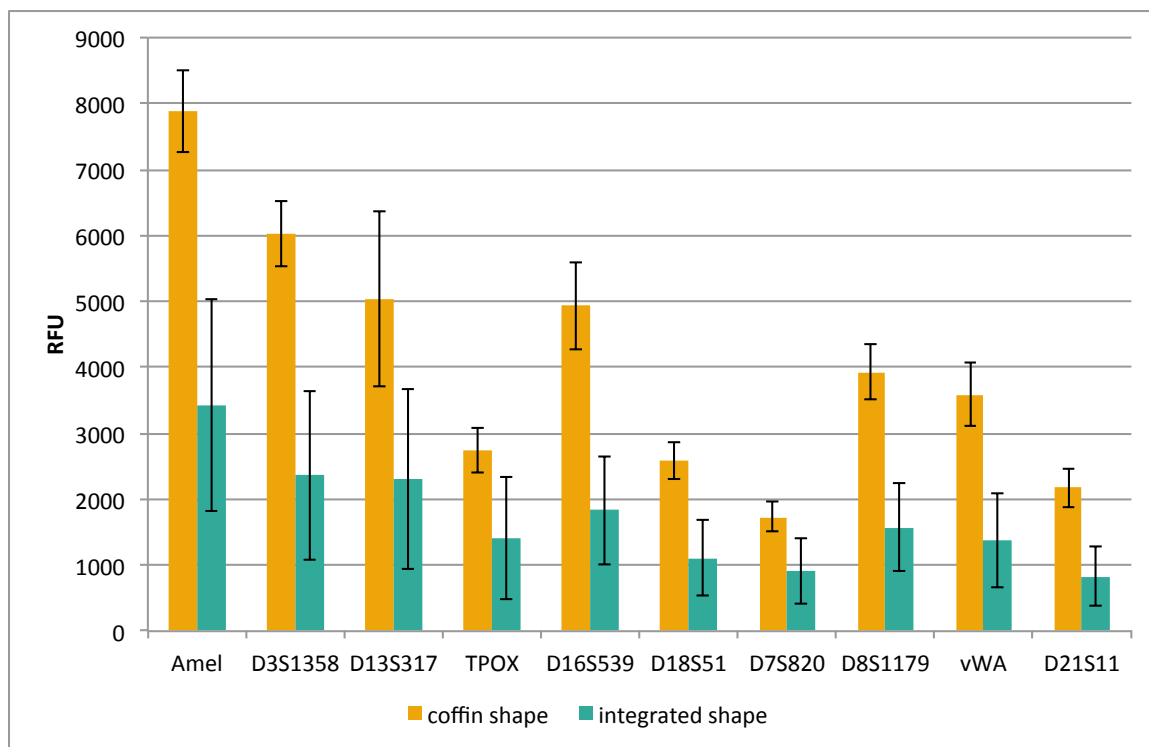


Figure 5-9. Results from on-chip PCR with new design. Peak height is compared for on-chip PCR using the old (coffin shape) vs. the new (integrated shape) chamber design. Decreased peak height is seen in the integrated shape.

and the integrated shape is concerning; however, since the average peak height for all markers was >1000 RFU with the integrated shape, we decided to move forward with integration of LE and PCR. The drop in peak height was attributed to the temperature gradient seen in Figure 5-8, likely due to the variability in clamping pressure across the surface of the dual-Peltier, leading to irregular thermocycling profiles and/or set temperatures that deviate from the desired set temperatures.

A buccal swab must be introduced into the microdevice for on-chip LE, and **Figure 5-10A** shows the custom-designed swab that was used for integrated LE-PCR. The swab head is designed to breakaway from the plastic handle, so that it can be easily inserted into the chamber (**Figure 5-10B**). After swab insertion, the chamber is covered with PCR tape. Fluidic flow between LE and PCR is achieved through the use of a laser

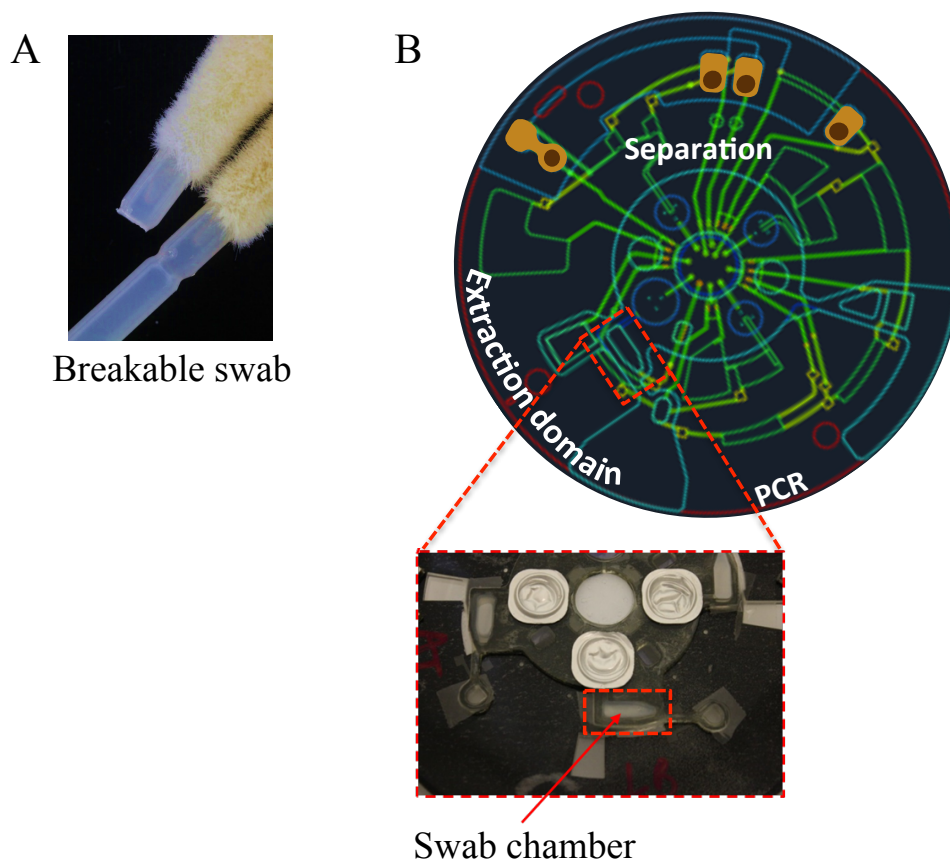


Figure 5-10. Integration of LE and PCR. A) Custom-designed swab with breakable head. Swab was designed for easy insertion into LE (swab) chamber. B) Integrated device shown with extraction domain highlighted. Inset shows swab chamber.

valve that allows the extracted DNA to be aliquoted and then mixed (in a separate mixing chamber) with PCR reagents. After the DNA and PCR reagents are mixed, the mixture flows into the PCR chamber for amplification via Peltier-mediated thermocycling.

The profile in **Figure 5-11A** was obtained using a modified 10-plex (TPOX primers were labeled with Fluorescein dye) with the optimized conditions described previously. Both processes (LE and PCR) were carried out on a single device, and heating for LE was achieved using the same Peltier clamping system described previously and utilized for PCR thermocycling.³⁵ The STR profile generated from integrated on-chip LE-PCR is well balanced, meaning all peaks contribute equally to the

overall peak height, and all peaks are >3000 RFU. **Figure 5-11B** shows the results from integrated on-chip LE-PCR from 10 different buccal swabs, and 91% of loci amplified have peak heights >1000 RFU. In 50% of the STR profiles generated, the locus with the lowest peak height is D8S1179, which has proven to be problematic in the past, in both the 6-plex and 10-plex PCR chemistries. This phenomenon will be explored further in future studies aimed at increasing the signal of the D8S1179 peaks by further modifying the primer concentration. These results indicate the successful integration of LE and PCR, with both assays and all fluidic movement achieved solely through the utilization of a centrifugally-driven microdevice.

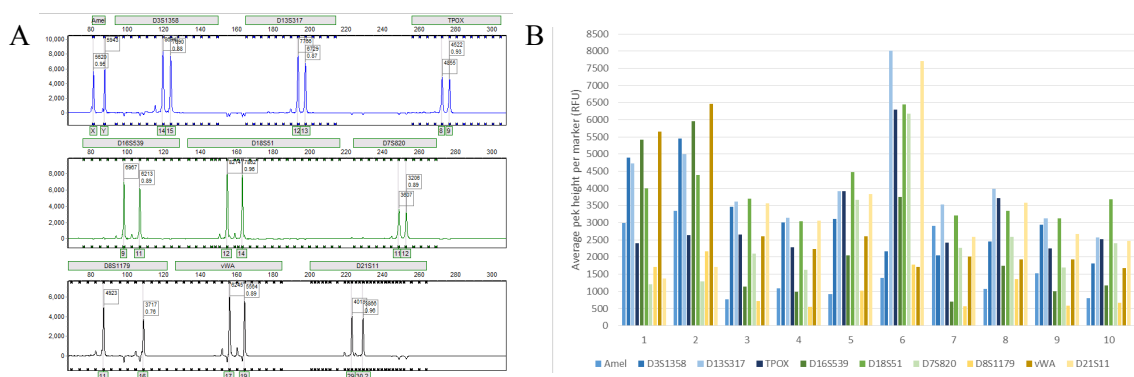


Figure 5-11. LE-PCR results. A) STR profile for integrated on-chip LE-PCR. All peaks >3000 RFU. B) Average peak height for integrated LE-PCR from 10 different runs. Average peak height >500 RFU for all markers across the 10 runs.

5.4.5 Integration of PCR and ME

Our group has previously shown the successful on-chip separation of the products generated from the 6-plex PCR described in Chapter 4.³⁷ Moving forward, however, it was necessary to demonstrate the separation of the 10-plex PCR, and to do so on an integrated microdevice. **Figure 5-12** shows the integrated microdevice, and the inset shows an expanded view of the separation domain. A custom-designed, injection molded

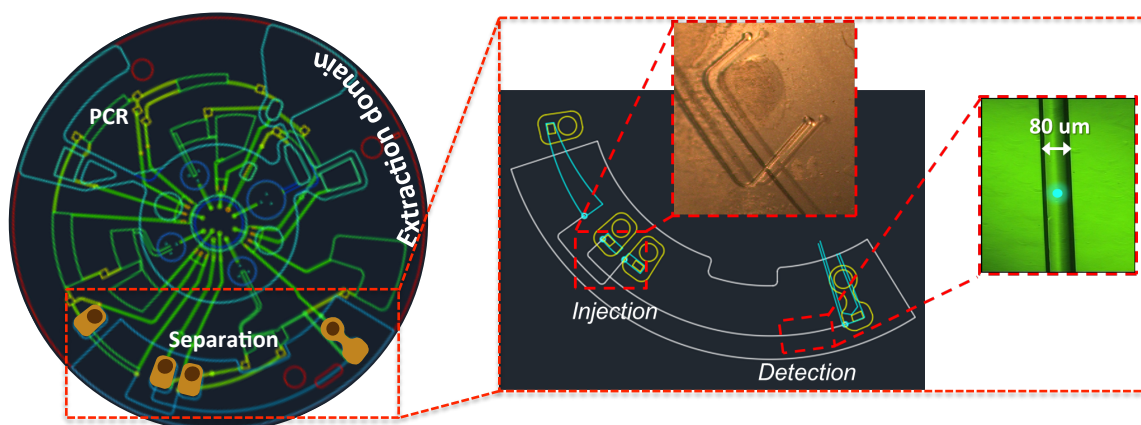


Figure 5-12. Integration of PCR and ME. Separation domain is highlighted in schematic. Inset shows cross-T structure and 80 μm channel width. Courtesy of Dr. Dan Nelson.

COC chip was used, which fits the curved shape of the disc. This curved shape is important because it allows for easier polymer loading by taking advantage of centrifugal force, and the channel has an effective length of 5 cm from injection to detection. The channel diameter is 80 μm , which provides higher resolution in order to meet the end goal of 2 base pair resolution. The gold leaf electrodes have been described previously by our lab³⁷, and provide an inexpensive alternative to traditional sputtering techniques (which requires expensive instrumentation). Furthermore, the gold leaf electrodes are simple to fabricate, and readily amenable to the PCL fabrication method.

Figure 5-13A shows the raw data of the preliminary results from integrated PCR-ME using DNA extracted on-chip with ZyGEM reagents; however, the LE was not fluidically integrated with the PCR-ME. The raw data was first collected using Lab View software, then converted and analyzed using GeneMarker, software to generate the STR profile shown in **Figure 5-13B**. All peaks are present, and the STR profile generated is 100% concordant with the conventional separation performed on the ABI 3130. In order to assign an allele number (i.e., the number of repeats present), an allelic ladder is run to

generate a profile with all the possible alleles for a given marker. The allelic ladder is used to generate a binning palette, which defines the allele number based on the migration time of a STR fragment. The binning palette used to analyze Figure 5-13B is based on the migration time of the allelic ladder on the ABI 3130, so it is not surprising that the peaks do not line up with the corresponding marker. For example, the TPOX fragment (labeled in Fluorescein, top right of STR profile) does not fall under the 300

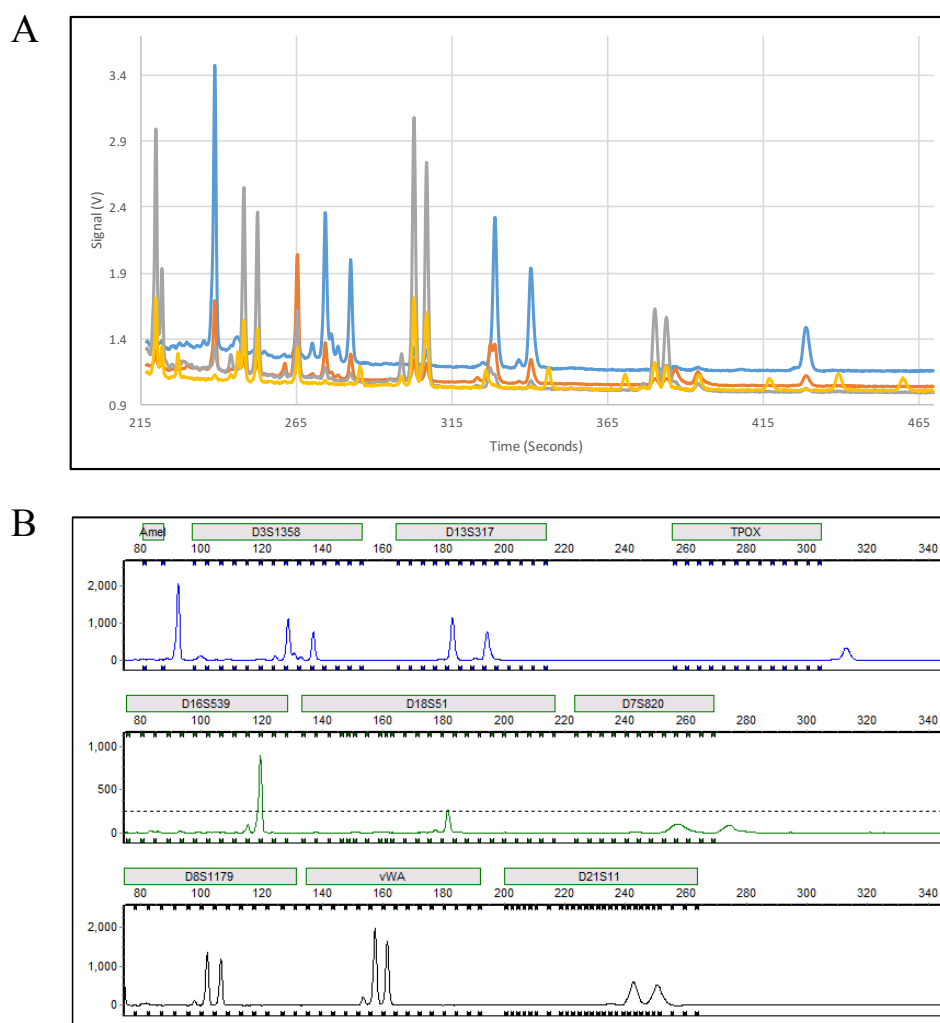


Figure 5-13. Results from integrated PCR-ME. A) Raw data collected in Lab View software. B) Data converted and analyzed using GeneMarker software to generate STR profile from integrated PCR-ME. All peaks are present, and results are 100% concordant with the results from conventional separation (on ABI 3130).

base limit, and therefore is not assigned the appropriate allele number. To correct this problem, the 10-plex allelic ladder was run on the custom-built ME system, as shown in **Figure 5-14A**. When the data is then analyzed using GeneMarker and the binning palette that is based upon the appropriate migration times for the custom-built system, the STR profile generated (**Figure 5-14B**) has the correct allele numbers assigned (shown in grey boxes below each peak).

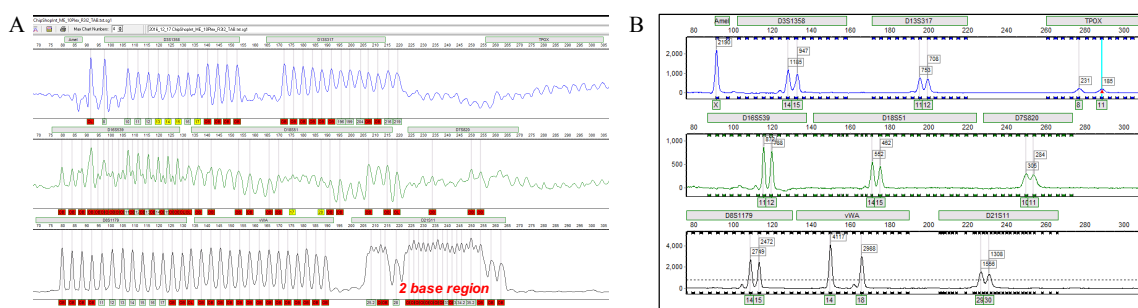


Figure 5-14. Results from integrated PCR-ME after allelic ladder was run. A) 10-plex allelic ladder was run on the ME setup to assign the correct allele numbers based on migration time. B) STR profile generated using corrected binning palette assigns the appropriate allele number to each STR fragment.

5.4.6 Integration of LE-PCR-ME

Fluidic flow and valving are important elements in the full integration of multiple assays onto a microfluidic platform. As described previously, our lab has successfully demonstrated the use of hydrophobic toner patches³⁸ as a method of passive valving. These hydrophobic valves impede aqueous fluid flow until the disc is spun at a speed high enough to overcome the burst pressure of the valve. Although these valves have been successfully utilized for a variety of applications, the number of fluidic steps required for full on-chip integration necessitates a more robust valving mechanism. The strength of the hydrophobic valves is changed based on the amount of toner printed on a given patch, referred to as gray scale, and the range of burst pressures available is,

therefore, limited. In order to integrate 24 chambers and 55 channels, a different valving mechanism is needed. Garcia-Cordero et al.³⁹ demonstrated laser valves in 2010, whereby an infrared laser is used to burn a hole through a physical barrier between fluidic layers of the disc (**Figure 5-15A**). This valving mechanism allows for the disc to be spun at high spin speeds (>2500 RPM) without risk of prematurely breaking valves that are needed for downstream fluid flow control (**Figure 5-15B**). Laser valves were therefore incorporated into the final integrated disc design, with 13 physical valves providing fluid flow control for metering, mixing, and aliquoting. The valves were printed with the same black toner that is used for hydrophobic valves; however, for future manufacturing, black Pe (previously tested for PCR inhibition) will be used to create the physical barrier between layers.

The final microdevice incorporates various inexpensive substrates, including: polyethylene terephthalate (Pe), polyethylene terephthalate toner (PeT), poly(methyl methacrylate) (PMMA), cyclic olefin copolymer (COC), heat sensitive adhesive (HSA), pressure sensitive adhesive (PSA), and gold leaf (**Figure 5-16A**). The disc consists of 10

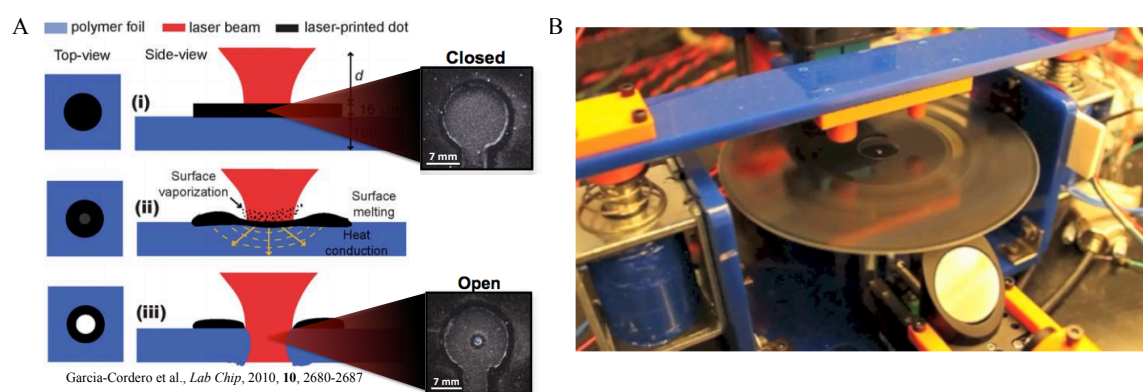


Figure 5-15. Fluidic flow control via laser valves. A) Schematic of laser valve principle. IR laser is used to burn a hole through a dark layer in order to fluidically connect multiple layers of the PeT device. B) Image of microdevice during spinning, allowing for fluid flow control.

distinct layers, 24 fluidic chambers, 55 channels, and 13 physical valves. A schematic of the final device is shown in **Figure 5-16B**, with each layer separated based on how the device is fabricated. All reagents are loaded into four central chambers prior to use, and include: ZyGEM reagents, PCR mixture (master mix and primers), internal lane standard (ILS), and polymer. The swab chamber is built into the PMMA layer (as shown in Figure 5-10B) and covered with PCR compatible tape. The air vents and outlets that are incorporated into the microdevice are located in the center, and covered with a hydrophobic polytetrafluoroethylene (PTFE) membrane to seal the device off from the external environment. This effectively eliminates the possibility for contamination once the swab has been inserted into the swab chamber and sealed, a distinct advantage for forensic applications.

A schematic of the integrated system designed to incorporate this device for complete STR analysis is shown in **Figure 5-17A**. The device is small (1700 in^3), inexpensive ($< \$10,000 \text{ USD}$ for all components) and run from a laptop computer (**Figure 5-17B**). Each microdevice is fitted with a 3D printed adaptor, which allows facile

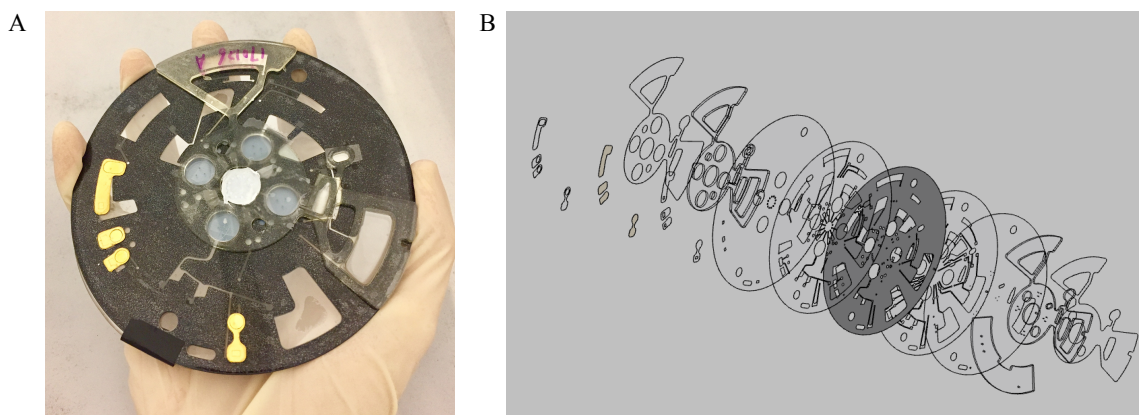


Figure 5-16. *Final integrated device.* A) Integrated microdevice with DNA extraction, PCR amplification, and electrophoretic separation for rapid human identification. B) Schematic of the device, showing each layer.

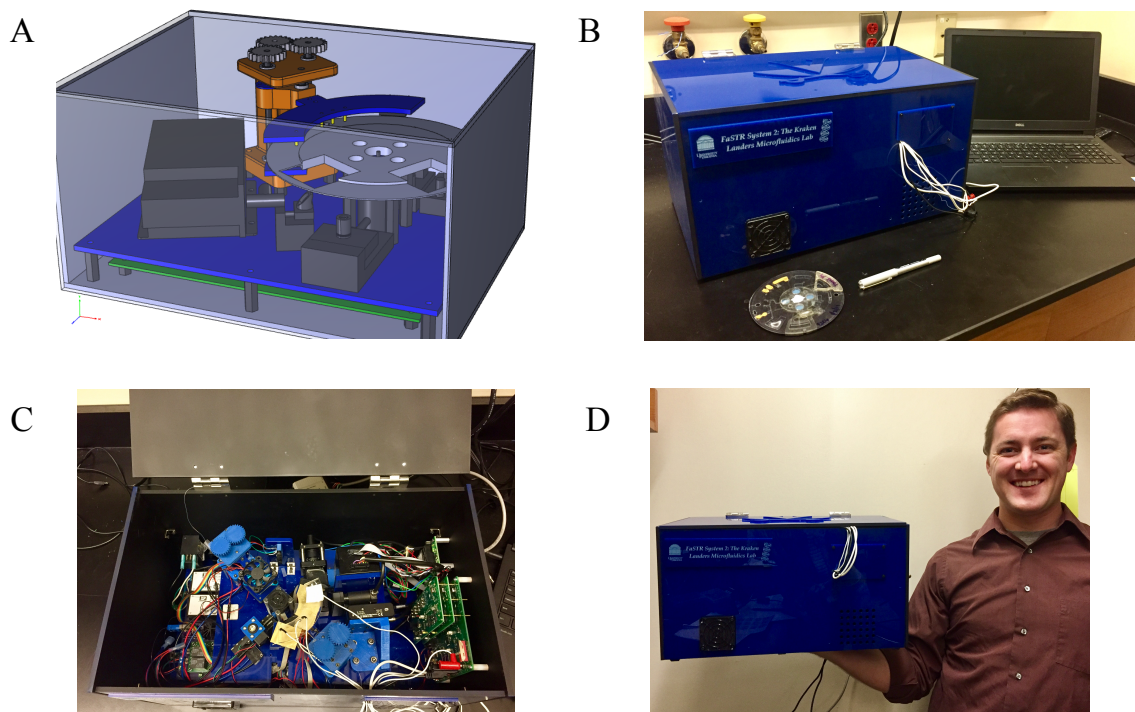
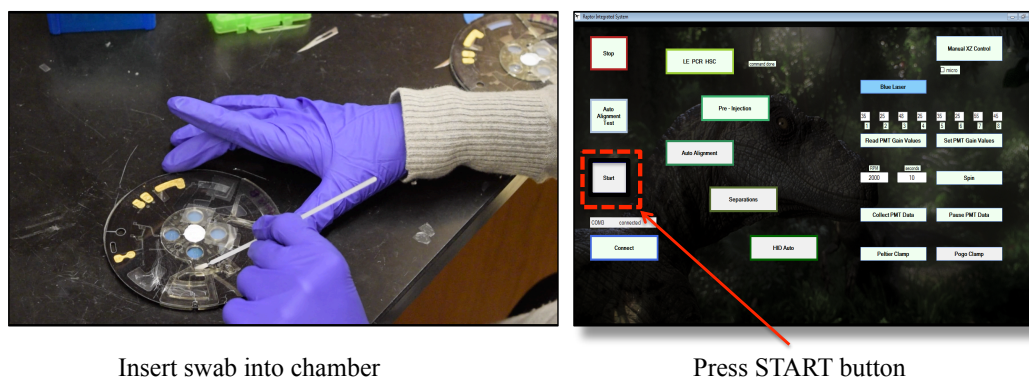


Figure 5-17. Hardware for integrated functionality. A) Solidworks drawing of all components necessary for fully integrated capability. B) System shown with associated laptop used to control instrument via graphical user interface (GUI). C) Inside view of the boxed system. D) System is designed for portability, and further work will focus on reducing the footprint of the instrument.

connection with a CD player mount. This advanced prototype instrument contains all of the hardware necessary for complete functionality, including: laser valving, spinning, clamping, Peltier-mediated heating and cooling, automated disc alignment, optical alignment and detection, high voltage application, and all of the associated printed circuit



Insert swab into chamber

Press START button

Figure 5-18. Limited user interaction. The user interacts with the system only to insert the swab into the swab chamber and press the “START” button on the GUI.

board (PCB) electronics (**Figure 5-17C**). Furthermore, the device is portable, and lightweight enough to be held in one hand (**Figure 5-17D**).

In order to control each function of the integrated system, custom software was designed that allows for limited user interaction with the device. A user simply inserts the swab into the swab chamber, loads the disc into the instrument, and presses the start button on the graphical user interface (GUI). This process is illustrated in **Figure 5-18**. The limited interaction of the user with the disc and equipment allows for a decreased risk of contamination, as well as the opportunity for use by untrained personnel. The

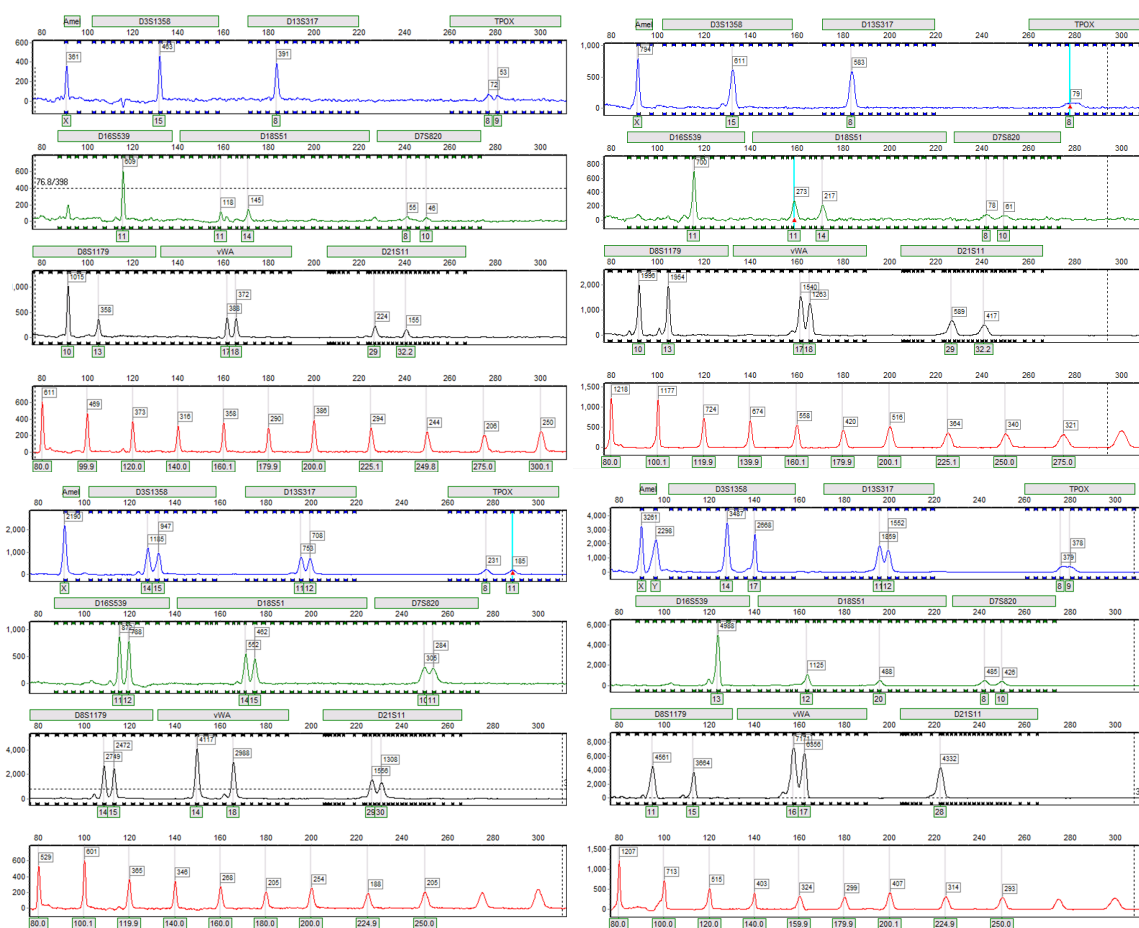


Figure 5-19. Integrated LE-PCR-ME results. Results from 4 of the 40 complete analyses. User inserted swab, loaded the disc onto the instrument, and pressed start. STR profiles were generated automatically, with final allele calling performed manually.

system was evaluated over 40 different runs, with an untrained user inserting the swab and pressing start. The resultant STR profiles generated were compared to truth data, which was amplified and separated conventionally for over 18 different DNA donors, and all profiles were 100% concordant. Analysis time, from swab insertion to STR profile generation, was averaged over the 40 runs to 73.9 minutes, well under the goal of 90 minutes. **Figure 5-19** shows the results from 4 of the 40 analyses, with the user inserting the swab, loading the instrument, and pressing start. The STR profile was generated automatically after the separation was complete, and allele calling was performed manually.

5.5 Conclusions

This work demonstrates the successful 15-minute and 19-minute amplification of a 10-plex kit for STR-based PCR and rapid human identification. The 10-plex chemistry has been previously optimized (Chapter 4), and further work was performed to decrease the overall thermocycling time, incorporate a simple extraction method (via ZyGEM reagents), demonstrate the compatibility with various new substrates, and integrate the PCR assay with upstream LE and downstream ME. A custom-built system capable of fluid flow control (via centrifugal force) and rapid thermocycling (via dual-Peltier clamping apparatus) was demonstrated, and additional functionality was incorporated to achieve a fully integrated system capable of extraction, amplification, and separation. The microdevice was designed and fabricated using the PCL method, thereby decreasing cost, and the final design consisted of 7 materials, 10 layers, 24 chambers, 55 channels, and 13 valves. The system allows for limited user interaction, and only requires insertion

of a buccal swab into the swab chamber, loading of the disc onto the instrument, and pressing the start button in the GUI. STR profiles for over 18 different DNA donors were generated and all profiles were 100% concordant with truth data. Furthermore, the device and associated instrumentation are inexpensive (<\$10,000 USD for all components) and small (1700 in³). Overall, this system represents a powerful advanced prototype instrument that is capable of rapid human identification via STR profile generation in a cost-effective and portable manner.

5.6 References

1. Le Roux, D.; Root, B. E.; Reedy, C. R.; Hickey, J. A.; Scott, O. N.; Bienvenue, J. M.; Landers, J. P.; Chassagne, L.; de Mazancourt, P., DNA Analysis Using an Integrated Microchip for Multiplex PCR Amplification and Electrophoresis for Reference Samples. *Analytical Chemistry* **2014**, *86* (16), 8192-8199.
2. Lounsbury, J. A.; Coult, N.; Miranian, D. C.; Cronk, S. M.; Haverstick, D. M.; Kinnon, P.; Saul, D. J.; Landers, J. P., An enzyme-based DNA preparation method for application to forensic biological samples and degraded stains. *Forensic Science International-Genetics* **2012**, *6* (5), 607-615.
3. Kloosterman, A.; Mapes, A.; Geradts, Z.; van Eijk, E.; Koper, C.; van den Berg, J.; Verheij, S.; van der Steen, M.; van Asten, A., The interface between forensic science and technology: how technology could cause a paradigm shift in the role of forensic institutes in the criminal justice system. *Philosophical Transactions of the Royal Society B-Biological Sciences* **2015**, *370* (1674), 10.

4. Mapes, A. A.; Kloosterman, A. D.; de Poot, C. J., DNA in the Criminal Justice System: The DNA Success Story in Perspective. *Journal of Forensic Sciences* **2015**, *60* (4), 851-856.
5. van Asten, A. C., On the added value of forensic science and grand innovation challenges for the forensic community. *Science & Justice* **2014**, *54* (2), 170-179.
6. Greenspoon, S. A.; Sykes, K. L. V.; Ban, J. D.; Pollard, A.; Baisden, M.; Farr, M.; Graham, N.; Collins, B. L.; Green, M. M.; Christenson, C. C., Automated PCR setup for forensic casework samples using the Normalization Wizard and PCR Setup robotic methods. *Forensic Science International* **2006**, *164* (2-3), 240-248.
7. Laurin, N.; Fregeau, C., Optimization and validation of a fast amplification protocol for AmpFISTR (R) Profiler Plus (R) for rapid forensic human identification. *Forensic Science International-Genetics* **2012**, *6* (1), 47-57.
8. Verheij, S.; Harteveld, J.; Sijen, T., A protocol for direct and rapid multiplex PCR amplification on forensically relevant samples. *Forensic Science International-Genetics* **2012**, *6* (2), 167-175.
9. Vallone, P. M.; Hill, C. R.; Butler, J. M., Demonstration of rapid multiplex PCR amplification involving 16 genetic loci. *Forensic Science International-Genetics* **2008**, *3* (1), 42-45.
10. Foster A, L. N., Development of a fast PCR protocol enabling rapid generation of AmpF/STR® Identifier ® profiles for genotyping of human DNA *Investigative Genetics* **2012**, *3* (6).
11. Aboud, M.; Oh, H. H.; McCord, B., Rapid direct PCR for forensic genotyping in under 25 min. *Electrophoresis* **2013**, *34* (11), 1539-1547.

12. Wheeler, E. K.; Hara, C. A.; Frank, J.; Deotte, J.; Hall, S. B.; Benett, W.; Spadaccini, C.; Beer, N. R., Under-three minute PCR: Probing the limits of fast amplification. *Analyst* **2011**, *136* (18), 3707-3712.
13. Vallone PM, H. C., Podien D, Butler JM, Rapid amplification of commercial STR typing kits. *Forensic Science International: Genetics Supplement Series* **2009**, *2* (1), 111-112.
14. Wang DY, C. C., Hennessy LK, Rapid STR analysis of single source DNA samples in 2 hours *Forensic Science International: Genetics Supplement Series* **2009**, *2* (1), 115-116.
15. Giese, H.; Lam, R.; Selden, R.; Tan, E., Fast Multiplexed Polymerase Chain Reaction for Conventional and Microfluidic Short Tandem Repeat Analysis. *Journal of Forensic Sciences* **2009**, *54* (6), 1287-1296.
16. Butts, E. L. R.; Vallone, P. M., Rapid PCR protocols for forensic DNA typing on six thermal cycling platforms. *Electrophoresis* **2014**, *35* (21-22), 3053-3061.
17. Wu, J. B.; Kodzius, R.; Cao, W. B.; Wen, W. J., Extraction, amplification and detection of DNA in microfluidic chip-based assays. *Microchimica Acta* **2014**, *181* (13-14), 1611-1631.
18. El-Ali, J.; Perch-Nielsen, I. R.; Poulsen, C. R.; Bang, D. D.; Telleman, P.; Wolff, A., Simulation and experimental validation of a SU-8 based PCR thermocycler chip with integrated heaters and temperature sensor. *Sensors and Actuators a-Physical* **2004**, *110* (1-3), 3-10.
19. Kopp, M. U.; de Mello, A. J.; Manz, A., Chemical amplification: Continuous-flow PCR on a chip. *Science* **1998**, *280* (5366), 1046-1048.

20. Obeid, P. J.; Christopoulos, T. K., Continuous-flow DNA and RNA amplification chip combined with laser-induced fluorescence detection. *Analytica Chimica Acta* **2003**, *494* (1-2), 1-9.
21. Obeid, P. J.; Christopoulos, T. K.; Crabtree, H. J.; Backhouse, C. J., Microfabricated device for DNA and RNA amplification by continuous-flow polymerase chain reaction and reverse transcription-polymerase chain reaction with cycle number selection. *Analytical Chemistry* **2003**, *75* (2), 288-295.
22. West, J.; Karamata, B.; Lillis, B.; Gleeson, J. P.; Alderman, J.; Collins, J. K.; Lane, W.; Mathewson, A.; Berney, H., Application of magnetohydrodynamic actuation to continuous flow chemistry. *Lab on a Chip* **2002**, *2* (4), 224-230.
23. Chen, Z. Y.; Qian, S. Z.; Abrams, W. R.; Malamud, D.; Bau, H. H., Thermosiphon-based PCR reactor: Experiment and modeling. *Analytical Chemistry* **2004**, *76* (13), 3707-3715.
24. Zhang, Y. H.; Ozdemir, P., Microfluidic DNA amplification-A review. *Analytica Chimica Acta* **2009**, *638* (2), 115-125.
25. Zhang, C. S.; Xu, J. L.; Ma, W. L.; Zheng, W. L., PCR microfluidic devices for DNA amplification. *Biotechnology Advances* **2006**, *24* (3), 243-284.
26. Beer, N. R.; Hindson, B. J.; Wheeler, E. K.; Hall, S. B.; Rose, K. A.; Kennedy, I. M.; Colston, B. W., On-chip, real-time, single-copy polymerase chain reaction in picoliter droplets. *Analytical Chemistry* **2007**, *79* (22), 8471-8475.
27. Kiss, M. M.; Ortoleva-Donnelly, L.; Beer, N. R.; Warner, J.; Bailey, C. G.; Colston, B. W.; Rothberg, J. M.; Link, D. R.; Leamon, J. H., High-Throughput

Quantitative Polymerase Chain Reaction in Picoliter Droplets. *Analytical Chemistry* **2008**, *80* (23), 8975-8981.

28. Liu, H. B.; Ramalingam, N.; Jiang, Y.; Dai, C. C.; Hui, K. M.; Gong, H. Q., Rapid distribution of a liquid column into a matrix of nanoliter wells for parallel real-time quantitative PCR. *Sensors and Actuators B-Chemical* **2009**, *135* (2), 671-677.

29. LaRue, B. L.; Moore, A.; King, J. L.; Marshall, P. L.; Budowle, B., An evaluation of the RapidHIT (R) system for reliably genotyping reference samples. *Forensic Science International-Genetics* **2014**, *13*, 104-111.

30. L. K. Hennessy, H. F., Y. Li, J. Buscaino, K. Chear, J. Gass, N. Mehendale, S. Williams, S. Jovanovich, D.; 2 3 Harris, K. E., W. Nielsen, Developmental validation studies on the RapidHIT^M Human DNA identification system. *Forensic Science International: Genetics Supplement Series* **2013**, *4* (1), e7-e8.

31. Vallone, P., http://www.cstl.nist.gov/strbase/pub_pres/Vallone_BCC_Talk_Sept2013.pdf.

32. Asogawa, M., Sugisawa, M., Aoki, K., Hagiwara, H., Mishina, Y., Yamashita, S., Yamada, Y., Development of portable and rapid human DNA analysis system aiming on-site screening. *Twelfth International Conference on Miniaturized Systems for Chemistry and Life Sciences (MicroTAS)*: 2008.

33. Le Roux, D.; Root, B. E.; Hickey, J. A.; Scott, O. N.; Tsuei, A.; Li, J. Y.; Saul, D. J.; Chassagne, L.; Landers, J. P.; de Mazancourt, P., An integrated sample-in-answer-out microfluidic chip for rapid human identification by STR analysis. *Lab on a Chip* **2014**, *14* (22), 4415-4425.

34. Thompson, B. L.; Ouyang, Y. W.; Duarte, G. R. M.; Carrilho, E.; Krauss, S. T.; Landers, J. P., Inexpensive, rapid prototyping of microfluidic devices using overhead transparencies and a laser print, cut and laminate fabrication method. *Nature Protocols* **2015**, *10* (6), 875-886.
35. DuVall, J. A.; Le Roux, D.; Tsuei, A. C.; Thompson, B. L.; Birch, C.; Li, J.; Nelson, D. A.; Mills, D. L.; Ewing, M. M.; McLaren, R. S.; Storts, D. R.; Root, B. E.; Landers, J. P., A rotationally-driven polyethylene terephthalate microdevice with integrated reagent mixing for multiplexed PCR amplification of DNA. *Analytical Methods* **2016**, *8* (40), 7331-7340.
36. Thompson, B. L.; Birch, C.; Li, J. Y.; DuVall, J. A.; Le Roux, D.; Nelson, D. A.; Tsuei, A. C.; Mills, D. L.; Krauss, S. T.; Root, B. E.; Landers, J. P., Microfluidic enzymatic DNA extraction on a hybrid polyester-toner-PMMA device. *Analyst* **2016**, *141* (15), 4667-4675.
37. Thompson, B. L.; Birch, C.; Nelson, D. A.; Li, J. Y.; DuVall, J. A.; Le Roux, D.; Tsuei, A. C.; Mills, D. L.; Root, B. E.; Landers, J. P., A centrifugal microfluidic device with integrated gold leaf electrodes for the electrophoretic separation of DNA. *Lab on a Chip* **2016**, *16* (23), 4569-4580.
38. Ouyang, Y. W.; Wang, S. B.; Li, J. Y.; Riehl, P. S.; Begley, M.; Landers, J. P., Rapid patterning of 'tunable' hydrophobic valves on disposable microchips by laser printer lithography. *Lab on a Chip* **2013**, *13* (9), 1762-1771.
39. Garcia-Cordero, J. L.; Kurzbuch, D.; Benito-Lopez, F.; Diamond, D.; Lee, L. P.; Ricco, A. J., Optically addressable single-use microfluidic valves by laser printer lithography. *Lab on a Chip* **2010**, *10* (20), 2680-2687.

Final Remarks

6.1 Conclusions

This dissertation has focused on the development of rapid systems for the detection of both pathogen and human nucleic acids following microfluidic nucleic acid amplification. The work in Chapter 2 demonstrated an inexpensive and simplistic method for pathogen detection utilizing commercially available, silica-coated magnetic beads. Loop-mediated isothermal amplification (LAMP) was utilized to produce amplicons of various sizes that were subsequently detected via product-inhibited bead aggregation (PiBA). PiBA builds upon a previously demonstrated magnetic bead assay, chaotrope-induced aggregation (CIA), whereby long strands of human genomic DNA bind to the surface of silica-coated magnetic beads and induce aggregation when exposed to a rotating magnetic field.¹ PiBA exploits the same DNA-silica particle interaction; however, the LAMP amplicons are too short to tether the beads together. When the magnetic beads are exposed to long strands of DNA (termed “trigger DNA”) in the presence of LAMP amplicons, the DNA is no longer able to access the silica surface of the beads (where the amplicons are bound), thereby inhibiting aggregation. The assay was successfully applied to several targets, including: Rift Valley fever virus (RVFV), *Salmonella enterica*, multiple strains of *Escherichia coli*, and human-specific thyroid peroxidase (TPOX) gene.

Chapter 3 focused on the transition of the PiBA assay from poly(methylmethacrylate) (PMMA) open microwells to a centrifugal platform and a polyester toner (PeT) substrate. PeT devices were fabricated using the print, cut,

laminate (PCL) method developed in our lab.² A custom-built system was designed to provide assay functionality, including: spinning, heating, and a rotating magnetic field. Both LAMP and PiBA were successfully demonstrated on PeT microdevices, and this new platform was shown for proof-of-concept with both Influenza H1N1 and multiple strains of *Clostridium difficile*.

In Chapter 4, a new project was introduced, which was aimed at developing a rapid, inexpensive, and portable system for human identification using short tandem repeat (STR) analysis. This chapter dealt mostly with the optimization of multiplexed STR-based PCR on PeT microdevices, coupled to a custom-built system. The dual integrated Peltier spinning (DIPS) system was designed for rapid thermocycling and fluid flow control via centrifugal force. Several STR kits, both commercial and custom, were demonstrated using this platform. Optimization of the kits was required for rapid PCR, and various master mix components, including DNA polymerase and MgCl₂, were titrated to achieve optimal results. For well-balanced STR profiles, where each locus contributes equally to the overall peak height, the various primer concentrations were modified for on-chip amplification. The successful amplification of 6-plex, 10-plex, and 18-plex STR kits was demonstrated in as little as 35 minutes.

A portable system for rapid human identification requires all analyses to be performed on a single device, including: DNA extraction, PCR amplification of genetic markers, and electrophoretic separation; therefore, the focus of Chapter 5 was assay integration. PCR time was reduced to 15 minutes, various new materials were demonstrated to be compatible with the novel 10-plex amplification, and ZyGEM-

extracted DNA was used as template. A fully-integrated microdevice was designed, which included 7 materials, 10 layers, 24 chambers, 55 channels, and 13 laser-actuated valves, for full assay functionality. The associated hardware was 1700 in³ in size and cost less than \$10,000 USD for all components, representing a truly portable and inexpensive device for rapid human identification. Over 40 analyses were performed, and the overall analysis time was only 74 minutes; furthermore, all STR profiles generated were 100% concordant with the truth data.

6.2 Future Directions

Many of the experiments and results presented in this dissertation demonstrate proof-of-concept for the rapid systems that have been developed; however, more work is required to bring the systems to a fully functional state for point-of-care (POC) testing.

*WHAT IF...*you could have a system that could detect infectious agents in resource-limited settings? Could the past outbreaks of, e.g., Ebola be handled in a way that would have a better outcome/containment? What if the system was cost-effective enough to do routine monitoring for *C. difficile* and *MRSA* in every room in every hospital in the country each day? Would HAI decrease?

*WHAT'S NEEDED...*is full integration of the PiBA system and associated hardware demonstrated in Chapter 2 and 3. Although both assays, LAMP and PiBA, have been demonstrated on PeT chips using the custom-built system, they are not fluidically integrated in their present state. Chip design will be a major focus of the work

going forward, with attention given to the challenge of metering the small volumes of LAMP product necessary for PiBA detection. The incorporation of laser valves could solve this problem and many of the other problems associated with hydrophobic valves, including the challenge of metering 1-2 μL at a time. Furthermore, the custom-built system demonstrated is capable of spinning, heating, and applying a rotating magnetic field; however, a slip ring has been incorporated so that the base plate of the system, which contains a resistive heater, is able to spin without disconnecting electronically. Additional work will address the motor requirements for spinning the slip ring, as well as the challenge of providing temperature feedback during the isothermal amplification, either using a thermocouple or thermistor. Detection using the cell phone app as demonstrated can also be improved, namely with additional features such as automatic cropping that will further simplify the image analysis step in the protocol.

With the two assays fluidically integrated, and the custom-built system fully functional, the LAMP-PiBA platform represents a powerful tool for pathogen screening. This device could be employed in numerous applications, the most important of which might be detection of biological warfare agents for implications in national security. Another powerful application of this technology would be for use by the Food and Drug Administration (FDA) for rapid screening of food-borne pathogens. A portable device would be an invaluable resource for pathogen screening at food packing sites, grocery stores, processing plants, etc. where an informed decision could be made before tainted meat or produce was disseminated. For diagnosis of lower respiratory infections, the PiBA device could be used to screen a nasopharyngeal swab for multiple pathogens

simultaneously, including: influenza A and B, respiratory syncytial virus, parainfluenza virus, and adenovirus.

The rapid and portable system for human identification, presented in Chapters 4 and 5, already represents a system that is capable of POC testing.

*WHAT IF...*we had the potential for on-site human identification at every crime scene in the country? Could we make more informed and less biased arrests of persons of interest? What if we could rapidly detect cancer mutations at the doctor's office, or determine genetic mutations that might lead to more informed decisions about which/how much medication to prescribe an ill patient?

*WHAT'S NEEDED...*is more research and development to decrease the overall analysis time required to generate a STR profile, and to make the system more portable. PCR represents the most time consuming step in the overall STR analysis, and experiments are currently underway to further reduce the thermocycling time. Smaller, faster Peltiers are being explored for more rapid heating and cooling, thereby reducing the overall time required per cycle. A reduction in the PCR chamber volume will allow for more rapid heat transfer, also contributing to a faster PCR thermocycling time. The hardware required for assay functionality is currently 1700 in³ in size, with a final goal of 500 in³, providing increased portability for field use. Together with the faster analysis time (end goal of < 30 minutes from start to finish), the smaller instrument will be capable of truly rapid, inexpensive, and portable human identification via STR profiling.

The portable device for genetic analysis has potential utility with applications outside of forensics as well. STR panels have been used to identify the origin of various strains of marijuana, and this portable system could be used on-site for the Drug Enforcement Agency in containing the influx of drugs into the United States. This device could also find utility in screening for cancer mutations by identifying various single nucleotide polymorphisms (SNPs) that increase the risk of developing certain types of cancer. Another important application of this device could be to detect genes specific for antibiotic resistance. The device currently has multiplex capabilities, allowing for the simultaneous detection of multiple bacterial genes associated with antibiotic resistance, including Methicillin-resistant *Staphylococcus aureus* (MRSA). The multiplex nature of the device would also allow for a single swab to be analyzed in terms of specific antibiotics that might be ineffective at treating the infection.

6.3 Summation

Microfluidics has been demonstrated to be an effective tool for developing rapid systems for the detection of pathogen and human nucleic acids. The systems demonstrated in this dissertation are simple, inexpensive, and offer increased portability over conventional methods for both pathogen detection, as well as human identification. With continued development, both platforms will be capable of POC use, and can be utilized for a range of applications.

6.4 References

1. D. C. Leslie, J. Y. Li, B. C. Strachan, M. R. Begley, D. Finkler, L. A. L. Bazydlo, N. S. Barker, D. M. Haverstick, M. Utz and J. P. Landers, *Journal of the American Chemical Society*, 2012, **134**, 5689-5696.
2. B. L. Thompson, Y. W. Ouyang, G. R. M. Duarte, E. Carrilho, S. T. Krauss and J. P. Landers, *Nature Protocols*, 2015, **10**, 875-886.